BIOCHIMICA ET BIOPHYSICA ACTA

BBA

BIOMEMBRANES

ELSEVIER

VOL. 1330 NO. 1 (13 NOVEMBER 1997)

ISSN 0005-2736 BBBMBS 1330(1) 1–102 (1997)

BIOCHIMICA ET BIOPHYSICA ACTA

International Journal of Biochemistry, Biophysics
& Molecular Biology

Editor-in-Chief: Peter C. van der Vliet (Utrecht, The Netherlands)

BBA comprises the following ten sections:

Subject area	Executive Editors
· Bioenergetics (including Reviews on Bioenergetics)	M. Wikström (Helsinki, Finland) P. Rich (London, UK)
· Biomembranes · Reviews on Biomembranes	A.G. Lee (Southampton, UK) P.L. Yeagle (Storrs, CT, USA)
· Lipids and Lipid Metabolism	H. van den Bosch (Utrecht, The Netherlands) D.E. Vance (Edmonton, AB, Canada)
· Protein Structure and Molecular Enzymology	G.H. Lorimer (Wilmington, DE, USA) Y. Lindqvist (Stockholm, Sweden)
· Molecular Cell Research	T.E. Kreis (Geneva, Switzerland) J. Avruch (Charlestown, MA, USA)
· Gene Structure and Expression	P.C. van der Vliet (Utrecht, The Netherlands) J.D. Gralla (Los Angeles, CA, USA)
· Molecular Basis of Disease	J.R. Riordan (Scottsdale, AZ, USA)
· General Subjects	M. Fukuda (La Jolla, CA, USA)
· Reviews on Cancer	D.M. Livingston (Boston, MA, USA)

Submission

Authors should submit their manuscripts (four copies) to one of the appropriate Executive Editors at either of the following Editorial Offices:

BBA Editorial Secretariat
P.O. Box 1345
1000 BH Amsterdam
The Netherlands

Tel. +31 20 4853510
Fax +31 20 4853506
E-mail: bba@elsevier.nl

BBA Editorial Secretariat
275 Washington Street
Newton, MA 02158
USA

Tel. +1 (617) 630-2244
Fax +1 (617) 630-2245
E-mail: bba.elsevier@cahners.com

Although most published *Review* articles are submitted on the invitation of the Executive Editor(s), authors of suitable (mini) reviews may also submit their work unsolicited (four copies) by sending their papers(s) to one of the Executive Editors of the appropriate section.

Copyright © 1997 Elsevier Science B.V. All rights reserved
Printed in The Netherlands

0005-2736/1997/$17.00

BIOCHIMICA ET BIOPHYSICA ACTA

BBA

VOL. 1330
(1997)

WORLD WIDE WEB PRESENCE:

For online access to information on the Aims & Scope, Editorial Board, Instructions to Authors, Table of Contents of recently published issues, subscription details and sample copy request procedure, please consult:

http://www.elsevier.nl/locate/BBA
or
http://www.elsevier.com/locate/BBA

BIOCHIMICA ET BIOPHYSICA ACTA

BBA

BIOMEMBRANES

EXECUTIVE EDITORS

A.G. Lee (Southampton, UK)
P.L. Yeagle (Storrs, CT, USA)

EDITORS

B. Andersson (Stockholm, Sweden)
J. Badwey (Boston, MA, USA)
M.T. Bayliss (London, UK)
C. Bevins (Cleveland, OH, USA)
R.J. Beynon (Liverpool, UK)
G. Cevc (Munich, Germany)
H. Chap (Toulouse, France)
C.M. Cohen (Boston, MA, USA)
H.W. Cook (Halifax, NS, Canada)
P.R. Cullis (Vancouver, BC, Canada)
M.L. DePamphilis (Nutley, NJ, USA)
B. Erni (Bern, Switzerland)
J. Fain (Memphis, TN, USA)
M. Gutman (Tel Aviv, Israel)
D.A. Harris (Oxford, UK)
R. Haselkorn (Chicago, IL, USA)
T. Hashimoto (Nagano, Japan)
T.D. Heath (Madison, IL, USA)
R.A. Houghten (San Diego, CA, USA)
S.W. Hui (Buffalo, NY, USA)
J.B. Jackson (Birmingham, UK)
B. Kemp (Melbourne, Australia)
R.N. McElhaney (Edmonton, AB, Canada)
D.J. McNamara (Washington, DC, USA)
A. Merill (Atlanta, GA, USA)
O.G. Mouritsen (Lyngby, Denmark)
K.H. Nierhaus (Berlin, Germany)
J.B. Ohlrogge (East Lansing, MI, USA)
C.R. Pace-Asciak (Toronto, ON, Canada)
P. Parker (London, UK)
M.C. Phillips (Philadelphia, PA, USA)
A.C.G. Porter (London, UK)
A.G. Porter (Singapore)
R. Prince (Annandale, NJ, USA)
K. Rajagopalan (Durham, NC, USA)
J. Riordan (Boston, MA, USA)
J.-M. Ruysschaert (Brussels, Belgium)
K. Sandhoff (Bonn, Germany)
R. Sen (Waltham, MA, USA)
C.N. Serhan (Boston, MA, USA)
J.R. Silvius (Montreal, PQ, Canada)
W.L. Smith (East Lansing, MI, USA)
F. Snyder (Oak Ridge, TN, USA)
S. Spiegel (Washington, DC, USA)
L.L. Spremulli (Chapel Hill, NC, USA)
U.P. Steinbrecher (Vancouver, BC, Canada)
H.G. Stunnenberg (Nijmegen, The Netherlands)
D.M. Tiede (Argonne, IL, USA)
K.F. Tipton (Dublin, Ireland)
B. Trüeb (Bern, Switzerland)
B. Tummler (Hannover, Germany)
J. Vanderkooi (Philadelphia, PA, USA)
L.M.G. van Golde (Utrecht, The Netherlands)
R. van Grondelle (Amsterdam, The Netherlands)
G. van Meer (Amsterdam, The Netherlands)
D.R. Voelker (Denver, CO, USA)
M. Waite (Winston-Salem, NC, USA)
M.J. Waring (Cambridge, UK)
R.J.P. Williams (Oxford, UK)
A.P. Wolffe (Bethesda, MD, USA)
J. Woodgett (Toronto, ON, Canada)
C. Yocum (Ann Arbor, MI, USA)
S. Yokoyama (Nagoya, Japan)

Reviews on Biomembranes, Reviews on Cancer and Reviews on Bioenergetics each have their own independent Editorial Advisory Board.

ASSOCIATE EXECUTIVE EDITOR
D.J. Waxman (Boston, MA, USA)

HONORARY EXECUTIVE EDITOR
E.C. Slater (Southampton, UK)

Founded in 1947 by H.G.K. Westenbrink
Managing Editor, 1947-1964

BBA is cited in: Current Contents/Life Sciences - Biological Abstracts - Chemical Abstracts - Index Chemicus - Index Medicus/MEDLINE - Cambridge Scientific Abstracts (CSA) - Excerpta Medica (EMBASE) - Reference Update - Current Awareness in Biological Sciences (CABS)

BIOCHIMICA ET BIOPHYSICA ACTA

BBA

INTERNATIONAL JOURNAL OF BIOCHEMISTRY, BIOPHYSICS
AND MOLECULAR BIOLOGY

BIOMEMBRANES

VOL. 1330 (1) (1997)

Executive Editors: A.G. Lee (Southampton, UK)
P.L. Yeagle (Storrs, CT, USA)

ELSEVIER

Amsterdam – Lausanne – New York – Oxford – Shannon – Tokyo

BBA — PUBLICATION SCHEDULE FOR 1997

BBA is published according to a volume-numbering scheme that embraces all sections of the journal.
Full subscription: 45 volumes plus Cumulative Index

BIO-ENERGETICS including Reviews on Bioenergetics	BIO-MEMBRANES	REVIEWS ON BIO-MEMBRANES	GENERAL SUBJECTS	PROTEIN STRUCTURE AND MOLECULAR ENZYMOLOGY	LIPIDS AND LIPID METABOLISM	GENE STRUCTURE AND EXPRESSION	MOLECULAR CELL RESEARCH	MOLECULAR BASIS OF DISEASE	REVIEWS ON CANCER
5 volumes	9 volumes *		3 volumes	7 volumes	6 volumes	5 volumes	5 volumes	3 volumes	2 volumes
1318-1	1323-1		1334-1	1337-1	1344-1	1350-1	1355-1	1360-1	1332-1
1318-2	1323-2			1337-2	1344-2	1350-2	1355-2		
1318-3					1344-3	1350-3	1355-3	1360-2	
	1324-1	1331-1	1334-2	1338-1					1332-2
1319-1	1324-2			1338-2	1345-1	1351-1	1356-1	1360-3	
1319-2			1334-3		1345-2	1351-2	1356-2		
1319-3	1325-1			1339-1	1345-3	1351-3	1356-3		
	1325-2		1335-1	1339-2	1346-1			1361-1	1332-3
1320-1	1326-1				1346-2	1352-1	1357-1		
1320-2	1326-2			1340-1	1346-3	1352-2	1357-2	1361-2	
1320-3		1331-2	1335-2	1340-2		1352-3	1357-3		
	1327-1				1347-1				1333-1
1321-1	1327-2		1335-3	1341-1	1347-2	1353-1	1358-1	1361-3	
1321-2				1341-2	1347-3	1353-2	1358-2		
1321-3	1328-1		1336-1		1348-1	1353-3	1358-3	1362-1	
	1328-2			1342-1	1348-2				1333-2
	1329-1			1342-2	1348-3			1362-2	
1322-1	1329-2	1331-3	1336-2		1349-1	1354-1	1359-1		
1322-2				1343-1	1349-2	1354-2	1359-2	1362-3	
1322-3	1330-1		1336-3	1343-2	1349-3	1354-3	1359-3		1333-3
	1330-2								

* Including Reviews on Biomembranes, Vol. 1331.

Copyright © 1997 Elsevier Science B.V. All rights reserved

0005-2736/1997/$17.00

This journal and the individual contributions contained in it are protected by the copyright of Elsevier Science B.V., and the following terms and conditions apply to their use:

Photocopying

Single photocopies of single articles may be made for personal use as allowed by national copyright laws. Permission of the Publisher and payment of a fee is required for all other photocopying, including multiple or systematic copying, copying for advertising or promotional purposes, resale, and all forms of document delivery. Special rates are available for educational institutions that wish to make photocopies for non-profit educational classroom use.

In the USA, users may clear permissions and make payment through the Copyright Clearance Center Inc., 222 Rosewood Drive, Danvers, MA 01923, USA. In the UK, users may clear permissions and make payment through the Copyright Licensing Agency Rapid Clearance Service (CLARCS), 90 Tottenham Court Road, London W1P 0LP, UK. In other countries where a local copyright clearance centre exists, please contact it for information on required permissions and payments.

Derivative Works

Subscribers may reproduce tables of contents or prepare lists of articles including abstracts for internal circulation within their institutions. Permission of the Publisher is required for resale or distribution outside the institution.

Permission of the Publisher is required for all other derivative works, including compilations and translations.

Electronic Storage

Permission of the Publisher is required to store electronically any material contained in this journal, including any article or part of an article. Contact the Publisher at the address indicated.

Except as outlined above, no part of this publication may be reproduced, stored in a retrieval system or transmitted in any form or by any means, electronic, mechanical, photocopying, recording or otherwise, without prior written permission of the Publisher.

No responsibility is assumed by the Publisher for any injury and/or damage to persons or property as a matter of products liability, negligence or otherwise, or from any use or operation of any methods, products, instructions or ideas contained in the material herein. Because of the rapid advances in the medical sciences, the Publisher recommends that independent verification of diagnoses and drug dosages should be made.

Advertising Information:

Advertising orders and enquiries may be sent to: *International* – Elsevier Science, Advertising Department, The Boulevard, Langford Lane, Kidlington, Oxford, OX5 1GB, UK; Tel: (+44) (0) 1865 843565; Fax (+44) (0) 1865 843976. *USA & Canada* – Weston Media Associates, Dan Lipner, P.O Box 1110, Greens Farms, CT 06436-1110, USA; Tel: +1(203) 261 2500; Fax +1(203) 261 0101. *Japan* – Elsevier Science Japan, Marketing Services, 1-9-15 Higashi-Azabu, Minato-ku, Tokyo 106, Japan; Tel: +81 3 5561 5033; Fax: +81 3 5561 5047.

Although all advertising material is expected to conform to ethical (medical) standards, inclusion in this publication does not constitute a guarantee or endorsement of the quality or value of such product or of the claims made of it by its manufacturer.

Printed in The Netherlands

♾ The paper used in this publication meets the requirements of ANSI/NISO Z39.48-1992 (Permanence of Paper).

ELSEVIER

Biomembranes

Vol. 1330, No. 1; 13 November 1997

BIOCHIMICA ET BIOPHYSICA ACTA

BBA

Contents

BBA is cited in: Current Contents / Life Sciences - Biological Abstracts - Chemical Abstracts - Index Chemicus - Index Medicus / MEDLINE - Cambridge Scientific Abstracts (CSA) - Excerpta Medica (EMBASE) - Reference Update - Current Awareness in Biological Sciences (CABS)

Information for Contributors *vii*

Regular papers

Inhibition of annexin V-dependent Ca^{2+} movement in large unilamellar vesicles by K201, a new 1,4-benzothiazepine derivative
N. Kaneko, R. Matsuda, M. Toda and K. Shimamoto (Japan) 1

Mechanism of adenovirus improvement of cationic liposome-mediated gene transfer
C. Meunier-Durmort, R. Picart, T. Ragot, M. Perricaudet, B. Hainque and C. Forest (France) 8

Pores formed by influenza hemagglutinin [1]
R. Jiricek, G. Schwarz and T. Stegmann (Switzerland) 17

Dual effects of extracellular Ca^{2+} on cardiotoxin-induced cytotoxicity and cytosolic Ca^{2+} changes in cultured single cells of rabbit aortic endothelium
Y.-J. Ou, Y.-M. Leung, S.-J. Huang and C.-Y. Kwan (China, Canada) 29

Potassium transport in opossum kidney cells: Effects of Na-selective and K-selective ionizable cryptands, and of valinomycin, FCCP and nystatin
A. Loiseau, C. Leroy and M. Castaing (France) 39

Evidence for extensive and non-specific translocation of oligopeptides across plasma membranes of mammalian cells
J. Oehlke, M. Beyermann, B. Wiesner, M. Melzig, H. Berger, E. Krause and M. Bienert (Germany) 50

Charge-dependent insertion of β-lactoglobulin into monoglyceride monolayers
J.M. Leenhouts, R.A. Demel, B. De Kruijff and J.-W.P. Boots (Netherlands) 61

Lysosome membrane permeability to amines
C.L. Andrew, A.R. Klemm and J.B. Lloyd (USA) 71

Activation of the Na^+/K^+ pump current by intra- and extracellular Li ions in single guinea-pig cardiac cells
A.N. Hermans, H.G. Glitsch and F. Verdonck (Belgium, Germany) 83

Na^+-dependent γ-aminobutyric acid (GABA) transport in the choroid plexus of rabbit
V.K. Ramanathan, C.M. Brett and K.M. Giacomini (USA) 94

ELSEVIER

BIOCHIMICA ET BIOPHYSICA ACTA

BBA

Information for Contributors

BBA – Aims and Scope

Biochimica et Biophysica Acta publishes papers reporting advances in the knowledge or understanding of any field of biochemistry or biophysics. More than forty volumes are published each year, each section featuring the latest scientific developments in its field of interest. BBA publishes Regular papers, Rapid reports, and Short sequence-papers and Promoter papers which contribute new and significant information to the fields of biochemistry and biophysics. Negative results will be accepted only when they can be considered to advance this knowledge significantly. Papers providing only confirmatory evidence or extending observations firmly established in one species to another will not normally be accepted. The journal is divided into ten specialized sections:

Bioenergetics covers the area of biological energy transfer and conversion, focusing on the kinetics and thermodynamics of molecular mechanisms involved in photosynthesis, mitochondrial and bacterial respiration, oxidative phosphorylation, motility and transport, as well as the underlying molecular structures. This section also includes Reviews on Bioenergetics.

Biomembranes has its main focus on membrane structure, function and biomolecular organization, membrane proteins, receptors, channels and anchors, fluidity and composition, model membranes and liposomes, membrane surface studies and ligand interactions, transport studies, and membrane dynamics.

Gene Structure and Expression covers DNA and RNA structure, DNA replication and expression, damage and repair, transcription mechanisms and factors, translation, RNA processing, control of gene expression, cell-cycle control, gene rearrangements and recombination, nucleic acid – ligand interactions, DNA-modifying enzymes, viral systems and molecular genetics. This section also includes Short sequence-papers describing DNA and RNA sequences for protein coding, regulatory or structural elements, and promoter papers describing sequence and functional analysis of promoter and enhancer regions. Short sequence-papers are also published in other sections of BBA when this is more appropriate.

General Subjects includes a wide diversity of papers and provides a vehicle for publication of novel and challenging subjects in developing areas of research not yet established, as well as completing BBA's coverage of other important areas of biochemistry (glycobiology and novel compounds) and biophysics for which no specialized section exists.

Lipids and Lipid Metabolism covers the novel aspects of lipid biosynthesis and metabolism, including protein lipid anchors, in all organisms. Emphasis is given to the enzymology and molecular biology of the enzymes involved in lipid metabolism. In addition, molecular genetics of the genes involved will be emphasized in the future.

Subsection: Lipids in Signalling and Recognition: concentrates on all biochemical and biophysical aspects of lipids and lipid-derived messenger molecules, including their structure, physicochemical properties and transport, regulation and enzymology of their biosynthesis and metabolic inactivation, and the recognition processes underlying their biological activities.

Molecular Cell Research focuses on cellular processes at the molecular level. These include aspects of intracellular trafficking, regulation of the secretory and endocytic pathways, sorting and targetting, organisation and dynamics of of cytoskeletal structures, cellular interactions, cell cycle regulation, cell/tissue differentiation and cellular enzymology. Also included are studies at the interface between Cell Biology and Biophysics which apply for example novel imaging methods for characterizing cellular processes. Excluded, however, are studies describing purely cellular or pharmacological aspects.

Subsection: Signal Transduction primarily focuses on hormone and neurotransmitter action, receptor structure and regulation, transmembrane signalling systems, second messengers, protein phosphorylation, and calcium in signal transduction.

Protein Structure and Molecular Enzymology covers protein structure, conformation and dynamics, protein-ligand interactions, enzyme mechanisms, models and kinetics, physical properties and spectroscopy. *Manuscripts, the principal purpose of which is to describe the purification of a protein, are considered outside the scope of BBA.* Concise and comprehensive reviews of recent developments are considered for publication. However, authors are strongly advised to consult with one of the Executive Editors before starting a review.

Molecular Basis of Disease addresses the biochemistry and molecular genetics of disease processes and their models. The section covers metabolic, membrane, receptor and immunological disorders as well as viral, bacterial and parasitological disorders, and includes the biochemistry of differentiation disorders, tissue damage and aging.

Reviews on Cancer and Reviews on Cancer Online (**ROCO**) are devoted to the rapid publication of critical views of leading investigators, who are invited to write on subjects of high current interest in cancer research. The current scope of this journal is the cell biology, genetics, and biochemistry of cancer, as well as the relationship of immunobiology to the disease. Four forms of reporting now comprise **ROCO**: *Mini-Reviews* focusing on topics in highly active segments of the field; *Opinion Corner*, a section devoted to the opinions of experts on newly evolving and/or controversial areas of special interest; *Meeting Reports*, a section devoted to focused reporting on scientific meetings of special interest; and *Oncology Corner*, a section devoted to analyses of new and interesting trends in translational research. **ROCO** is aimed at a diverse audience of scientists and clinical investigators who need to know what is new and important in this rapidly changing field of science.

Reviews on Cancer Online available on the World Wide Web at: http://www.elsevier.nl/locate/roco or http://www.elsevier.com/locate/roco

Reviews on Biomembranes publishes cutting-edge reviews of new developments in the field of biomembranes.

BBA Reviews. BBA also publishes Reviews that present a concise yet comprehensive overview of recent developments in the field of interest in any other section. Reviews are usually submitted on invitation.

Submission of manuscripts

A submission letter should always accompany the submitted paper, providing the following information:
(a) The full name and address of the corresponding author (including telephone and fax numbers, and e-mail address).
(b) Any known changes of address within a period of six months after submission of the paper.
(c) The type of paper (Regular paper, Rapid report, Short sequence/Promoter paper or Review) and possibly a preferred section of the journal for eventual publication.
(d) The full title of the submitted paper.
(e) The names and addresses of at least three suitable potential reviewers (including telephone and fax numbers, and e-mail address). If there are compelling reasons for excluding some individuals as potential reviewers, these can be mentioned. However, choice of reviewers is at the editors' discretion.

Four copies are required of all material submitted, including the submission letter.

All figures should be provided in quadruplicate and all four sets of figures should be labelled.

Copies of relevant papers that are submitted elsewhere or 'in press', should be provided.

Manuscripts for publication in BBA should be mailed to one of the Executive Editors via one of the receiving offices. **[Four copies of the hard-copy printout plus the electronic file of the manuscript.]**

Editorial Secretariat
Biochimica et Biophysica Acta
P.O. Box 1345, 1000 BH Amsterdam
Molenwerf 1, 1014 AG Amsterdam
The Netherlands
Fax: +31 (20) 4853506
E-mail: bba@elsevier.nl

Biochimica et Biophysica Acta
Elsevier Science Inc.
275 Washington Street
Newton, MA 02158
USA
Fax: (617) 630 2245
E-mail: bba.elsevier@cahners.com

The Executive Editors are responsible for processing and professional review of the manuscripts. Authors are free in their choice of an editorial office, irrespective of their country of residence, for submission of Regular papers and Rapid reports. Short sequence-papers and Promoter papers must always be mailed to the BBA Editorial Secretariat in The Netherlands.

All materials submitted become the property of BBA. While manuscripts and figure copies of refused manuscripts will be returned to the authors whenever possible, this cannot be guaranteed.

Submission of a manuscript implies that the work described has not been published before (except in the form of an abstract or as part of a published lecture or academic thesis), that it is not under consideration for publication elsewhere, that its publication has been approved by all the authors and tacitly or explicitly by the responsible authorities in the laboratories where the work was carried out and that, if accepted, it will not be published elsewhere in the same form, in either the same or another language, without the consent of the editors and the publisher. Reference should be made to previously published abstracts, etc. in the introductory section. Responsibility for the accuracy of the material in the manuscript, including bibliographic citations, lies entirely with the authors.

Ethics

When conducting scientific research using human tissue and which is intended for publication in BBA, authors should follow procedures that are in accordance with the ethical standards as formulated in the Helsinki Declaration of 1975 (revised in 1983). When conducting experiments on animals, authors should follow the institution's or the National Research Council's guide for the care and use of laboratory animals.

Revisions and publication dates

Papers requiring revision and/or condensation will be returned to the authors by the Executive Editors, specifying the requested alterations and including the (anonymous) referee reports.

Authors are requested to resubmit the revised paper within 6 months. Papers not resubmitted within six months will be treated as new submissions.

Proofreading

Authors of Regular papers and Reviews will receive proofs. Since acceptance is based upon the submitted version of the paper, it is essential that no new material be inserted in the text at the time of proofreading; furthermore, no alteration to style or meaning will be permitted at this stage. Any new material that the authors wish to introduce for reasons of scientific accuracy will be checked by the Executive Editors, and a charge may be made for corrections. Authors are encouraged to return their proofs by fax. Proofs of Rapid reports (including Short sequence-papers and Promoter papers) may be faxed to authors upon request, where issue scheduling permits: corrections must then be faxed or telephoned to the Publisher within 48 hours of receipt. If no fax number is provided for Rapid reports, proofs will not be sent.

No page charges; 50 offprints free of charge

Fifty offprints are provided free of charge to the corresponding author of each article. There are no page charges for BBA. An offprint order form, price list and copyright transfer form are sent upon receipt of the manuscript at the Publisher so that extra offprints may be ordered. It is also essential that copyright be transferred at this stage.

Publication

For information concerning your **accepted** manuscript, proof, etc., please contact the Issue Manager at Elsevier Science B.V. Fax +31 20 485 2775; Tel. +31 20 485 3425. Postal address: P.O. Box 2759, 1000 BM Amsterdam, The Netherlands. Courier address: Sara Burgerhartstraat 25, 1055 KV Amsterdam, The Netherlands. Always quote 'BBA' and the article number.

Electronic publishing

Authors are required to submit electronic manuscripts. Typesetting from computer files has several advantages, not the least of which is the avoidance of re-keying errors in the article.

The following points should be taken into account in preparing electronic manuscripts:

1. Files produced by most commercial wordprocessing software packages (but preferably WordPerfect) can be used directly by the publisher. Save your files as usual on a floppy disk (the preferred storage medium is a 5.25- or a 3.5-inch disk in the MS-DOS (or compatible) system). Apple Macintosh or NEC is also suitable; if you use NEC, please submit your article on a double density or high density 5.25 inch disk or double density 3.5 inch disk (not a high density 3.5 inch disk). For other systems please contact the BBA Editorial Secretariat first. Please do not save your text as ASCII or similar: this will cause all special formatting codes to be lost.
2. Authors should not use (or allow their word processor to introduce) any hyphenation or word splits and they should not use a 'justified' layout.
3. Authors should ensure that the digit '1' and the letter 'l' (also the digit '0' (zero) and the capital letter 'O') have been used properly. The letter X and the 'times' sign, the apostrophe and the prime, and the hyphen and dash (for minus, etc.) represent further sources of confusion.
4. If the word processor or printer has any special characters, e.g., ä, $\hbar$, ê, Ø, Greek letters and mathematical symbols, they should be used consistently throughout the text.
5. Non-reproducible characters should not be left as blank spaces in the file, but should be replaced by characters or codes not used elsewhere, and should be used consistently, e.g., sigma, cap for Σ, and sigma, l.c. for σ. A list of such characters (codes) and a lexicon of what they actually represent should be added as a separate file on the disk.
6. All instructions given on style and arrangement of Regular papers should also be followed when preparing electronic manuscripts. This is especially important for the References section. Consistency in all operations is of vital importance in the preparation of articles. Facilities for 'automatic' numbering of references and footnotes must not be used.
7. In any case of doubt, authors are welcome to contact the publisher before keying in an article.

The following points should be taken into account in submitting electronic manuscripts:

1. The file must contain the final corrected version of the article and must match exactly the accompanying hard-copy printout – the final (revised) manuscript.
2. The output from specific desk-top publishing (DTP) equipment includes a considerable amount of coding which will interfere with normal file processing. Such DTP output should therefore be avoided.
3. **Four copies are required of the hard-copy printout.**
4. Figures and tables are also handled electronically.
5. The disk should be labelled with:
– the name of the author who will receive the proofs
– the manuscript reference number (when known)

– the soft- and hardware used
– the names of the files.
6. **The disk and the four copies of the hard-copy printout should be accompanied by a submission letter (see above).**
7. **Any revised version of a manuscript should be accompanied by a new set of figures and a disk containing the final revised version of the paper.**

BBA's publications

BBA publishes English-language papers only. Papers may be written in either American or British English, provided that the preferred spelling is used consistently throughout.

Many readers of the journal are not native speakers of English. It is therefore important to write succinctly and clearly, using short, simple sentences and avoiding long adjectival phrases and laboratory jargon. The following types of paper are published:

Regular papers

A Regular paper is the normal medium of publication. Although there is no fixed length, Regular papers should be as concise as possible, while providing sufficient information for the work to be repeated and for the claims of the authors to be judged by the readers.

Rapid reports

Rapid reports should meet the following conditions:
(1) encompass a complete piece of work of special significance and timeliness;
(2) be concise and not normally exceeding 4 printed pages (i.e., up to 12 pages of double spaced typescript, including tables and figures up to a total number of 4);
(3) comprise no separate sections, except for a summary and the reference list.

Authors should note that:
(a) Submission of a rapid report should be accompanied by a letter briefly describing why the author believes his paper to be deserving of rapid publication. Failure to provide this information can lead to delays in the manuscript handling.
(b) Proofs are not normally sent unless specifically requested. In this case a fax number must be given to enable turnaround of corrected proofs in 48 h.
(c) Rapid reports will be added to the beginning of issues currently in production.
(d) An accepted Rapid report will generally be published within 8 weeks of the date of receipt at the Publisher's office, depending on issue scheduling.

Short sequence / Promoter papers

These are published in the 'Gene Structure and Expression' section, and conform in style and format to BBA Rapid reports. Short sequence-papers should include a comparison of related sequences, a description of salient features of the sequence and significant data on expression of the genes described. Papers presenting sequences presumably coding for a protein must be accompanied by sufficient evidence, e.g., expression data, that the gene indeed codes for such a protein. If the paper only confirms in one organism what is already known for several other species, it will not be considered eligible for publication in BBA.

Promoter papers include data on promoter or enhancer sequences or other regulatory regions required for gene expression. In addition to the sequence itself, these papers should include novel information on the transcription start site and functional studies, e.g., using reporter genes. Such studies could entail a deletion analysis or otherwise establish functional regions in the promoter that act either positively or negatively. In addition, information on the recognition of these functional regions by transcription factors could be included, e.g., using band shifts or footprints.

Manuscripts should be marked 'Short Sequence/Promoter paper' and the accompanying submission letter should state explicitly that a Short sequence/Promoter paper is being submitted. They are handled as Rapid reports, but must be submitted to the Amsterdam address.

Sequences should be deposited in one of the usual data banks **before** submission. Accession numbers should be mentioned in the submission letter and in a footnote to the Short sequence/Promoter paper. If an author does not want merely to refer to a sequence by its accession number, the sequence should be presented as a figure.

Reviews

BBA reviews are published in the independent sections Reviews on Cancer and Reviews on Biomembranes, and in all other sections of the journal. They are contributed by scientists who are leading specialists in their field of expertise, normally at the invitation of the Executive Editors. Authors wishing to contribute a review paper are advised first to contact one of the responsible Executive Editors (listed in the issues of BBA) to avoid overlap with Reviews already commissioned.

Preparation of papers

Authors should consult a recent issue of the journal to make themselves familiar with the conventions and layout of articles.

The entire text, including figure and table legends and the reference list, should be typed (or printed out) with double or triple spacing on one side of the paper, leaving a left margin of approx. 3 cm. All pages should be numbered consecutively, starting with the title page of the manuscript. Every new paragraph should be clearly indented. Handwritten characters should be clearly defined in the margin. Expressions of Latin origin, for example, in vivo, in vitro, et al., per se, should be typed in normal typeface. They should be neither italicized nor underlined.

Equations should be numbered in the right margin as follows:

$$A + B \rightarrow C + D \qquad (1)$$

Title page

The title should be concise, descriptive and informative. The names of the authors should be followed by their addresses and indicated by corresponding letters. Changes in address should be indicated by footnotes. The author(s) to whom correspondence and proofs should be sent should be indicated, giving a full address (including fax number and e-mail address).

Authors are requested to select a maximum of six key words and to present them on the title page of the typescript. These key words will be used in the compilation of the annual cumulative index. They should cover precisely the contents of the submitted paper and should give readers sufficient information as to the relevance of the paper to his/her particular field.

Summary

The second page of the typescript should be reserved for the Summary. This should be self-explanatory and intelligible without reference to the body of the paper.

A Regular paper should have a Summary of 100–200 words; Rapid reports and Short sequence-papers should have summaries of approximately 50 words.

Since summaries are increasingly used by abstracting services which will cut off after a fixed number of words, it is important not to exceed the maximum number of words and to avoid bibliographic references and non-standard abbreviations.

Regular papers

After the Summary, Regular papers are usually divided into the sections Introduction, Materials and methods, Results, Discussion and Acknowledgements.

Introduction

This is a short section in which the authors should state the reasons for performing the work, with brief reference to relevant previous work.

Materials and methods, Results, Discussion

The section Materials and methods should be detailed enough for readers to reproduce the experiments. Authors should always refer to other work on the same subject, indicating whether or not their experimental results are in agreement with previous work. Conclusions drawn from experiments described in the tables or figures can often appear most conveniently in the Results section. The overall conclusions based on the work reported should be given in the Discussion. In shorter papers the Results and Discussion sections may be combined.

Acknowledgements

Acknowledgements should be presented at the end of the main text in a separate section.

Rapid reports, Short sequence- and Promoter papers

These types of paper are not divided into sections after the summary, except for the reference list. The first paragraph serves as an introduction; acknowledgements are added as a final paragraph before the reference list.

References and citations

The numerical system of references should be used. References in the text should be cited by numbers in square brackets in the order of their citation.

References are listed together in their order of appearance in a separate section at the end of the text under the heading References. All references should be numbered consecutively. References to journals should contain initials and names of all authors, article title, abbreviation of the name of the journal according to the *List of Serial Title Word Abbreviations* (International Serials Data System, 20, rue Bachaumont, 75002 Paris, France. ISBN 2-904938-02-8), volume number, year of publication (between brackets), and page numbers. References to books should also include the title (of series and volumes), initials and names of the editor(s), the publisher and place of publication.

Examples

[1] M. Wikström, J.E. Morgan, M.I. Verkhovshy, Proton and electrical charge translocation by cytochrome-*c* oxidase, Biochim. Biophys. Acta 1318 (1997) 299–306.

[2] E.C. Slater, Biochimica et Biophysica Acta: The Story of a Biochemical Journal, Elsevier Science Publishers, Amsterdam, 1986.

[3] D.E. Vance, Glycerolipid biosynthesis in eukaryotes, in: D.E. Vance, J.E. Vance (Eds.), New Comprehensive Biochemistry, vol. 31, Biochemistry of Lipids, Lipoproteins and Membranes, Elsevier Science B.V., Amsterdam, 1996, pp. 153–181.

Reference to a paper as 'in press' implies that it has been accepted for publication. Evidence (e.g., a photocopy of the note of acceptance from the journal concerned) should accompany the submitted typescript. Papers that are 'in press' should be included as a number in the text. Other papers submitted before or simultaneously with the paper in question should be included as a number in the text and in the References section, stating the name of the journal. Copies of papers that are submitted elsewhere should be provided for inspection by the Editors. Omission of this information will delay publication and may lead to redating of a submitted manuscript. Papers presented at scientific meetings that are not available in published form should not be cited as references in the References section.

Unpublished results should not be listed in the References section. In the text they are mentioned as follows: '(M.V. Tervoort and J. Glimcher, unpublished data)'. When unpublished results are cited, the data should be provided for the Editors' information when essential for proper evaluation, or if requested.

A personal communication should be mentioned in the text as follows: '(M.V. Tervoort, personal communication)'. Authors should not make unauthorized use of personal communications. Personal communications are not to be included in the References section.

Tables

Tables should be used sparingly; they should be used only when the data cannot be presented clearly in the text. Authors are requested to consult recent issues of BBA for the proper table layout.

Each table, including its legend, should be typed on a separate page. The heading of the table should make its general meaning understandable without reference to the text.

Figures and illustrations

Figures should be used to illustrate experimental results clearly. As figures are often reduced to a one-column width, authors should bear in mind the size of BBA's printed page and they should ensure that symbols, lettering and lines are sufficiently large and clear to be legible after reduction. (Column width is 8.4 cm, preferred figure size is approximately double this).

Legends should be collated and typed with double or triple spacing on a separate sheet. A legend should consist of an opening sentence constituting a brief title (without extra capitalization), followed by a brief description of the figure.

All figures should be in a form suitable for reproduction, e.g., drawn in black, on waterproof drawing or tracing paper, or as sharp, glossy prints. Each figure should bear the figure number, the name of the corresponding author and the (shortened) title of the paper on the reverse side. Figures should never be folded and they should never be mounted on heavy card. Continuous or half-tone figures should have their labelling supplied as an overlay, or be supplied in duplicate.

The size of symbols in relation to lettering should be chosen carefully.

Photographs of gels, micrographs, etc., should be glossy and as rich in contrast as possible. For photographs of electrophoretic patterns and electron micrographs four high-quality prints must be provided. If the content of a photograph is likely to suffer as a result of reduction, it should be provided in a size that will fit within BBA's format without reduction (preferred size is 8.4 cm $\times$ 11 cm). In the case of electron micrographs, unit length must be indicated on the figure by a labelled bar.

When essential to the understanding of a paper, figures may be reproduced in colour, at the author's own expense. The price of a single printed full-colour page is Dfl. 750.00, exclusive of sales tax. Two, three or four full-colour pages in combination will cost Dfl. 500.00 per additional page excluding sales tax. Authors should take into consideration that colour illustrations reproduced from a slide provide a better-quality, clearer result than those reproduced from a photograph.

ELSEVIER

Biochimica et Biophysica Acta 1330 (1997) 1–7

BIOCHIMICA ET BIOPHYSICA ACTA
BBA

Inhibition of annexin V-dependent Ca^{2+} movement in large unilamellar vesicles by K201, a new 1,4-benzothiazepine derivative

Noboru Kaneko [a,*], Ryuko Matsuda [b], Masashi Toda [b], Ken Shimamoto [a]

[a] *Department of Cardiology, The Heart Institute of Japan, Tokyo Women's Medical College, 8-1 Kawada-cho, Shinjuku-ku, Tokyo 162, Japan*

[b] *Department of Anatomy, Tokyo Women's Medical College, 8-1 Kawada-cho, Shinjuku-ku, Tokyo 162, Japan*

Received 20 January 1997; revised 20 May 1997; accepted 26 May 1997

Abstract

Examination was made of the effect of annexin V on Ca^{2+} movement into large unilamellar vesicles (LUV) using fura-2, a calcium-sensitive fluorescent dye. To avoid the possible difficulties relating to the addition of annexin V and/or Ca^{2+} in fura-2-loaded LUV, the burst method was used. LUV, preincubated with rat annexin V in the presence of Ca^{2+}, were collected by centrifugation and resuspended, and then burst with Triton X-100 in the presence of fura-2. Inward Ca^{2+} movement across the artificial lipid membrane was measured by determination of fura-2 fluorescence due to the leaked Ca^{2+} from ruptured LUV. The observed Ca^{2+} signal increased dependent on annexin V and Ca^{2+} concentrations, whereas bovine serum albumin did not affect this signal up to 1 μM. Thus, annexin V shows Ca^{2+} channel activity in LUV. K201, a novel 1,4-benzothiazepine, inhibited inward Ca^{2+} movement into LUV caused by annexin V in a dose-dependent manner. In the presence of 50 nM annexin V and 400 μM Ca^{2+}, 3 μM K201 showed significant inhibition of Ca^{2+} movement due to annexin V, and 50% inhibition was achieved at 25μM K201. On the other hand, diltiazem had no such effect even at 30 μM. K201 is thus shown to have inhibitory activity on inward Ca^{2+} movement due to annexin V in artificial vesicles and may prove useful as a probe for elucidating the functions of annexin V in vivo. © 1997 Elsevier Science B.V.

Keywords: K201; Annexin V; Ca^{2+} movement; Large unilamellar vesicle; Fura-2

1. Introduction

Annexin V is a member of the annexin family which binds to phospholipid and actin, in a Ca^{2+}-dependent manner [1,2]. This protein has been suggested to have such actions as anticoagulant activity [3], anti-inflammatory activity [4] and inhibition of protein kinase C [5] in vitro.

Annexin V has been found to express calcium channel activity by the patch clamp method [6], and its molecular structure as an ion channel model has been proposed based on the crystal structure [7]. The biological roles of annexin V have yet to be fully determined in vivo, but if a low molecular weight compound that binds to annexin V and inhibits its function can be made available, considerable clarification in this regard should be possible.

A novel 1,4-benzothiazepine derivative, 4-[3-{1-(4-benzyl) piperidinyl} propionyl]-7-methoxy-2,3,4,5-tetrahydro-1,4-benzothiazepine, K201 (Fig. 1), has been found to have potential for preventing

* Corresponding author. Fax: +81-3-33560441.

0005-2736/97/$17.00 © 1997 Elsevier Science B.V. All rights reserved.
PII S0005-2736(97)00132-6

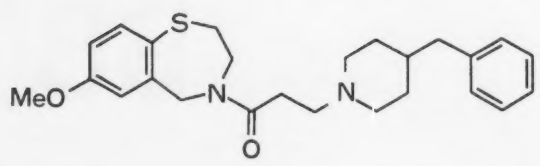

4-[3-[1-(4-benzyl)piperidinyl]propionyl]-7-methoxy-2,3,4,5-tetrahydro-1,4-benzothiazepine

Fig. 1. Chemical structure of K201.

cardiac cell damage due to calcium overload [8]. It was also found capable of protecting the myocardium from damage induced by six hour ischemia using a rat Langendorff model [9]. On the other hand, K201 exhibited an inhibitory effect on binding of cardiac annexin V with actin in a Ca^{2+}-dependent manner [8] and was demonstrated to bind to annexin V by X-ray crystallography (unpublished observation, submitted for publication).

In order to clarify the calcium ion channel activity of annexin V, the present study was conducted to examine the inhibitory effect of K201 on inward Ca^{2+} movement across large unilamellar vesicles (LUV) due to annexin V using fura-2 [10], a Ca^{2+}-dependent fluorescent agent. The effect of K201 was also compared with that of diltiazem [11], a 1,5-benzothiazepine derivative. For this purpose, the burst method was employed to measure the amount of influxed Ca^{2+} in the collected LUV after preincubation with annexin V and Ca^{2+}, to avoid possible difficulties such as LUV disintegration caused by annexin V and/or Ca^{2+}.

2. Materials and methods

2.1. Purification of annexin V

As in our previous study [12], annexin V was purified from the hearts of 50 mature male Wistar strain rats using a Sephacryl S-300 (Pharmacia, Uppsala, Sweden) column (3.3 × 55 cm), and then a DEAE Bio-Gel Agarose (Bio Rad Laboratories, Richmond, CA, USA) column (1.0 × 10 cm). Identification of annexin V was made by partial amino acid sequencing. Quantitative protein analysis was conducted according to the modified method of Lowry et al., using bovine serum albumin (BSA) as a standard protein [13].

2.2. Preparation of LUV

LUV were prepared by the procedure of Reeves and Dowben [14], with modification and by that of Berendes et al. [15]. Briefly, a solution of phosphatidylserine and phosphatidylethanolamine (w/w 9:1) dissolved in methanol/chloroform (v/v 1:2) to a total volume of 1115 μl was poured into a round bottom flask. Treatment of the mixture with a rotary evaporator (Tokyo-Rikakikai, type N-1N, Tokyo) led to the formation of a dehydrated film under N_2 gas. This film, comprised of lipids, was further dehydrated for 30 min by the evaporator under water-saturated nitrogen. After gently pouring 2 ml buffer A [180 μM EGTA, 162 mM sucrose, 10 mM HEPES, pH 7.4 (tetramethylammonium hydroxide; TMA)] into the flask, the lipid film was saturated with nitrogen gas and the flask was sealed with a rubber cap and left to stand at 37°C for 2 h to produce LUV. The multilamellar vesicles were removed by centrifugation. The LUV solution was centrifuged in a Beckman Avanti 30 compact centrifuge at 12 000 × g for 10 min at 4°C. To the sediment containing LUV, dilution buffer B [180 μM EGTA, 160 mM sucrose, 10 mM HEPES, pH 7.4 (TMA)] was added to adjust the total volume to 100 μl. This procedure was performed twice, and the suspension of LUV (200 μl) was used to perform at least twenty experiments. The total lipid concentration of liposomes was estimated as inorganic phosphate by phosphate analysis [16].

2.3. Burst method

The burst method was used to examine inward Ca^{2+} movement into LUV due to annexin V. To 442 μl dilution buffer B containing ca. 0–450 μM Ca^{2+}, a suspension containing LUV (8 μl) and annexin V ca. 0–100 nM (50 μl) were added, followed by preincubation at 26°C for 10 min. After adding 400 μM EGTA, the solution was centrifuged at 4°C for 10 min at 7000 × g to collect LUV. The collected LUV were suspended in buffer B solution (480 μl) containing 1 μM fura-2. After incubation in a cuvette

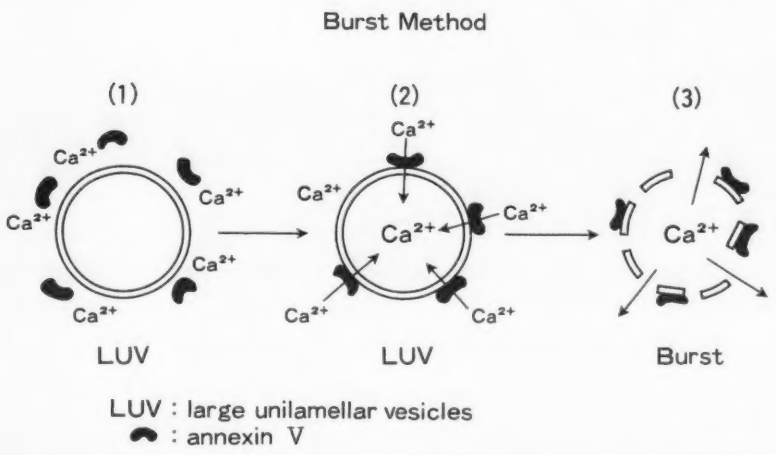

Fig. 2. Burst method: (1) LUV were added to buffer solution containing Ca^{2+} and then annexin V with or without reagent was added. Concentration of phospholipid in LUV suspension was 20 mM. The final amount of phospholipid used in each experiment was 0.125 μmol $cell^{-1}$. (2) Incubation was conducted at 26°C for 10 min. LUV were recollected by centrifugation following the addition of 400 μM EGTA. (3) Resuspended LUV were burst by addition of 0.2% Triton X-100 in 1 μM fura-2 solution.

at 37°C for 1 min, a burst was made with 0.2% Triton X-100 (10% w/w, 10 μl) (Fig. 2). The effect of BSA (ca. 0–1000 nM) on Ca^{2+} movement into LUV was also investigated.

To prove that there is no influence of K201 on the liposomes, Ca^{2+}-incorporated LUV were made. Ca^{2+}-incorporated LUV were prepared by addition of 400 μM Ca^{2+} in buffer A at the time of preparation of LUV. These were incubated with ca. $0–10^{-4}$ M K201 at 26°C for 10 min, and then recollected and burst as above.

The influence of K201 on the ability of annexin V to bind to liposomes in the presence of Ca^{2+} was estimated by measurement of the amount of annexin V binding to LUV incubated in various concentrations of K201. LUV (containing only buffer A) were incubated with 50 nM annexin V and ca. $0–10^{-4}$ M K201 in the presence of 400 μM Ca^{2+} at 26°C for 10 min. Recollected LUV were burst with 0.2% Triton X-100 and then the concentrations of annexin V were measured by ELISA, as previously reported [17].

Ca^{2+} concentration was measured by a JASCO CAF-110 fluorescence spectrophotometer (Nihon Bunkou, Tokyo, Japan). Data were obtained at excitation wavelengths of 340 and 380 nm and at an emission wavelength of 500 nm. K201 or diltizem at ca. 0.1–100 μM was first incubated with annexin V at 26°C for 30 min, and then these were added to the reaction buffer B solution containing LUV, and the effects of both drugs were examined.

2.4. Materials

Phosphatidylserine, phosphatidylethanolamine, BSA (fatty acid free) and TMA were obtained from Sigma (St. Louis, MO). HEPES and EGTA were from Nacarai Tesque (Kyoto), fura-2 from Dojin Laboratories (Kumamoto, Japan) and Triton X-100 from Millipore (San Francisco, CA). The reagents used were K201 (Japan Tobacco, Central Pharmaceutical Research Institute, Osaka, Japan) and diltiazem (Sigma), which were dissolved in distilled water for use in the experiments.

2.5. Statistics

Student's *t*-test was conducted for statistical analysis of the data; *P* values less than 0.05 were considered significant.

3. Results

The amino acid segment of annexin V purified from rat heart was shown to be YMTIS-GFQIEETIDR, corresponding to 213–227 of previously reported annexin V from human placenta [3]. Examination of the effects of K201 and diltiazem on

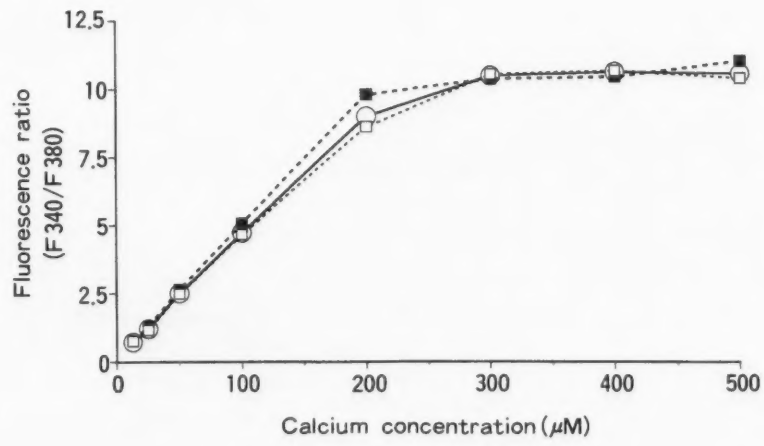

Fig. 3. Effects of K201 and diltiazem on fluorescence intensity in fura-2 solution. Composition of solution: 180 μM EGTA, 160 mM sucrose, 10 mM HEPES, 1 μM fura-2, pH 7.4 (TMA). Open circles: control. Open squares: 100 μM K201. Closed squares: 100 μM diltiazem. Both K201 and diltiazem had no effect on the fluorescence ratio.

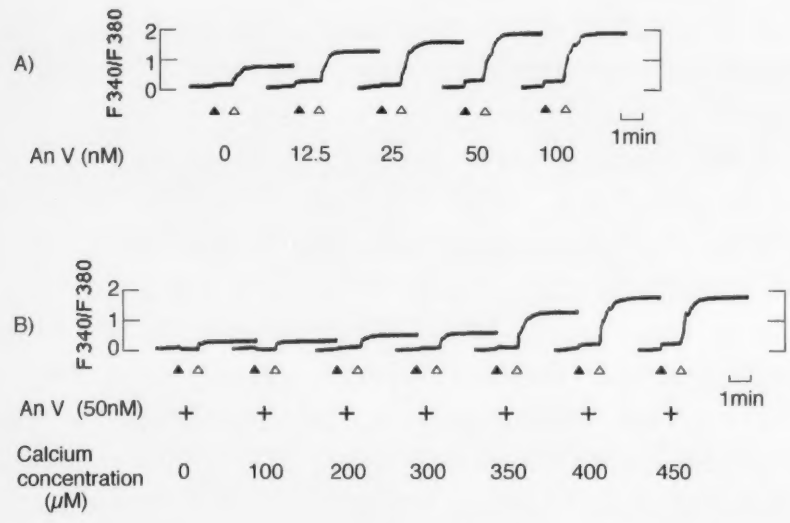

Fig. 4. (A) Effects of annexin V on fluorescence intensity. LUV were preincubated with annexin V (ca. 0–100 nM) in the presence of Ca^{2+} (400 μM). (B) Effects of calcium on fluorescence intensity. LUV were incubated with annexin V (50 nM) in the presence of Ca^{2+} (ca. 0–450 μM). Closed triangles: Time of resuspension of LUV. Open triangles: Time of addition of Triton X-100. An V: Annexin V

fura-2-calcium complex was made by addition of Ca^{2+} to buffer B solution containing 1 μM fura-2. The 340/380 fluorescence ratio indicated neither K201 nor diltiazem to have any effect (Fig. 3).

Fluorescence signals due to the leakage of trapped Ca^{2+} were recognized by the burst of LUV preincubated with annexin V in the presence of Ca^{2+}. The degree of fluorescence signal emission was dependent on annexin V concentration. When the annexin V concentration in the incubation solution increased, the fluorescence ratio increased dose dependently and reached the maximum at 50 nM in the presence of 400 μM Ca^{2+} (Fig. 4A). LUV, following preincubation with 50 nM annexin V, also showed an increase in fluorescence ratio with Ca^{2+} concentration. Fluorescence ratio reached a plateau at Ca^{2+} concentrations higher than 400 μM (Fig. 4B). BSA did not affect this fluorescence signal up to 1 μM in the presence of 400 μM Ca^{2+} (Fig. 5).

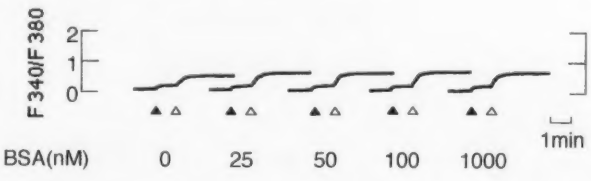

Fig. 5. Effects of BSA (ca. 0–1000 nM) on fluorescence intensity. LUV were incubated with BSA (ca. 0–1000 nM) in the presence of Ca^{2+} (400 μM). Closed triangles: Time of resuspension of LUV. Open triangles: Time of addition of Triton X-100.

The effect of K201 and diltiazem on inward Ca^{2+} movement into LUV was measured in the presence of 50 nM annexin V and 400 μM Ca^{2+}. K201 was shown to inhibit inward Ca^{2+} movement dose dependently (Fig. 6A). Under the same conditions (in the presence of 50 nM annexin V and 400 μM Ca^{2+}), K201 at 0.1 or 1 μM had no significant effect, but

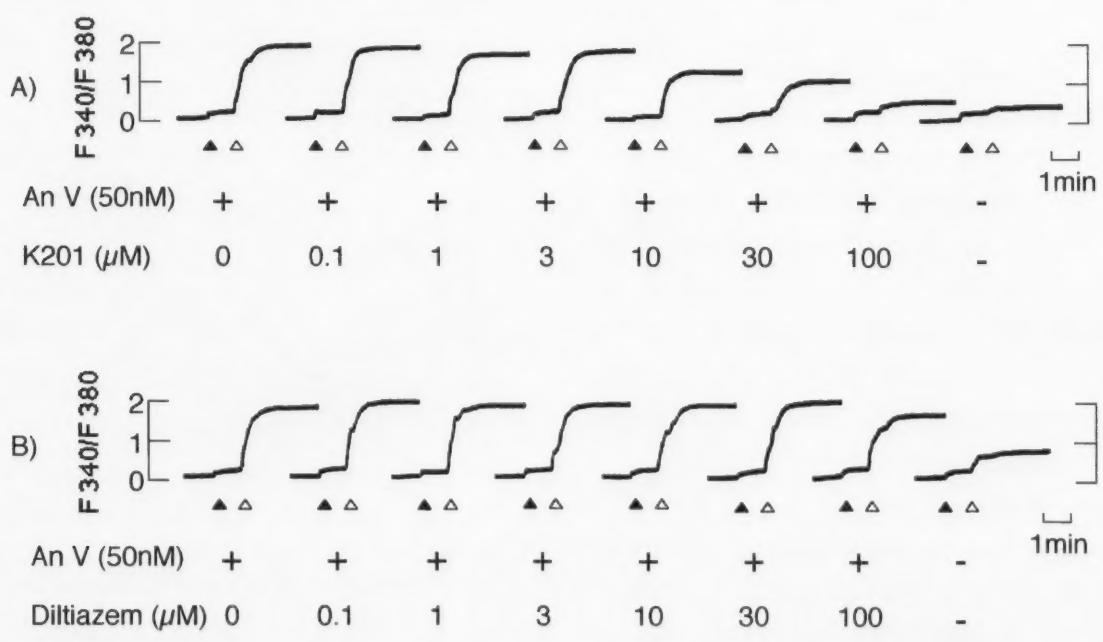

Fig. 6. (A) Effects of K201 on fluorescence intensity. (B) Effects of diltiazem on fluorescence intensity. LUV were incubated with annexin V (50 nM) and each reagent in the presence of Ca^{2+} (400 μM). Closed triangles: Time of resuspension of LUV. Open triangles: Time of addition of Triton X-100. An V: Annexin V.

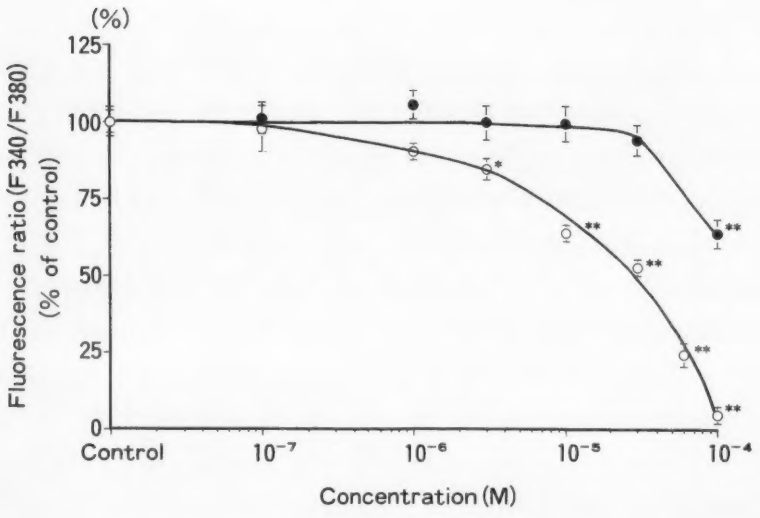

Fig. 7. Relationship between fluorescence intensity and concentrations of K201 and diltiazem. Open circles: K201, Closed circles: diltiazem. Horizontal bars show mean ± standard error. Each experimental group contained 4 or 5 cases ($n = 4$ or 5). $^{*}P < 0.05$, $^{**}P < 0.001$ (control vs. each group).

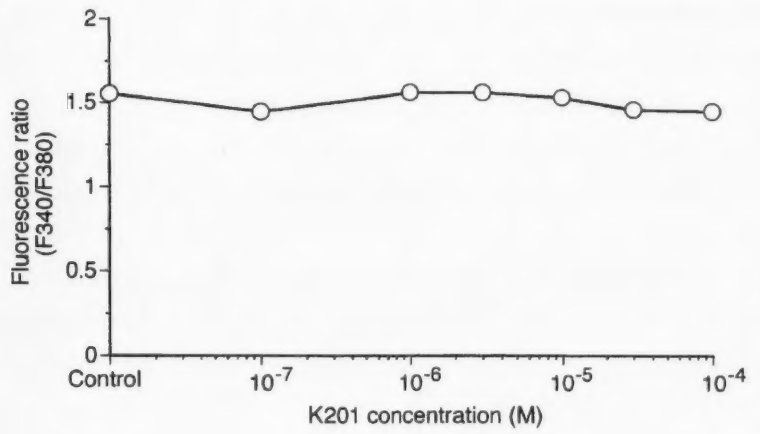

Fig. 8. Relationship between concentration of K201 and Ca^{2+} signal due to bursting of Ca^{2+}-incorporated LUV. Ca^{2+}-incorporated LUV were incubated with ca. $0–10^{-4}$ M K201 at 26°C for 10 min.

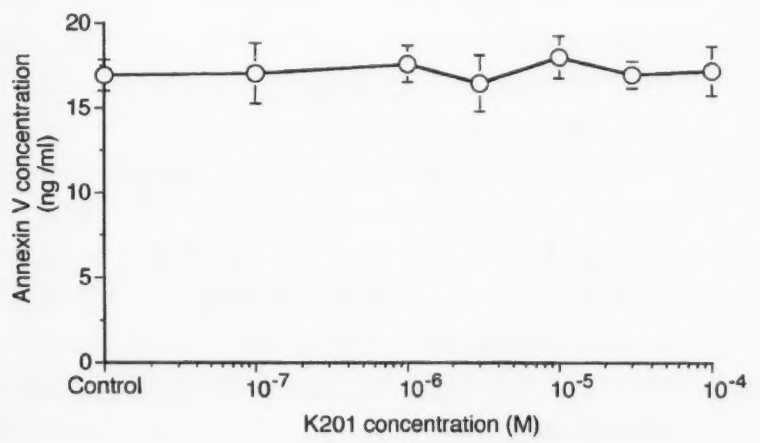

Fig. 9. Relationship between concentration of K201 and amount of annexin V binding to LUV. LUV were incubated with 50 nM annexin V and ca. $0–10^{-4}$ M K201 in the presence of 400 μM Ca^{2+} at 26°C for 10 min.

fluorescence ratio decreased significantly at 3 μM and higher (Fig. 7). The dose for 50% inhibition of inward Ca^{2+} movement was found to be 25 μM. Diltiazem did not show any effect at 30 μM, and showed an inhibitory effect only at very high concentrations (100 μM) (Fig. 6BFig. 7).

In the experiments using Ca^{2+}-incorporated LUV, no influence of K201 on the liposomes was recognized. Recollected Ca^{2+}-incorporated LUV incubated with $0–10^{-4}$ M K201 showed almost the same Ca^{2+} signal by burst method (Fig. 8). K201 also had no influence on the ability of annexin V to bind to liposomes. The amount of annexin V binding to LUV in the presence of Ca^{2+} did not change under the conditions of $0–10^{-4}$ M K201 (Fig. 9).

4. Discussion

In the annexin family, annexin I [18], II [19], V [6,7], VI [20,21], and VII [22] have been revealed to have voltage-dependent Ca^{2+} channel activity in vitro using patch clamp and dipping techniques. There have been some reports that suggest that annexin V has Ca^{2+} transport activity, using LUV and fura-2. Berendes et al. noted annexin V at 25 to 200 nM to exhibit calcium transport activity using fura-2-incorporated LUV, thereby promoting calcium influx in the presence of Ca^{2+} [15]. On the other hand, Goossens et al. could detect no Ca^{2+} channel activity even following the addition of 150 nM recombinant annexin V and native annexin V purified from human placenta to LUV in the presence of Ca^{2+} using fura-2-incorporated LUV, and concluded that annexin V in the presence of low concentrations of Ca^{2+} causes disruption of the lipid membrane with consequent leakage of fura-2, rather than inward Ca^{2+} transport [23]. Views on the functions of annexin V in experiments using fura-2-incorporated LUV are thus at variance.

Here, a study was conducted to determine whether rat native annexin V is capable of inducing inward Ca^{2+} movement across lipid membranes. Our preliminary study using fura-2-incorporated LUV indicated that annexin V induces an increase in the fluorescence ratio following centrifugation in the presence of a high concentration of Ca^{2+}. This result suggests

that a high concentration of Ca^{2+} makes LUV susceptible to disruption. However, addition of EGTA to the solution prevented this disruption by centrifugation. For the purpose of clarifying the effect of annexin V on inward Ca^{2+} movement into LUV, usage of fura-2-incorporated LUV as in the previous reports [15,23] would not be suitable, because it could not be determined whether an increase in fluorescence ratio in solution containing fura-2-incorporated LUV was due to an increase in inward Ca^{2+} movement into LUV or due to leakage of fura-2 from LUV. On the other hand, the burst method as shown in Fig. 2 reflects the Ca^{2+} content in LUV, which results from influx from the outside of LUV, so this method can avoid the artificial results described above.

Since Goossens et al. [23] reported that a very high concentration of Ca^{2+} (2.5 mM) and bovine serum albumin (5 g l^{-1} = about 80 μM) caused a significant increase in fluorescence with excitation and emission wavelengths of 340 and 500 nm using fura-2-loaded LUV, we measured the effect of BSA on inward Ca^{2+} movement into LUV by this burst method. BSA did not show any effect on fluorescence ratio up to 1 μM (Fig. 5). A high concentration of proteins such as BSA might cause nonspecific disturbance of LUV as described by Reeves and Dowben [14] and Goossens et al. [23]. Therefore, we used relatively low concentrations of annexin V (0 to 100 nM) and Ca^{2+} (0 to 450 μM) in this study to avoid nonspecific and/or artificial disturbance.

After disruption by Triton X-100, the fluorescence ratio of LUV solution was increased by annexin V and Ca^{2+} dose dependently as shown in Fig. 4. Maximum response was achieved at 50 nM annexin V in the presence of 400 μM Ca^{2+}, and at 400 μM Ca^{2+} in the presence of 50 nM annexin V. Thus, native rat annexin V induces Ca^{2+} movement into LUV and shows calcium influx activity in artificial phospholipid membrane in vitro.

Burger et al. [24] noted the X-ray crystal structure of annexin V to have features of channel-forming membrane protein. Recently, we found by protein X-crystallography that K201 binds with the central region of annexin V formed by domains II, III, and IV (unpublished observation: submitted for publication). K201, thus, shows not only ability to bind to annexin V but also inhibitory activity on annexin V-dependent inward Ca^{2+} movement into LUV in a dose-dependent manner (Fig. 7). K201 did not show effects to stabilize or destroy liposomes (Fig. 8) and there was no influence of K201 on the ability of annexin V to bind to liposomes (Fig. 9). Diltiazem, a 1,5-benzothiazepine, did not affect inward Ca^{2+} movement into LUV even at 30 μM and showed an inhibitory effect at 100 μM, and hardly bound to the same site in annexin V as K201 as shown by computer associated drug design method based on X-ray crystallography of annexin V (data not shown). Therefore, inhibition of diltiazem appears to be nonspecific, not being dependent on concentration.

Although K201 has been demonstrated to have a strong cardioprotective effect [8], the mechanisms of this action are unclear at the present time. Annexin V hardly associates with phosphatidylcholine and sphingomyelin, but it has a high affinity for the acidic phospholipids, such as phosphatidylserine [2]. Since phosphatidylserine is mainly located in the inner layer of the plasma membrane, annexin V, which is an intracellular protein, might reveal its function in the cytoplasmic site of cells under normal conditions. Recently, it has been reported that the translocation of phosphatidylserine from the inner side of the plasma membrane to the outer layer occurs in abnormal conditions, such as in the early stage of apoptosis and cell injury, and the annexin V binding site appeared in the outer membrane in these conditions [25–27]. On the other hand, we demonstrated that annexin V is displaced from its ordered distribution in the plasma membrane in the ischemic heart by immunohistochemical studies [12]. Furthermore, we also found that annexin V levels in plasma were substantially increased in patients with acute myocardial infarction [17]; that is, annexin V is released into the plasma in some forms of injury. These results suggest that intrinsic annexin V acts not only in the inner part of cells but also in the outer membrane in abnormal conditions. In this study, K201 inhibited the calcium channel activity of annexin V, and it acted as a cytoprotective agent in certain abnormal conditions and/or injuries, such as a myofibrillar overcontraction model of isolated rat heart [8], demonstrating myocardial preservation in the rat in vitro [9]. Although the role of annexin V channels in vivo is unclear at present, it is possible that annexin V causes deterioration of abnormal cellular functions

via accelerating inward Ca^{2+} current through its channel. In order to clarify this hypothesis, further studies, such as demonstrating the presence of annexin channels in apoptotic and injured cells, are necessary and K201 might be a good tool as an inhibitor of this channel.

Acknowledgements

We appreciate the proof reading and helpful suggestions of Dr. K. Iwata and Dr. M. Miyano.

References

[1] S.E. Moss, The Annexins. Portland Press Res. Monograph Ser. No. 2., Portland Press, London, 1992.
[2] P. Raynal, H.B. Pollard, Biochim. Biophys. Acta 1197 (1994) 63–93.
[3] A. Iwasaki, M. Suda, H. Nakao, T. Nagoya, Y. Saino, K. Arai, T. Mizoguchi, F. Sato, H. Yoshizaki, M. Hirata, T. Miyata, Y. Shidara, M. Murata, M. Maki, J. Biochem. 102 (1987) 1261–1273.
[4] N.G. Ahn, D.C. Teller, M.J. Bienkowski, B.A. McMullen, E.W. Lipkin, C. de Haën, J. Biol. Chem. 263 (1988) 18657–18663.
[5] D.D. Schlaepfer, J. Jones, H.T. Haigler, Biochemistry 31 (1992) 1886–1891.
[6] E. Rojas, H.B. Pollard, H.T. Haigler, C. Parra, A.L. Burns, J. Biol. Chem. 265 (1990) 21207–21215.
[7] R. Huber, R. Berendes, A. Burger, M. Schneider, A. Karshikov, H. Luecke, J. Römisch, E. Paques, J. Mol. Biol. 223 (1992) 683–704.
[8] N. Kaneko, Drug Dev. Res. 33 (1994) 429–438.
[9] M. Hachida, N. Kaneko, A. Ohkado, H. Hoshi, M. Nonoyama, S. Saitou, Y. Bonkohara, N. Hanayama, M. Miyagishima, H. Koyanagi, Transplant. Proc. 29 (1997) 1346–1348.
[10] G. Grynkiewicz, M. Poenie, R.Y. Tsien, J. Biol. Chem. 260 (1985) 3440–3450.
[11] T. Nagao, T. Ikeo, M. Sato, Jpn. J. Pharmacol. 27 (1977) 330–332.
[12] N. Kaneko, R. Matsuda, F. Chiwaki, S. Hosoda, Heart Vessels 9 (1994) 148–154.
[13] O.H. Lowry, N.J. Rosebrough, A.L. Farr, R.J. Randall, J. Biol. Chem. 193 (1951) 265–275.
[14] J.P. Reeves, R.M. Dowben, J. Cell. Physiol. 73 (1969) 49–60.
[15] R. Berendes, A. Burger, D. Voges, P. Demange, R. Huber, FEBS Lett. 317 (1993) 131–134.
[16] G.R. Bartlett, J. Biol. Chem. 234 (1959) 466–468.
[17] N. Kaneko, R. Matsuda, S. Hosoda, T. Kajita, Y. Ohta, Clin. Chim. Acta 251 (1996) 65–80.
[18] H.B. Pollard, H.R. Guy, N. Arispe, M. de la Fuente, G. Lee, E.M. Rojas, J.R. Pollard, M. Srivastava, Z.-Y. Zhang-Keck, N. Merezhinskaya, H. Caohuy, A.L. Burns, E. Rojas, Biophys. J. 62 (1992) 15–18.
[19] A. Burger, R. Berendes, S. Liemann, J. Benz, A. Hofmann, P. Göttig, R. Huber, V. Gerke, C. Thiel, J. Römisch, K. Weber, J. Mol. Biol. 257 (1996) 839–847.
[20] M. Díaz-Muñoz, S.L. Hamilton, M.A. Kaetzel, P. Hazarika, J.R. Dedman, J. Biol. Chem. 265 (1990) 15894–15899.
[21] J. Benz, A. Bergner, A. Hofmann, P. Demange, P. Göttig, S. Liemann, R. Huber, D. Voges, J. Mol. Biol. 260 (1996) 638–643.
[22] H.B. Pollard, E. Rojas, Proc. Natl. Acad. Sci. USA 85 (1988) 2974–2978.
[23] E.L.J. Goossens, C.P.M. Reutelingsperger, F.H.M. Jongsma, R. Kraayenhof, W.T. Hermens, FEBS Lett. 359 (1995) 155–158.
[24] A. Burger, D. Voges, P. Demange, C.R. Perez, R. Huber, R. Berendes, J. Mol. Biol. 237 (1994) 479–499.
[25] G. Koopman, C.P.M. Reutelingsperger, G.A.M. Kuijten, R.M.J. Keehnen, S.T. Pals, M.H.J. van Oers, Blood 84 (1994) 1415–1420.
[26] M.R. Bennett, D.F. Gibson, S.M. Schwartz, J.F. Tait, Circ. Res. 77 (1995) 1136–1142.
[27] M. Sugimura, R. Donato, V.V. Kakkar, M.F. Scully, Blood Coag. Fibrinol. 5 (1994) 365–373.

ELSEVIER

Biochimica et Biophysica Acta 1330 (1997) 8–16

BIOCHIMICA ET BIOPHYSICA ACTA
BBA

Mechanism of adenovirus improvement of cationic liposome-mediated gene transfer

Claire Meunier-Durmort [a], Renée Picart [b], Thierry Ragot [c], Michel Perricaudet [c], Bernard Hainque [d], Claude Forest [a,*]

[a] *Centre de Recherche sur l'Endocrinologie Moléculaire et le Développement, CNRS UPR 9078, 9 rue Jules Hetzel, 92190 Meudon, France*

[b] *INSERM U36, Collège de France, 11 place Marcelin Berthelot, 75231 Paris cedex 05, France*

[c] *CNRS URA 1301, Institut Gustave Roussy RP2, 39 rue Camille Desmoulins, 94805 Villejuif, France*

[d] *Laboratoire de Biochimie, Groupe Hospitalier Pitié-Salpétrière, 47 bd de l'hôpital, 75651 Paris cedex 13, France*

Received 3 April 1997; revised 21 May 1997; accepted 29 May 1997

Abstract

Substantial effort has been focused on the development of highly efficient gene transfer strategies. Although viral and non-viral methods have been elaborated, mechanisms of gene delivery are still poorly understood. We exploited our recent observation that replication-deficient type 5 adenovirus dramatically enhances lipofectAMINE-mediated gene transfer (lipoadenofection) in differentiated cells to elucidate the mechanism of adenovirus action in this process. Heat-induced denaturation of viral capsid abolishes adenovirus action whereas inactivation of viral genome by short treatment with UV has no effect. Electron microscopic observations reveal the formation of a complex containing adenovirus and lipofectAMINE which probably carries DNA into cells via endocytosis. Anti-adenovirus antiserum or monoclonal anti-$\alpha_v\beta_3$ integrin antibody inhibits lipoadenofection, at least partially. Neutralization of endosomal compartments with chloroquine, ammonium chloride or monensin does not prevent adenovirus improvement of gene transfer. Hence, adenovirus–lipofectAMINE–DNA complexes in which viral particles are each encompassed by three lipid layers, penetrate cells via an endocytic pathway involving probably the adenovirus receptor and $\alpha_v\beta_3$ integrin. The resulting efficient transfer and expression of plasmid DNA proceeds from a mechanism in which adenoviral endosomolytic activity appears to be required while viral genome is not essential. © 1997 Elsevier Science B.V.

Keywords: Cationic liposome; Adenovirus; Gene transfer; Adipocyte; Integrin; Endocytosis

1. Introduction

Gene transfer by non-viral methods remains a poorly efficient process, particularly in terminally differentiated cells. Two types of vectors have been widely employed. Soluble DNA-protein complexes utilize the targeting capacity of a ligand that is recognized by a specific receptor at the cell surface and is conjugated to poly-L-lysine to which plasmid DNA is associated [1,2]. Cationic liposomes or polyethylenimine (PEI) allow formation of a condensed structure in which positive charges of the vector interact with negatively-charged phosphate DNA [3–5]. At least in the case of lipid–DNA complexes, receptor-independent endocytosis has been demonstrated as being the major pathway of entry into cells [6,7]. The limiting

* Corresponding author. Fax: +33-1-45075890.

0005-2736/97/$17.00 © 1997 Elsevier Science B.V. All rights reserved.
PII S0005-2736(97)00133-8

step for efficient gene transfer using non-viral methods is the intra-endosomal DNA breakdown consecutive to fusion of endosomes to lysosomes [7]. With the aim of overcoming this degradation process, the idea has emerged that the endosomolytic property of adenovirus could be exploited.

In the past few years, we and others have developed approaches using the association of replication-deficient adenovirus and either naked plasmid DNA [8], poly-L-lysine–DNA conjugates [2,9–11], cationic liposomes [12–16] or PEI [17] in a covalent [10,11] or non-covalent [2,9,12–17] manner. Such associations actually dramatically enhance gene transfer efficiency in various cell types. Moreover, combination of adenovirus with either lipofectAMINE or PEI has been proved adequate for transfection of plasmid DNA in cultured adipocytes, muscle or hepatocytic cells, three highly differentiated cells almost impervious to efficient transfection by other means [12].

Mechanisms by which adenovirus improves non-viral-mediated gene transfer are poorly documented. It is known however that covalent coupling of adenovirus to poly-L-lysine–DNA conjugates induces formation of a complex which enters cells at least in part through adenovirus receptor-mediated endocytosis [18]. In this report, we have addressed the question of how non-covalent association of adenovirus to cationic liposome–DNA complexes permits a better lipofection efficiency in differentiated cells. We demonstrate that a complex between adenovirus, lipofectAMINE and plasmid DNA penetrates adipose cells via an endocytic process which probably involves the adenovirus receptor and a cellular integrin. We show also that neutralization of endosomal pH is not deleterious to gene transfer enhancement.

2. Materials and methods

2.1. Plasmid and cell culture

The plasmid pSV2-CAT (SV40 promoter fused to the chloramphenicol acetyltransferase (CAT) gene) was described elsewhere [19]. Plasmid was prepared by two successive equilibrium centrifugations in cesium chloride/ethidium bromide gradient. 3T3-F442A adipoblasts [20] were cultured in 60 mm dishes (Falcon) at 37°C in a humidified atmosphere of 10% CO_2/90% air. Cells were grown in Dulbecco's modified Eagle medium (DMEM) (Gibco BRL) containing 200 IU ml^{-1} penicillin, 50 mg l^{-1} streptomycin, 8 mg l^{-1} biotin, 4 mg l^{-1} pantothenate and 3.7 g l^{-1} bicarbonate and supplemented with 10% fetal calf serum. Adipose differentiation was achieved in the same medium supplemented with 0.02 μM insulin for 7 days. Medium was changed every other day.

2.2. Adenovirus propagation and treatment

The replication-deficient recombinant type 5 adeno-virus Ad-RSV-nlsLacZ (Rous sarcoma virus promoter driving the nlsLacZ gene) [21] was propagated in human embryonic kidney cell line 293 (ATCC collection) as previously described [22]. Adenovirus was purified by banding on two successive cesium chloride gradients, dialyzed against phosphate buffered saline containing 10% glycerol, and stored at −80°C. Viral titers were determined by plaque assay using 293 cells. For genome inactivation, adenovirus was exposed to 260 nm UV light source on ice at 4 cm from the lamp, for 1, 2 or 5 min. For alteration of capsid protein, virus was heated at 45°C for 10 min [23].

2.3. Gene transfer procedure

Plasmid DNA (5 μg) and 18.6 μl lipofectAMINE (Gibco BRL) were separately diluted into 50 μl of DMEM in polystyrene tubes, then gently mixed together (10 ± charge ratio). After 10 min, adenovirus (200 plaque forming units (pfu) $cell^{-1}$) was added or not to the lipid–DNA complex prior dilution in 2 ml of serum-free medium which was subsequently added to a 60 mm dish containing ca. 3×10^6 differentiated cells. 7 h later, medium was changed to 4 ml of DMEM containing 10% fetal calf serum. Cells were harvested 16 h later.

2.4. Adenovirus infection and CAT and β-galactosidase assays

Preparation of cell homogenates for CAT assays was performed as detailed elsewhere [12]. The method of Seed and Sheen [24] was used for determination of CAT activity. For measurement of adenovirus infec-

tivity, cells were incubated in 2 ml of culture medium containing 200 pfu cell^{-1} of native or UV light-treated adenovirus for 7 h. β-galactosidase was detected 16 h later either by determination of enzymatic activity as described previously [25] or by staining as follows. Cells were rinsed with phosphate buffered saline, fixed and stained with 5-bromo-4-chloro-3-indolyl-β-D-galactoside as described [26]. Blue nuclei corresponding to β-galactosidase expressing cells were counted under the microscope 8 h after staining.

2.5. Electron microscopy

Negatively stained material for gene transfer were observed by electron microscopy. Lipid–DNA complexes were achieved with 5 μg of pSV2-CAT and lipofectAMINE in a 1/10 positive charge ratio, then adenovirus was added (200 pfu cell^{-1}) or not. Transfection materials were adsorbed on colodion coated nickel grids, air dried, stained with 0.5% aqueous solution of phosphotungstate and visualised with a transmission electron microscope. Lipofection or lipoadenofection were carried out on 3T3-F442A adipocytes cultured in 35 mm dishes for 30 min, then fixed with 1% glutaraldehyde for 2 h at 4°C. Standard electron microscopy procedure was achieved as previously described [27]. Briefly, cells were post-fixed in 1% osmium tetroxide and dehydrated in graded series of ethanol. Embedded Eponate blocks were sectioned. Sections were stained with uranyl acetate and lead then examined with a transmission electron microscope.

2.6. Neutralization with antibodies

Adenovirus was treated with a polyclonal antiserum from rabbit which had been obtained after three intramuscular immunizations with adenovirus serotype 5 [28]. This antiserum contains neutralizing antibodies directed against proteins of the adenoviral capsid. This serum was used at a dilution of 1/100 for 30 min at 37°C prior addition to the lipid–DNA complex. Pre-immune serum was used under the same conditions as a control. To neutralize $\alpha_v\beta_3$ integrin, cells were treated with hamster anti-mouse monoclonal anti-β_3 IgG (25 μg ml^{-1}) (Pharmingen) in serum-free DMEM for 30 min before proceeding to lipoadenofection.

2.7. Cell treatment with weak bases and ionophores

Differentiated cells were incubated with either 100 μM chloroquine, 10 mM ammonium chloride or 5 μM monensin for 30 min. Then lipoadenofection was carried out in the presence of these agents. For controlling acidification of endosomes, 3T3-F442A adipocytes were pretreated with either 100 μM chloroquine, 10 mM ammonium chloride or 5 μM monensin for 30 min then 1 μM acridine orange was added for 30 min. Acridine orange accumulates in acidic compartments resulting in fluorescent red staining. Cells were immediately observed under microscope with a 546 nm filter.

3. Results and discussion

3.1. Adenovirus capsid but not viral genome is essential for lipoadenofection

Adenovirus binding to the plasma membrane, internalization and endosome-disruption activity are three crucial steps intervening in adenovirus infection [29,30]. Short treatment of adenovirus with UV has been reported to be without effect on adenovirus infectivity, suggesting that viral genome plays no obvious role in this process [31]. We wondered whether UV-treated adenovirus would be efficient for lipoadenofection. We used a complex of pSV2-CAT with lipofectAMINE in a 1/10 positive charge ratio for lipofection of 3T3-F442A adipocytes in the absence or in the presence of either native or UV-treated non-replicative type 5 adenovirus. As expected from our previous findings [12], the presence of adenovirus is highly beneficial to lipofection, with a 50-fold increase in CAT activity (Fig. 1). Lipoadenofection efficiency was entirely conserved at 1 min of treatment of adenovirus with a 260 nm UV light, reduced by about 30% at 2 min and by 60% at 5 min (Fig. 1). In contrast, a 1 min UV-treatment was sufficient to prevent adenovirus infection by 90%, as determined by Ad-RSV-nlsLacZ-mediated β-galactosidase expression (Fig. 1). Longer exposure to UV light totally inhibited infection. The deleterious effect of 1 min UV-treatment on adenovirus infectivity, together with the maintenance of maximal transfer of the plasmid indicated that integrity of the viral genome was not

required for lipoadenofection. This result was in accordance with previous observations showing that UV-treated adenovirus still supported delivery of either naked DNA [32] or transferrin–polylysine–DNA conjugates [31] into cultured cells, while its ability to replicate on 293 cells was obviated.

Next we exposed the adenovirus preparation to 45°C for 10 min. Such a treatment was reported to alter capsid proteins in such a way that a large decrease in adenovirus infectivity [29] and endosomolytic activity [23] was observed. This heat-inactivated adenovirus was used in lipoadenofection experiments. As shown in Fig. 1, CAT activity remained identical to that obtained with lipofectAMINE alone, showing that viral capsid was essential for the enhancement of liposome-mediated gene transfer by adenovirus. A similar dependence of unaltered adenoviral capsid proteins for gene transfer accomplished by the receptor-mediated transferrin–polylysine system has been described already [33].

3.2. DNA, liposomes and adenovirus form a complex that enter cells via the adenovirus-mediated endocytic process

We wondered whether adenovirus would associate with the lipofectAMINE–DNA complex to form a higher ordered complex that would penetrate cells via endocytosis. Electron microscopy observations showed that negatively stained lipofectAMINE–DNA complexes appeared as dense aggregates resembling those observed with other cationic lipids [3,7], although much larger as a consequence of using anionic (aggregating) phosphotungstate instead of uranyle acetate as contrasting agent (Fig. 2A). Adenovirus bound avidly to these condensed structures (Fig. 2B). 3T3-F442A cells were treated for 30 min with a suspension containing the resulting ternary complex, the fate of which was examined by electron microscopy. Condensed structures were found in the vicinity of the cell membrane and in endocytic vesicles holding several lipid-coated adenovirus particles (Fig. 2C–D). Adenovirus-free lipofectAMINE–DNA complexes were also found in endocytic vesicles (not shown) as expected from previous works [7,6]. Periodicity of the lamellar structures was of approximately 5.5–7 nm a size close to that reported using different cationic lipids [7,34], giving rise to multilamellar structures of 70–150 nm (Fig. 2E). In the course of lipoadenofection, each adenovirus particle with a core of 65 nm, was encompassed by 3 lipidic bilayers of identical sizes (3.5–5 nm) separated each by 3 nm and presenting an hexaedric conformation (Fig. 2F). The resulting highly ordered structure had a diameter of 110 nm. In such a structure, the plasmid DNA is likely to be condensed between the lipid bilayers [35].

We next wondered whether the route taken by adenovirus to penetrate cells was of importance for the lipoadenofection process. Adenovirus enters cells by endocytosis after binding to a still unidentified cellular receptor (see *Note* on p. 15) via penton fiber, a protein of the capsid, 37.6 nm in length [36–38]. Internalization requires intervention of $\alpha_v\beta_3$ and $\alpha_v\beta_5$ integrins thought to interact with the RGD sequence of penton base, another protein of the capsid [39–42]. Because of the size of the lipofectAMINE–DNA–adenoviral core complex (see above and Fig. 2F) we postulated that part (about 12 nm) of

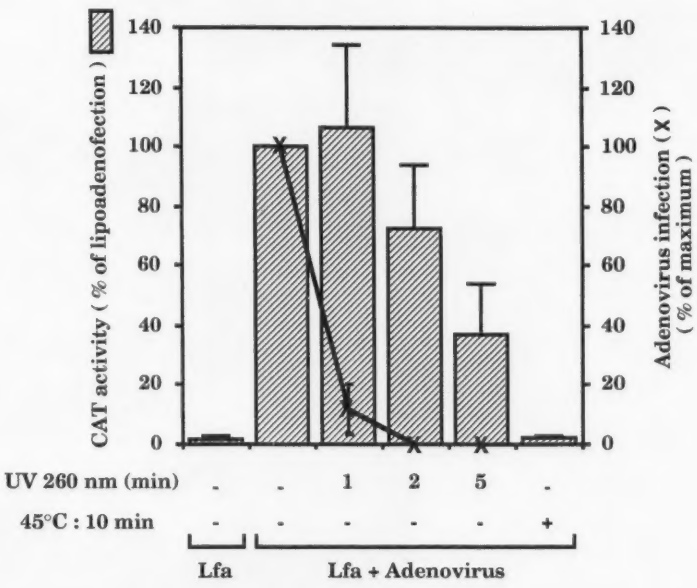

Fig. 1. Role of adenovirus capsid and viral genome for lipoadenofection efficiency. 3T3-F442A adipocytes were transfected for 7 h by lipofection (Lfa) or lipoadenofection (Lfa + adenovirus). Either native adenovirus (200 pfu cell^{-1}), or adenovirus treated with UV for 1, 2 or 5 min or with heat (45°C) for 10 min was used or not. After transfection, cells were incubated with serum-containing medium for 17 h before harvesting and determination of CAT activity. Values of CAT activity are expressed in percent of that obtained by lipoadenofection carried out with native adenovirus. Each value represents the mean ± SEM of data obtained from three independent experiments with duplicate dishes. 100% represents 231 ± 61 mU CAT mg protein^{-1}.

the penton fibre protruded out of the complex and remained able to interact with the adenovirus receptor (Fig. 3).

For blocking penton fiber, we used a polyclonal adenovirus antiserum previously obtained in immunization experiments [28]. We incubated adenovirus with either this antiserum or the pre-immune counterpart before mixing with the lipofectAMINE–DNA complex and proceeding to lipoadenofection of 3T3-F442A adipocytes. Results are presented in Fig. 4. As expected, adenovirus augmented lipofectAMINE-mediated gene transfer as quantified by CAT activity measurement. Adenovirus anti-serum prevented this increase by 80%, whereas pre-immune serum had no effect. Hence, we could speculate that lipofectAMINE–DNA–adenovirus ternary complex formation did not impair interaction of penton fiber to the adenovirus receptor. Therefore, in our transfection procedure like in those employing either naked DNA [32] or transferrin–polylysine–DNA conjugates [18], adenovirus appeared to use its own receptor for increasing gene transfer efficiency.

For neutralizing $\alpha_v\beta_3$ integrin, we incubated cells with a specific $\alpha_v\beta_3$ monoclonal antibody before lipoadenofection. As shown in Fig. 4, this treatment inhibited by about 40% the adenovirus-mediated increase in CAT activity. Such a partial neutralization was consistent with the potential involvement of a second receptor, the $\alpha_v\beta_5$ integrin, in adenovirus internalisation [41,43]. The mechanism by which the

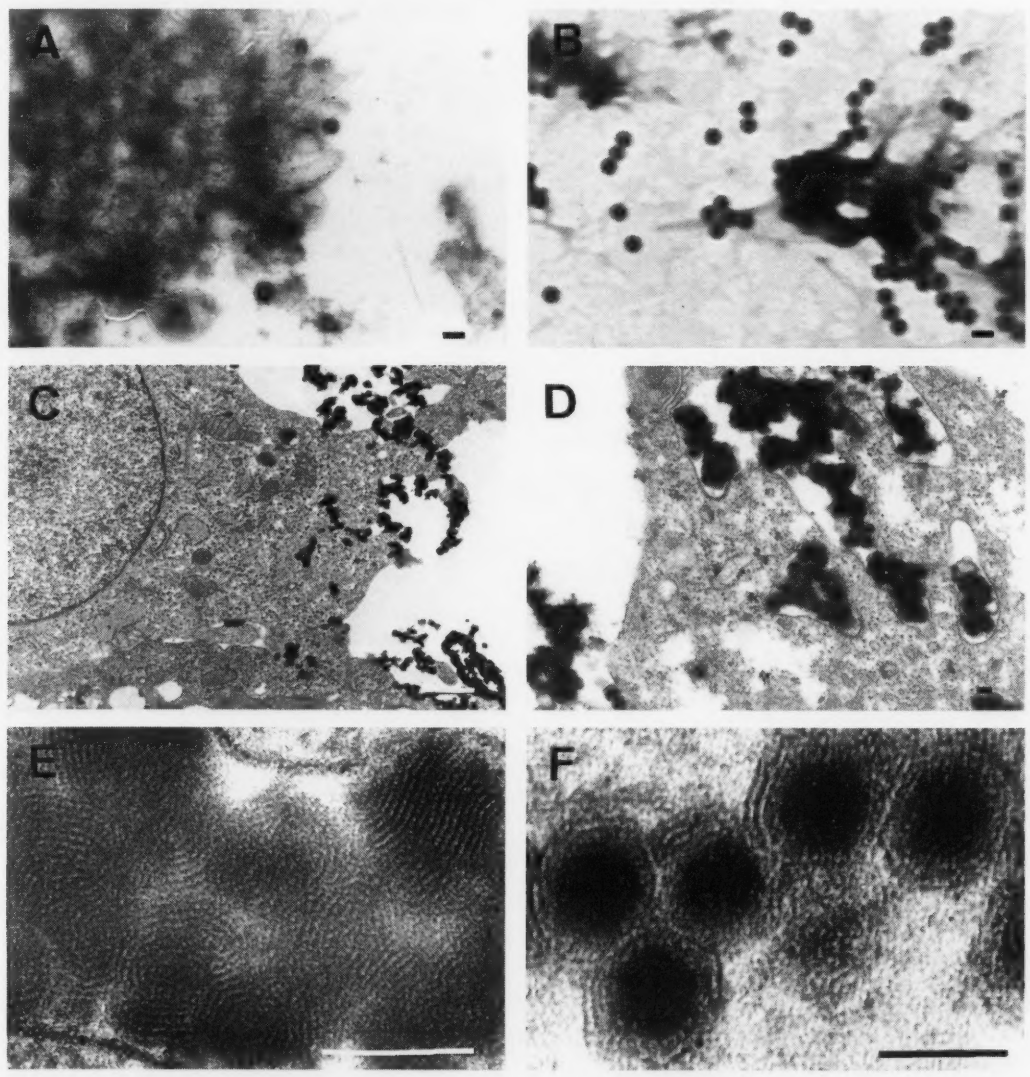

Fig. 2. Electron photomicrographs of gene transfer reagents and of 3T3-F442A adipocytes transfected by lipoadenofection. Lipid–DNA complex was prepared at a charge ratio of 10+ then adenovirus was added or not. These reagents were observed under electron microscope after negative stain or incubated with adipocytes for 30 min before electron microscopy. Negatively stained lipofectAMINE–DNA complex are presented without (panel A) or with adenovirus (panel B). Panels C and D show cells transfected by lipoadenofection, at different magnifications. Panels E and F show endosomes containing lipid–DNA complexes without (panel E) or with adenovirus (panel F). Panels A, B, D, E, F: bar represents 100 nm. Panel C: bar represents 1 μM.

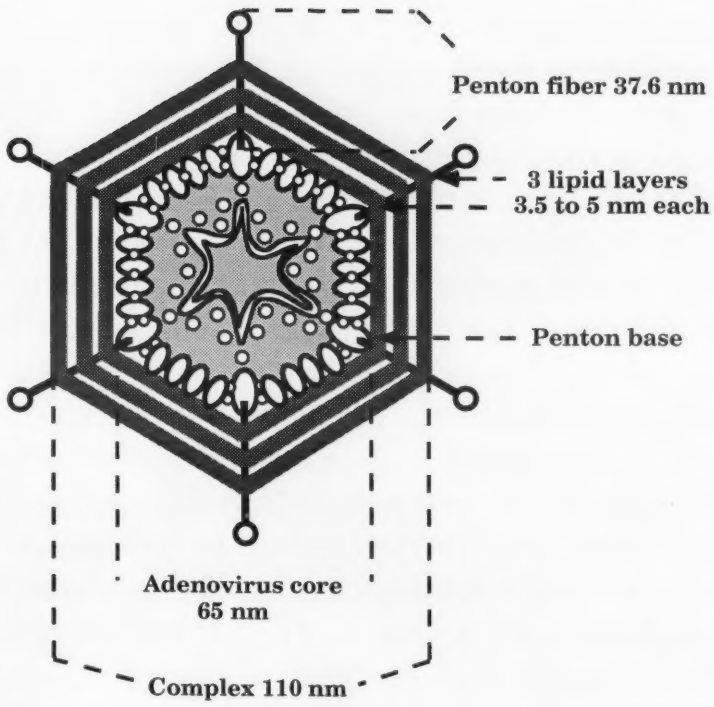

Fig. 3. Schematic representation of the lipofectAMINE–adenovirus complex. Figure drawn from electron microphotographs identical to that of Fig. 2F represents adenovirus encapsulated in 3 lipid bilayers.

RGD sequence of penton base interact with integrins for allowing lipoadenofection to proceed is presently unknown.

Hence, both adenovirus receptor and $\alpha_v\beta_3$ integrin appeared to play a role in the adenovirus-induced increase in lipofection. These results associated to the electron microscopic observations strongly suggested that lipofectAMINE–DNA–adenovirus ternary complexes penetrated cells via receptor-mediated endocytosis, leading to lipoadenofection.

3.3. Neutralization of endosomal pH does not affect lipoadenofection

We wondered whether both components of the vector system, i.e., adenovirus and lipofectAMINE were equally important for plasmid delivery from the endosomal compartment to the cytoplasm. One alternative to dissociate the respective roles of liposome and adenovirus was to neutralize the pH of intracellular compartment. We treated cells with either weak bases (chloroquine, ammonium chloride) or a ionophore (monensin), all agents known to be efficient for neutralizing pH of the intracellular compartments [44,45]. We controlled this neutralizing action by incubating cells for 30 min with these agents then 30 min with acridine orange, a fluorescent molecule able to specifically stain acidic intracellular compartments [46]. Indeed, fluorescent spots were strongly attenuated in cells incubated with the neutralizing agents when compared to those present in acridine orange-only treated cells (Fig. 5).

Cells were transfected by lipoadenofection in the presence or not of either chloroquine, ammonium chloride or monensin and CAT gene expression was measured. A 3.6-fold increase in CAT activity was obtained when chloroquine was used, whereas ammonium chloride or monensin had no effect (Table 1). In contrast, in lipofectAMINE only-transfected cells, reductions of 40%, 75% or 95% in gene transfer were obtained by treatments with respectively chloroquine, ammonium chloride or monensin (Table 1). One interpretation for these results could be that these reductions would be the consequence of a decrease in the endosomolytic potential of dioleoylphosphatidyl

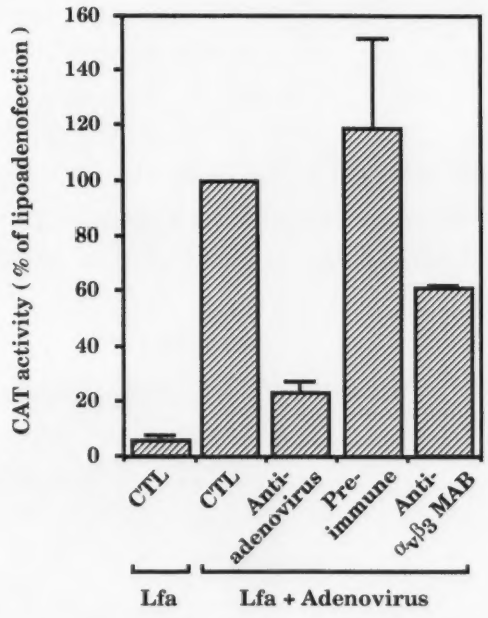

Fig. 4. Effect of anti-adenovirus and anti $\alpha_v\beta_3$ integrin antibodies on lipoadenofection efficiency. 3T3-F442A Adipocytes were transfected as described in the legend to Fig. 1 using either native or neutralized adenovirus (200 pfu cell^{-1}). Adenovirus was treated with either a polyclonal adenovirus antiserum from rabbit or the pre-immune counterpart for 30 min at 37°C. For $\alpha_v\beta_3$ integrin neutralization, adipocytes were pretreated with hamster anti-mouse monoclonal anti-β_3 IgG (Anti-avb3 MAB) for 30 min before proceeding to lipoadenofection. Cells were next incubated with serum-containing medium for 17 h before harvesting and determination of CAT activity. Values of CAT activity are expressed in percent of that achieved by lipoadenofection performed with native adenovirus. Each value represents the mean ± SEM of data obtained from three independent experiments with duplicate dishes. 100% represents 164 ± 57 mU CAT mg protein^{-1}. Lfa, lipofectAMINE; CTL, control.

Table 1
Effect of weak bases and ionophores on transgene expression

	Transgene expression (% of control)			
	Control	Chloroquine (100 μM)	Ammonium chloride (10 mM)	Monensin (5 μM)
Lipoadenofection	100	357 ± 43	108 ± 9	99 ± 32
Lipofection	100	64 ± 14	24 ± 10	4.4 ± 1.2
Infection	100	145 ± 17	99 ± 2	114 ± 18

3T3-F442A adipocytes were pretreated with either 100 μM chloroquine, 10 mM ammonium chloride or 5 μM monensin for 30 min, then lipoadenofection (LipofectAMINE 10+ associated with Ad-RSV-nlsLacZ, 200 pfu cell^{-1}), lipofection (LipofectAMINE 10+) or infection (Ad-RSV-nlsLacZ, 200 pfu cell^{-1}) were carried out for 7 h. 17 h later cells were harvested and CAT (lipofection, lipoadenofection) or β-galactosidase (infection) activities were determined. Values of transgene expression are expressed in percent of that of control cells. Each value represents the mean ± SEM of data obtained from three independent experiments with duplicate dishes. 100% CAT activity represents 227 ± 70 mU mg protein^{-1} and 11 ± 3 mU mg protein^{-1} for lipoadenofection and lipofection, respectively. 100% β-galactosidase activity represents 374 ± 36 mU μg^{-1} h^{-1} for adenovirus infection.

ethanolamine (DOPE) present in lipofectAMINE, when pH is raised to neutral as reported [47]. Interestingly, β-galactosidase activity from adenovirus-infected cells augmented 1.45-fold in the presence of chloroquine and was unaffected by ammonium chloride or monensin (Table 1). This result was at first glance unexpected considering the dogma that adenovirus-mediated disruption of membranes of endocytic vesicles required the acidic pH of endosomes [48,49]. However, validity of this dogma is still a matter of debate. Indeed, recent data indicate that weak base amines do not alter adenovirus uncoating [50] and our results are in agreement with this observation.

The beneficial effect of chloroquine on lipoadenofection efficiency cannot be attributed to the prevention of plasmid DNA degradation by lysosomal nucleases since ammonium chloride and monensin do not augment CAT activity (Table 1). Rather, chloroquine may act by binding DNA in endosomes thereby dissociating lipofectAMINE–DNA complex in a manner similar to that postulated for glycosylated polylysine–DNA complex [51]. Taken together, our results show that endosomotropic agent-linked modulations of gene expression follow a similar pattern after adenoviral infection or lipoadenofection and show opposite traits after lipofection. Hence, delivery of DNA to the cytoplasm during lipoadenofection is likely to be the result of adenovirus endosomolytic activity.

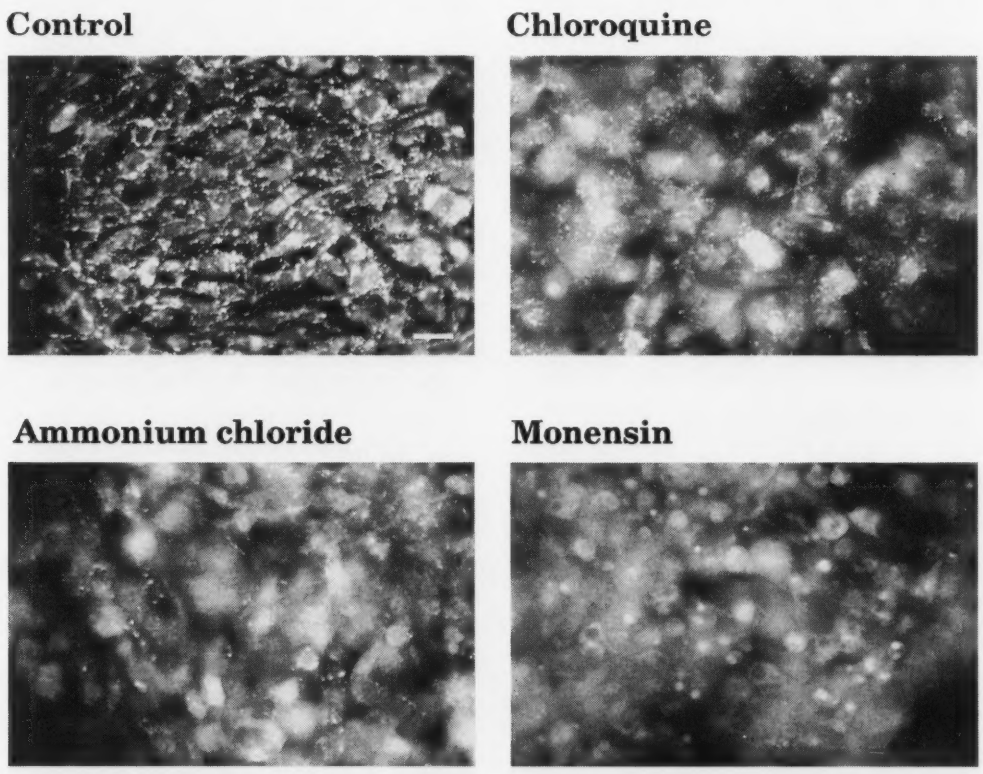

Fig. 5. Acridine orange stained adipocytes. 3T3-F442A adipocytes were incubated in serum-free medium (control: panel A) containing either 100 μM chloroquine (panel B), 10 mM ammonium chloride (panel C) or 5 μM monensin (panel D) for 30 min then 1 μM acridine orange was added for 30 min. Cells were immediately observed under fluorescent microscope with a 546 nm filter. Bar indicates 100 μm.

In conclusion, the association of adenovirus and lipofectAMINE permits the efficient transfer and expression of plasmid DNA in differentiated cells via a process which involves the adenovirus receptor and $\alpha_v\beta_3$ integrin for endocytosis of the ternary complex and in which viral genome is not essential whereas adenoviral endosomolytic activity seems to be required. Determining the structural conformation of the active complex and delineating the mechanism by which adenovirus enhances cationic liposome-mediated gene transfer are prerequisites towards the design of adequate synthetic vectors for gene therapy procedures.

Note added in proof

While this paper was under review, Hong et al. [52] reported that the conserved region of MHC class I $\alpha 2$ domain represents a high affinity receptor for adenovirus type 5 fiber knob.

Acknowledgements

We are grateful to Dr. Howard Green for providing us with the 3T3-F442A cell line. We thank Drs. Claude Tougard (Collège de France, Paris) and Christian Vannier (Ecole Normale Supérieure, Paris) for helpful discussions. C.M.-D. was recipient of a fellowship from the French Ministère de l'Education Nationale, de l'Enseignement Supérieur et de la Recherche (1993–1996). This work was supported by a grant from the Association Française contre les Myopathies to C.F.

References

[1] G.Y. Wu, C.H. Wu, J. Biol. Chem. 262 (1987) 4429–4432.
[2] E. Wagner, M. Zenke, M. Cotten, H. Beug, M.L. Birnstiel, Proc. Natl. Acad. Sci. USA 87 (1990) 3410–3414.
[3] H. Gershon, R. Ghirlando, S.B. Guttman, A. Minsky, Biochemistry 32 (1993) 7143–7151.
[4] J.P. Behr, B. Demeneix, J.P. Loeffler, J. Perez-Mutul, Proc. Natl. Acad. Sci. USA 86 (1989) 6982–6986.
[5] O. Boussif, F. Lezoualc'h, M.A. Zanta, M.D. Mergny, D. Scherman, B. Demeneix, J.P. Behr, Proc. Natl. Acad. Sci. USA 92 (1995) 7297–7301.
[6] D.S. Friend, D. Papahadjopoulos, R.J. Debs, Biochim. Biophys. Acta 1278 (1996) 41–50.
[7] J. Zabner, A.J. Fasbender, T. Moninger, K.A. Poellinger, M.J. Welsh, J. Biol. Chem. 270 (1995) 18997–19007.
[8] K. Yoshimura, M.A. Rosenfeld, P. Seth, R.G. Crystal, J. Biol. Chem. 268 (1993) 2300–2303.
[9] R.J. Cristiano, L.C. Smith, S.L.C. Woo, Proc. Natl. Acad. Sci. USA 90 (1993) 2122–2126.
[10] E. Wagner, K. Zatloukal, M. Cotten, H. Kirlappos, K. Mechtler, D.T. Curiel, M.L. Birnstiel, Proc. Natl. Acad. Sci. USA 89 (1992) 6099–6103.
[11] G.Y. Wu, P.L. Zhan, L.L. Sze, A.R. Rosenberg, C.H. Wu, J. Biol. Chem. 269 (1994) 11542–11546.
[12] C. Meunier-Durmort, N. Ferry, B. Hainque, J. Delattre, C. Forest, Eur. J. Biochem. 237 (1996) 660–667.
[13] R. Raja-Walia, J. Webber, J. Naftilan, G.D. Chapman, A.J. Naftilan, Gene Ther. 2 (1995) 521–530.
[14] J. Kreuzer, S. Denger, F. Reifers, C. Beisel, K. Haack, J. Gebert, W. Kübler, Atherosclerosis 124 (1996) 49–60.
[15] M. Honda, P.C. Hu, C.H. Huang, H. Matsui, S.M. Lemon, J. Virol. Meth. 58 (1996) 41–58.
[16] P. Seth, U. Brinkmann, G.N. Schwartz, D. Katayose, R. Gress, I. Pastan, K. Cowan, Cancer Res. 56 (1996) 1346–1351.
[17] C. Meunier-Durmort, H. Grimal, L. Sachs, B. Demeneix, C. Forest, Gene Ther. (1997) in press.
[18] S.I. Michael, C.H. Huang, M.U. Romer, E. Wagner, P.C. Hu, D.T. Curiel, J. Biol. Chem. 268 (1993) 6866–6869.
[19] C.M. Gorman, L.F. Moffat, B.H. Howard, Mol. Cell. Biol. 2 (1982) 1044–1051.
[20] H. Green, O. Kehinde, Cell 7 (1976) 105–113.
[21] L.D. Stratford-Perricaudet, I. Makeh, M. Perricaudet, P. Briand, J. Clin. Invest. 90 (1992) 626–630.
[22] F.L. Graham, L. Prevec, Meth. Molec. Biol. (1991) 109–128.
[23] C. Defer, M.T. Belin, M.L. Caillet-Boudin, P. Boulanger, J. Virol. 64 (1990) 3661–3673.
[24] B. Seed, J.Y. Sheen, Gene 67 (1988) 271–277.
[25] P. Herbomel, B. Bourachot, M. Yaniv, Cell 39 (1984) 653–662.
[26] N. Ferry, O. Duplessis, D. Houssin, O. Danos, J.M. Heard, Proc. Natl. Acad. Sci. USA 88 (1991) 8377–8381.
[27] B.R. Brinkley, P. Murphy, C. Richardson, J. Cell Biol. 35 (1967) 279–283.
[28] T. Ragot, M. Eloit, M. Perricaudet, In: O. Cohen-Haguenauer, M. Boiton (Eds.), Human Gene Transfer, Editions INSERM, Paris, 1991, pp. 249–260.
[29] D.T. Brown, B.T. Burlingham, J. Virol. 12 (1973) 386–396.
[30] Y. Chardonnet, S. Dales, Virology 40 (1970) 462–477.
[31] M. Cotten, E. Wagner, K. Zatloukal, S. Phillips, D.T. Curiel, M.L. Birnstiel, Proc. Natl. Acad. Sci. USA 89 (1992) 6094–6098.
[32] P. Seth, M. Rosenfeld, J. Higginbotham, R.G. Crystal, J. Virol. 68 (1994) 933–940.
[33] D.T. Curiel, S. Agarwal, E. Wagner, M. Cotten, Proc. Natl. Acad. Sci. USA 88 (1991) 8850–8854.

[34] B. Sternberg, F.L. Sorgi, L. Huang, FEBS Lett. 356 (1994) 361–366.
[35] J.O. Rädler, I. Koltover, T. Salditt, C.R. Safinya, Science 275 (1997) 810–814.
[36] C.E.G. Wohlfart, U.K. Svensson, E. Everitt, J. Virol. 56 (1985) 896–903.
[37] C. Devaux, M. Adrian, C. Berthet-Colominas, S. Cusack, B. Jacrot, J. Mol. Biol. 215 (1990) 567–588.
[38] R.W.H. Ruigrok, A. Barge, C. Albiges-Rizo, S. Dayan, J. Mol. Biol. 215 (1990) 589–596.
[39] T.J. Wickham, P. Mathias, D.A. Cheresh, G.R. Nemerow, Cell 73 (1993) 309–319.
[40] M. Bai, B. Harfe, P. Freimuth, J. Virol. 67 (1993) 5198–5205.
[41] P. Mathias, T. Wickham, M. Moore, G. Nemerow, J. Virol. 68 (1994) 6811–6814.
[42] P.L. Stewart, C.Y. Chiu, S. Huang, T. Muir, Y. Zhao, B. Chait, P. Mathias, G.R. Nemerow, EMBO J. 16 (1997) 1189–1198.
[43] T.J. Wickham, E.J. Filardo, D.A. Cheresh, G.R. Nemerow, J. Cell Biol. 127 (1994) 257–264.
[44] F.R. Maxfield, J. Cell Biol. 95 (1982) 676–681.
[45] A.M. Tartakoff, Cell 32 (1983) 1026–1028.
[46] D.J. Yamashiro, S.R. Fluss, F.R. Maxfield, J. Cell Biol. 97 (1983) 929–934.
[47] H. Farhood, N. Serbina, L. Huang, Biochim. Biophys. Acta 1235 (1995) 289–295.
[48] P. Seth, D.J.P. Fitzgerald, M.C. Willingham, I. Pastan, J. Virol. 51 (1984) 650–655.
[49] E. Prchla, C. Plank, E. Wagner, D. Blaas, R. Fuchs, J. Cell Biol. 131 (1995) 111–123.
[50] E. Rodriguez, E. Everitt, J. Virol. 70 (1996) 3470–3477.
[51] P. Erbacher, A.C. Roche, M. Monsigny, P.M. Monsigny, Exp. Cell Res. 225 (1996) 186–194.
[52] S.S. Hong, L. Karayan, J. Tournier, D.T. Curiel, P. Boulanger, EMBO J. 16 (1997) 2284–2306.

ELSEVIER

Biochimica et Biophysica Acta 1330 (1997) 17–28

BIOCHIMICA ET BIOPHYSICA ACTA
BBA

Pores formed by influenza hemagglutinin [1]

Rolf Jiricek, Gerhard Schwarz, Toon Stegmann *

Department of Biophysical Chemistry, Biozentrum of the University of Basel, Klingelbergstrasse 70, CH 4056 Basel, Switzerland [2]

Received 2 January 1997; revised 26 May 1997; accepted 29 May 1997

Abstract

Low pH-induced fusion mediated by the hemagglutinin (HA) of influenza virus involves a conformational change in the protein that leads to the insertion of a ''fusion peptide'' of the protein into the target membrane. It has been suggested that this insertion, aided by the formation of a complex of multiple HA trimers, would lead to perturbation of the bilayer structure of the membrane, initiating fusion. Here we present data showing that the interaction of the bromelain released ectodomain of the protein (BHA) with liposomal membranes at low pH leads to pore formation, at least at low temperatures. Strongly temperature-dependent low pH-induced inactivation of BHA resulted in a complete lack of activity of BHA above 10°C. Even at 0°C, only about 5% of the BHA participated in pore formation. Viral HA was less rapidly inactivated and still induced pores at 37°C. BHA-induced pore formation showed a sigmoidal time course. Once BHA had formed a pore in one liposome, it did not form a pore in a further liposome. Quantitative analysis of pore formation indicated that one single BHA trimer sufficed to produce a pore. These data indicate that fusion peptide insertion perturbs the membrane and that the formation of a complex of trimers is not a prerequisite for the perturbation. © 1997 Elsevier Science B.V.

Keywords: Membrane fusion; Pore formation; Hemagglutinin; Influenza virus; Liposome

1. Introduction

Fusion of influenza virus with target membranes is mediated by the trimeric integral membrane protein, hemagglutinin (HA) (for reviews, see [1–3]). Each monomer of the trimer consists of two disulfide-linked subunits [4], the smaller one of which, HA2, is membrane-anchored and has a hydrophobic N-terminus, the so-called ''fusion peptide''. Low pH induces a conformational change in the protein [5], which results in the insertion of the fusion peptide into the target membrane [6,7] and the viral membrane [8]. The expression of HA on the surface of cells causes their fusion with neighbouring cells at low pH [9]. On the basis of experiments with cell

Abbreviations: BHA, Bromelain released ectodomain of influenza hemagglutinin; EDTA, ethylenediaminetetraacetic acid; HA, hemagglutinin; HEPES, 4-(2-hydroxyethyl)-1-piperazine-ethanesulfonic acid; MES, 2-morpholinoethane-sulfonic acid monohydrate; *N*-Rh-PE, *N*-(lissamine Rhodamine B sulfonyl) phosphatidylethanolamine; *N*-NBD-PE, *N*-(7-nitro-2,1,3-benzoxadiazol-4-yl) phosphatidylethanolamine

* Corresponding author. Current address: Institut de Pharmacologie et de Biologie Structurale, 205 Route de Narbonne, 31077 Toulouse, France. Fax: +33 5 6117 5994; E-mail: Stegmann@opium.ipbs.fr

[1] This study was supported by grant 3100-042953.95/1 (to T.S.) and 31-32188.91 and 31-42045.94 (to G.S) of the Swiss National Science Foundation.

[2] Fax.: +41 61 267 2189; E-mail: Stegmann@ubaclu.unibas.ch

0005-2736/97/$17.00 © 1997 Elsevier Science B.V. All rights reserved.
PII S0005-2736(97)00134-X

lines that expressed varying densities of HA, it was demonstrated that multiple HA trimers are required for fusion [10,11]. Some data indicate that these trimers interact cooperatively [10,11]. It is often assumed that several HA trimers form a higher order oligomer or ''fusion complex''.

Insertion of the fusion peptide could change the structure of the lipid bilayer of the target membrane locally, particularly if the formation of a fusion complex would concentrate these peptides. Fusion of influenza virus with erythrocytes induces hemolysis [12–14] and the leakage of small molecular weight substances from liposomes [12], indicating that during fusion, pores are formed in the membrane of the fusion product. In this paper, the term pore is used to indicate any kind of defect leading to the leakage of substances across a membrane. Shangguan et al. [15] have shown that a rather large pore is generated during the fusion of influenza virus with liposomes, allowing the leakage of dextrans with a molecular weight of 10 000. However, it is not clear if this is the result of fusion with a leaky viral membrane or is caused directly by fusion peptide–membrane interactions. On the one hand, a preparation of membrane-free HA aggregates that are held together by hydrophobic interactions between the membrane anchors (HA rosettes) also had lytic activities at low pH [16–18]. HA rosettes are made by detergent solubilization of viral membranes, followed by purification of the protein and removal of the detergent [16]. On the other hand, the ectodomain of HA, prepared by bromelain digestion of HA (BHA), induced no [16] or very slow [17] hemolysis, although the fusion peptide of BHA is known to insert into the target membrane [19,20]. Therefore, it seems possible that residual detergent at least contributed to the lytic activities of HA rosettes. Alternatively, the lack of activity of BHA could be due to its instability at low pH values [21,22].

It was often suggested that changes in the structure of the bilayer created by fusion peptide insertion could be crucial for fusion (see reviews [1,23]), since, in order to merge the viral and the target membrane, the lipids at the site of fusion have to deviate at least temporarily from a bilayer structure [24]. Thus, structural changes in the membrane induced by HA resulting in pore formation might be related to the formation of lipid intermediate structures that are required for fusion. In this way, the lipid intermediates in the bilayers would lead to the formation of the first aqueous connection between the viral and the target membrane interior, the ''fusion pore''. However, electrophysiological measurements have shown that the fusion pores form before significant lipid mixing takes place, and that the pores may be entirely proteinaceous, resembling an ion channel made of HA trimers [25].

In this paper, we present data showing that BHA is able to interact with liposomal target membranes at low pH values, resulting in pore formation, at least at low temperatures. Strongly temperature-dependent low pH-induced inactivation of BHA was responsible for a complete lack of activity of BHA at temperatures above 10°C. Only a fraction of the BHA participated in pore formation even at 0°C. In contrast, viral HA was less rapidly inactivated, and still induced pores at 37°C. The use of BHA trimers instead of HA rosettes or viral HA allowed us to establish that one single BHA trimer was able to make a pore.

2. Materials and methods

2.1. Liposome preparation

Multilamellar vesicles were produced by resuspension of dry lipid films of egg phosphatidylcholine, egg phosphatidylethanolamine (both from Avanti Polar Lipids, Birmingham, AL, USA), gangliosides (Sigma, St. Louis, MO, USA; type III from bovine brain, estimated molecular weight 1500 g/mol) at a molar ratio of 6:3:1 in buffer containing 145 mM NaCl, 2.5 mM HEPES and 1 mM EDTA, pH 7.4. Subsequently, the suspension was frozen and thawed five times and large unilamellar vesicles were made from the multilamellar vesicles by extrusion (five–ten times) through 0.1 μm defined-pore polycarbonate filters (Nucleopore, Pleasanton, CA, USA) [26]. After extrusion, residual multilamellar liposomes were removed by centrifugation. Phospholipid phosphate was determined according to Böttcher et al. [27]. The size distribution of the liposomes was determined by dynamic laser light scattering at 632 nm using a He–Ne laser, an ALV-125 goniometer and an ALV-5000 correlator.

2.2. Virus

The X-31 recombinant strain of influenza A virus (from plaque C-22 [28]) was grown for us by the Schweizerisches Serum- und Impfstoffinstitut (Bern, Switzerland) in the allantoic cavity of embryonated eggs, and purified, handled and stored essentially as described before [29]. Viral phospholipid was extracted according to Folch et al. [30] and phospholipid phosphate was determined according to Böttcher et al. [27].

2.3. BHA preparation

BHA was prepared as described by Brand and Skehel [31] with minor modifications as specified by Harter et al. [19]. Briefly, virus was pelleted by centrifugation and resuspended in 100 mM Tris–HCl buffer, 57 μM 2-mercaptoethanol, pH 8.0. The protein was then released from the virus by digestion with 2 mg/ml bromelain (Calbiochem, La Jolla, CA, USA) at 37°C for 20 h. Subsequently, virus was removed by centrifugation and BHA was purified from the supernatant by molecular sieve chromatography on Sephadex G-75 in buffer containing 3.5 mM HEPES, 1 mM EDTA and 145 mM NaCl. As assessed by sodium dodecyl sulfate–polyacrylamide gel electrophoresis (SDS–PAGE), the protein was more than 95% pure. Protein concentrations were determined according to Bradford [32] using the BioRad protein assay (BioRad Laboratories, Hercules, CA, USA; using bovine serum albumin as the reference).

2.4. Calcein leakage measurements

Leakage of the small molecular weight fluorescent dye, calcein, from liposomes was assessed by monitoring its fluorescence at 515 nm, with excitation at 495 nm, using an SLM 8000 D spectrofluorimeter. At high concentrations, the fluorescence of calcein is self-quenched. Dilution of liposome-entrapped calcein into the aqueous buffer (5 mM HEPES, 10 mM MES, 15 mM sodium citrate, 135 mM NaCl, 1.0 mM EDTA, pH 5.0) surrounding the liposomes therefore leads to an increase in fluorescence intensity. Calcein was entrapped into liposomes by hydrating the lipid film in buffer containing 2.5 mM HEPES, 1 mM EDTA, 100 mM NaCl and 50 mM calcein at pH 7.4 or in buffer containing 5 mM HEPES, 10 mM MES, 15 mM citrate, 85 mM NaCl, 1.0 mM EDTA and 50 mM calcein at pH 5.0, respectively. Non-entrapped dye was then removed by molecular sieve chromatography on Sephadex G-75 with buffer containing 3.5 mM HEPES, 1 mM EDTA and 145 mM NaCl at pH 7.4 or in buffer containing 135 mM NaCl, 15 mM sodium citrate, 10 mM MES, 5 mM HEPES and 1 mM EDTA at pH 5.0, respectively. For evaluation of the kinetic measurements, the fluorescence data were normalized. The fluorescence intensity, F_∞, of completely dequenched calcein was obtained after lysis of the liposomes with the detergents Triton X-100 (7.6 mM) or octaethyleneglycol mono *n*-dodecyl ether (C12E8, Nikko Chemicals, Tokyo, Japan; 5.0 mM). The efflux of dye function, E(t), was calculated from the relative fluorescence intensities, F(t), according to Eq. (1), where F_0 represents the initial fluorescence

$$E(t) = (F_\infty - F(t))/(F\infty - F_0) \quad (1)$$

For easier comparison with the fusion data, 1 − E(t) is plotted in some of the figures, rather than E(t). This function has an initial value of zero and reaches a value of 1 when all liposomes are lysed. We observed an increase in fluorescence intensity, probably due to spontaneous leakage, when liposomes were kept at low concentrations, especially at 37°C or when the solution was stirred, even if no protein or virus was added. The increase in fluorescence intensity after 24 hours was about 15 to 35% of the difference between F_0 and F_∞. For that reason, long time experiments were done without further stirring, after mixing the components for several seconds. In this case, the fluorescence intensity F_s of a liposome solution, which was incubated for the same time under the same conditions, but in the absence of BHA, was taken as the initial level of fluorescence. The efflux E(24 h) was then calculated according to:

$$E(24h) = [F_\infty - F(24h)]/(F_\infty - F_s) \quad (2)$$

The lag time before the onset of leakage was defined as the time between the addition of BHA or virus and the intercept of the tangent to the inflection point of the leakage curve with the time axis [33], as first proposed by Bentz [34].

2.5. Fusion measurements

Fusion between virus and labeled liposomes was measured with a resonance energy transfer assay [35].

Labeled liposomes contained 0.6 mol.% each of *N*-(lissamine Rhodamine B sulfonyl)dioleoylphosphatidylethanolamine (*N*-Rh-PE) and *N*-(7-nitro-2,1,3-benzoxadiazol-4-yl)phosphatidylethanolamine (*N*-NBD-PE). Fluorescence was recorded at excitation and emission wavelengths of 465 and 530 nm, respectively, with a 515-nm long-pass filter placed between the cuvette and the emission monochromator [36] on a SLM 8000 D spectrofluorimeter with continuous stirring in a thermostated cuvette holder. All measurements were carried out in buffer containing 135 mM NaCl, 15 mM sodium citrate, 10 mM MES, 5 mM HEPES and 1 mM EDTA at pH 5.0 or 7.4. For calibration of the fluorescence scale, the initial residual fluorescence intensity, F_0, was taken as the zero level and the intensity at infinite probe solution, F_∞, as the maximum. The latter value was obtained by lysis of the liposomes with 5.0 mM octaethyleneglycol mono *n*-dodecyl ether (C12E8, Nikko Chemicals) with correction for dilution. Hence, the calibrated fluorescence, F_n, was obtained by:

$$F_n = [F(t) - F_0]/(F_\infty - F_0) \quad (3)$$

In some experiments, dextran (MW 19600 g/mol), at a concentration of 4.1 mM, was incorporated into liposomes containing *N*-NBD-PE and *N*-Rh-PE. A much higher pressure was needed to extrude the liposomes in this case, but a similar extrusion protocol as described above was followed.

3. Results

3.1. BHA induces pore formation in liposomes at 0°C

Influenza virus and HA rosettes have hemolytic activity and induce the leakage of small molecular weight markers from liposomes at low pH [12–17]. However, BHA, which, in contrast to HA rosettes, is not prepared in the presence of detergent, had little or no lytic activity [16,17]. Therefore, the activity of HA rosettes could be due to residual detergent and, in this case virus-induced lysis, could be a consequence of fusion, in line with the results obtained by Shangguan et al. [15], rather than resulting from the interaction of HA with target membranes. On the other hand, BHA is not very stable at low pH values and, thus, the lack of activity could be due to its inactivation [21].

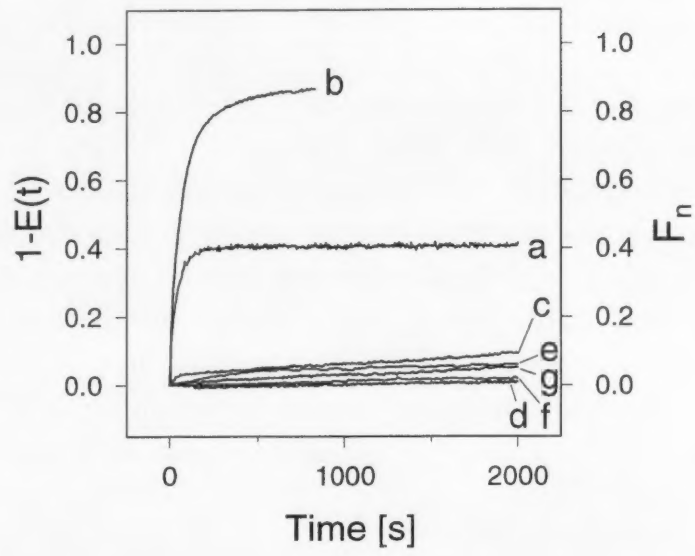

Fig. 1. Comparison of fusion and leakage at 37°C. At time 0, virus (a, b, d, e) or BHA (c, f) was injected into a cuvette containing liposomes at pH 5.0 (a, b, c, g) or pH 7.4 (d, e, f). The liposomes either contained calcein and leakage of this substance from liposomes was measured (b, c, e, f, g) as described in Section 2, or fusion was measured (a, d). In the latter case, liposomes contained the fluorescent phospholipid analogues *N*-NBD-PE and *N*-Rh-PE and fusion was measured by a resonance energy transfer assay, as described in Section 2. F_n: normalized NBD fluorescence. The leakage data are expressed as $1-E(t)$ (see Section 2) for ease of comparison with the fusion data. The Eq. (1) $-E(t)$ represents the amount of calcein that has leaked from the liposomes. All experiments were done at 37°C, at 5 μM liposomal phospholipid and 25 nM BHA or 5 μM viral phospholipid (a, b, d, e). (g) Leakage from liposomes under the same conditions as in c but in the absence of BHA.

To investigate these issues, we first compared the fusion of virus with large unilamellar liposomes (composed of phosphatidylcholine, phosphatidylethanolamine and gangliosides in a 6:3:1 ratio) with virus-induced leakage at pH 5.0, 37°C (Fig. 1). Fusion, measured using the resonance energy transfer assay of Struck et al. [35], leveled off at a fluorescence increase of 41% at pH 5.0, corresponding to 82% fusion [37,38]. Virus-induced leakage of the small molecular weight substance, calcein, from liposomes, measured by the relief of self-quenching of the dye upon its dilution in aqueous buffer, reached a level of 86%. At this pH and temperature, BHA induced less than 5% leakage (Fig. 1). At neutral pH, there was neither leakage nor fusion. BHA does not induce fusion [17].

To investigate if the lack of activity of BHA at this

temperature was due to the instability of BHA at 37°C, fusion and leakage were also investigated at 0°C (Fig. 2). In the absence of target membranes, the fusion activity of viral HA is rapidly affected by low pH incubation at 37°C, but not at 0°C [39]. At 0°C, virus-induced leakage reached 91% after 30 min, but fluorescence dequenching measurements of fusion had reached only 8% at this time point, corresponding to 16% fusion. Therefore, in contrast to the data published by Shangguan et al. [15], these data indicate that leakage was also from liposomes that did not fuse with the virus, suggesting that it could be caused by interactions of HA with liposomes, rather than being a secondary consequence of fusion. Significantly, at this temperature, BHA was found to induce 69% leakage within 30 min at pH 5.0. Both fusion and leakage showed a sigmoidal time course. No leakage or fusion took place at neutral pH (Fig. 2). The detailed pH-dependence of BHA-induced pore formation confirmed that a conformational change in the protein, which exposes the fusion peptide, was involved (Fig. 3).

Thus, it seemed likely that the lack of activity of BHA at 37°C was due to strongly temperature-dependent inactivation. To investigate this in more detail, the activity of BHA was measured at a range of temperatures (Fig. 4, panel A). We found that the rate of BHA-induced leakage decreased with increasing

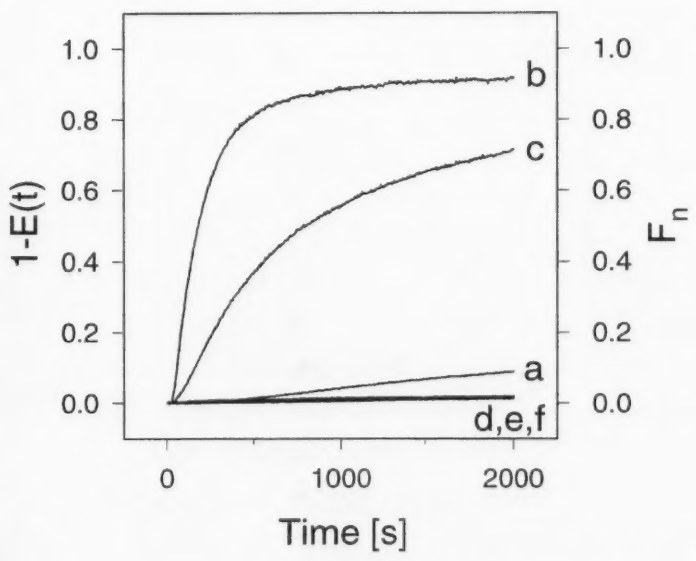

Fig. 2. Comparison of fusion and leakage at 0°C. At time 0, virus (a, b, d, e) or BHA (c, f) was injected into a cuvette containing liposomes at pH 5.0 (a, b, c) or pH 7.4 (d, e, f) at 0°C. Leakage (b, c, e, f) and fusion (a, d) were measured as in Fig. 1. All other conditions were as in Fig. 1.

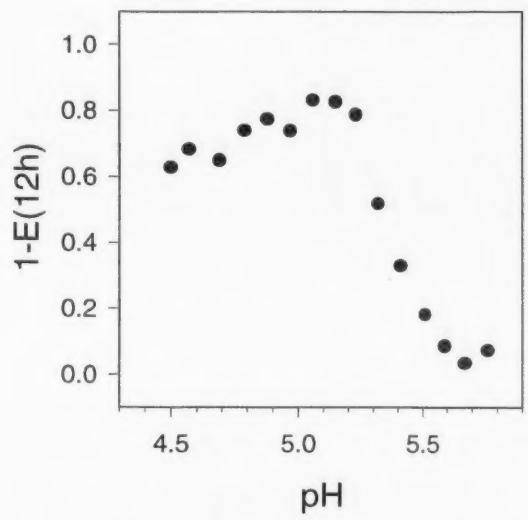

Fig. 3. Dependence of leakage on pH. BHA (1.15 nM) was incubated with calcein-containing liposomes (2.5 mM phospholipid) at 0°C and at various pH values. The extent of leakage was measured after 24 h, as described in Section 2. 1 − E(12 h) = amount of calcein that has leaked from the liposomes after 24 h.

temperature. Moreover, when BHA was incubated at low pH for 10 min at 0°C before the addition of liposomes, the rate of leakage was much reduced (Fig. 4, panel B). These data indicate that BHA is more rapidly inactivated at low pH than is viral HA, and that this inactivation is much faster at higher temperatures. Doms and Helenius [21] have shown that BHA trimers dissociate at low pH and at room temperature. In accordance with their data, we found that, as measured by high-performance liquid chromatography (HPLC) gel filtration, about 50% of BHA (1.0 μM) dissociated after a treatment at 25°C and pH 5 for 10 min, followed by reneutralization (data not shown). At lower concentrations, there should be at least as much dissociation.

The leakage of calcein across the membrane was the result of a membrane defect induced by HA, and not the result of complete destruction of the liposomes, as evidenced by the capacity of the liposomes to undergo fusion (Fig. 1). Also, negative stain electron microscopy showed intact liposomes after incubation with BHA at pH 5 (results not shown). Moreover, if liposomes containing dextran (MW 19600) were prepared as described in Section 2, they could, in contrast to liposomes containing buffer, be pelleted by centrifugation in an Eppendorf centrifuge. After incubation with various concentrations of BHA at pH 5, 0°C, under conditions where calcein would have leaked completely (16 μM liposomal lipid, 3 nM

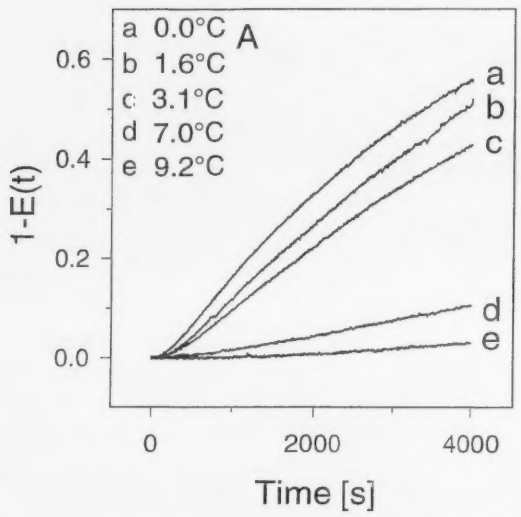

Fig. 4. Inactivation of BHA. Panel A: 10 nM BHA, pH 7.4, was added to a solution of calcein-loaded liposomes (10 μM phospholipid) in acidic buffer to a final pH of 5.0 at various temperatures. 1−E(24 h): as in Fig. 3. Panel B: BHA (29 nM) was incubated at pH 5.1 and 0°C for 0 s (a), 200 s (b) or 600 s (c) prior to the addition of calcein-loaded liposomes (2.5 μM phospholipid) at time 0, and leakage was measured.

BHA, 30 min), 92% of the liposomes could still be pelleted, indicating that high molecular weight molecules were retained in their interior.

BHA-induced leakage apparently reached a final level after incubation for several hours. To investigate if BHA caused leakage of only a fraction of liposomes or lysed all liposomes eventually, various amounts of BHA were incubated with liposomes at 0°C and pH 5.0 for 2, 24, 48 and 170 h. As shown in Fig. 5, leakage reached a constant level after 24 h. Further incubation did not increase the extent of leakage. If calcein-loaded liposomes were added to a sample of BHA and liposomes that had already reached a final level of leakage, no further BHA-induced leakage was observed (data not shown). Therefore, the interaction of BHA with liposomes was most likely irreversible; once a BHA molecule has bound to a liposome and formed a pore, it is not able to form a pore in a further liposome. To investigate at which point pore formation became irreversible, empty liposomes were incubated with BHA at low pH and, after various periods of time, calcein-loaded liposomes were added to the mixture. As shown in Fig. 6, after preincubation of BHA with liposomes for 10 min, less than 10% of the subsequently added

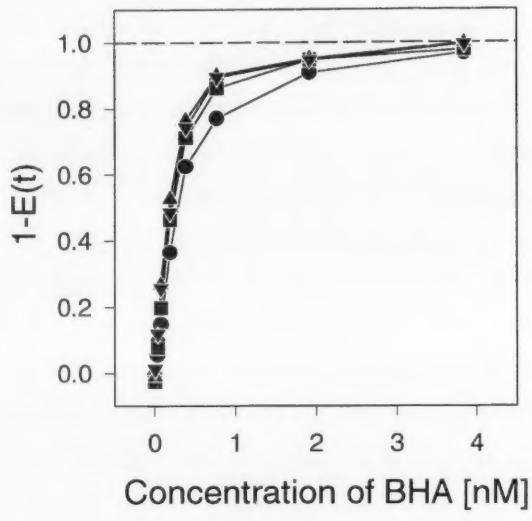

Fig. 5. Leakage from liposomes versus BHA concentration. BHA was added to calcein-containing liposomes (2.5 μM phospholipid) at pH 5.1, 0°C. The extent of leakage was measured after 2 h (circles), 24 h (squares), 46 h (triangles) and 170 h (inverted triangles).

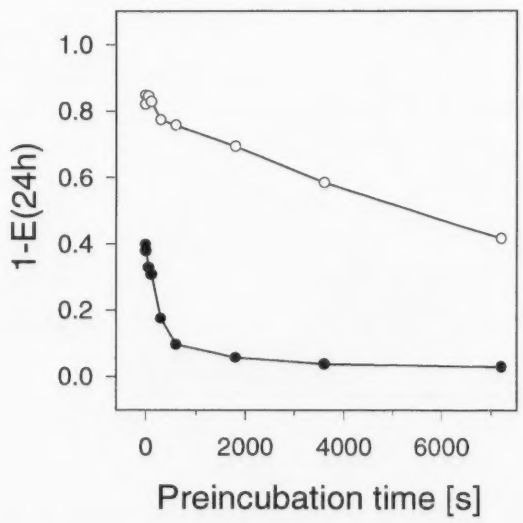

Fig. 6. Preincubation of BHA with liposomes at pH 5.0, 0°C. BHA (1.15 nM) was incubated with unlabelled liposomes (2.5 μM phospholipid) without calcein (dots) or without liposomes (circles) at pH 5.0, 0°C for a certain period of time. Then, calcein-loaded vesicles were added (2.5 μM). Leakage was measured after 24 h.

calcein-loaded liposomes (which would have been lysed if BHA was incubated at low pH in the absence of liposomes) were lysed under these circumstances.

3.2. Determination of the minimum number of BHA trimers required to form a pore

To determine the minimum number of BHA-trimers per liposome required to form a pore, we assumed that the binding of the protein to liposomes is non-cooperative, i.e., that the trimers bind to liposomes independently. Furthermore, it was taken into account that one BHA trimer induced leakage in only one liposome, as shown above. The fraction of emptied liposomes can then be calculated as a function of the protein/liposome ratio, assuming that the liposomes are of equal size. Dynamic laser light scattering measurements, as described in Section 2, showed that the size distribution of the liposomes, which were made by repeated extrusion through defined-pore filters, was very narrow, as described previously [26], around a mean diameter of 103 nm. In that case, the fraction $P_\mu(m)$ of liposomes with exactly m proteins are Poisson-distributed according to:

$$P_\mu(m) = e^{-\mu}\mu^m/m! \quad (4)$$

where μ is the average number of BHA trimers per liposome. The fraction of liposomes with one or more pores can be calculated from the efflux function, E(t), provided that the mode of leakage (''all or none'' or more gradual) is known. To determine the mode of leakage, we first measured the self-quenching of calcein incorporated in liposomes at a range of concentrations (not shown). Liposomes containing 50 mM calcein were then incubated at pH 5, 0°C with various concentrations of BHA for 24 h, resulting in a variety of leakage levels (Fig. 7). The liposomes were separated from the free dye by gel filtration chromatography, and the quenching of the calcein remaining in the liposomes was determined [40]. It was found that, even under conditions where more than 80% of the calcein had leaked out of the liposomes, the quenching in those that still contained the dye was still close to the quenching of 50 mM calcein (Fig. 7), clearly indicating an ''all or none'' mode of leakage for BHA. In this case, the fraction of emptied liposomes equals $[1 - E(t)]$. Assuming that m_p proteins are required to form a pore, then the

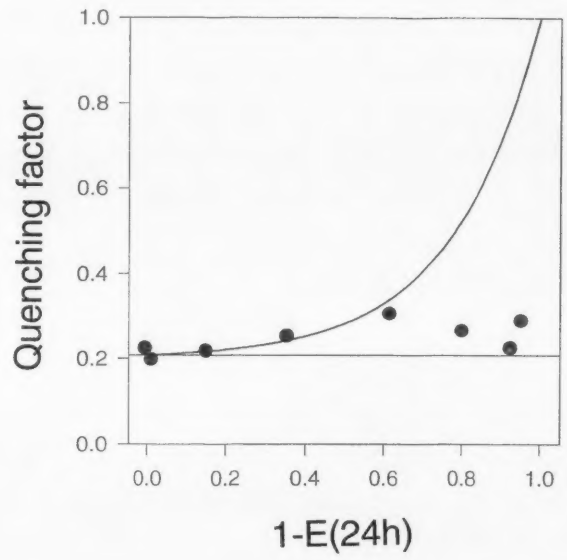

Fig. 7. ''All or none'' mode of leakage. Liposomes containing calcein (50 mM) were incubated with various concentrations of BHA at pH 5, 0°C and, after 24 h, the liposomes were separated from the leaked dye, and the quenching of calcein remaining in the liposomes was determined as described in the text (dots). The quenching expected in the case of an ''all or none'' mode of leakage is represented by a straight line and the curve shows the quenching expected for a gradual release of dye.

fraction of liposomes that do not lose their content equals the sum of all fractions of liposomes with less than m_p proteins:

$$E(\mu,m_p) = SP_\mu(i),\ i = 0 \ldots m_p - 1 \quad (5)$$

and the fraction of emptied liposomes becomes:

$$1 - E(\mu,m_p) = 1 - SP_\mu(i),\ i = 0 \ldots m_p - 1 \quad (6)$$

The final extent of leakage at several different concentrations of liposomes and BHA was calculated according to Eq. (6) (Fig. 8, panel A) and measured (Fig. 8, panel B). The measured data points were fitted using Eq. (6). Best fits were obtained with $m_p = 1$, yielding an exponential function, with a mean square residue of 0.009. For $m_p = 2$, the mean square residue was 0.015 and for $m_p = 3$, it was 0.021. These data indicate that the minimum number of BHA trimers required to form a pore was one. However, the concentrations of BHA at which lysis occurred were twenty-fold higher than expected if every BHA trimer would be active, as shown graphically in Fig. 8, panel B. Therefore, these data could either mean that only 5% of the BHA had pore-forming activity, or that the formation of very large complexes of BHA trimers (of the order of twenty trimers) in the solution was required prior to binding

to the liposomes in order to produce a pore. Considering that BHA is rapidly inactivated at low pH (Fig. 4) and that fragments of BHA containing the fusion peptide were found to bind to liposomes singly [41], the former possibility is more likely.

3.3. The kinetics of leakage

As can be seen most clearly in Fig. 4, panel A, BHA-induced leakage showed a sigmoidal time course. The occurrence of a ''lag phase'' before the onset of leakage indicated that there were at least two rate-limiting steps in the reaction leading to leakage. These steps could involve the conformational change in BHA, binding of the protein to the liposomes, insertion of the fusion peptide into the target membrane, and the perturbation of the target bilayer, which leads to pore formation. Preincubation of BHA with liposomes at pH 7.4 did not significantly shorten the lag, indicating that BHA-receptor binding was not rate-limiting. As preincubation of BHA at low pH in the absence of liposomes seemed to shorten the lag phase (cf. Fig. 4, panel A), we investigated whether or not the conformational change in BHA was rate-limiting. To this end, we preincubated BHA at 0°C, pH 5.0 for various times, in the absence of liposomes, and determined the lag, as described in Section 2 (Fig. 9). It was found that preincubation for up to 200 s shortened the lag, but longer preincubations did not shorten it further. Therefore, the conformational change contributes to the measured lag, but is not solely responsible for it. These data indicate that there were more than two steps leading to leakage.

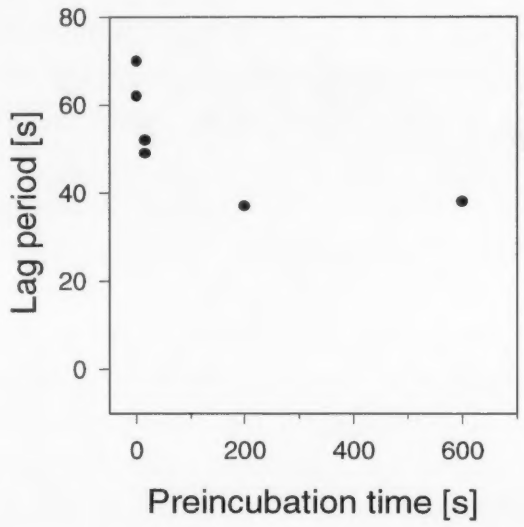

Fig. 9. Lag versus preincubation time of BHA at a low pH value. BHA (29 nM) was incubated at 0°C and pH 5.1 for the time indicated. Then, liposomes (2.5 μM phospholipid) were added and calcein leakage was monitored. The lag time was determined graphically, from the injection of BHA to the intercept of a tangent to the leakage curve at its inflection point, as described in Section 2.

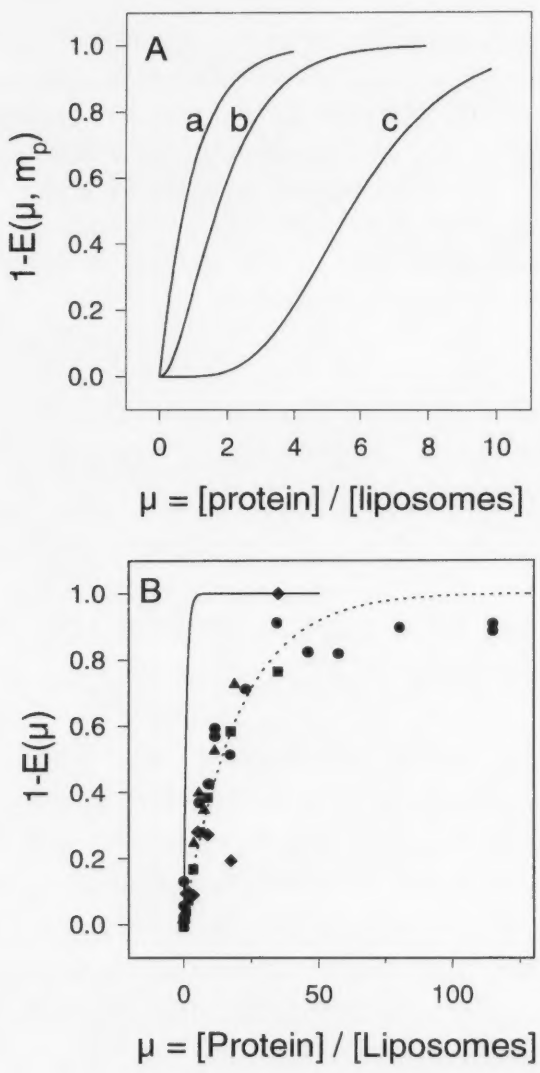

Fig. 8. Leakage from liposomes at different BHA trimer concentrations. Panel A: The fraction of emptied liposomes $[1-E(\mu, m_p)]$ was calculated using Eq. (6) (see text) for $m_p = 1$ (a), 2 (b) and 6 (c) and plotted versus the protein/liposome ratio, μ. Panel B: BHA was added to calcein-containing liposomes at pH 5.1, 0°C. The extent of leakage $[1-E(\mu)]$ was measured after 24 h as described in Section 2. The final phospholipid concentrations were 2.5 μM (circles), 20 μM (squares), 25 μM (triangles) and 50 μM (rhombi). Solid line: theoretical curve for $m_p = 1$ was calculated as described for panel A; dotted line: theoretical curve for $m_p = 1$ and interaction of one twentieth of the protein.

4. Discussion

In this paper, we have shown that a single trimer of BHA, the soluble ectodomain of HA, is able to

form a pore in a liposome at the pH of HA-induced fusion. BHA was rapidly inactivated at low pH in a strongly temperature-dependent fashion and, therefore, significant pore formation at pH 5 was seen at temperatures below 10°C only. BHA-induced pore formation was preceded by a lag phase. Receptor binding of the molecule to liposomes did not appreciably contribute to the lag phase, and there still was a (shortened) lag after the low pH-induced conformational change in BHA, indicating that there were more than two rate-limiting steps in the reaction.

Temperature-dependent low pH-induced inactivation is probably the reason why previous experiments with BHA at 37°C showed no [16] or only very slow [17] hemolysis. The fusion and hemolytic activities of viral HA and HA rosettes are also inactivated at low pH values in a similar temperature-dependent fashion [16,39] but much more slowly than BHA, indicating that the transmembrane C-terminal part of HA is important for the stability of the molecule [21]. Even at 0°C, we found that only 5% of BHA participated in pore formation. Most likely, the remainder of the BHA was inactivated before it could interact with the membrane. For membrane-anchored HA, inactivation probably involves insertion of the fusion peptide in the membrane containing HA, rather than the target membrane [8], and also aggregation of HA trimers [42], most likely through hydrophobic interactions between their fusion peptides. Two mechanisms are likely to contribute to the inactivation of BHA. At low pH values, BHA molecules were shown to aggregate into rosettes, which are held together by hydrophobic interactions between the fusion peptides in the center of the rosette [43]. Since inactivation was irreversible and BHA trimers were shown to interact singly with the target membrane [41], BHA molecules aggregated in this fashion are most likely to no longer be capable of interactions with the membrane. Also, dissociation of the trimers of the low pH form of BHA contributed to the inactivation [21]. Alternatively, it is possible that some BHA trimers did bind to liposomes and insert their fusion peptides, but without forming a pore. However, binding experiments (R. Jiricek, unpublished) seem to indicate that the fraction of BHA that binds to liposomes is not very much larger than the fraction that causes pore formation.

The kinetic distinction between virus-induced leakage and fusion at 0°C (Fig. 2) and the pore-forming activity of BHA indicate that the leakage, which was shown to occur during influenza virus–liposome fusion [15], is caused by the interaction of HA with the target membrane. It remains a possibility that lipid mixing during fusion is also a leaky process, as suggested by Shangguan et al. [15], and that there is leakage after fusion, because the viral membrane has defects, as suggested by Young et al. [44]. It should be noted that Shangguan et al. [15] used a strain of virus whose HA has considerable sequence differences from the one used here.

HA-induced fusion may require the cooperative interaction of multiple HA trimers [10,11]. Cooperativity was first demonstrated using two cell lines expressing 1.9-fold different densities of the protein, which showed a 4.4-fold difference in the extent of fusion with liposomes [11]. Moreover, on the basis of the duration of the lag phase that preceded the fusion of nine cell lines expressing different densities of HA with erythrocytes, it was concluded that fusion involved the cooperative action of three to four trimers [10]. Originally, it was suggested that multiple HA trimers have to form a higher order oligomer or ''fusion complex'' in order to initiate fusion. In that case, most of the lag was thought to arise from the formation of the fusion complex. However, the data presented by Danieli et al. [10] and the results of other experiments with cell-surface-expressed HA [45] suggested that the cooperativity was not at this stage of the reaction, but at a later stage. In agreement with these observations, BHA-induced pore formation was also preceded by a lag phase, and the pores were formed by single trimers, as we have shown here. If the events that take place during the lag preceding BHA-induced lysis are comparable to those that take place during the lag preceding fusion, then it is most likely that fusion peptide–target membrane lipid interactions are rate-limiting and that these could play a key role in fusion.

In the case of BHA, these interactions may involve the formation of a certain arrangement of two or three fusion peptides in the membrane at the site of fusion. It is not clear how insertion of the fusion peptide would lead to pore formation. Pores are induced by synthetic fusion peptides, but, in most cases, small unilamellar vesicles were used as targets [46–49] and, because of the curvature strain on these

membranes, they are easily lysed. On using large unilamellar vesicles as targets, a clear correlation was found between the ability of synthetic influenza fusion peptides with different sequences to produce pores and the fusion activity of the corresponding wild-type or mutant HAs [50]. Typical lytic amphipathic helical peptides, which differ from the fusion peptide because they have positive charges, have been proposed to induce leakage either by forming pores according to a barrel–stave mechanism, involving clusters of transmembrane helices [51], or by increasing the negative curvature strain on membranes [52]. Fusion peptides probably do not form pores of the barrel–stave type. Studies with photoactivatable lipids have indicated that the fusion peptide of BHA is inserted as an α-helix [20]. The orientation of the inserted peptide has been found to be parallel to the plane of the membrane [53], or oblique [54,55]. The tryptophan residue of the molecule is close to the hydrocarbon/polar interface [56]. Even though there may be differences between BHA and viral HA, in the sense that viral HA might penetrate deeper into the target membrane [6], there are no indications that fusion peptides would span the membrane, like they should in a barrel–stave model. Moreover, other viruses that have fusion proteins with internal, rather than N-terminal, fusion peptides, also cause hemolysis and induce pore formation in membranes [13,57] and it is hard to imagine how these would span the membrane.

Alternatively, fusion peptides could have lytic properties because they increase the negative curvature strain on membranes, a mechanism proposed for lytic amphipathic peptides [58]. Synthetic influenza fusion peptides were shown to have effects that are compatible with this proposal, at low pH values, and peptides corresponding to mutants that lack fusion activity did not have these [59]. Although this seems to provide a plausible link between fusion and lytic activities of fusion peptides, considering that the formation of structures with negative curvature is thought to be required for fusion [1,23], it was recently shown that changes in the composition of the membrane that would affect the negative curvature strain have little effect on fusion or leakage [15]. Whether BHA is actually capable of altering membrane curvature or not remains to be determined.

The pore-forming activities of other peptides that do not span the membrane or resemble amphipathic lytic peptides, like magainin 2 [60] or melittin [61,62], cannot be easily understood. Most of these peptides presumably induce pore formation only as multimers, indicating the formation of a larger, defined structure. Considering the orientation of the influenza fusion peptide in the membrane, and the fact that a single trimer of BHA has pore-forming activity, the mechanism of pore formation by these types of peptides might give the most relevant information on BHA-induced pore formation.

Although influenza HA is the most extensively studied membrane fusion protein, and many details of the conformational change in the protein at the pH of fusion are known, how the protein succeeds in mixing the lipids of the viral and target membrane is not understood. Insertion of the fusion peptide into the target membrane seems to play a key role in the process. Studies with synthetic fusion peptides modeled after wild-type- or mutant fusion peptides almost invariably show a positive correlation between the pore-forming ability of the synthetic peptide and the fusion activity of the corresponding HA [48–50,59]. Therefore, it is likely that the effect of these peptides on the membrane, which gives rise to pore formation, is comparable to that which gives rise to lipid mixing. Such studies can now be performed with BHA, providing a more sophisticated model for observing the changes in the lipid membrane and obtaining information on the lipid intermediates that are involved in fusion.

Acknowledgements

We thank Dr. R. Glück and R. Mischler of the Swiss Institute for Serum and Vaccines for the preparation of influenza virus, A. Arbuzova for helpful discussions and Dr. M. Winterhalter for critical review of the paper.

References

[1] J.E. Bentz, Viral Fusion Mechanisms, CRC Press, Boca Raton, FL, 1993.

[2] J. Zimmerberg, S.S. Vogel, L.V. Chernomordik, Ann. Rev. Biophys. Biomol. Struct. 22 (1993) 433–466.
[3] F.M. Hughson, Curr. Biol. 5 (1995) 265–274.
[4] I.A. Wilson, J.J. Skehel, D.C. Wiley, Nature 289 (1981) 366–375.
[5] P.A. Bullough, F.M. Hughson, J.J. Skehel, D.C. Wiley, Nature 371 (1994) 37–43.
[6] T. Stegmann, J.M. Delfino, F.M. Richards, A. Helenius, J. Biol. Chem. 266 (1991) 18404–18410.
[7] M. Tsurudome, R. Glück, R. Graf, R. Falchetto, U. Schaller, J. Brunner, J. Biol. Chem. 267 (1992) 20225–20232.
[8] T. Weber, G. Paesold, C. Galli, R. Mischler, G. Semenza, J. Brunner, J. Biol. Chem. 269 (1994) 18535–18538.
[9] J. White, A. Helenius, M.-J. Gething, Nature 300 (1982) 658–659.
[10] T. Danieli, S.L. Pelletier, Y.I. Henis, J.M. White, J. Cell Biol. 133 (1996) 559–569.
[11] H. Ellens, J. Bentz, D. Mason, F. Zhang, J. White, Biochemistry 29 (1990) 9697–9707.
[12] T. Maeda, K. Kawasaki, S.I. Ohnishi, Proc. Natl. Acad. Sci. U.S.A. 78 (1981) 4133–4137.
[13] J. Lenard, D.K. Miller, Virology 110 (1981) 479–482.
[14] R.T. Huang, R. Rott, H.-D. Klenk, Virology 110 (1981) 243–247.
[15] T. Shangguan, D. Alford, J. Bentz, Biochemistry 35 (1996) 4956–4965.
[16] S.B. Sato, K. Kawasaki, S.I. Ohnishi, Proc. Natl. Acad. Sci. U.S.A. 80 (1983) 3153–3157.
[17] S.A. Wharton, J.J. Skehel, D.C. Wiley, Virology 149 (1986) 27–35.
[18] S. Günther-Ausborn, A. Praetor, T. Stegmann, J. Biol. Chem. 270 (1995) 29279–29285.
[19] C. Harter, T. Bächi, B. Semenza, J. Brunner, Biochemistry 27 (1988) 1856–1864.
[20] C. Harter, P. James, T. Bächi, G. Semenza, J. Brunner, J. Biol. Chem. 264 (1989) 6459–6464.
[21] R.W. Doms, A. Helenius, J. Virol. 60 (1986) 833–839.
[22] R.W. Doms, A. Helenius, in: S. Ohki, D. Doyle, T.D. Flanagan, S.W. Hui, E. Mayhew (eds.), Molecular Mechanisms of Membrane Fusion, Plenum, New York, 1987, pp. 385–398.
[23] D.P. Siegel, Biophys. J. 65 (1993) 2124–2140.
[24] J. Wilschut, D. Hoekstra, Chem. Phys. Lipids 40 (1986) 145–166.
[25] M. Lindau, W. Almers, Curr. Opin. Cell Biol. 7 (1995) 509–517.
[26] L.D. Mayer, M.J. Hope, P.R. Cullis, Biochem. Biophys. Acta 858 (1986) 161–168.
[27] C.J.F. Böttcher, C.M. Van Gent, C. Fries, Anal. Chim. Acta 24 (1961) 203–204.
[28] R.W. Doms, M.J. Gething, J. Henneberry, J. White, A. Helenius, J. Virol. 57 (1986) 603–613.
[29] S. Nebel, I. Bartoldus, T. Stegmann, Biochemistry 34 (1995) 5705–5711.
[30] J. Folch, M. Lees, G.H. Sloane-Stanley, J. Biol. Chem. 226 (1957) 497–509.
[31] C.M. Brand, J.J. Skehel, Nature New Biol. 238 (1972) 145–147.
[32] M.M. Bradford, Anal. Biochem. 72 (1976) 248–254.
[33] T. Stegmann, I. Bartoldus, J. Zumbrunn, Biochemistry 34 (1995) 1825–1832.
[34] J. Bentz, Biophys. J. 63 (1992) 448–459.
[35] D.K. Struck, D. Hoekstra, R.E. Pagano, Biochemistry 20 (1981) 4093–4099.
[36] T. Stegmann, D. Hoekstra, G. Scherphof, J. Wilschut, Biochemistry 24 (1985) 3107–3113.
[37] S. Nir, T. Stegmann, J. Wilschut, Biochemistry 25 (1986) 257–266.
[38] T. Stegmann, S. Nir, J. Wilschut, Biochemistry 28 (1989) 1698–1704.
[39] T. Stegmann, F.P. Booy, J. Wilschut, J. Biol. Chem. 262 (1987) 17744–17749.
[40] G. Schwarz, A. Arbuzova, Biochim. Biophys. Acta 1239 (1995) 51–57.
[41] S.A. Wharton, L.J. Calder, R.W.H. Ruigrok, J.J. Skehel, D.A. Steinhauer, D.C. Wiley, EMBO J. 14 (1995) 240–246.
[42] D. Gutman, T. Danieli, J.M. White, Y.I. Henis, Biochemistry 32 (1993) 101–106.
[43] R.W. Ruigrok, A. Aitken, L.J. Calder, S.R. Martin, J.J. Skehel, S.A. Wharton, W. Weis, D.C. Wiley, J. Gen. Virol. 69 (1988) 2785–2795.
[44] J.D.-E. Young, G.P.H. Young, Z.A. Cohn, J. Lenard, Virology 128 (1983) 186–194.
[45] M.J. Clague, C. Schoch, R. Blumenthal, J. Virol. 65 (1991) 2402–2407.
[46] M. Murata, Y. Sugahara, S. Takahashi, S. Ohnishi, J. Biochem. 102 (1987) 957–962.
[47] C. Schoch, R. Blumenthal, J. Biol. Chem. 268 (1993) 9267–9274.
[48] N. Düzgünes, F. Gambale, FEBS Lett. 227 (1988) 110–114.
[49] S.A. Wharton, S.R. Martin, R.W. Ruigrok, J.J. Skehel, D.C. Wiley, J. Gen. Virol. 69 (1988) 1847–1857.
[50] M. Rafalski, A. Ortiz, A. Rockwell, L.C. van Ginkel, J.D. Lear, W.F. DeGrado, J. Wilschut, Biochemistry 30 (1991) 10211–10220.
[51] D.M. Ojcius, D.-E. Young, Trends Biochem. Sci. 16 (1991) 225–229.
[52] M.E. Tytler, J.P. Segrest, R.E. Epand, S.-Q. Nie, R.F. Epand, G.M. Anatharamaiah, J. Biol. Chem. 268 (1993) 22112–22118.
[53] R. Ishiguro, M. Matsumoto, S. Takahashi, Biochemistry 35 (1996) 4976–4983.
[54] J. Lüneberg, I. Martin, F. Nuessler, J.-M. Ruysschaert, A. Herrmann, J. Biol. Chem. 270 (1995) 27606–27614.
[55] C. Gray, S.A. Tatulian, S.A. Wharton, L.K. Tamm, Biophys. J. 70 (1996) 2275–2286.
[56] M.J. Clague, J.R. Knutson, R. Blumenthal, A. Herrmann, Biochemistry 4 (1991) 5491–5497.

[57] K. Mifune, M. Ohuchi, K. Mannen, FEBS Lett. 137 (1982) 293–296.
[58] R.M. Epand, Y. Shai, J.P. Segrest, G.M. Anatharamaiah, Biopolymers 37 (1995) 319–338.
[59] R.M. Epand, R.F. Epand, Biochem. Biophys. Res. Commun. 202 (1994) 1420–1425.
[60] K. Matsuzaki, O. Murase, K. Miyajima, Biochemistry 34 (1995) 12553–12559.
[61] M. Pawlak, S. Stankowski, G. Schwarz, Biochim. Biophys. Acta 1062 (1991) 94–102.
[62] G. Schwarz, R. Zong, T. Popescu, Biochim. Biophys. Acta 1110 (1992) 97–104.

ELSEVIER

Biochimica et Biophysica Acta 1330 (1997) 29–38

BIOCHIMICA ET BIOPHYSICA ACTA
BBA

Dual effects of extracellular Ca^{2+} on cardiotoxin-induced cytotoxicity and cytosolic Ca^{2+} changes in cultured single cells of rabbit aortic endothelium

Yi-Jun Ou [a,1], Yuk-Man Leung [b], Shou-Jian Huang [b,2], Chiu-Yin Kwan [b,*]

[a] *Department of Physiology, Faculty of Medicine, The University of Hong Kong, 5 Sassoon Road, Hong Kong, China*
[b] *Department of Biomedical Sciences, Faculty of Health Sciences, McMaster University, 1200 Main Street West, Hamilton, Ontario L8N 3Z5, Canada*

Received 18 February 1997; revised 13 May 1997; accepted 28 May 1997

Abstract

The effects of extracellular Ca^{2+} on cytotoxicity induced by cardiotoxin (CTX), isolated from Chinese cobra venom, were investigated in cultured rabbit aortic endothelial cells (RAECs). In Hank's buffered saline solution (HBSS) containing 1.2 mM Ca^{2+}, CTX (1–30 μM) caused cell necrosis and cell death in a concentration-dependent manner, as determined by trypan blue exclusion test performed after a 20-min CTX treatment. The concentration of CTX that caused 50% cell death was about 6.5 μM. CTX (10 μM)-induced RAEC damage was also evident but less prominent in Ca^{2+}-free medium and almost completely prevented in medium containing 7–10 mM Ca^{2+}. Therefore, Ca^{2+} appears to provoke CTX-induced injury at physiological concentrations, but protects against it at high concentrations. The protection of RAECs from CTX-induced injury could also be achieved by high concentrations of Ni^{2+} and Mg^{2+}. Using the fura-2 fluorescence technique to measure the cytosolic free Ca^{2+} concentration ($[Ca^{2+}]_i$) of single RAEC, it was shown that in 1.2 mM Ca^{2+}-containing HBSS, treatment of RAECs with 10 μM CTX for 7–35 min resulted in a tremendous and irreversible $[Ca^{2+}]_i$ elevation, suggestive of cell membrane damage and extracellular Ca^{2+} entry. Ni^{2+} could also enter the cytosol of these damaged RAECs. However, there was no $[Ca^{2+}]_i$ elevation or Ni^{2+} entry in RAECs that were preincubated in HBSS containing 7 mM Ca^{2+} or Ni^{2+} before CTX exposure. In RAECs protected with 7 mM Ca^{2+}, the intracellular Ca^{2+} signals triggered by 100 μM extracellular ATP or 10 μM bradykinin in CTX-treated groups were similar to those in the untreated control groups. Taken together, the results indicate that high extracellular Ca^{2+} concentrations protected RAECs from CTX-induced injury, and preserved the ability of CTX-treated RAECs to generate Ca^{2+} signals in response to physiological stimuli. © 1997 Elsevier Science B.V.

Keywords: Calcium; Cardiotoxin; Cytotoxicity; Endothelium; Direct lytic factor; Aorta

* Corresponding author. Fax: +1 (905) 304 3748; E-mail: kwancy@fhs.csu.mcmaster.ca

[1] YJO and YML contributed equally to this work.

[2] Present address: Department of Pharmacology, Sun Yat-Sen University of Medical Sciences, Guangzhou, China.

0005-2736/97/$17.00 © 1997 Elsevier Science B.V. All rights reserved.
PII S0005-2736(97)00136-3

1. Introduction

Cardiotoxin (CTX) is a membrane-active polypeptide that has been purified from cobra snake venom [1]. It exerts many effects, including membrane depolarization, contraction of cardiac and skeletal muscles, and modulation of a number of enzymes, such as phospholipase C and the plasmalemmal Ca^{2+} pump [2,3]. CTX has also been named cytotoxin or direct lytic factor because continuous exposure to this toxin leads to hemolysis and cytolysis [4–7]. The manner by which CTX interacts with the plasma membrane is not fully understood, but there is evidence that suggests that the positively charged amino acid residues of CTX interact with some anionic domains of the plasmalemmal lipid molecules, thus leading to disorganization of the plasma membrane [8–11]. In concordance with this notion, it has been shown that high concentrations of extracellular Ca^{2+} can prevent the action of CTX, presumably by competing with CTX for the same anionic sites. For instance, Chen et al. [12] and Jiang et al. [6] reported that 10 mM Ca^{2+} inhibited CTX-induced hemolysis. Leung et al. [4] also demonstrated that CTX-induced cytolysis of Ehrlich ascites tumor cells was attenuated by high Ca^{2+} concentrations. In addition, high Ca^{2+} concentrations also inhibited the contracture of skeletal and cardiac muscles that was triggered by CTX [13–15]. High concentrations of Ca^{2+} could also block the binding of radiolabeled CTX to membranes of axons [8], skeletal muscles [13] and erythrocytes [16].

Vascular endothelial cells respond to many vasoactive substances by releasing a number of factors, such as the endothelium-derived relaxation factor (now known as nitric oxide) and endothelin, which can modulate the tone of the underlying vascular smooth muscle [17]. The endothelium is in immediate contact with CTX, once this toxin invades the circulatory system. We previously showed that, in endothelium-intact rat aortic rings, CTX-induced contraction was preceded by a small and transient relaxation and that CTX could also transiently suppress phenylephrine-induced contraction in an endothelium-dependent manner [18]. These functional studies suggest that CTX damaged the endothelial plasmalemma, thus permitting Ca^{2+} influx and subsequent nitric oxide release. However, despite the well-recognized hemodynamic effects of CTX, direct toxic effects of CTX on isolated endothelial cells have not been demonstrated hitherto. Whether or not high levels of Ca^{2+} can also protect endothelial cells from CTX-induced injury is therefore unknown. Furthermore, previous studies on CTX effects used either cell membranes or a group (population) of cells, and there has not been any work reporting changes in single cells after CTX treatment. In this study, using the trypan blue exclusion test and the fura-2 microfluorimetric technique to measure $[Ca^{2+}]_i$ in single cells, it was shown that in 1.2 mM Ca^{2+}-containing HBSS, treatment of rabbit aortic endothelial cells (RAECs) with CTX led to a substantial $[Ca^{2+}]_i$ elevation prior to plasma membrane damage and eventual cell lysis. However, RAECs preincubated in medium containing high Ca^{2+} levels (7–10 mM) were protected from CTX-induced injury. Although there have been many reports showing that high Ca^{2+} (or divalent cation) concentrations could protect cells from CTX-induced structural damage, whether functional integrity is preserved or not in these protected cells has not been demonstrated hitherto. Here, we show that CTX-treated RAECs that were protected by high levels of Ca^{2+} could generate Ca^{2+} signals (in response to agonists), similar to those of untreated cells, suggesting that high levels of Ca^{2+} could maintain the functional integrity of CTX-challenged endothelium.

2. Materials and methods

2.1. Materials

Medium 199, penicillin, streptomycin and fetal bovine serum (FBS) were obtained from Gibco BRL (Gaithersburg, MD, USA). Fura-2 AM, trypan blue, mepacrine, neomycin and ATP were purchased from Sigma (St. Louis, MO, USA). Bradykinin was purchased from Peninsula Laboratories, (Belmont, CA, USA). CTX was purified from the venom of *Naja naja atra* by a three-step column chromatography method, as previously described [15]. Phospholipase A_2 (PLA_2) activity was found to be very low (0.05–0.15%) in the purified CTX using a standard pH–stat assay [15]. Mepacrine, an inhibitor of PLA_2, did not prevent the cytotoxic action of CTX (see Section 3), suggesting that the CTX-induced cytotoxicity was not due to the trace amount of contaminating PLA_2.

Neurotoxin was also purified from the same snake venom by carboxymethyl (CM) Sephadex G-25 column chromatography [15]. All other chemicals were of reagent grade.

2.2. Culture of endothelial cells

Endothelial cells were isolated from the thoracic aorta of New Zealand white rabbits (weighing 1.5 to 2.5 kg) in the following manner. Under sterile conditions, the thoracic aorta was removed and placed in Hank's balanced salt solution (HBSS) without Ca^{2+} and Mg^{2+} (Gibco). After careful removal of the surrounding fat and connective tissue, the luminal surface was incubated in HBSS containing 0.25% trypsin and 1 mM EDTA (Gibco) for 5 min at 37°C. Thereafter, the luminal surface was gently flushed with Medium 199 supplemented with 20% FBS, penicillin (100 U/ml) and streptomycin (100 μg/ml) (enriched Medium 199). The effluent was collected and centrifuged (200 *g*) for 10 min. The cell pellet was resuspended in enriched Medium 199 and seeded onto six-well tissue culture plates (Costar, Cambridge, MA, USA). The cells were maintained in the same culture medium in a humidified atmosphere of 5% CO_2 at 37°C and were passaged about once a week. HBSS containing 0.05% trypsin and 0.53 mM EDTA (Gibco) was used to detach cells. All RAECs used in this study were between passage numbers four and ten.

The identity of the endothelial cells was indicated by their typical cobblestone appearance (Fig. 3a) and confirmed by positive immunofluorescence using an anti-von Willebrand factor VIII antibody (Sigma) (not shown).

2.3. Determination of cell viability

HBSS, composed of (mM) 138 NaCl, 5.3 KCl, 0.8 $MgSO_4$, 1.2 $CaCl_2$, 0.44 KH_2PO_4, 0.34 Na_2HPO_4, 5 glucose and 25 HEPES, buffered at 7.4, was used for washing and incubation. RAECs were gently washed once and cell viability was examined by the trypan blue (0.1% final concentration) exclusion test, which was performed after treatment with or without CTX for 20 min (except in Fig. 5) at room temperature. In each experiment, 100 cells in each treatment group were counted at random under a light microscope.

2.4. Fura-2 fluorescence measurement in a single RAEC

The cytosolic free Ca^{2+} concentration ($[Ca^{2+}]_i$) in a single RAEC was measured using the Ca^{2+}-sensitive fluorescence dye, fura-2. HBSS, having the composition mentioned above, was used for washing and for fluorescence measurements. RAECs were grown on glass coverslips for 24–48 h, washed once with HBSS and then incubated in Medium 199 containing 2% FBS and 1 μM fura-2 acetoxy methylester for 30 min at 37°C. Thereafter, the fura-2-loaded cells were washed twice with HBSS, bathed in 500 μl of HBSS and the coverslip was mounted in a small plastic chamber. The latter was then put on the stage of an inverted microscope (Nikon, Tokyo, Japan). Single cells were selected using a rectangular diaphragm that was fitted into the emission port of the microscope, which was, in turn, coupled to a photomultiplier of the fluorescence instrument (Photon Technology International, South Brunswick, NJ, USA). The selected cell was excited alternately at 340 and 380 nm and the emitted fluorescence was detected at 510 nm. After the fluorescence signals stabilized, drugs or agonists were added in small volumes (≤ 5 μl) followed by very gentle mixing. All experiments were performed at room temperature.

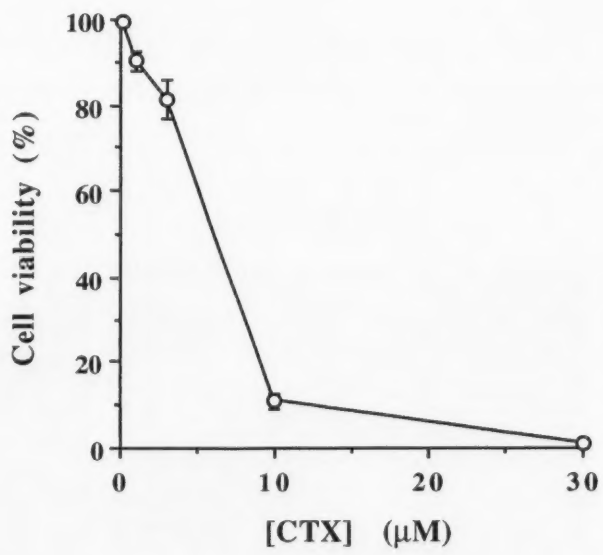

Fig. 1. CTX caused the concentration-dependent death of RAECs. Cells in HBSS containing 1.2 mM Ca^{2+} were treated with different concentrations of CTX for 20 min prior to a trypan blue exclusion test. Results are expressed as the mean ± SE of four separate experiments.

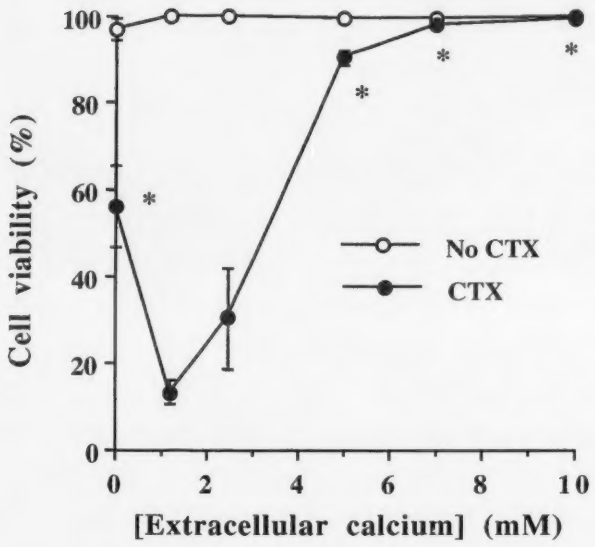

Fig. 2. Effects of extracellular Ca^{2+} concentration on CTX-induced RAEC death. Cells in HBSS containing various concentrations of Ca^{2+} were incubated with (solid circle) or without (open circle) CTX (10 μM) for 20 min and cell viability was then examined. Under Ca^{2+}-free conditions, 50 μM EGTA was added. Results are expressed as the mean ± SE of six separate experiments. An * indicates statistical significance compared to CTX-treated RAECs in HBSS containing 1.2 mM Ca^{2+} ($P < 0.05$).

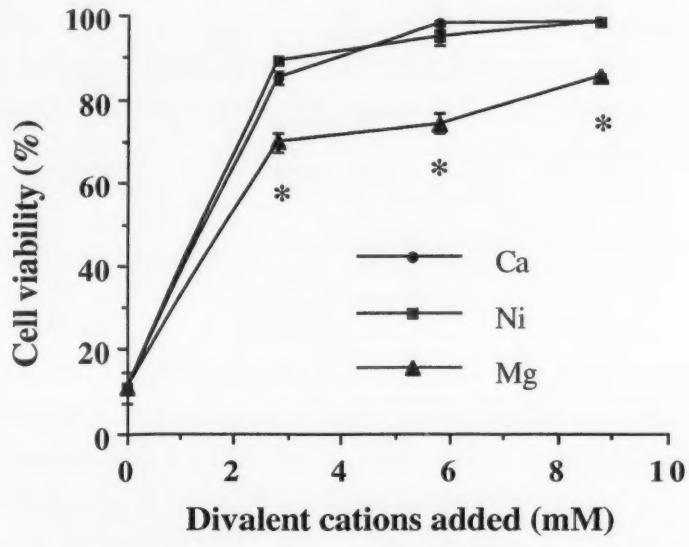

Fig. 4. The protective effects of high Ca^{2+}, Ni^{2+} and Mg^{2+} on CTX-induced cell death. Cells were initially bathed in 1.2 mM Ca^{2+}-containing HBSS. Various concentrations of Ca^{2+}, Ni^{2+} and Mg^{2+}, and CTX (10 μM) were then added for 20 min prior to the trypan blue exclusion test. Results are expressed as the mean ± SE of four separate experiments. * The protective effect of Mg^{2+} was significantly less prominent than that of Ca^{2+} or Ni^{2+} ($P < 0.05$).

2.5. Statistical analysis

The results were expressed as mean ± SEM. The Student's paired *t*-test was employed and differences were considered significant when $P < 0.05$.

3. Results

Fig. 1 shows that CTX (1–30 μM) caused cell death in 1.2 mM Ca^{2+} medium in a concentration-dependent manner. The concentration of CTX that caused 50% cell death was about 6.5 μM. As a negative control, neurotoxin, also present in snake venom and having structural similarity to CTX, did not cause cell death, even at a concentration of 50 μM (cell viability = 99.7 ± 0.3%; $n = 3$). Fig. 2 shows that extracellular Ca^{2+} exhibited a concentration-dependent biphasic effect on CTX-induced cytotoxicity. CTX-induced cytotoxicity was higher in 1.2 mM Ca^{2+}-containing HBSS than in Ca^{2+}-free HBSS. However, increasing the concentration of Ca^{2+} in

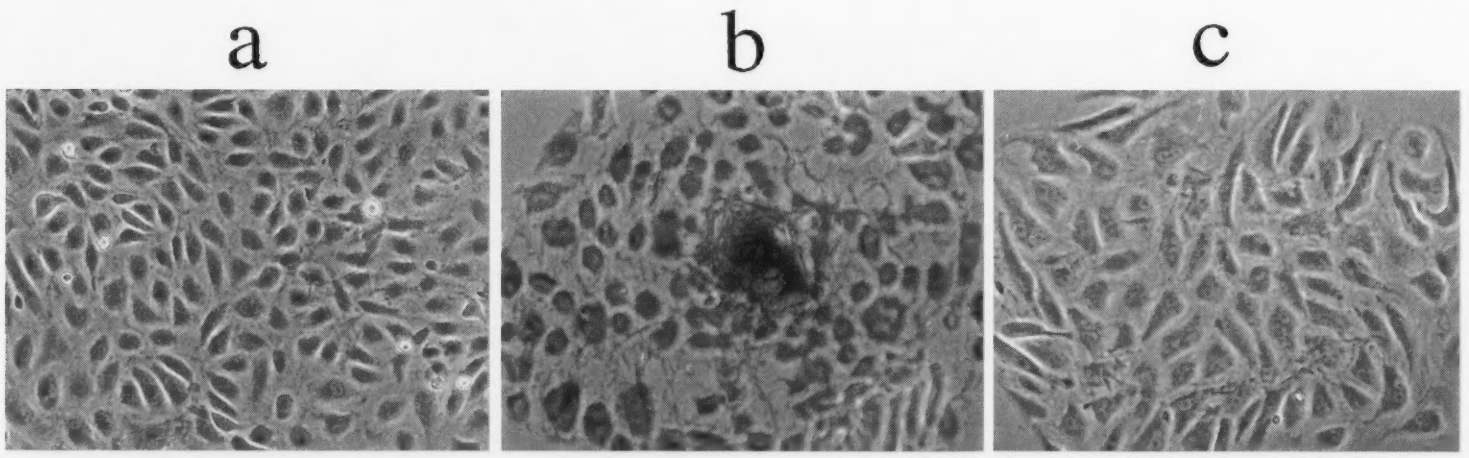

Fig. 3. Protective effect of high levels of Ca^{2+} on CTX-induced RAEC damage. (a) Untreated control cells in 1.2 mM Ca^{2+}-containing HBSS. (b) and (c) Cells were treated with 10 μM CTX in HBSS containing, 1.2 and 7 mM Ca^{2+} for 20 min, respectively. Thereafter, trypan blue (0.1% final concentration) was added. Magnification = 400 ×.

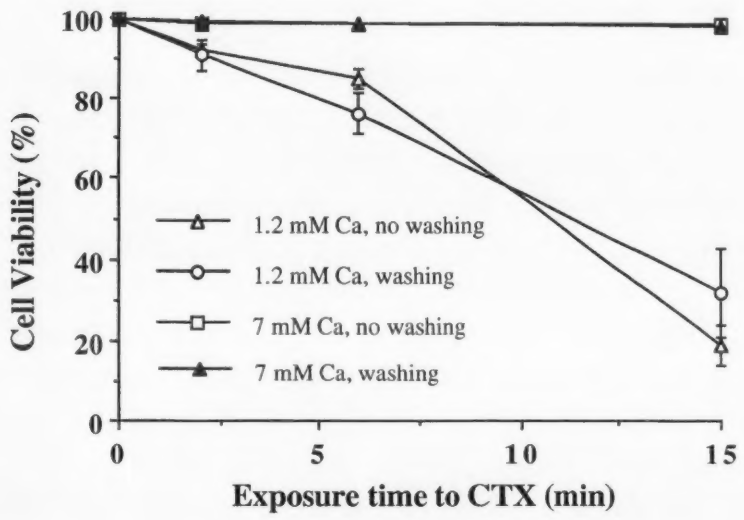

Fig. 5. The effect of the washing out of CTX on cell death during the course of CTX treatment. RAECs were initially bathed in 1.2 mM Ca^{2+} or 7 mM Ca^{2+}-containing HBSS. CTX (10 μM) was then added and cell death was determined at 2, 6 and 15 min (open triangle, square). CTX (10 μM) was also added to other groups, which were washed extensively for 30 s with 1.2 mM Ca^{2+}-containing HBSS at 2, 6 or 15 min (circle, closed triangle). These groups were then bathed in 1.2 mM Ca^{2+}-containing HBSS for a further 13, 9 or 0 min, respectively, before the trypan blue exclusion test was performed. Results are expressed as the mean ± SE of five separate experiments.

HBSS attenuated CTX-induced cytotoxicity so that in 7–10 mM Ca^{2+} HBSS, nearly all cells were protected. CTX-induced cytotoxicity and the protective effects of high Ca^{2+} were also obvious when cell morphology was examined. Fig. 3a and b show, respectively, the morphology of RAEC incubated in the absence and presence of CTX (10 μM) in 1.2 mM Ca^{2+} HBSS for 20 min. The majority of CTX-treated cells exhibited necrosis and were stained with trypan blue. However, in 7 mM Ca^{2+} HBSS, almost all the CTX-treated cells retained normal morphology (Fig. 3c).

We also tested to see if other divalent cations could prevent CTX-induced cytotoxicity in RAECs. Fig. 4 shows that high concentrations of Ni^{2+} were as effective as high concentration of Ca^{2+} in inhibiting the action of CTX. Mg^{2+} also elicited a substantial protective effect, but was significantly less effective than Ca^{2+} or Ni^{2+} ($P < 0.05$).

We next tested the reversibility of CTX action (Fig. 5). Treatment of RAECs with 10 μM CTX in 1.2 mM Ca^{2+} medium resulted in a time-dependent

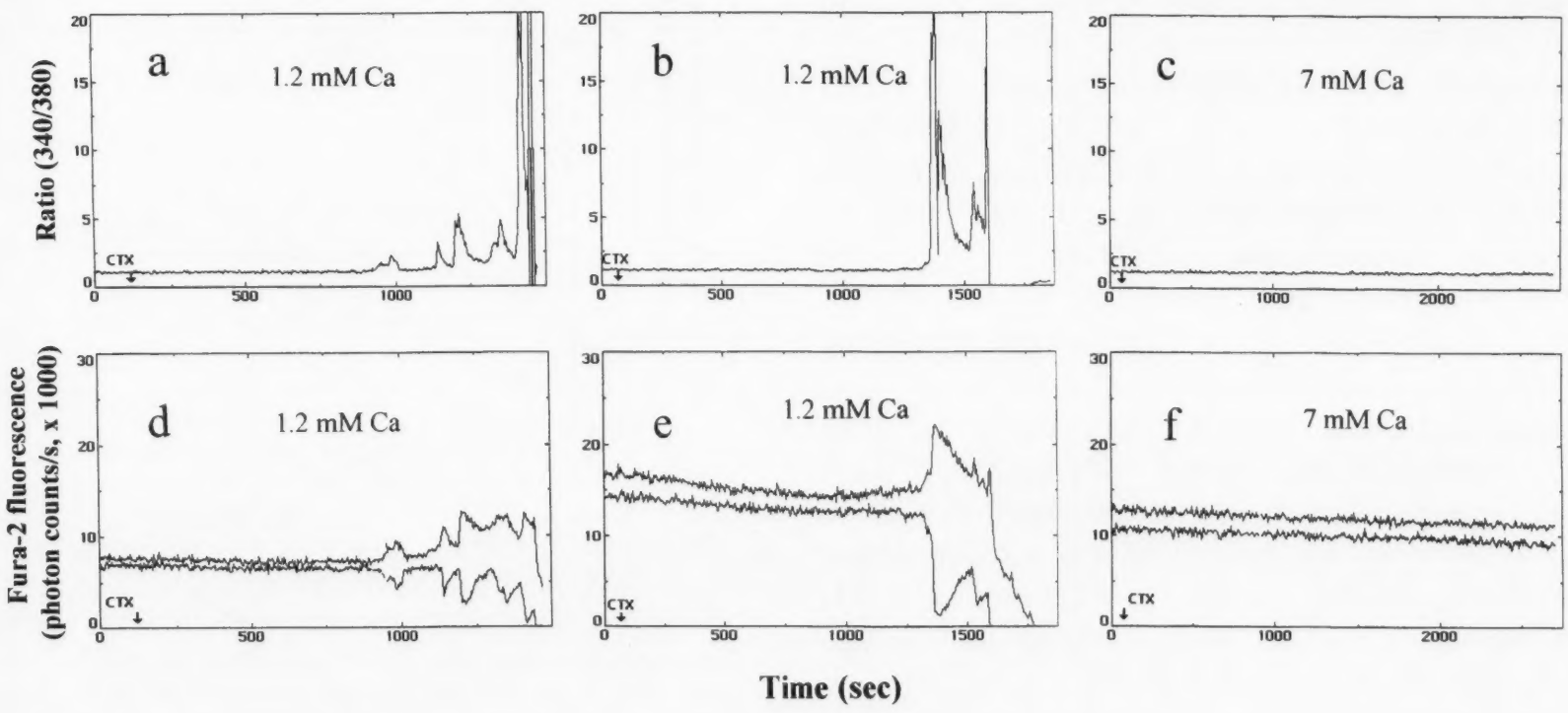

Fig. 6. The effect of CTX on $[Ca^{2+}]_i$ of a single RAEC. A fura-2-loaded RAEC in 1.2 mM Ca^{2+}-containing HBSS (a and b) or 7 mM Ca^{2+}-containing HBSS (c) was treated with 10 μM CTX (arrow). The *y*-axis represents the fura-2 fluorescence ratio of 340 nm/380 nm. Small fluctuations in $[Ca^{2+}]_i$ before the substantial $[Ca^{2+}]_i$ elevation (a) was observed in eight out of eleven cells, while the other three cells did not exhibit fluctuation before the large $[Ca^{2+}]_i$ surge (b). In (a) and (b), there was a variation in the time (7–35 min) between CTX exposure and the abrupt increase (''burst'') in the ratio value. The result shown in (c) was observed in at least three other cells tested. (d), (e) and (f) show the corresponding fluorescence at 340 nm (upper trace) and 380 nm (lower trace) of samples (a), (b) and (c), respectively.

increase in cell death. If RAECs were treated with CTX for 2 min, then washed extensively and checked for viability after 13 min, the degree of cytotoxicity was similar to that observed at the 2-min time point. This result suggests that CTX could be washed away so that there was no further cell damage during the 13 min incubation. A similar result was obtained at the 6-min time point. Ca^{2+} (7 mM) offered almost complete protection against CTX-induced cytotoxicity at all time points, regardless of whether the ''wash-out'' protocol was employed or not.

CTX has been known to activate PLA_2 and phospholipase C [3]. We investigated if the CTX-induced toxicity was due to activation of these enzymes. Mepacrine (100 μM, an inhibitor of PLA_2) did not prevent CTX-induced cytotoxicity in Ca^{2+}-containing medium (cell viability = 4.4 ± 1.0% in CTX-treated group versus 5.1 ± 1.1% in CTX- and mepacrine-treated group; $n = 8$) or Ca^{2+}-free medium (cell viability = 17.1 ± 0.7% in CTX-treated group versus 14.2 ± 1.0% in CTX- and mepacrine-treated group; $n = 8$). Neomycin (100 μM, an inhibitor of phospholipase C) also did not prevent CTX-induced cytotoxicity in Ca^{2+}-containing medium (cell viability = 5.9 ± 0.7% in CTX-treated group versus 6.6 ± 0.8% in CTX- and neomycin-treated group; $n = 8$) or Ca^{2+}-free medium (cell viability = 16.4 ± 1.0% in CTX-treated group versus 16.1 ± 1.4% in CTX- and neomycin-treated group; $n = 8$). Therefore, activation of PLA_2 and phospholipase C did not appear to mediate the cytotoxic action of CTX.

The protective effects caused by high concentrations of divalent cations on CTX-induced membrane damage were also demonstrated using the fura-2 fluorescence technique. In HBSS containing 1.2 mM Ca^{2+}, a single RAEC treated with CTX (10 μM) showed a tremendous (340 nm/380 nm fluorescence ratio > 20) $[Ca^{2+}]_i$ elevation after a variable period of 7–35 min (26.5 ± 4.2 min; $n = 11$; mean ± SEM) (Fig. 6a–b). A smaller $[Ca^{2+}]_i$ elevation was observed prior to the tremendous $[Ca^{2+}]_i$ elevation in eight out of eleven cells tested (Fig. 6a). Fig. 6d–e show the fluorescence changes (at 340 and 380 nm) of the experiment shown in Fig. 6a–b, respectively. The fluorescence changes at these two wavelengths were opposite (i.e., rise and fall at 340 and 380 nm, respectively) and, therefore, genuinely reflects $[Ca^{2+}]_i$ elevation. Note that at the very late stage, the ratio fluctuated dramatically and subsequently dropped to zero (Fig. 6a–b). The corresponding fluorescence at 340 and 380 nm also eventually dropped to zero (Fig. 6d–e), probably due to the leakage of fura-2 from the severely damaged single cell, being infinitely diluted by the large volume of the extracellular medium. The addition of 7 mM Ca^{2+} during or immediately after the large $[Ca^{2+}]_i$ elevation did not prevent the cell from disruption (not shown). However, there was no persistent elevation in $[Ca^{2+}]_i$ in CTX-treated RAECs for 40 min, if the HBSS already contained 7 mM Ca^{2+} at the beginning of the experiment (Fig. 6cFig. 6f). The protective effect of high Ca^{2+} concentrations could also be achieved by 7 mM Ni^{2+} (Fig. 7), which quenches fura-2 fluorescence at all excitation wavelengths [19]. When RAECs were treated with 10

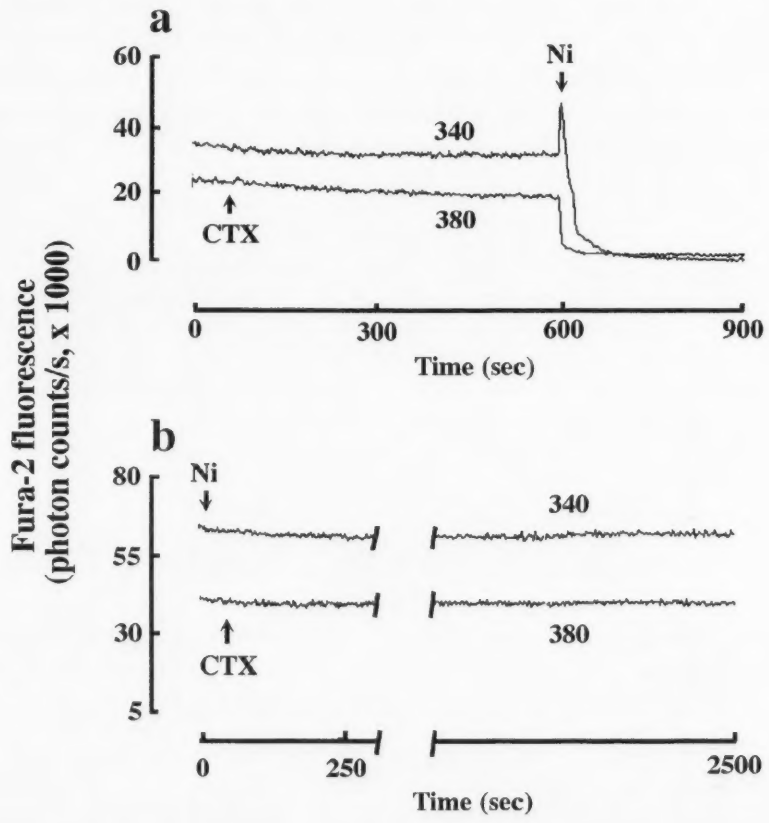

Fig. 7. High Ni^{2+} prevented CTX-induced plasma membrane leakiness in single RAECs. In (a) and (b), the upper and lower traces represent fura-2 fluorescence at 340 and 380 nm, respectively. (a) A fura-2-loaded RAEC in 1.2 mM Ca^{2+}-containing HBSS was exposed to 10 μM CTX. As soon as the fluorescence at 340 and 380 nm began to increase and decrease, respectively, 7 mM Ni^{2+} was added. (b) A fura-2-loaded RAEC in 1.2 mM Ca^{2+}-containing HBSS was treated with 7 mM Ni^{2+} before CTX (10 μM) challenge. Similar results were obtained in four other separate experiments. In (a), there was a variation in the time (7–30 min) between CTX exposure and the changes in fluorescence at both wavelengths.

μM CTX in 1.2 mM Ca^{2+} HBSS for some 3–30 min, there was an increase and decrease in fura-2 fluorescence at 340 and 380 nm, respectively, indicating Ca^{2+} influx and, hence, CTX-induced permeabilization (Fig. 7a). When Ni^{2+} was then added, the fura-2 fluorescence at both 340 and 380 nm was completely quenched, indicating the entrance of Ni^{2+} into the cytosol. However, when RAECs were preincubated with Ni^{2+} before CTX treatment, there was no change in fluorescence at both wavelengths for 40 min (Fig. 7b), suggesting that neither $[Ca^{2+}]_i$ elevation nor Ni^{2+} entry took place. The results in Figs. 6 and 7 thus suggest that high Ca^{2+}- or Ni^{2+} concentrations could prevent CTX-induced membrane damage.

The results obtained so far indicate that high concentrations of divalent cations could maintain the structural integrity of the plasma membrane of CTX-treated RAECs, thus preventing the cells from membrane leakiness and necrosis. However, whether such protected cells remain functionally intact or not is unclear. One approach to examine this is to test how well the protected RAECs respond to physiological agonists by generating Ca^{2+} signals. In cells bathed in 1.2 mM Ca^{2+}, or 7 mM Ca^{2+}, or cells bathed in 7 mM Ca^{2+} and treated with 10 μM CTX, bradykinin evoked a surge in $[Ca^{2+}]_i$, followed by a gradual decline to a plateau level that was slightly above the resting $[Ca^{2+}]_i$ (Fig. 8a–c). There is no significant difference in magnitude between the bradykinin-stimulated Ca^{2+} responses (peak and tonic) under the three different conditions used (Fig. 8d). Similar results were obtained when extracellular ATP was used as an agonist (Fig. 8e). We did not use high Mg^{2+} and Ni^{2+} in this experiment, as these two cations, besides protecting the RAECs, may exert inhibitory effects on plasmalemmal Ca^{2+} channels [20].

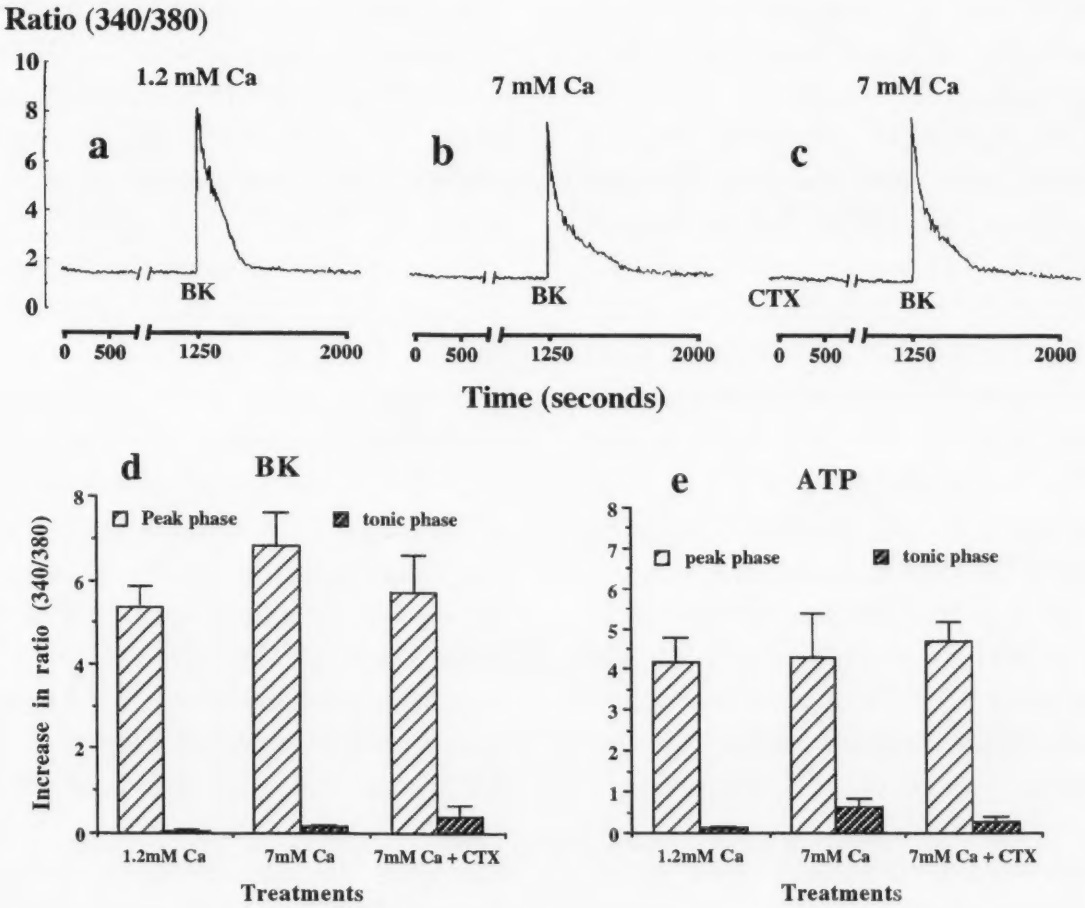

Fig. 8. Agonist-induced Ca^{2+} signaling was unaffected in high Ca^{2+}-protected, CTX-treated RAECs. Single fura-2-loaded RAECs in HBSS containing 1.2 or 7 mM Ca^{2+}, with or without CTX (10 μM) pretreatment for 20 min, were stimulated with bradykinin (BK, 10 μM) (a–c). The *y*-axis represents the fura-2 fluorescence ratio of 340 nm/380 nm. Results are quantified and shown in (d). The ratio increase at peak is taken as the difference between the pre-stimulation ratio and the highest ratio after agonist addition. The ratio increase at tonic phase is the difference between the pre-stimulation ratio and the ratio at 12.5 min after agonist stimulation. Results are expressed as the mean ± SE of eight separate experiments. Similar protocols were done using ATP (100 μM) as the agonist (e). Results are the mean ± SE of ten–thirteen separate experiments.

4. Discussion

Although there have been a number of publications demonstrating the interactions of CTX with various types of tissues [3] and its effect on the circulatory system [14,15,18,21], our report is the first to directly demonstrate the cytotoxic actions of CTX on isolated endothelial cells and the protection of these cells from CTX-induced injury by divalent cations. Our studies are of interest as endothelial cells are in immediate contact with CTX once this toxin invades the circulation. The uptake of trypan blue, membrane necrosis, and substantial leakiness to Ca^{2+} and Ni^{2+} observed in CTX-treated RAECs (Figs. 1, 3, 6 and 7), consistently suggest that CTX caused elevation of permeability to ions at the plasma membrane, eventually leading to membrane degeneration and cell death. The percentage of cell death increased with the exposure time to CTX (Fig. 5), a fact that is in concordance with the variable lag periods (7–35 min) between CTX application and the considerable rise in plasmalemmal permeability to Ca^{2+} and Ni^{2+} in a single RAEC (Figs. 6 and 7). These results suggest a heterogeneity in the sensitivity of individual RAECs to CTX. Our work (presented here) provides the first report showing the effects of CTX at the single-cell level. Tzeng and Chen [21] previously measured $[Ca^{2+}]_i$ changes induced by CTX in single neonatal rat cardiomyocytes. Since the $[Ca^{2+}]_i$ responses were averaged over those obtained from a large number of cell samples, this may account for their finding that $[Ca^{2+}]_i$ rose gradually during the 10-min CTX treatment. Such averaged results may mask the variable lag periods (between CTX application and $[Ca^{2+}]_i$ elevation) in individual cells, as we observed in single RAECs (Figs. 6 and 7). In our case, after the lag period in CTX-treated RAECs, $[Ca^{2+}]_i$ elevation was manifested as an abrupt ''burst'', with or without the preceding fluctuation in $[Ca^{2+}]_i$ (Fig. 6a–b; also, see below).

When RAECs were treated with CTX for 2 and 6 min, then washed extensively and checked for viability after 13 and 9 min, respectively, the degrees of cytotoxicity were similar to those checked immediately at the two time points (Fig. 5). These results indicate that, first, those cells that CTX had already damaged could not be recovered; second, those that had not yet been damaged by CTX could be prevented from cell death by extensive washing. Hence, there appears to be a critical stage during CTX-induced pore formation (permeabilization), after which membrane damage becomes irreversible. This proposal is further supported by the observation that the increase in plasmalemmal Ca^{2+} permeability in CTX-treated RAECs was abrupt, tremendous and was followed by severe membrane disruption (Fig. 6a–b). At the latter ''critical'' moment, the plasma membrane was damaged to an extent that Ni^{2+}, which usually does not permeate cells (also see Fig. 7b), could rapidly enter the cytosol (Fig. 7a).

High concentrations of Ca^{2+} have been known to inhibit CTX actions. For example, CTX-induced hemolysis, contracture of skeletal muscles and guinea pig papillary muscles were strongly suppressed by > 10 mM Ca^{2+} [12,13,15]. In a consistent manner, such high concentrations of Ca^{2+} inhibited the binding of radiolabeled CTX to axonal membranes and chick skeletal muscles [8,13]. In the present study, when added prior to CTX, high Ca^{2+} concentrations completely suppressed CTX-induced cytotoxicity (Figs. 2 and 4). It should be emphasized that such high Ca^{2+} concentrations merely represent an experimental condition rather than a pathophysiological situation. Suppression of CTX action could be mimicked by high concentrations of two other divalent cations, Mg^{2+} and Ni^{2+} (Figs. 4 and 7). The prevention of CTX actions by high concentrations of divalent cations has been demonstrated previously in hemolysis, cytolysis and contractility studies [4,6,13,15]. All these data support the hypothesis that CTX and Ca^{2+} compete for the same anionic sites at the plasmalemma [4,13]. Such anionic sites may be located in the phospholipids [9,11]. If Ca^{2+} competes with CTX at the same sites, the activity of CTX would be expected to be highest under Ca^{2+}-free conditions. It was, in fact, observed that the rate of CTX-induced hemolysis and the binding of radiolabeled CTX to erythrocytes were both enhanced when Ca^{2+} in the physiological saline was removed by excess EGTA [7,16]. Likewise, CTX-induced contraction in the rat skeletal muscle was enhanced in Ca^{2+}-free medium [22]. However, in the same study, CTX-induced contraction in human skeletal muscle was considerably depressed in Ca^{2+}-free medium. It was also found that CTX-induced contracture in guinea pig taenia coli was strongly attenuated under

Ca^{2+}-free conditions [23]. We observed that CTX-induced cytotoxicity was much lower in Ca^{2+}-free than in 1.2 mM Ca^{2+}-containing HBSS (Fig. 2). This observation also suggests that Ca^{2+} entry leading to the elevation of $[Ca^{2+}]_i$ caused by CTX may not be a necessary condition to initiate cell damage; it is more likely that it acts by aggravating the injury process leading to cell death. It should also be noted that the concentration of CTX also profoundly affects its interaction with extracellular Ca^{2+} and the subsequent damage (eg. hemolysis) at the plasma membrane [6]. We used 10 μM CTX throughout this work, but other concentrations should be investigated in future.

The prevention of CTX-induced plasmalemmal leakiness by high Ca^{2+}- and Ni^{2+} concentrations is illustrated in Figs. 6 and 7. There was no change in basal fura-2 fluorescence at all in CTX-treated cells protected by high Ca^{2+}- or Ni^{2+} concentrations, indicating that no increases in permeability to Ca^{2+} and Ni^{2+} had taken place. This experimental protocol, while demonstrating how high concentrations of Ca^{2+} and Ni^{2+} could prevent CTX-induced cytolysis, has some advantages over previous methods, such as the hemolysis assay: (1) Small molecules (i.e., Ca^{2+} and Ni^{2+}) were used as ''leakage markers'' instead of much bigger molecules such as hemoglobin; (2) the fura-2 fluorimetric method offers a much more sensitive and real-time measurement. Thus, our data further confirm that high concentrations of divalent cations can preserve the integrity of the plasma membrane of CTX-treated cells.

CTX has been known to modulate the activities of a number of enzymes at the plasma membrane. For instance, studies using purified enzymes or isolated membranes reveal that CTX inhibits Na^+/K^+-ATPase, stimulates phosphatidylinositol 4-kinase, enhances Ca^{2+}–Mg^{2+} ATPase and adenylate cyclase [2,24–26]. Whether or not high concentrations of Ca^{2+} can prevent such modulatory activities by CTX is unknown. Therefore, although the plasmalemmal integrity of CTX-treated RAECs was preserved at high concentrations of divalent cations, it still remains unknown in such protected cells whether the plasmalemmal enzyme activities were altered by CTX or not. In line with this, there is no previous report showing if high Ca^{2+}-protected, CTX-treated cells stay functionally intact or responsive to physiological stimuli. One approach to solve this problem is to test how well CTX-treated, high Ca^{2+}-protected RAECs could generate Ca^{2+} signals in response to agonists. Endothelial cells have been shown to express functional ATP (P_{2U}- and P_{2Y}-purinoceptors) and bradykinin (B_1 and B_2) receptors [27–29]. These receptors are coupled, via a G-protein ($G_{q/11}$), to phospholipase C [30], which cleaves phosphatidyl inositol 4,5-bisphosphate to form inositol 1,4,5-trisphosphate ($InsP_3$) and diacylglycerol [31]. $InsP_3$ releases Ca^{2+} from intracellular stores and, subsequently, the empty state of the stores stimulates extracellular Ca^{2+} entry [32,33]. The decline of a Ca^{2+} signal depends on the sequestration of Ca^{2+} back into the intracellular stores, and Ca^{2+} extrusion into the extracellular space achieved by the plasmalemmal Ca^{2+} pump and/or the Na^+–Ca^{2+} exchanger [34]. In high Ca^{2+} medium, the Ca^{2+} responses triggered by ATP and bradykinin in CTX-treated groups were qualitatively and quantitatively similar to those in the untreated control groups (Fig. 8), suggesting that there are intact $[Ca^{2+}]_i$ homeostatic mechanisms in CTX-treated cells. Therefore, in high Ca^{2+}-protected RAECs, CTX was unlikely to have significant effects on plasmalemmal receptors and Ca^{2+}-handling machineries, and did not seem to cause general adverse effects on plasmalemmal functions. Intracellular Ca^{2+} signalling plays an important role in endothelial cell functions. For example, an increase in endothelial $[Ca^{2+}]_i$ triggers the release of vasoactive substances, such as prostacyclin, nitric oxide and endothelin, which modulate the vascular tone [17]. The preservation of functional integrity in high Ca^{2+}-protected CTX-challenged RAECs may render the latter with the ability to control the contractility of the underlying smooth muscles.

Acknowledgements

This work was supported by grants from the Hong Kong Research Grant Council and the Heart and Stroke Foundation of Ontario. CYK is a recipient of the Heart and Stroke Foundation of Ontario. Y.M.L is a recipient of the Croucher Foundation Postdoctoral Fellowship. S.J.H. and Y.J.O are visiting scientists from the Department of Pharmacology and the Department of Histology and Embryology, respec-

tively, Sun Yat-Sen University of Medical Sciences, Guangzhou, China. S.J.H was a recipient of the Sino-British Trust Fund Visiting Fellowship.

References

[1] E. Condrea, Experientia 30 (1974) 121–129.
[2] J.L. Huang, W.R. Trumble, Toxicon 29 (1991) 31–41.
[3] J.E. Fletcher, M.S. Jiang, Toxicon 31 (1993) 669–695.
[4] W.W. Leung, W.M. Keung, Y.C. Kong, Naunyn. Schmiedeberg's Arch. Pharmacol. 292 (1976) 193–198.
[5] C.L. Hinman, E. Lepisto, R. Stevens, I.N. Montgomery, H.C. Rauch, R.A. Hudson, Toxicon 25 (1987) 1011–1014.
[6] M.S. Jiang, J.E. Fletcher, L.A. Smith, Toxicon 27 (1989) 1297–1305.
[7] L.P. Vernon, A. Rogers, Toxicon 30 (1992) 701–709.
[8] J.P. Vincent, H. Schweitz, R. Chicheportiche, M. Fosset, M. Balerna, M.C. Lenoir, M. Lazdunski, Biochemistry 15 (1976) 3171–3175.
[9] O.S. Ksenzhek, V.S. Gevod, A.M. Omel'chenko, S.N. Semenov, A.I. Sotnichenko, Mol. Biol. Mosk. 12 (1978) 1057–1065.
[10] P. Bougis, M. Tessier, J. Van Rietschoten, H. Rochat, J.F. Faucon, J. Dufourcq, Mol. Cell. Biochem. 55 (1983) 49–64.
[11] B. Gilquin, C. Roumestand, S. Zinn-Justin, A. Menez, F. Toma, Biopolymers 33 (1993) 1659–1675.
[12] Y.H. Chen, C.T. Hu, J.T. Yang, Biochem. Int. 8 (1984) 329–338.
[13] S.Y. Lin-Shiau, M.C. Huang, C.Y. Lee, J. Pharmacol. Exp. Ther. 196 (1976) 758–770.
[14] A.L. Harvey, R.J. Marshall, E. Karlsson, Toxicon 20 (1982) 379–396.
[15] S.J. Huang, C.Y. Kwan, Res. Commun. Mol. Pathol. Pharmacol. 94 (1996) 103–110.
[16] L.P. Vernon, A. Rogers, Toxicon 30 (1992) 711–721.
[17] H.M. Himmel, A.R. Whorton, H.C. Strauss, Hypertension 21 (1993) 112–127.
[18] K.H. Ho, C.Y. Kwan, S.J. Huang, J.P. Bourreau, FASEB J. 10 (1996) A440.
[19] J.E. Merritt, R. Jacob, T.J. Hallam, J. Biol. Chem. 264 (1989) 1522–1527.
[20] B. Hille, in: Ionic channels of excitable membranes, Sinauer, Massachusetts, 1992, pp. 83–114.
[21] W.F. Tzeng, Y.H. Chen, Biochem. J. 256 (1988) 89–95.
[22] J.E. Fletcher, F.H. Lizzo, Toxicon 25 (1987) 1003–1010.
[23] S.Y. Lin-Shiau, H.C. Huang, C.Y. Lee, Toxicon 24 (1986) 131–139.
[24] C.C. Chen, S.Y. Lin-Shiau, Biochem. Pharmacol. 34 (1985) 2335–2341.
[25] D.H. Walker, L.J. Pike, Biochim. Biophys. Acta 1055 (1990) 295–298.
[26] W. Huang, L.P. Vernon, J.D. Bell, Toxicon 32 (1994) 789–797.
[27] A. Bowden, V. Patel, C. Brown, M.R. Boarder, Br. J. Pharmacol. 116 (1995) 2563–2568.
[28] C. Brown, B. Tanna, M.R. Boarder, Br. J. Pharmacol. 116 (1995) 2413–2416.
[29] J.A. Smith, C. Webb, J. Holford, G.M. Burgess, Mol. Pharmacol. 47 (1995) 525–534.
[30] S.P. Watson, D. Girdlestone, Trends Pharmacol. Sci. Receptor and ion channel nomenclature supplement (7th edition) (1996) 54.
[31] M.J. Berridge, Annu. Rev. Biochem. 56 (1987) 159–193.
[32] M.J. Berridge, R.F. Irvine, Nature 341 (1989) 197–205.
[33] J.W. Putney Jr., Cell Calcium 11 (1990) 611–624.
[34] D.E. Clapham, Cell 80 (1995) 259–268.

ELSEVIER

Biochimica et Biophysica Acta 1330 (1997) 39–49

BIOCHIMICA ET BIOPHYSICA ACTA
BBA

Potassium transport in opossum kidney cells: Effects of Na-selective and K-selective ionizable cryptands, and of valinomycin, FCCP and nystatin

Alain Loiseau *, Christine Leroy, Madeleine Castaing

U-426 INSERM, BP 416, F-75870 Paris Cedex 18, France

Received 1 April 1997; revised 29 May 1997; accepted 5 June 1997

Abstract

The effects of two ionizable cryptands, the Na-selective $(221)C_{10}$ and the K-selective $(222)C_{10}$, and of valinomycin, FCCP and nystatin on K^+ fluxes in opossum kidney (OK) cells have been quantified. The Na,K-ATPase (ouabain-sensitive ^{86}Rb influx) was stimulated by nystatin ($\geq 20\%$), and inhibited by the other ionophores (50–80%), by barium (K-channel blocker) (61%) and by amiloride (Na entry blocker) (34%). The V_{max} of the Na,K-ATPase phosphatase activity was unmodified by the ionophores, indicating the absence of direct interaction with the enzyme. The ATPi content was unmodified by the inhibitors and nystatin, but was lowered by $(221)C_{10}$ (47%), $(222)C_{10}$ (75%), valinomycin (72%) and FCCP (88%). Amiloride was found to partially remove the inhibition caused by $(222)C_{10}$ (51%) and valinomycin (49%). Rb efflux was stimulated by nystatin (32%), unmodified by valinomycin, and was inhibited by $(221)C_{10}$ (19%), $(222)C_{10}$ (19%) and FCCP (10%). Barium (39%) and amiloride (32%) inhibited this efflux and, in their presence, the nystatin effect persisted, whereas that of the other ionophores vanished. At pH 6.4, the Rb efflux decreased by 14% of its value at pH 7.4, with no additional inhibition by cryptands. Cryptands are shown to inhibit the pH-sensitive K^+-conductance, probably by inducing a K^+–H^+ exchange at the plasma membrane, and by uncoupling oxidative phosphorylation by inducing the entry of K^+ and H^+ (and possibly Ca^{2+}) ions into the mitochondria. © 1997 Elsevier Science B.V.

Keywords: OK (opossum kidney) cell; Ionizable and neutral ionophore; K^+ flux; Na,K-ATPase activity; Cell ATPi content; Inhibitor

1. Introduction

One third of the energy requirement of animal cells is expended in keeping K^+ inside and Na^+ outside the plasma membrane. Whether cells maintain high Na^+ and K^+ gradients simply to preserve their metabolic integrity or, as in kidney, because transport of these ions is inherent to the function of the organ, they all use essentially the same basic mechanism utilizing the sodium- and potassium-activated adenosine triphosphatase (Na,K-ATPase), an enzyme located in the plasma membrane [1]. Since this enzyme helps maintain the osmotic balance across

Abbreviations: $(221)C_{10}$-cryptand, diaza-1,10-decyl-5-penta-oxa-4,7,13,16,21-bicyclo[8.8.5]tricosane; $(222)C_{10}$-cryptand, diaza-1,10-decyl-5-hexaoxa-4,7,13,16,21,24-bicyclo[8.8.8]hexacosane; Na-selective $(221)C_{10}$-cryptand, Na^+ over K^+ selective $(221)C_{10}$-cryptand; K-selective $(222)C_{10}$-cryptand, K^+ over Na^+ selective $(222)C_{10}$-cryptand; FCCP, carbonylcyanide *p*-trifluoro-methoxyphenyl-hydrazone; ouabain-sensitive Rb influx, ouabain-sensitive ^{86}Rb influx; Rb efflux, ^{86}Rb efflux; V_{max}, maximal rate of the Na,K-ATPase phosphatase activity; ATPi content, cell ATP content; HEPES, *N*-[2-hydroethyl]piperazine-*N'*-[2-ethane-sulfonic acid]

* Corresponding author. Fax: (33) 1 42 28 15 64.

0005-2736/97/$17.00 © 1997 Elsevier Science B.V. All rights reserved.
PII S0005-2736(97)00140-5

cell membranes, by keeping the intracellular Na concentration low, balancing the negatively charged organic molecules, confined inside the cell, is performed largely by K^+. This ion is actively pumped into the cell by the Na,K-ATPase and can also move freely in or out through the K^+ leak channels in the plasma membrane [2].

For the purpose of understanding the molecular basis of cellular processes controlled by ions, ionophores have been widely used by cell biologists over the past thirty years as tools to increase the ion permeability of cell membranes. Among these ionophores, the K^+-selective carrier, valinomycin, the H^+-carrier, FCCP, and the channel-forming compound, nystatin, deserve special attention. Valinomycin, a neutral antibiotic, has been used to investigate the involvement of K^+ gradients, membrane potentials and K^+ permeability within cell membranes [3,4]. While inducing K^+ entry into the mitochondrial matrix, valinomycin also promotes the uncoupling of oxidative phosphorylation from respiration [5,6]. The protonophore, FCCP, a lipid-soluble weak acid, has been used mainly as a potent uncoupler of mitochondrial phosphorylation [6,7], and also has frequently been used to allow H^+ exchange across membranes against alkali cations carried by ionophores like valinomycin [8]. The polyene antibiotic, nystatin, which displays a channel-forming activity, increases the permeability of sterol-containing membranes to anions, and to Li^+, Na^+, K^+ and H^+ ions [9,10]. This compound has been used essentially to stimulate the Na,K-ATPase activity by increasing intracellular Na [11], and it does not exert an uncoupling effect on the mitochondria [12]. A detailed study of the effects of these three ionophores on K^+ transport in the proximal tubule has shown that their actions were localized at the plasma membrane (nystatin), the mitochondrial membrane (FCCP), or at both (valinomycin) [12].

More recently, another type of ionophore, i.e., the synthetic agents called cryptands, have attracted increasing interest [13]. These compounds form very stable complexes with various substrates, especially with monovalent and divalent cations [14] (Table 1), and it has been demonstrated that the (221)C_{10} and (222)C_{10} lipophilic cryptands induced the transport of competing K^+ and Na^+ ions through thin lipid membranes [15,16]. Due to the stated difference in specificity, these two cryptands may be expected to produce different effects. However, the affinity of either cryptand is sufficient to bind cellular concentrations of either Na^+ or K^+ [15,16]. Outside the cell, where K^+ is low, either cryptand should bind and transport Na^+; whereas inside, where Na^+ is low, the same may be true for K^+. Also (since they are ionizable), these cryptands have been found to elicit a cation-H^+ exchange across membranes without the need for a proton carrier [17,18].

Table 1
Ionic radii of cations and association constants (K_a) of cations to cryptands, in water at 25°C [14]

Ionic radius (Å)		K_a (M^{-1})	
		(221)-cryptand	(222)-cryptand
		Cavity radius 1.1 Å	Cavity radius 1.4 Å
Na^+	0.98	$2.5 \cdot 10^5$	$7.9 \cdot 10^3$
K^+	1.33	$8.9 \cdot 10^3$	$2.5 \cdot 10^5$
Rb^+	1.49	$3.5 \cdot 10^2$	$2.2 \cdot 10^4$
Ca^{2+}	1.06	$8.9 \cdot 10^6$	$2.5 \cdot 10^4$
Ba^{2+}	1.43	$2.0 \cdot 10^6$	$3.2 \cdot 10^9$

The Na^+ over K^+ selectivity of the hydrophilic (221)-cryptand and the K^+ over Na^+ selectivity of the hydrophilic (222)-cryptand, calculated using the K_a values, are equal to ~ 30.
Note: When competing Na^+ and K^+ ions are transported through thin lipid membranes at identical concentrations, the competitive transport selectivities have lower values, i.e., the Na^+ over K^+ transport selectivity of the (221)C_{10}-cryptand and the K^+ over Na^+ transport selectivity of the (222)C_{10}-cryptand at 25°C are equal to 1.5 and 2.5, respectively [15,16].
Our interpretations of the present data are based upon this observation.

Due to the selectivity of (221)C_{10} for Na^+ over K^+ and its potential ability to carry Ca^{2+} ions under physiological conditions, whereas (222)C_{10} exhibits selectivity for K^+ over Na^+ and might be blocked by barium (K^+-channel blocker), it seemed of interest to investigate the action of such compounds at the cellular level. Until now, it has only been shown that (221)C_{10} was as efficient as nystatin at reversing the cellular Na^+ and K^+ gradients [19], and at stimulating the oxidative metabolism of isolated tubules of rat nephron [20]. However, the molecular mechanisms underlying these effects have not yet been elucidated.

The present study is the first to focus on the effects of ionizable cryptands on K^+ transport by an established cell line, the opossum kidney (OK) cell, de-

rived from the cortex of the American opossum. These cells are known to express several K^+ channels [21–24], and K^+-conductance, via these pathways, is intracellular pH-sensitive and can be blocked by barium [21,23]. Besides, K^+ exit from these cells also occurs via a K/H antiporter that, under normal conditions, would participate in intracellular pH regulation [25], together with an amiloride-sensitive Na/H exchanger [26]. As in other animal cells, a major part of K^+ entry into OK cells is ensured by the Na,K-ATPase and, to a limited extent, by a Na,K/2Cl cotransporter. Because the complex interplay between the intracellular pH and Na^+, and the K^+ fluxes across their apical and basolateral membranes, is well known, the OK cells present a unique opportunity to study the effects of two ionophores transporting Na^+, K^+ and H^+ ions, i.e., the Na-selective $(221)C_{10}$ and the K-selective $(222)C_{10}$. This study quantifies the effects of the $(221)C_{10}$- and $(222)C_{10}$-cryptands on: The ouabain-sensitive ^{86}Rb influx, which is attributable to the functioning of the Na,K-ATPase; the maximal rate of the Na,K-ATPase phosphatase activity (V_{max}); the cells' ATP content and ^{86}Rb efflux, in the presence or absence of barium (K^+-channel blocker) and amiloride (Na^+-channels and Na/H antiporter blocker). The effects of valinomycin, FCCP and nystatin on these parameters have also been quantified and compared to those of the two cryptands. The results are discussed in terms of the ionic selectivities of the ionophores and of their structural characteristics. They are interpreted in terms of the ionophore's action at the plasma membrane (nystatin), or at the mitochondrial membrane (valinomycin) or both [$(221)C_{10}$, $(222)C_{10}$ and FCCP].

2. Materials and methods

2.1. Materials

$^{86}RbCl$ (0.5–10 mCi/mg Rb) was obtained from Amersham (Buckinghamshire, UK) and the Quicksafe A scintillator was from Zinsser Analytic (Frankfurt, Germany). The ATP assay kit was purchased from Calbiochem (San Diego, CA, USA) and FCCP was from Boëhringer (Mannheim, Germany). $(221)C_{10}$-cryptand, $(222)C_{10}$-cryptand, absolute ethanol for spectroscopy, NaCl, KCl, $MgSO_4$, $CaCl_2$, 2 H_2O, D-glucose, NaOH, KOH, $MgCl_2$, 6 H_2O, perchloric acid (70–72%), $BaCl_2$, 2 H_2O, NaH_2PO_4, H_2O, hydrochloric acid (37%) and ammonium heptamolybdate tetrahydrate were obtained from Merck (Darmstadt, Germany). Ouabain, amiloride, valinomycin, nystatin, dimethyl sulfoxide, trypan blue, ATP(2Na), BRIJ (polyoxyethylene-20-cetyl ether), triton X-100 and HEPES were purchased from Sigma (St. Louis, MO, USA). D-Mannitol and sulfuric acid (98% min.) were from Prolabo (Paris, France) and HCl was from Prosciences (Paris, France). Culture media and reagents were from Gibco-BRL (Paisley, UK), except for sodium selenite, insulin, transferrin and hydrocortisone, which were purchased from Sigma. Plastic-ware was from Costar (Cambridge, MA, USA).

The liquid scintillation counter was an LKB-Wallac 1209 RackBeta from EGG Wallac (Turku, Finland) and was used for β-emission counting. The production of inorganic phosphate by the cell homogenates was measured at 390 nm using a Uvikon 930 spectrophotometer from Kontron Instruments (Milan, Italy). The light emitted by the luciferin/luciferase system, which was used to quantify the ATP content of the supernatants, was measured using a luminometer (LUMAT LK 9501/16) from EGG Berthold (Bad Wilbad, Germany).

$(221)C_{10}$-cryptand, $(222)C_{10}$-cryptand, valinomycin and FCCP were dissolved in absolute ethanol. Nystatin, ouabain and amiloride were dissolved in dimethyl sulfoxide, and triton X-100 and $BaCl_2$, 2 H_2O in water. Final overall ethanol plus dimethyl sulfoxide concentrations never exceeded 0.6%; control experiments demonstrated that these solvent concentrations had no detectable effect on the parameters measured. The percentage of viable cells was over 99% under all experimental conditions under study (trypan blue exclusion procedure).

2.2. Cell culture

OK cells (passages 19–27) were grown to confluence in 6- or 24-well trays in a medium consisting of a 1:1 (v/v) mixture of Dulbecco's modified Eagle's medium (DMEM) and Ham's F12 medium, which, in addition, contained 21.5 mM $NaHCO_3$, 15 mM HEPES, 4 mM L-glutamine, 0.5 mM sodium pyru-

vate, 100 nM sodium selenite, 50 IU/ml penicillin, 50 μg/ml streptomycin, 10 μg/ml insulin, 5 μg/ml transferrin, 50 nM hydrocortisone and 2.5% fetal calf serum. Cultures were maintained at 37°C in an atmosphere of 5% CO_2/95% air, and the medium was changed on alternate days. Cells were fed with hormone- and serum-free medium 24 h before experiments were started, and they were studied when confluent, after six to seven days. They were subcultured weekly using 0.05% trypsin and 0.02% EDTA in saline solution (Puck-modified) and seeded (approx. $1 \cdot 10^6$ cells/disk) onto 100-mm plastic petri dishes. Since trypsin might modify K^+ transport systems, it should be stressed that any tryptic activity present in the initial passaging would be inhibited by the added serum and reduced to negligible levels by dilution, as each culture was fed three times before experimental study, with all old media being aspirated and replaced by fresh medium.

2.3. Unidirectional K^+ flux

Unidirectional K^+ flux was measured using ^{86}RbCl following procedures adapted from the methods by Cheval and Doucet [27] for K^+ influx measurements, and by Venglarik et al. [28] for K^+ efflux measurements. Cells were preincubated in a buffered solution adjusted to 340 mOsm with D-mannitol and containing (in mM): 137 NaCl, 5.4 KCl, 1.2 $MgSO_4$, 1 D-glucose, 1 $CaCl_2$, 14 HEPES (pH 6.4 or 7.4). Then, transport was induced by incubation in the same buffer without D-glucose and supplemented with the components to be investigated (inhibitors, ionophores, tracer).

The ^{86}Rb influx was determined as follows: after removal of the culture medium, the monolayers were washed three times with 500 μl/well of the buffer solution and were preincubated for variable times at 37°C in 250 μl of buffer, with or without ionophores and inhibitors. After removing this solution, ^{86}Rb uptake was induced by adding 250 μl of the D-glucose-free buffer, supplemented with 0.2 μCi/ml ^{86}RbCl (0.5–10 mCi/mg Rb) in the presence or absence of inhibitors. At 3 min, the uptake was stopped by washing the monolayers three times with 500 μl/well of ice-cold rinsing solution, adjusted to 340 mOsm with D-mannitol and containing (in mM): 137 *N*-methyl glucamine, 3 $BaCl_2$, 1 ouabain, 1 amiloride, 14 HEPES (pH 6.4 or 7.4). The cells were then solubilized in 500 μl/well of 0.5% triton X-100 and the tracer activity was measured by liquid scintillation counting using 400 μl aliquots. The protein concentration was measured according to the method of Bradford [29]. Ouabain-sensitive ^{86}Rb influx, calculated as the difference between the values of the ^{86}Rb influxes measured in the presence or absence of 1 mM ouabain, was used as an indicator of Na,K-ATPase activity. It was expressed in nmoles K^+/mg protein/3 min.

^{86}Rb efflux was determined as follows: after removal of the culture medium, the monolayers were washed three times with 500 μl/well of the buffer solution and were preincubated for 60 min at 37°C in 250 μl of buffer solution containing 0.4 μCi/ml ^{86}RbCl, in the presence or absence of inhibitors. After removing the loading solution by suction, the monolayers in one of the 24-well plates experimented on were washed three times with 500 μl/well of ice-cold rinsing solution. Then, the cells were solubilized in 500 μl/well of 0.5% triton X-100, and the tracer activity of the cell layer was determined by liquid scintillation counting, in order to determine the total ^{86}Rb load (qRb_0) under each experimental condition. Following removal of the loading solution, the monolayers in the wells of the other plates being used for experiments were washed four times with 500 μl/well of warmed D-glucose-free buffer solution (1.5 min total time). Then, Rb efflux was induced by adding 250 μl of the glucose-free buffer, with or without the ionophores and the inhibitors. At 5 min, the efflux was stopped by rinsing the monolayers three times, as indicated above. Cells were then solubilized in 0.5% triton X-100 and the tracer activity remaining in the cell layer (qRb_t) was counted. Results are expressed as the percentage of the total ^{86}Rb load that was released in 5 min, i.e., $100(qRb_0 - qRb_t)/qRb_0$.

2.4. Maximal rate of the Na,K-ATPase phosphatase activity (V_{max})

Ouabain-sensitive phosphatase activity was measured according to the method of Post and Sen [30] on cell homogenates with 1 mM ouabain and 3 mM ATP. The release of inorganic phosphate from ATP was measured by spectrophotometric absorption at

390 nm using a procedure adapted from the method of Atkinson et al. [31]. The results are expressed in μmoles Pi/mg protein/h.

2.5. Cell adenosine triphosphate content (ATPi)

For these experiments, cells were grown to confluence in six-well plates. After removal of the culture medium, the monolayers were washed three times with 2 ml/well of the buffer solution and were then preincubated for 40 min at 37°C in 1 ml of buffer, with or without ionophores and inhibitors. After removing this solution, 1 ml/well of the glucose-free buffer, with or without inhibitors, was added for 3 min, i.e., ^{86}Rb influx procedure without tracer. The monolayers were then washed three times with 2 ml/well of ice-cold rinsing solution and twice with 2 ml/well of ice-cold 0.9% NaCl, and were extracted with 1 ml/well of ice-cold 0.3 N perchloric acid. After scraping off the monolayers from the bottom of the wells with a plastic cell scraper, the extracts were centrifuged for 30 min at 4°C (14 000 rpm ~ 88 *g*) and the supernatant was collected. The remaining protein pellet in the tube was dissolved in 1 ml of NaOH and the protein concentration was determined according to Bradford [29]. The supernatant was neutralized to pH 7 with 3 M and 0.3 M KOH at 4°C, and was maintained for 30 min at this temperature and centrifuged for 30 min at 4°C and 14000 rpm. ATP was measured in the supernatant using Calbiochem's ATP assay kit, which uses the luciferin/luciferase system. The emitted light produced by the enzymatic reaction, which is proportional to the ATP content of the sample, was measured using a luminometer. The results are expressed in nmoles ATP/mg protein.

2.6. Statistical treatment

Data are expressed as means ± SEM. Means were compared by variance analysis with repeated measurements for the ionophore factor followed either by a Dunnet's test for comparisons to the control (''ionophore effect'') or the standard conditions (''inhibitor effect''), or by a Newman-Keul's test for comparisons between the ionophores (''inter-ionophores differences'') or the pH (''inter-pH differences''). Differences were considered as significant for $P < 0.05$.

3. Results

3.1. Ouabain-sensitive ^{86}Rb influx

At 40 min preincubation, about 90% of the overall Rb influx observed at pH 7.4 was ouabain-sensitive and, therefore, was attributable to the functioning of the Na,K-ATPase. In many cell types, K^+ enters cells via a Na,K/2Cl cotransport system. The presence of such a cotransport system in OK cells was therefore checked, using bumetanide as an inhibitor (not shown). At 500 μM bumetanide and a preincubation time of 40 min, only 7% of the overall Rb influx was ouabain-resistant and bumetanide-sensitive and, therefore, attributable to the Na,K/2Cl cotransporter. Thus, bumetanide was not used in future experiments.

In preliminary experiments, the effect of cryptands on ouabain-sensitive Rb influx in OK cells was studied after preincubating the monolayers in HEPES (pH 7.4) for various times and carrier concentrations. It was found that $(221)C_{10}$ and $(222)C_{10}$ inhibited ouabain-sensitive Rb influx in a time- and concentration-dependent manner (not shown). Regardless of the cryptand concentration, in the 2 to 20 μM range (or 5.4 to 54.0 nmoles/mg protein), the inhibition reached a steady-state within 40 min of preincubation.

The effects of the Na-selective $(221)C_{10}$ and K-selective $(222)C_{10}$ (10 μM or 27 nmoles/mg protein) on the ouabain-sensitive Rb influx were then compared to those of valinomycin, a K^+-selective antibiotic (1 μM or 3 nmoles/mg protein), nystatin, a channel-forming compound that increases the permeability of membranes to Na^+, K^+ and H^+ ions (50 μM or 125 nmoles/mg protein), and of the protonophore FCCP, an uncoupler of oxidative phosphorylation (10 μM or 26 nmoles/mg protein). The experiments were performed with or without inhibitors (3 mM barium, a K^+-channel blocker, or 1 mM amiloride, a Na^+-channel and Na/H antiporter blocker), and 40 min was chosen for the preincubation period so that the effects of all the ionophores and inhibitors were nearly at steady-state levels (Fig. 1).

Under standard conditions, ouabain-sensitive Rb influx was equal to 247.8 ± 19.0 nmoles/mg pro-

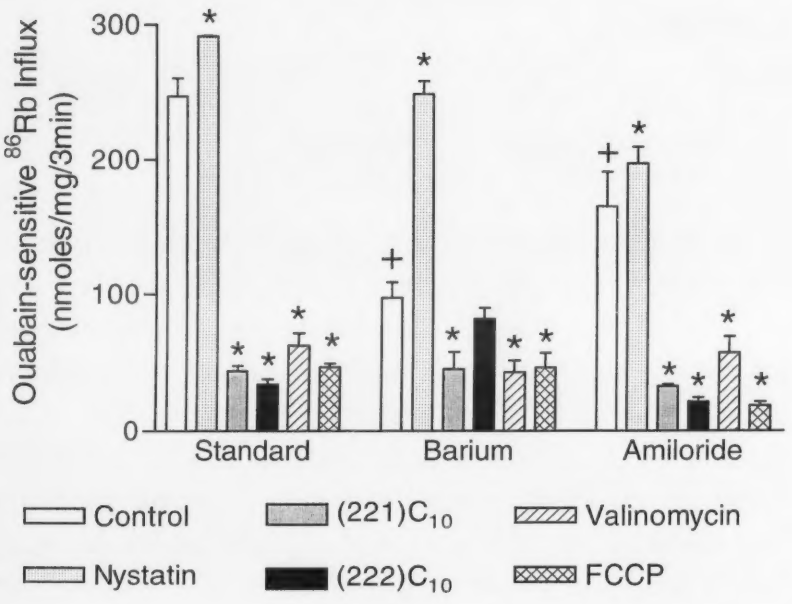

Fig. 1. Effect of ionophores and inhibitors on the ouabain-sensitive ^{86}Rb influx in OK cells. OK cells were preincubated for 40 min in HEPES buffer (pH 7.4), with or without nystatin (50 μM or 125 nmoles/mg protein), (221)C_{10} (10 μM or 27 nmoles/mg protein), (222)C_{10} (10 μM or 27 nmoles/mg protein), valinomycin (1 μM or 3 nmoles/mg protein) and FCCP (10 μM or 26 nmoles/mg protein), in the presence or absence of 3 mM barium or 1 mM amiloride. Ouabain-sensitive Rb influx was measured after 3 min incubation in glucose-free buffer (pH 7.4) containing 0.2 μCi/ml ^{86}RbCl, with or without 3 mM barium or 1 mM amiloride. Each value (± SEM) is the mean of five–seven experiments (in duplicate) for the control, (221)C_{10}, (222)C_{10} and valinomycin, two–four experiments (in duplicate) for FCCP and two experiments (in duplicate) for nystatin. The statistical significance (at least $P < 0.05$) of the ionophore effect (*), i.e., ionophore vs. appropriate control, and of the inhibitor effect (+), i.e., control plus inhibitor vs. control standard, are indicated on the figure.

tein/3 min. This value was significantly decreased by 3 mM barium (61%) and 1 mM amiloride (34%).

Whether or not inhibitors were present, nystatin induced a significant increase (≥ 20%) of the ouabain-sensitive Rb influx, whereas all of the other ionophores decreased this influx significantly (50–80%), with the exception of (222)C_{10} in the presence of barium. In the latter case, the stability of the complexes formed with Ba^{2+} being 10^4 times greater than with K^+ [14], the binding and transport of K^+ ions by (222)C_{10} were prevented (Table 1).

3.2. Maximal rate of the Na,K-ATPase phosphatase activity (V_{max})

In order to check if the ouabain-sensitive Rb influx decrement induced by cryptands, valinomycin and FCCP was due to a direct interaction between the ionophores and the Na,K-ATPase or its lipidic environment, the maximal rate of the Na,K-ATPase phosphatase activity (V_{max}) of OK cell homogenates was quantified at 37°C and pH 7.4, in the presence and absence of the ionophores. The V_{max} of the phosphatase activity of the enzyme was determined at final substrate concentrations of 120 mM Na^+, 20 mM K^+ and 3 mM ATP (Mg/ATP = 1.2), in the presence or absence of 1 mM ouabain. The ionophore concentrations used here were the same as in Rb influx experiments, when expressed in nmoles/mg protein (Fig. 2). Statistical treatment of the data indicated that none of the ionophores had a significant effect on the V_{max} value.

3.3. Adenosine triphosphate cell content (ATPi)

In an attempt to explain, at the molecular level, the ouabain-sensitive Rb influx inhibition by an uncoupling effect of cryptands, valinomycin and FCCP, the ATPi content of OK cells was quantified following a 40-min preincubation of the cell monolayers in

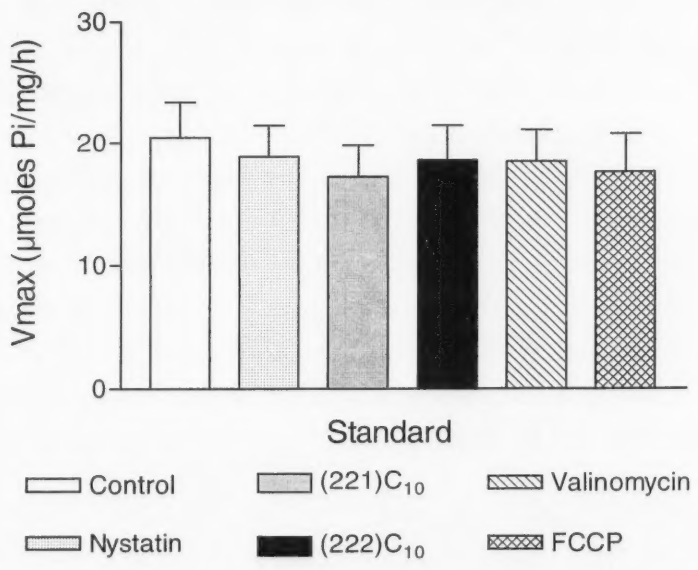

Fig. 2. Effect of ionophores on the maximal rate of Na,K-ATPase phosphatase activity (V_{max}) in OK cells. The maximal rate of Na,K-ATPase phosphatase activity of OK cell homogenates was measured according to the method of Post and Sen [30], with or without nystatin (6.23 μM or 125 nmoles/mg protein), (221)C_{10} (1.35 μM or 27 nmoles/mg protein), (222)C_{10} (1.35 μM or 27 nmoles/mg protein), valinomycin (0.12 μM or 3 nmoles/mg protein) and FCCP (1.30 μM or 26 nmoles/mg protein). Each value (± SEM) is the mean of five experiments (in duplicate). No statistically significant differences were found between the ionophores and the control.

HEPES (pH 7.4), with or without inhibitors and ionophores, and a 3-min incubation in glucose-free HEPES (pH 7.4), with or without inhibitors, i.e., under the same conditions as used for Rb influx experiments performed without tracer.

Fig. 3 shows the effects of the various ionophores and inhibitors on the cells' ATP content. Under standard conditions (absence of inhibitor), the ATPi content of the control was equal to 40.7 ± 7.4 nmoles/mg protein. This value was not significantly modified by 3 mM barium (37.6 ± 6.4 nmoles/mg protein), 1 mM amiloride (41.0 ± 7.5 nmoles/mg protein) or 1 mM ouabain (41.6 ± 7.5 nmoles/mg protein). Also, under standard conditions, nystatin did not significantly modify the ATPi content, whereas $(221)C_{10}$, $(222)C_{10}$, valinomycin and FCCP decreased this content significantly by 47, 75, 72 and 88% of the control value, respectively. In addition,

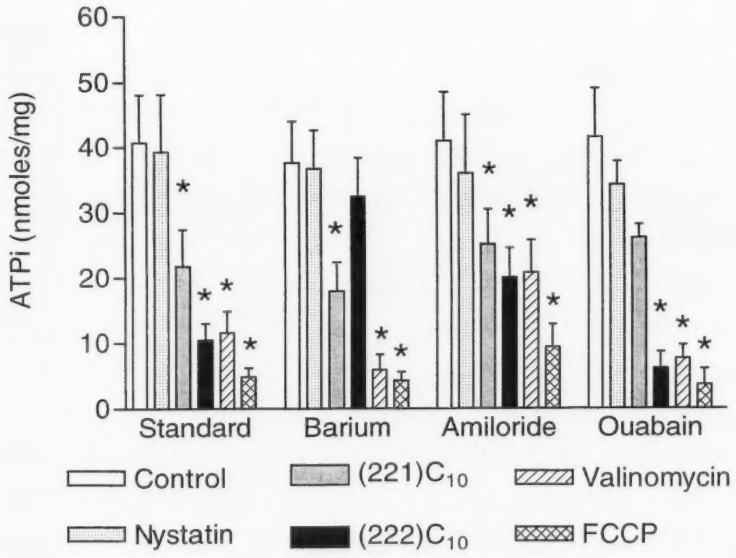

Fig. 3. Effect of ionophores and inhibitors on the ATP content (ATPi) of OK cells. OK cells were preincubated for 40 min in HEPES buffer (pH 7.4), with or without nystatin (50 μM or 125 nmoles/mg protein), $(221)C_{10}$ (10 μM or 27 nmoles/mg protein), $(222)C_{10}$ (10 μM or 27 nmoles/mg protein), valinomycin (1 μM or 3 nmoles/mg protein) and FCCP (10 μM or 26 nmoles/mg protein), in the presence or absence of 3 mM barium, 1 mM amiloride or 1 mM ouabain. They were next incubated for 3 min in glucose-free buffer (pH 7.4) in the presence of the corresponding inhibitor, i.e., the Rb influx procedure performed without tracer, and then checked for the cells' ATP content. Each value (±SEM) is the mean of five–six experiments, except for the ionophores in the presence of ouabain ($n = 2$). The statistical significance (at least $P < 0.05$) of the ionophore effect (*), i.e., ionophore vs. appropriate control, and of the inhibitor effect (+), i.e., control plus inhibitor vs. control standard, are indicated on the figure.

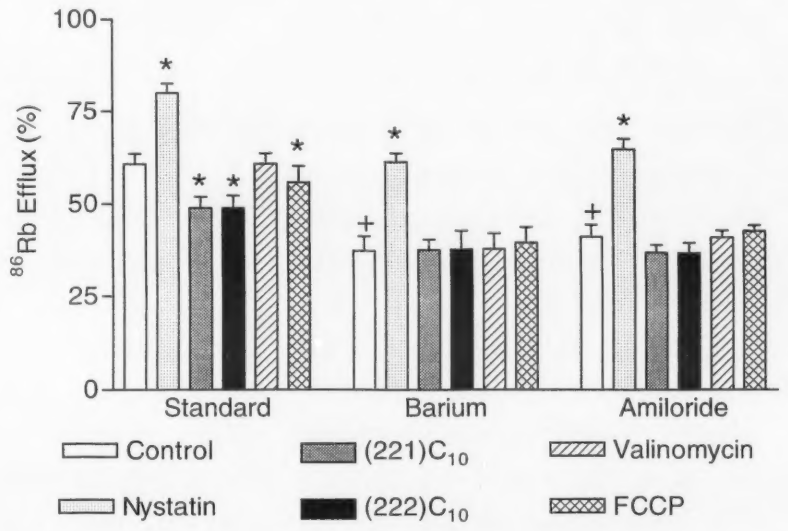

Fig. 4. Effect of ionophores and inhibitors on ^{86}Rb efflux from OK cells. OK cells were preloaded for 1 h in HEPES buffer (pH 7.4) containing 0.4 μCi/ml $^{86}RbCl$, in the presence or absence of 3 mM barium or 1 mM amiloride. Rb efflux was measured after an incubation period of 5 min in the glucose-free buffer (pH 7.4), with or without nystatin (50 μM or 125 nmoles/mg protein), $(221)C_{10}$ (10 μM or 27 nmoles/mg protein), $(222)C_{10}$ (10 μM or 27 nmoles/mg protein), valinomycin (1 μM or 3 nmoles/mg protein) and FCCP (10 μM or 26 nmoles/mg protein), in the presence or absence of 3 mM barium or 1 mM amiloride. Each value (±SEM) is the mean of four–six experiments (in duplicate) for the control, $(221)C_{10}$, $(222)C_{10}$ and valinomycin, and of two–four experiments (in duplicate) for FCCP and nystatin. The statistical significance (at least $P < 0.05$) of the ionophore effect (*), i.e., ionophore vs. appropriate control, and of the inhibitor effect (+), i.e., control plus inhibitor vs. control standard, are indicated on the figure.

the effects of $(222)C_{10}$ and valinomycin on the ATPi content were similar, being significantly greater than that of $(221)C_{10}$ and significantly lower than that of FCCP.

In the presence of 3 mM barium, 1 mM amiloride or 1 mM ouabain, the effects of ionophores resembled those observed under standard conditions, except that: (i) $(222)C_{10}$ no longer caused a significant decrease in the ATPi content in the presence of barium. As indicated above, the irreversible binding of Ba^{2+} ions to the $(222)C_{10}$-cryptand prevented the formation of K^+-complexes; (ii) the magnitude of the $(222)C_{10}$ and valinomycin effects on the ATPi content did not differ significantly from that of $(221)C_{10}$ in the presence of amiloride and (iii) the effect of $(221)C_{10}$ was not found to be significant in the presence of ouabain, probably because of the limited number of experiments performed under these conditions ($n = 2$).

3.4. ^{86}Rb efflux

In an attempt to quantify the effect of the ionophores at the plasma membrane, the efflux of ^{86}Rb from OK cells was measured after loading the cells for 1 h in HEPES buffer (pH 7.4), with or without inhibitors. Fig. 4 compares the effects of cryptands to those of the other ionophores when acting on Rb efflux for 5 min.

Under standard conditions, Rb efflux was stimulated to a high and significant extent by nystatin (32%), was unmodified by valinomycin, and was significantly inhibited by (221)C_{10} (19%), (222)C_{10} (19%) and FCCP (10%).

The control Rb efflux was significantly decreased by 3 mM barium (39%) and 1 mM amiloride (32%). In the presence of these inhibitors, the significant stimulation of Rb efflux by nystatin persisted, whereas the other ionophores were without effect.

When lowering the pH from 7.4 to 6.4, control Rb efflux was decreased insignificantly, by 14% of its value at pH 7.4, i.e., nearly the magnitude of the inhibition induced here by cryptands at pH 7.4 (19%) (Table 2). The Rb efflux was still stimulated by nystatin and unchanged by valinomycin, while the inhibition by (221)C_{10}, (222)C_{10} and FCCP vanished.

Table 2
pH-Dependence of the effect of ionophores on ^{86}Rb efflux from OK cells

^{86}Rb Efflux (%)	pH 7.4	pH 6.4
Control	60.6 ± 2.8	52.3 ± 4.3
(221)C_{10}	48.9 ± 2.9[a]	51.0 ± 2.0
(222)C_{10}	48.9 ± 3.2[a]	52.6 ± 0.6
Valinomycin	60.7 ± 2.8	53.9 ± 1.2
Nystatin	80.0 ± 2.6[a]	72.0 ± 4.8[a]
FCCP	54.3 ± 3.3[a]	51.6 ± 1.2

OK cells were preloaded for 1 h in HEPES buffer (pH 6.4 and 7.4) containing 0.4 μCi/ml $^{86}RbCl$. The Rb efflux was measured after a 5-min incubation period in the glucose-free buffer (pH 6.4 and 7.4), with or without nystatin (50 μM or 125 nmoles/mg protein), (221)C_{10} (10 μM or 27 nmoles/mg protein), (222)C_{10} (10 μM or 27 nmoles/mg protein), valinomycin (1 μM or 3 nmoles/mg protein) and FCCP (10 μM or 26 nmoles/mg protein).

Means ± SEM are the result of four–six experiments (in duplicate) at pH 7.4 and of two experiments (in duplicate) at pH 6.4 (ongoing experiments).

[a]The ionophore effect is statistically significant at least at the $P < 0.05$ level, i.e., ionophore vs. appropriate control, is indicated in the table.

4. Discussion

The following discussion is based on the data and comments presented in Table 1. With the exception of Ba^{2+} ions blocking the (222)C_{10} cryptand cavity, all of the other cations were alternative substrates of the two cryptands. Also, due to the high affinity of the (221)C_{10} for Ca^{2+} ions, which are present in the buffer at a low concentration and are almost absent from the cellular media (0.1 μM), it is likely that Ca^{2+} was easily carried inside by (221)C_{10} and, to a lesser extent, by (222)C_{10}. In efflux experiments, it was thought likely that Rb^+ traced the K^+ exit by the two cryptands.

In the present study, about 90% of the Rb influx in OK cells was found to be ouabain-sensitive and, therefore, attributable to the functioning of the Na,K-ATPase. At pH 7.4 and 37°C, the control ouabain-sensitive Rb influx value (Fig. 1) was in agreement with previous data [32,33]. This value was decreased by barium, as already found by Sjodin and Ortiz [34], and by amiloride, two inhibitors that have no effect on the ATPi content (Fig. 3). The K^+-channels blockade by barium leads to down-regulation of the Na,K-ATPase by mechanisms that have not yet been elucidated [34–37]. Amiloride blocks sodium entry through Na^+-channels and via the Na/H antiporter. The latter has been shown to be very active in regulating the internal pH (pH_i) [26] and its blockade by amiloride reduces both the Na_i and pH_i [25]. An inhibition of the Na,K-ATPase activity was therefore expected because (i) Na_i is one of the major determinant of the pump's activity [1]; (ii) intracellular acidosis directly blocks the Na,K-ATPase [38]; (iii) K^+ permeability in OK cells is down-regulated when the pH_i decreases [21]. This, in turn, reduces the pump's activity [35] and (iv) amiloride directly inhibits the Na,K-ATPase [39]. Independent of the presence of inhibitors, all of the ionophores significantly modified the ouabain-sensitive Rb influx

in OK cells, except for $(222)C_{10}$ in the presence of barium. Nystatin increased the control value (in agreement with the data of Middleton et al. [32]) by its ability to increase the Na_i (and K_i) [10]. The inhibition of the ouabain-sensitive Rb influx by the other ionophores (mobile carriers) was independent of their ionic selectivity.

The control V_{max} of the Na,K-ATPase phosphatase activity (20.5 ± 2.9 μmole Pi/mg protein/h) was in agreement with previous data [40], and was not modified by the ionophores under investigation (Fig. 2). Hence, direct interactions with the Na,K-ATPase or its lipidic environment could probably be excluded. Besides, ouabain-sensitive Rb influx inhibition by $(222)C_{10}$ was entirely removed when Ba^{2+} ions irreversibly bound to the cryptand, confirming the absence of any effect of the cryptand's aliphatic chain within the Na,K-ATPase.

Another mechanism for the ouabain-sensitive Rb influx inhibition by the ionophores was their potential uncoupling activity [12] (Fig. 3). ATP synthesis in mitochondria is driven by an electrochemical proton gradient within the inner mitochondrial membrane [2,6]. ATP synthesis blockade may arise from a decrease in the membrane potential (ΔV) and/or of the proton concentration gradient (ΔpH). It is now clearly established that FCCP dissipates the ΔpH [6,41], whereas valinomycin decreases the ΔV [6]. The cryptands' effects on ATP synthesis were expected to reflect a valinomycin-like effect on ΔV, combined with an FCCP-like effect on ΔpH (see below).

The control ATPi content of OK cells had a slightly higher value than that determined by Li et al. [42,43]. Under standard conditions (Fig. 3), the marked decrease in the ATPi content by valinomycin and FCCP is typical of those expected from mitochondrial uncouplers [12]. The K-selective $(222)C_{10}$ reduced the ATPi content to the same level as valinomycin, whereas $(221)C_{10}$ was less efficient. Several reasons may have accounted for this result: (i) $(221)C_{10}$ possesses a Na^+ over K^+ selectivity and, therefore, its ability to decrease the ΔV may have been less than that of $(222)C_{10}$; (ii) the ionization constants of $(221)C_{10}$ are higher than those of $(222)C_{10}$ [14]. $(221)C_{10}$, therefore, may have reduced the ΔpH to a lesser extent than $(222)C_{10}$ and (iii) $(221)C_{10}$ can bind and transport Ca^{2+} ions [14,44]. $(221)C_{10}$ may have carried Ca^{2+} ions into the mitochondria, thus stimulating ATP synthesis [45]. Due to the linear ouabain-sensitive Rb influx vs. ATPi content relationship [46,47], the large inhibition of ouabain-sensitive Rb influx by $(221)C_{10}$ was not mediated entirely through an effect on ATP synthesis. In addition, $(221)C_{10}$ may have reduced the ouabain-sensitive Rb influx (i) by exchanging K^+ for H^+ ions across the plasma membrane (see Rb efflux discussion), an event which decreased the pH_i and, in turn, the Na,K-ATPase activity [38] and (ii) possibly by increasing the free Ca_i, thus decreasing the Na,K-ATPase activity [48–50]. In summary, it is likely that the inhibition of ouabain-sensitive Rb influx by $(222)C_{10}$ was due mainly to its effect on ATP synthesis, whereas that by $(221)C_{10}$ was mediated through its combined effects on ATP synthesis and on the pH_i- and Ca_i-dependent Na,K-ATPase activity.

In an attempt to quantify the effect of the ionophores at the plasma membrane, a study of Rb efflux from OK cells was performed (Fig. 4). In agreement with previous data [12,19], the large nystatin effect arose from the dissipation of the K^+ (and Na^+) gradient. Independent of their ionic selectivities, cryptands inhibited Rb efflux, an effect reproduced to a lesser extent by FCCP. This H^+-carrier has been shown to acidify the intracellular pH of OK cells [51]. Cryptands were expected to mimic concomitantly the behavior of the Na/H and K/H antiporters of OK cells. However, due to their internal interface localization ($\sim 90\%$) [17,18], they would have behaved here mainly like K^+–H^+ exchangers. The results at variable pH values (Table 2) strongly suggested that Rb efflux from OK cells was pH-sensitive, as already shown by Graber [52], and that inhibition of Rb efflux by cryptands and FCCP at pH 7.4 arose from the ionophores ability to decrease the pH_i. Besides, no effects of $(221)C_{10}$ and of FCCP could be observed with barium, indicating that these carriers did not modify the K/H antiporter activity of OK cells (Fig. 4). Hence, cryptands and FCCP may have acted mainly on the pH-sensitive barium-blockable K^+-channels of OK cells.

In agreement with the data of Graber [52], barium decreased the control values of Rb efflux by blocking the barium-sensitive K^+-channels [21]. Nystatin increased this efflux, whereas the other ionophores were without effect. This suggested that $(221)C_{10}$ and FCCP could not induce an additional pH effect on the

remaining K^+-conductance, i.e., according to Graber [52], the K/H antiporter. Due to the decrease in the pH_i induced by amiloride, inhibition of the pH_i-sensitive barium-blockable K^+-channels was expected, as occurred in the presence of barium. Hence, the ionophore effects were similar with amiloride and barium.

In conclusion, comparing cryptand effects to those of commonly used ionophores has shown a variety of responses on K^+ transport in OK cells. It has been found that the ionophore's action is localized at the plasma membrane (nystatin), or at the mitochondrial membrane (valinomycin) or both [$(221)C_{10}$, $(222)C_{10}$ and FCCP]. Cryptands were shown to inhibit the pH-sensitive K^+-conductance of OK cells by inducing a K^+–H^+ exchange at the plasma membrane, and to uncouple oxidative phosphorylation by inducing the entry of K^+ and H^+ (and possibly Ca^{2+}) ions into the mitochondria, thereby inhibiting the Na,K-ATPase. Moreover, their ability to inhibit ATP synthesis to different levels, together with the specific removal of the $(222)C_{10}$ effects by barium, arose from their different ionic selectivities only. This study emphasizes the importance of understanding metabolic and transport effects of ionizable ionophores, such as cryptands. The reversal of Na^+ and K^+ gradients of proximal tubules by $(221)C_{10}$, which was previously interpreted as occurring by cation transport across the plasma membrane [19], thus appears to have arisen from inhibition of Na,K-ATPase, through changes at the mitochondrial and plasma membranes.

Acknowledgements

The authors are grateful to Professor G. Friedlander of U-426 INSERM, Paris, for encouraging the progress of this work in his laboratory, and to Professor F. Morel, Paris, for his constant interest in the cryptands' study throughout the years. They would like also to thank B. Escoubet, D. Prié, R. Radjerison, C. Clerici, C. Planes, M. Blot-Chabaud, N. Farman and J. Teulon for their helpful comments during the course of this work, and L. René-Corail for technical assistance.

References

[1] A.I. Katz, Am. J. Physiol. 242 (1982) F207–F219.
[2] B. Alberts, D. Bray, J. Lewis, M. Raff, K. Roberts, J.D. Watson, in: Molecular Biology of the Cell, Garland, New York, 1994, pp. 507–549.
[3] Y.A. Ovchinnikov, V.T. Ivanov, A.M. Shkrob, in: Membrane-Active Complexones, BBA Library, Vol. 12, Elsevier, Amsterdam, 1974, pp. 331–406.
[4] B.C. Pressman, Biological applications of ionophores, Annu. Rev. Biochem. 45 (1976) 501–530.
[5] W.C. McMurray, R.W. Begg, Arch. Biochem. Biophys. 84 (1959) 546–548.
[6] A.L. Lehninger, D.L. Nelson, M.M. Cox, in: Principles of Biochemistry, Worth, New York, 1993, pp. 542–597.
[7] J. Cunarro, M.W. Weiner, Biochim. Biophys. Acta 387 (1975) 234–240.
[8] H. Murer, U. Hopfer, R. Kinne, Biochem. J. 154 (1976) 597–604.
[9] A. Cass, A. Finkelstein, V. Krespi, J. Gen. Physiol. 56 (1970) 100–124.
[10] A. Cass, M. Dalmark, Nat. New Biol. 244 (1973) 47–49.
[11] S.J. Harris, R.S. Balaban, L. Barrett, L.J. Mandel, J. Biol. Chem. 256 (1981) 10319–10328.
[12] S.P. Soltoff, L.J. Mandel, J. Membr. Biol. 94 (1986) 153–161.
[13] J.M. Lehn, Struct. Bond. 16 (1973) 1–69.
[14] J.M. Lehn, J.P. Sauvage, J. Am. Chem. Soc. 97 (1975) 6700–6707.
[15] A. Loiseau, M. Hill, G.M. Mulliert, M. Castaing, Biochim. Biophys. Acta 1235 (1995) 21–32.
[16] A. Loiseau, M. Hill, L. René-Corail, M. Castaing, Biochim. Biophys. Acta 1238 (1995) 107–117.
[17] M. Castaing, F. Morel, J.M. Lehn, J. Membr. Biol. 89 (1986) 251–267.
[18] M. Castaing, J.M. Lehn, J. Membr. Biol. 97 (1987) 79–95.
[19] R.M. Rajerison, M. Faure, F. Morel, VIe Congrès Européen de Physiologie Rénale, 23–28 May 1988, Varna, Bulgaria.
[20] A. Hus-Citharel, F. Morel, VIe Congrès Européen de Physiologie Rénale, 23–28 May 1988, Varna, Bulgaria.
[21] J.S. Schwegler, A. Henner, S. Silbernagl, Pflüg. Arch. Eur. J. Physiol. 415 (1989) 183–190.
[22] T. Ohno-Shosaku, T. Kubota, J. Yamaguchi, M. Fukase, T. Fujita, M. Fujimoto, Pflüg. Arch. Eur. J. Physiol. 413 (1989) 562–564.
[23] T. Ohno-Shosaku, T. Kubota, J. Yamaguchi, M. Fujimoto, Pflüg. Arch. Eur. J. Physiol. 416 (1990) 138–143.
[24] H.A. Kolb, Renal Physiol. Biochem. 13 (1990) 26–36.
[25] M. Graber, E. Pastoriza-Munoz, Am. J. Physiol. 265 (1993) F773–F783.
[26] A. Moran, M.H. Montrose, H. Murer, Biochim. Biophys. Acta 969 (1988) 48–56.
[27] L. Cheval, A. Doucet, Am. J. Physiol. 259 (1990) F111–F121.
[28] C.J. Venglarik, R.J. Bridges, R.A. Frizzell, Am. J. Physiol. 259 (1990) C358–C364.

[29] M.M. Bradford, Anal. Biochem. 72 (1976) 248–254.
[30] R.L. Post, A.K. Sen, Methods Enzymol. 10 (1967) 762–768.
[31] A. Atkinson, A.D. Gatenby, A.G. Lowe, Biochim. Biophys. Acta 320 (1973) 195–204.
[32] J.P. Middleton, W.A. Khan, G. Collinsworth, Y.A. Hannun, R.M. Medford, J. Biol. Chem. 268 (1993) 15958–15964.
[33] S.P. Soltoff, L.J. Mandel, J. Gen. Physiol. 84 (1984) 601–622.
[34] R.A. Sjodin, O. Ortiz, J. Gen. Physiol. 66 (1975) 269–286.
[35] B.C. Kone, H.R. Brady, S.R. Gullans, Proc. Natl. Acad. Sci. U.S.A. 86 (1989) 6431–6435.
[36] A.G. Ramsay, D.L. Gallagher, R.L. Shoemaker, G. Sachs, Biochim. Biophys. Acta 436 (1976) 617–627.
[37] W. Nagel, Biochim. Biophys. Acta 552 (1979) 346–357.
[38] D.C. Eaton, K.L. Hamilton, K.E. Johnson, Am. J. Physiol. 247 (1984) F946–F954.
[39] S.P. Soltoff, L.J. Mandel, Science 220 (1983) 957–959.
[40] B. Escoubet, K. Djabali, C. Amiel, Am. J. Physiol. 256 (1989) C322–C328.
[41] B. Alberts, D. Bray, J. Lewis, M. Raff, K. Roberts, J.D. Watson, in: Molecular Biology of the Cell, Garland, New York (1994) pp. 655–696.
[42] H.-Y. Li, L.-J. Dai, C. Krieger, G.A. Quamme, Biochim. Biophys. Acta 1181 (1993) 307–315.
[43] H.-Y. Li, L.-J. Dai, C. Krieger, G.A. Quamme, J. Lab. Clin. Med. 122 (1993) 260–272.
[44] M. Kirch, in: Thèse de Doctorat ès Sciences Physiques Strasbourg, France, 1980, pp. 38–95.
[45] R.M. Denton, J.G. McCormack, Am. J. Physiol. 249 (1985) E543–E554.
[46] T. Ikehara, H. Yamaguchi, K. Hosokawa, T. Sakai, H. Miyamoto, J. Cell Physiol. 119 (1984) 273–282.
[47] S.P. Soltoff, L.J. Mandel, J. Gen. Physiol. 84 (1984) 643–662.
[48] D.R. Yingst, Ann. Rev. Physiol. 50 (1988) 291–303.
[49] W. Huang, A. Askari, Arch. Biochem. Biophys. 216 (1982) 741–750.
[50] D.R. Yingst, R.M. Jones, D.M. Polasek, Biophys. J. 49 (1986) 549a.
[51] C. Knoblauch, M.H. Montrose, H. Murer, Am. J. Physiol. 256 (1989) C252–C259.
[52] M. Graber, Am. J. Kidney Dis. 22 (1993) 436–444.

ELSEVIER

Biochimica et Biophysica Acta 1330 (1997) 50–60

BIOCHIMICA ET BIOPHYSICA ACTA
BBA

Evidence for extensive and non-specific translocation of oligopeptides across plasma membranes of mammalian cells

Johannes Oehlke [a,*], Michael Beyermann [a], Burkhard Wiesner [a], Mathias Melzig [b], Hartmut Berger [a], Eberhard Krause [a], Michael Bienert [a]

[a] *Institute of Molecular Pharmacology, Alfred-Kowalke-Strasse 4, D-10315 Berlin, Germany*
[b] *Institute of Pharmacy, Humboldt University, Goethestrasse 54, D-13086 Berlin, Germany*

Received 4 March 1997; revised 4 June 1997; accepted 11 June 1997

Abstract

After exposure of bovine aortic endothelial cells to various small peptides (tetra- to undeca-mer), extensive transport of the peptides across the plasma membrane was observed in the concentration range 10^{-7} to 10^{-2} M. The observed transport events, which contradict the generally anticipated poor permeability of peptides across plasma membranes, exhibited high complexity and showed no saturability up to a concentration of 10^{-2} M. Evidence was found for the involvement of mdrp-like transporters as well as of energy-independent facilitated diffusion events. The peptide levels within the cells approximated those of the incubation solution within 30 min, indicating high capacity and velocity for the involved transport processes. Correspondingly, preloaded cells exported about 80% of the internalized peptide within 5 min at 37°C. Analogous results were found after peptide exposure to several other mammalian cell types, indicating a more general importance of the transport phenomena described here. Our findings contradict the prevailing opinion that the often observed lack of activity of externally administered peptides against their targets within intact cells is accounted for primarily by poor cellular uptake and point to export processes counteracting the uptake to be more important in this context. © 1997 Elsevier Science B.V.

Keywords: Peptide transport; Cellular uptake; Mammalian cell

1. Introduction

The value of small peptides as biological agents is compromised according to the prevailing opinion, apart from metabolic instability, primarily by poor permeability across biological membranes [1–3]. Metabolic degradation appears to be of lesser importance in this context, since there exist multiple approaches to improve the enzymatic stability of peptides. To overcome the poor propensity of peptides to cross lipidic membranes, however, provides principal

Abbreviations: AEC, bovine aortic endothelial cells; BEC, porcine brain microvessel endothelial cells; BSP, sulfobromophthalein; CLSM, confocal laser scanning microscopy; DNP-SG, S-(2,4-dinitrophenyl)glutathione; DOG, 2-deoxy-D-glucose; DPBSG, Dulbecco's phosphate-buffered saline supplemented with 1g/l D-glucose; FLUOS-, 5(6)-carboxyfluoresceinyl; NBD-, 7-nitrobenz-2-oxa-1,3-diazol-4-yl; PBS, phosphate-buffered saline

* Corresponding author. Fax.: (49-30) 51551 206; E-mail: bienert@fmp-berlin.de

0005-2736/97/$17.00 © 1997 Elsevier Science B.V. All rights reserved.
PII S0005-2736(97)00141-7

problems. Besides insufficient lipophilicity, this low permeability is accounted for primarily by the high hydrogen-bonding potential of the peptide backbone's amide groups [4], which often cannot be reduced by structural alterations without affecting the affinity for the biological target. Numerous attempts to improve the permeability by simply increasing the lipophilicity of the molecule have not met with success [5].

The existence of peptide carriers in the plasma membrane of mammalian cells, which could circumvent this principal obstacle, has been demonstrated to date only for di- and tripeptides [6,7]. Additionally, evidence has been provided for the presence of peptide transporters at the blood–brain barrier, exhibiting, however, high structural specificity for a limited number of centrally active peptides [8,9].

In this study, we found evidence that, in contrast to prevailing opinion, oligopeptides (tetra- to at least undeca-mers) can extensively and non-specifically cross the plasma membranes of mammalian cells. Our findings point to the presence of multiple transport facilities for oligopeptides in the plasma membrane of mammalian cells which, if considering counteracting export processes, appear exploitable for non-specifically translocating oligopeptides into living cells. Such a possibility seems to be of particular interest with respect to an introduction into intact cells of small peptides that have appropriate sequences for blocking associations between signal-transducing proteins [10]. So far, competition experiments of this kind have only been carried out in cell free systems, permeabilized cells or by means of microinjection techniques.

2. Materials and methods

2.1. Materials

^{3}H-DAMGO and 5(6)-carboxyfluorescein-*N*-hydroxysuccinimide ester (FLUOS) were purchased from Amersham and Boehringer, Mannheim, respectively. DNP-SG was synthesized according to Hinchman et al. [11]. Buserelin (HOE 766) was a generous gift from Dr. J. Sandow (Hoechst). Other chemicals and reagents, if not specified, were purchased from Sigma or Bachem.

2.2. Peptide synthesis

The peptides were synthesized manually by the solid phase method using standard Fmoc chemistry. Boc-Lys(Fmoc)-OH was coupled to *o*-chloro-trityl resin in the presence of two equivalents of ethyl-diisopropylamine. After Fmoc-deprotection by 20% piperidine/dimethylformamide (DMF), subsequent couplings of Fmoc-Leu, Fmoc-Phe, Fmoc-Gly and Fmoc-Tyr(tBu) were carried out by means of TBPipU [12]. The crude peptide was obtained from the final cleavage in acetic acid–trifluoroethanol–methylene dichloride (2:2:6, v/v/v) for 1 h and purified using preparative reversed-phase high-performance liquid chromatography (RP-HPLC). The peptide purity (> 98%) was determined by analytical RP-HPLC (220 nm) and the identity was confirmed by electrospray mass spectrometry.

Nitrobenzoxadiazole (NBD)- and FLUOS-derivatives were obtained by reacting the Fmoc-deprotected resin-bound peptides with two equivalents of 7-chloro-4-nitrobenz-2-oxa-1,3-diazole or 5(6)-carboxyfluorescein-*N*-hydroxysuccinimide ester, respectively, for about 48 h at pH 8–9 and ambient temperature.

2.3. Tritiated peptides

With the exception of [^{3}H]DAMGO, which was purchased from Amersham, the tritiated peptides were synthesized as described previously [13–15]. Before use, the labelled peptides, all exhibiting specific radioactivities of about 1 Tbq/mmol, were cleaned up by HPLC to a radioactive purity > 95% and were mixed with the respective inactive parent compound to attain the required peptide concentration.

2.4. Cell culture

Calf aortic endothelial cells (BkEz-7; AEC), a 12.–20. subculture of a cell line that was established and characterized by Halle et al. [16], were cultured to almost confluency (four days) in 24-well plates (10^{5} cells/well) at 37°C in a humidified 3% CO_2 in air environment in Dulbecco's modified Eagle's medium (DMEM) (Biochrom, Berlin, Germany) containing 4.5 mg/ml of glucose, 100 U/ml of peni-

cillin, 100 μg/ml streptomycin and supplemented with 290 mg/l glutamine and 10% fetal bovine serum (FBS; Sigma, Deisenhofen, Germany).

Porcine endothelial cells (SEZ; MEM/5% FBS), human endothelial cells (ECV 304; M199/10% heat inactivated FBS), murine corticotrophic pituitary tumour cells (AtT-20; DMEM/10% FBS), human neuroblastoma cells (SK-N-SH; MEM Eagle's/10% FBS supplemented with 1% non-essential amino acids, 1% sodium pyruvate and 1% glutamine (Biochrom), human embryonic kidney tumour cells (HEK; MEM Earle's/10% FBS supplemented with 1% non-essential amino acids) and human hepatoma cells (Hep G2; MEM Eagle's/10% FBS supplemented with 1% non-essential amino acids, 1% sodium pyruvate and 1% glutamine) were cultured analogously.

Brain microvessel endothelial cells (BEC) were isolated from fresh porcine brains, as described by Mertsch et al. [17]. The cells were plated into 24-well plates at an initial density of $5 \cdot 10^4$ cells/well and were cultured as outlined for AEC. In addition, the wells were coated with gelatine (Sigma, St. Louis, MO, USA) before plating and 1 ng/ml basic fibroblast growth factor (Promega, Madison, WI, USA), 100 μg/ml Heparin (H-3149, Sigma, St. Louis, MO, USA) and 0.5 μg/ml amphotericin (Biochrom) were added to the medium. The obtained monolayers proved to be more than 95% endothelial in origin and exhibited properties regarded to be typical for the blood–brain barrier (presence of tight junctions, γ-glutamyl transpeptidase-, alkaline phosphatase- and angiotensin-converting enzyme activities, Factor VIII antigen) [17].

2.5. Uptake experiments

After removing the culture medium, the cells were rinsed twice at 37°C with PBS–Dulbecco's (Biochrom), supplemented with 1 g/l glucose (DPBSG) and subsequently exposed to the substrates dissolved in DPBSG (150 μl/well) for the indicated periods. Subsequently, the substrate solution was aspirated off and the cells were washed four times with ice cold PBS (within 2 min) and lysed by allowing them to stand for about 20 h at room temperature in a 0.1% solution of Triton X-100 containing 10 mM trifluoroacetic acid (200 μl/well). For performing efflux experiments, the preloaded and washed cells were incubated with DPBSG (200 μl/well) at 37°C for indicated periods prior to lysis. For determination of the acid-sensitive bound proportion of cell-associated peptide, in some cases, an acid-wash step (incubation with 200 μl/well of 0.2 M acetic acid/0.05 M NaCl for 5 min at 0°C) was inserted between the normal wash process and lysis. The obtained extracts or lysates were utilized without further treatment for HPLC quantitation or liquid scintillation counting.

Parts of the Triton-lysates were used for determining the protein content, according to the method of Bradford [18]. In order to correlate the amount of protein with cell number, monolayers, grown under identical conditions in separate wells, were trypsinized and counted. For AEC, a ratio of 200 μg protein/10^6 cells was found by this procedure. The average volume of AEC was determined to be 1.4 pl by means of a coulter-ZM counter (Coulter Electronics, Luton, UK).

2.6. HPLC analysis

HPLC was performed using a Bischoff HPLC gradient system (Leonberg, Germany) equipped with a Kromasil 100 C_{18}, 5-μm column (250 × 4 mm I.D.), precolumns containing the same sorbent and a Rheodyne-RH 8125 injection valve with a 50-μl sample loop. The elution was performed with 0.01 M trifluoroacetic acid (TFA) (A) and acetonitrile–water (9:1, v/v) (B) (gradient from 30 to 60% B within 20 min). Detection was performed by fluorescence using a fluorescence detector RF-551 (Shimadzu, Japan) at 520 nm after excitation at 445 nm for prepurified FLUOS-labelled peptides (see below), at 350 nm after excitation at 285 nm for tryptophan-containing peptides and at 540 nm after excitation at 470 nm for NBD-labelled derivatives. The peaks corresponding to the intact peptides and their des-tyrosine metabolites were quantified using a Hyperdata Integration Workstation S I (Bischoff, Leonberg, Germany) on the basis of calibration lines established previously with pure references. If not specified otherwise, the so-determined quantities of incorporated peptide are generally indicated as the sum of intact peptide and detyrosinated metabolite.

The cells' own fluorescently active components did not interfere with detection of the peptides, even in the case of tryptophan-containing derivatives, so

that pretreatment of the cell lysates could be avoided at the cost of a somewhat more frequent replacement of the precolumn.

2.7. FLUOS derivatization

To 70 μl of the sample solution, 10 μl of 2 M K_2HPO_4, 10 μl of 23 μM cyclohexylalanine solution (internal standard) and 5 μl of a solution containing 4.9 mg of 5(6)-carboxyfluorescein-*N*-hydroxysuccinimide ester (Boehringer) in 100 μl of dimethylsulfoxide were added and allowed to react for about 20 h at room temperature. Subsequently, the solution was mixed with 4 μl of 8 M NaOH and, after standing for at least 30 min, with 11 μl of 1.4 M H_3PO_4. HPLC was first carried out by eluting with 0.04 M phosphate buffer, pH 7.4 (A) and acetonitrile–water (9:1, v/v) (B) with gradients from 9–28% B (0–20 min) and 28–85% B (20–30 min) at a flow-rate of 1.0 ml/min. UV Detection was at 242 nm. The eluates containing the derivatized peptides and their aminopeptidase degradation products (16 to 21 min) were collected and concentrated to dryness by means of a vacuum centrifugal evaporator (Jouan, Unterhaching, Germany). Residuals, corresponding to 1 ml of the eluate, were dissolved in 100 μl of 0.5 M TFA containing 25% acetonitrile and subjected to the HPLC protocol described above for quantitation.

2.8. Confocal laser scanning microscopy (CLSM)

Cells ($1 \cdot 10^4$) were plated on 22 × 22 mm coverslips, glued (with silicones RTV 615A/615B, Paul Hellermann, Pinneberg, Germany) above the hole (15 mm D) of punched plastic Costar culture dishes (35 mm D; Integra Biosciences, Germany) and cultured for four days, as described above. After removing the culture medium, the cells were exposed to solutions of the fluorescently labelled peptides in DPBSG (10–500 μM) for 60 min at 37°C. Subsequently, the cells were washed four times with ice-cold PBS and covered with about 200 μl of PBS. Microscopy was conducted within 10 min at room temperature using an LSM 410 inverted confocal laser scanning microscope (Carl Zeiss Jena, Jena, Germany). Excitation was performed at 488 nm by means of an argon–krypton laser and a dichroitic mirror (FT 510) for wavelength selection. Emission was measured at 515 nm using a cut-off filter (LP 515) in front of the detector. For optical sectioning in the *z*-direction, sixteen frames were made, with a thickness of 1 μm. Subsequent HPLC investigations of the incubation solution and of Triton X-100 lysates of the cells gave no indication of any metabolic breakdown of the peptides.

3. Results

3.1. Evidence for peptide incorporation after millimolar exposure of endothelial cells to enkephalin-derived peptides

With the initial intention of examining the possibility of whether or not natural amino acid transporters could be exploited for translocating small central active peptides through the blood–brain barrier, we exposed aortic- (AEC) and brain microvessel endothelial cells (BEC) to several enkephalin-derived peptides. Surprisingly, in all cases, we observed high degrees of peptide association onto the cells (Fig. 1). Incubation at 0–4°C (2 mM peptide, 60 min; precooling the cells for 30 min) resulted in virtually no association to the cells (< 0.1 nmol/mg protein) so that non-specific adsorption could be ruled out as contributing noticeably and actual uptake into the cell interior had to be taken into consideration.

Since both derivatives bearing an intact α-carboxy- and α-amino group (for recognition by amino acid

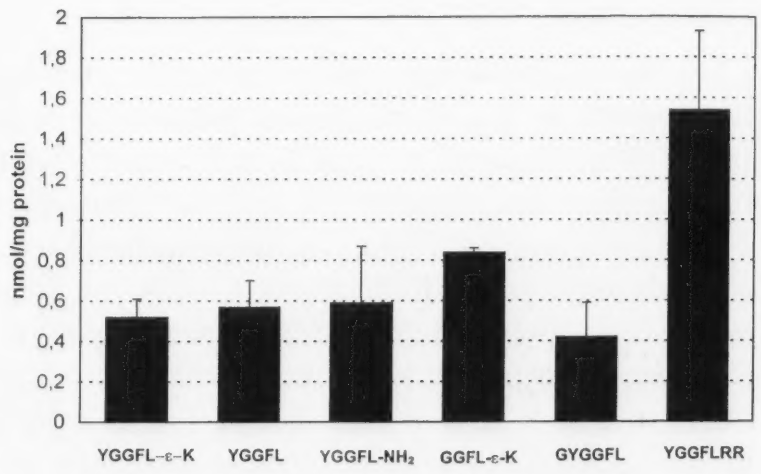

Fig. 1. Quantity of cell-associated peptide after exposure of aortic endothelial cells to 2 mM solutions of various enkephalin-derived peptides in DPBSG for 30 min at 37°C. Each bar represents the mean of three samples ± SEM.

transporters, according to Smith [19]) and unmodified peptides exhibited comparable degrees of association to the cells (Fig. 1), the observed peptide uptake appeared to resemble more general phenomena, unlike our initial intention. Therefore, we extended our investigations with the goal of gaining insights into the mode and structural requirements for the transport events that were found.

In order to facilitate detection and to render the degree of degradation by plasma membrane-associated peptidases negligible, millimolar peptide concentrations (0.2–10 mM) were employed in the first experiments. That the observed transport phenomena did not reflect artifacts, accounted for by these unphysiologically high peptide concentrations, was ascertained in subsequent investigations conducted in the low micromolar range using tritium-labelled peptides (see below).

3.2. Time dependency of peptide translocation

The uptake by the cells reached an equilibrium at about 20 min (Fig. 2). The efflux out of preloaded cells exhibited a complex course, indicating location of the cell-associated substrate within distinct compartments (Fig. 3). From BEC, the release of the incorporated substrate proceeded considerably more rapidly than that from AEC (Fig. 3), suggesting a relation to the lower degree of uptake into BEC (Fig. 3).

3.3. Influence of the peptide structure on cellular uptake

In order to obtain information about the structural requirements for the found peptide import, we modified the N- and C-terminal amino- and carboxy-groups of Leu-enkephalin, respectively, and incorporated basic and acidic residues and glycine into the N-terminal, C-terminal and middle regions of the molecule. Phenylalanine was generally replaced by tryptophan in this series to permit fluorescence detection during HPLC analysis. Since amidation of the C-terminus did not attenuate the uptake, in most cases, the more conveniently available amides were used (Table).

The performed structural modifications only slightly influenced peptide import (Table), indicating poor structural specificity for the transport mechanism. Generally, a positive effect of basic modification and, more surprisingly, of incorporation of glycine, is suggested by the data displayed in Table 1.

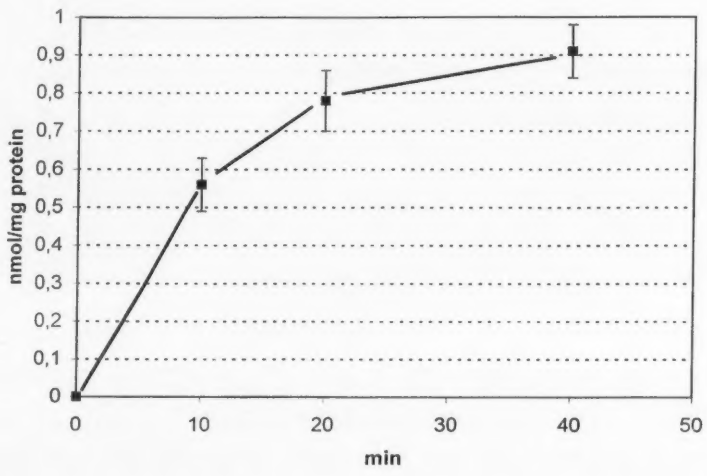

Fig. 2. Quantity of cell-associated peptide after exposing AEC to 2 mM YGGFL-ϵ-K at 37°C for different periods of time. Each point represents the mean of three samples ± SEM.

3.4. CLSM imaging after cell exposure to fluorescently labelled peptides

The poor structural specificity that was found should justify the use of N-terminally fluorescently labelled derivatives for directly demonstrating peptide uptake by CLSM, in spite of substantial alterations to the charge and lipophilicity, which were associated with the introduction of fluorescence labels into peptides. We, therefore, performed CLSM

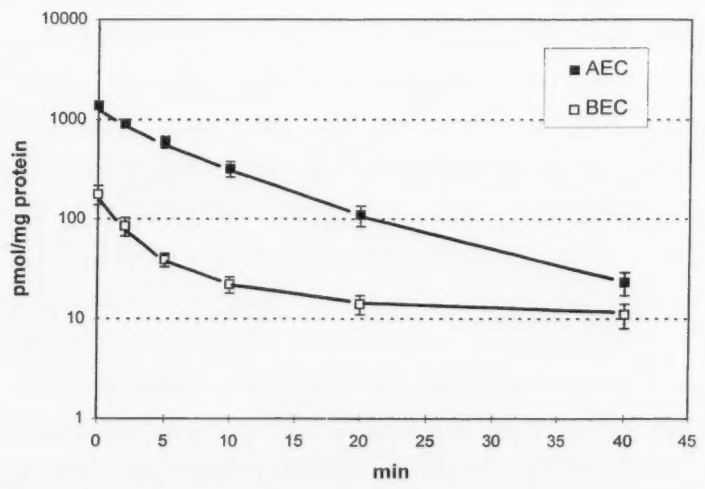

Fig. 3. Liberation of cell-associated peptide at 37°C from AEC and BEC, which had been previously exposed to 2 mM YGGFL-ϵ-K for 60 min at 37°C. Each point represents the mean of three samples ± SEM.

with AEC that had been previously exposed to the fluorescently labelled peptides NBD-GGFL, NBD-GGFL-ϵ-K, NBD-RR-all-D-LWGGY-NH_2 and all-D-RPRPQQFO-(FLUOS)GLM-NH_2 (all-D-FLUOS-SP). The CLSM images in all cases revealed actual peptide import into the cell interior and exhibited a similar pattern to that displayed by NBD-GGFL in Fig. 4. Analogous results to those found with AEC were also obtained with BEC (NBD-GGFL-ϵ-K), primary hypophysis cells (NBD-RR-all-D-LWGGY-NH_2; Furkert et al., in prep.) and mast cells (FLUOS-SP and all-D-FLUOS-SP; Lorenz et al., in prep) (not shown).

3.5. Cell viability and peptide degradation

No differences were detectable between controls and cells treated with 2 mM peptide according to the protocol outlined above with respect to trypan blue exclusion and the MTT-viability test [20].

Due to the high peptide concentrations used, the proportion of the peptide that was degraded by peptidases during exposure to the cells remained clearly below 10%, so that the influence of enzymatic breakdown upon the uptake was neglected. Correspondingly, the addition of 0.4 mM bestatin, a potent inhibitor of aminopeptidase N, the predominant peptidase activity residing on the surface of AEC [21,22], did not influence the amount of cell-associated peptide under the conditions used in this study.

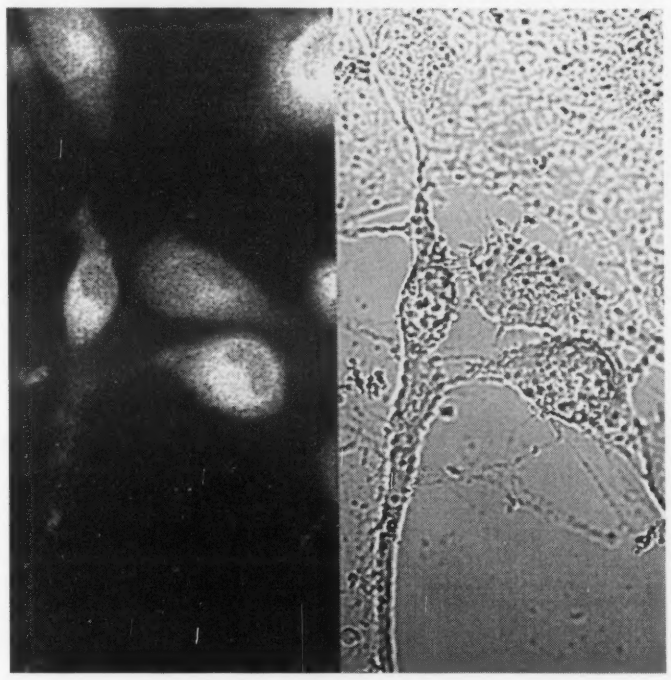

Fig. 4. Confocal laser scanning microscopy image of a 1-μm thick central horizontal optical section through AEC that had previously been exposed to 0.7 mM NBD-GGFL in DPBSG for 30 min at 37°C. Inset: The same section viewed in transmission mode.

In order to obtain information about the possible effects of endogenous peptidases on the internalized substrate, YGGFL-ϵ-K and YGGFL were exposed to Triton X-100 lysates of AEC or BEC at pH 7.2 [$1 \cdot 10^5$ cells, 1% Triton X-100 in 0.5 ml PBS–H_2O (1/9, v/v); 0.2 mM peptide; 60 min, 37°C]. The modified peptide proved to be substantially more stable than leucine enkephalin under these conditions. About 50% of YGGFL-ϵ-K remained intact, whereas 95% of YGGFL was degraded. After exposure of the cells to acidic lysates (10 mM TFA in 0.1% Triton X-100), no cleavage of the peptides could be detected within 24 h at ambient temperature.

3.6. Reproduction of the translocation events in the micromolar range

Beside the metabolically stable enkephalin analog, [^{3}H]DAMGO, we utilized several tritiated peptides

Table 1
Quantity of cell-associated substrate after exposure of aortic endothelial cells to various enkephalin-derived peptides [a]

Peptide	nmol/mg protein
YGGFL	0.57(±0.13)
YGGWL	0.60(±0.17)
N-Methyl-GYGGWL-NH_2	0.71(±0.05)
N-Dimethyl-GYGGWL-NH_2	0.63(±0.19)
SuccinylYGGWL-NH_2	0.80(±0.04)
YGGWLE-NH_2	0.67(±0.13)
DAMGO	0.89(±0.09)
AcYGGWL-NH_2	0.97(±0.22)
YGGWL-NH_2	1.12(±0.11)
EYGGWL-NH_2	1.30(±0.13)
GYGGWL-NH_2	1.29(±0.26)
all-D-YGGWL-NH_2	1.48(±0.27)
YGGEWL-NH_2	1.61(±0.19)
RYGGWL-NH_2	1.65(±0.56)
KYGGWL-NH_2	1.90(±0.08)
AcKYGGWL-NH_2	1.85(±0.27)
YGGWLR-NH_2	1.98(±0.23)
YGGRWL-NH_2	2.12(±0.65)
all-D-LWGGY-NH_2	2.56(±0.36)
YGGWLG-NH_2	2.40(±0.26)
YGGGWL-NH_2	2.99(±0.24)

[a] Incubation with 2 mM peptide dissolved in DPBSG for 30 min at 37°C (mean of three samples ± SEM).

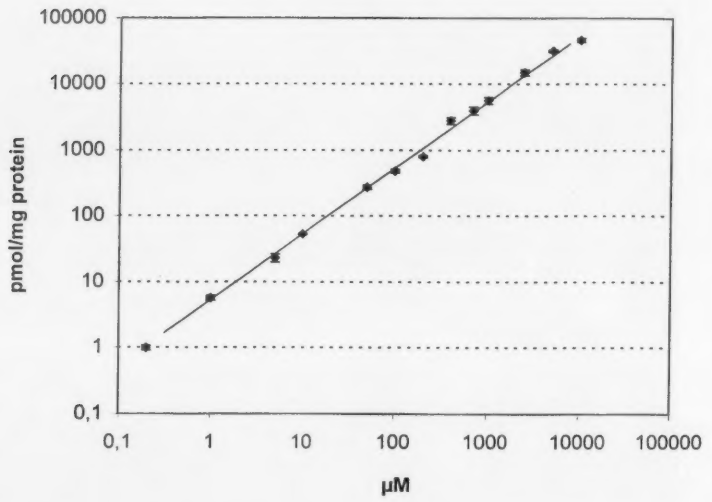

Fig. 5. Quantity of cell-associated peptide after exposing AEC to different concentrations of tritiated DAMGO for 30 min at 37°C. Each point represents the mean of three samples ± SEM.

that differed with respect to charge, size and modification of the N- or C-terminus (R-P-K-P-G-[^{3}H]Y-OH; R-K-E-V-[^{3}H]Y-OH; AcR-AcK-E-V-[^{3}H]Y-OH and [^{3}H]buserelin) for conducting transport experiments in the micromolar concentration range, in a manner analogous to that used in the millimolar range.

To minimize the influences of enzymatic degradation, we generally performed the uptake experiments in the presence of 0.2 mM bestatin. Under these conditions, more than 90% of the radioactivity in the incubation solution was attributable (by HPLC) to the intact peptide after exposure to the cells. From the cell-associated peptide portion, at least 40% coeluted with the intact peptide during subsequent HPLC analysis, indicating uptake of the intact peptide.

3.7. Concentration dependency of uptake

The uptake of the enkephalin analog, DAMGO, into AEC proved to be linear from 10^{-2} up to 10^{-7} M (Fig. 5), rendering peculiarities for the high concentration range unlikely. Uptake investigations performed with the other labelled and unlabelled peptides in the range $5 \cdot 10^{-4}$ to 10^{-7} M and from 10^{-2} to $2 \cdot 10^{-4}$ M led to analogous results (not shown).

Generally, the quantities of internalized peptide approached values corresponding to an equilibrium between intra- and extracellular peptide concentrations (taking into account the cell volume of 1.4 pl

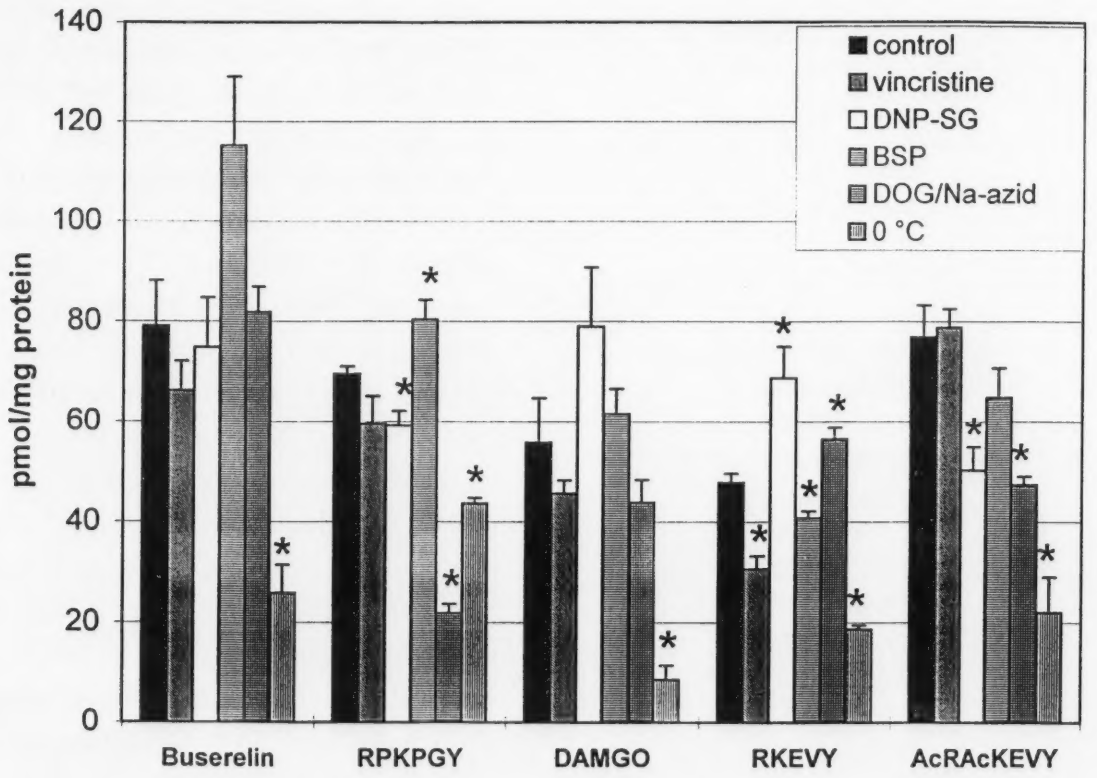

Fig. 6. Quantity of cell-associated peptide after exposing AEC, pretreated with DPBSG or 25 mM 2-deoxyglucose–10 mM sodium azide in DPBS, respectively, for 60 min at 37 and 0°C, to 10 µM tritiated peptide in DPBSG without additives and in the presence of 25 mM 2-deoxyglucose–10 mM sodium azide in DPBS, 20 µM vincristine in DPBSG, 100 µM 2,4-dinitrophenyl-*S*-glutathione (DNP-SG) in DPBSG and 100 µM sulfobromophthalein (BSP) in DPBSG for 60 min at 37 and 0°C. Each bar represents the mean of three samples ± SEM. The differences between the respective controls and the asterisk-labelled bars are statistically significant at $P \leq 0.05$ (Student's *t*-test).

and the protein content of 200 μg protein/10^6 cells given in the Section 2).

3.8. Influences of metabolic and transport inhibitors

To gain an insight into the mechanism of the observed peptide uptake, we exposed the cells to the peptides in the presence of various agents that are known to affect metabolism and transport events. Energy depletion and treatment with vincristine, an inhibitor of the multidrug resistance mediating efflux pump, P-glycoprotein [23], in most cases resulted in a slight reduction in uptake (Fig. 6). The presence of DNP-*S*-glutathione (DNP-SG) and bromosulfophthalein, known to serve as substrates for multidrug resistance-associated protein, glutathione conjugates- and large anion transporters [24–27], augmented or attenuated, respectively, the peptide incorporation, depending on the respective substrate (Fig. 6). This complex behaviour suggests the involvement of multiple energy-consuming transporters exhibiting distinct preferences for the inward or outward direction, respectively, and prevents clear kinetic characterization.

That these reagents also influence the efflux out of the cells is illustrated in Fig. 7 for DNP-SG-treated cells. Conclusions concerning the reduced efflux rate in the presence of DNP-SG, which is apparent in Fig. 7 for the period from 5 to 30 min, and its relation to the enhanced uptake, can be drawn, however, only with caution. Because of a delayed onset of the effects, the agents had to be added prior to the preloading of cells, which resulted in different peptide levels for control- and reagent-treated cells and, probably, in the occupation of distinct compartments by the peptides.

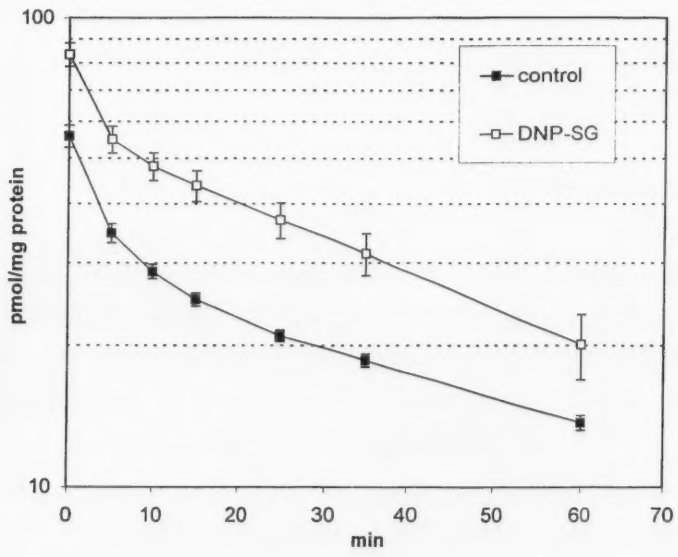

Fig. 7. Liberation of cell-associated peptide at 37°C from AEC into DPBSG without additives and in the presence of 100 μM 2,4-dinitrophenyl-*S*-glutathione (DNP-SG), exposed previously to 10 μM tritiated DAMGO for 60 min at 37°C alone or in the presence of 100 μM DNP-SG, respectively. Each point represents the mean of three samples ± SEM.

Brefeldin A, an inhibitor of vesicular transport [28], did not significantly affect the uptake (not shown), which argues against considerable contributions being made by endocytic processes.

The major part of the observed peptide uptake, however, remained uninfluenced by energy depletion and, therefore, must proceed in an energy independent way (Fig. 6). The substantially reduced uptake at 0°C renders simple diffusion as unlikely to be involved and points to facilitated diffusion as the mechanism for this energy-independent transport. Evidence for cotransport of protons or Na^+, however, often found associated with such a mechanism [29], could not be found. Alterations of the pH in the range of 7.2–5.5, treatment with the acidotropic agent, monensin (20 μM) [30], and replacement of Na^+ by choline, performed in this context, had no effect on peptide uptake (not shown).

3.9. Discrimination between acid-sensitive and acid-resistant portions of cell-associated peptide by acid washes

The levels of cell-associated peptide attained after incubation with 10 μM peptide at 0–4°C (Fig. 6) were relatively higher than those found in the millimolar concentration range, suggesting enhanced contributions of non-specific adsorption in the low concentration range. To obtain information about the degree of this non-specific adsorption, we performed an additional wash step with acetic acid–NaCl for 5 min at 0°C, commonly thought to strip off adsorbed peptides [31]. Fig. 8 displays the cell-associated peptide, which was split into acid-sensitive and an acid-resistant (internalized) parts. Generally (except for RPKPGY at 0°C), the acid-sensitive portion remained clearly below 50% of the total amount, which argues for an actual uptake of the greater part of the observed cell-associated peptide. Moreover, the signifi-

cant reduction in the acid-sensitive bound peptide portion observed in several cases after energy depletion (Fig. 8) raises questions regarding the assumption that the acid extract contains only surface-bound peptide. More likely, this finding suggests export from the cell interior, proceeding also throughout the extraction period at 0°C. That the cells exert residual transport activities at 0°C is also suggested by the considerable amount of acid-resistant bound (internalized) peptide found after incubation at this temperature (Fig. 8).

3.10. Reproducing the transport events with other cell types

In order to rule out the possibility that the found transport phenomena would reflect a peculiarity of AEC, we exposed several cell lines originating from different species and tissues to 10 μM tritiated DAMGO at 37°C and 0°C and after energy depletion. The results of these experiments are displayed in Fig.

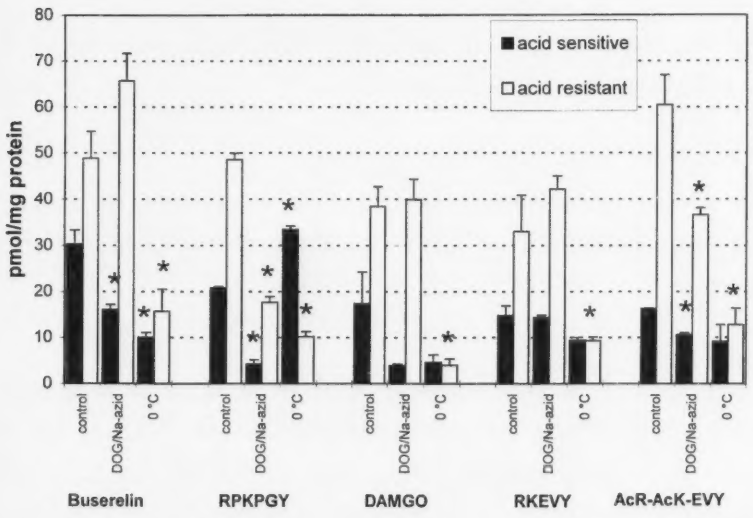

Fig. 8. Acid-sensitive and acid-resistant quantities of cell-associated peptide after exposing AEC, pretreated with DPBSG or 25 mM 2-deoxyglucose–10 mM sodium azide in DPBS, respectively, for 60 min at 37 and 0°C, to 10 μM tritiated peptide in DPBSG without additives and in the presence of 25 mM 2-deoxyglucose–10 mM sodium azide in DPBS for 60 min at 37 and 0°C. The acid-sensitive and acid-resistant proportions of the cell-associated peptide were assessed after incubating the washed cells in 0.2 M acetic acid containing 0.05 M NaCl for 5 min at 0°C before lysing the cells and measuring the radioactivities of both the acid extract and the lysate. Each bar represents the mean of three samples ± SEM. The differences between the respective controls and the asterisk-labelled bars are statistically significant at $P \leq 0.05$ (Student's *t*-test).

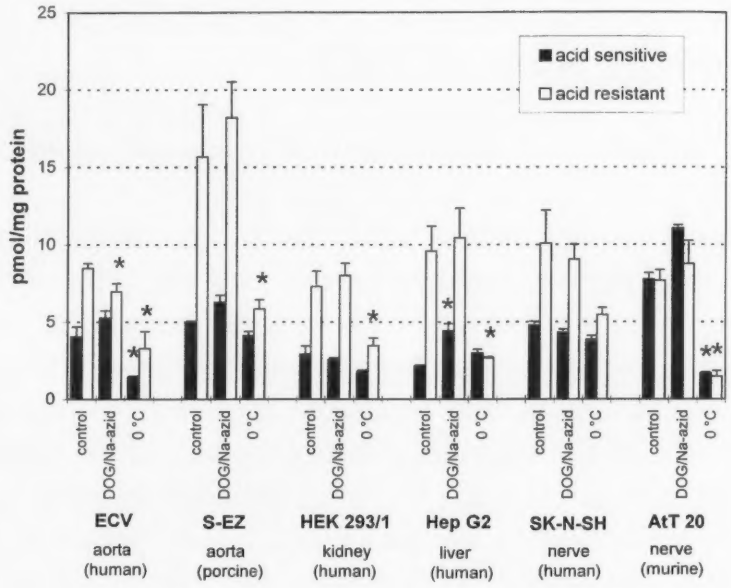

Fig. 9. Acid-sensitive and acid-resistant quantities of cell-associated peptide after exposing various cell types originating from different species and organs to 10 μM tritiated DAMGO, according to the conditions specified in the legend to Fig. 8. Each bar represents the mean of three samples ± SEM. The differences between the respective controls and the asterisk-labelled bars are statistically significant at $P \leq 0.05$ (Student's *t*-test).

9 and reveal, despite clear quantitative differences, considerable analogy to that found previously with AEC. This finding supports the notion that the observed transport phenomena would reflect a more general behaviour of mammalian cells, which has been suggested also by the above outlined analogies found between the results obtained with AEC and BEC, respectively, in the millimolar range, and of AEC and various cell types in CLSM studies.

4. Discussion

This study provides evidence that oligopeptides containing more than five amino acid residues are capable of extensively crossing plasma membranes of living cells. So far, such an ability was demonstrated only for di- and tripeptides [6,32,33] and for a limited number of oligopeptides possessing specific transporters at the blood–brain barrier [8,9].

Our findings contradict prevailing opinion that the repeatedly reported inefficiency of externally administered oligopeptides against recognition domains of signal proteins or intracellular enzymes would be accounted for primarily by poor permeability of peptides across the plasma membranes and point to

export processes being a more decisive factor in this context.

This notion appears reconcilable with recent speculation about the residence of, as yet undetected, peptide transporters of the ABC-transporter type in the plasma membrane of mammalian cells being operative preferably as efflux pumps [34–36]. The influence of energy depletion on the cellular uptake process, and of the P-glycoprotein- and MRP-substrates, vincristine and DNP-SG, respectively, [23–25], observed in the current work, support such speculations. Likewise, these observations provide the first clues to the mechanism for one part of the found translocation events.

The majority of the peptide transport described here, however, proceeded by energy-independent mechanisms. The energy independence, in conjunction with the levels of internalized peptide, approaching an equilibrium between external and internal concentrations, and the substantially reduced uptake at 0°C, point to facilitated diffusion as the mechanism for this part of peptide translocation.

Non-specific adsorptive endocytosis or pinocytosis can only partly explain the transport phenomena found in the present study, taking into consideration the high intracellular peptide levels attained and presuming a total volume for endocytic vesicles of only about 10% of that of the entire cell [37]. An explanation by these mechanisms is further compromised by the observed high exchange rates, of the order of minutes, considering that periods of 1–2 h are commonly required for the turnover of endocytic vesicles between a cell's interior and the plasma membrane [38]. Moreover, brefeldin A, an inhibitor of vesicular transport [28], had no influence upon peptide uptake.

The very specific transporters for enkephalin-like peptides [8,9] can be ruled out as accounting for the transport phenomena observed here, because of the lack of saturability and poor structural specificity. These features tempt one to speculate that the peptides might be capable of exploiting transport facilities that were originally destined for non-peptidic substrates. Preliminary experiments point to amino acid transporters and putative protein channels as probable candidates for mediating such transport. Other preliminary experiments suggest an analogy to the behaviour of several membrane-permeable amphipathic peptides, which have been reported to extensively cross the plasma membrane of mammalian cells by an unknown mechanism [39–41]. These issues will be addressed in future studies.

This study provides evidence for the existence of efficient and non-specific facilities for translocating small peptides in the plasma membranes of mammalian cells. The ability of peptides to extensively cross plasma membranes calls for altered strategies to attain intracellular activity that consider not only metabolic stability and propensity to traverse lipidic membranes, the currently most widespread practice, but also efforts to minimize peptide export out of the cells.

Acknowledgements

We thank Mrs. B. Dekowski, B. Eilemann, A. Klose and D. Smettan for excellent technical assistance, Dr. K. Mertsch and Dr. I.E. Blasig for preparing brain microvessel endothelial cells and Dr. J. Sandow (Hoechst AG) for kindly providing buserelin (HOE 766).

References

[1] W.A. Banks, A.J. Kastin, C.M. Barrera, Pharm. Res. 8 (1991) 1345–1350.
[2] P.L. Smith, D.A. Wall, C.H. Gochoco, G. Wilson, Adv. Drug Deliv. Rev. 8 (1992) 253–290.
[3] B.J. Aungst, J. Pharm. Sci. 82 (1993) 979–987.
[4] M.S. Karls, B.D. Rush, K.F. Wilkinson, T.J. Vidmar, P.S. Burton, M.J. Ruwart, Pharm. Res. 8 (1991) 1477–1481.
[5] P.S. Burton, R.A. Conradi, A.R. Hilgers, Adv. Drug Deliv. Rev. 8 (1991) 93–113.
[6] Y.-J. Fei, Y. Kanai, S. Nussberger, V. Ganapathy, F.H. Leibach, M.F. Romero, S.K. Singh, W.F. Boron, M.A. Hediger, Nature 368 (1994) 563–566.
[7] R. Liang, Y.-J. Fei, P.D. Prasad, S. Ramamoorthy, H. Han, T.L. Yang-Feng, M.A. Hediger, V. Ganapathy, F.H. Leibach, J. Biol. Chem. 270 (1995) 6456–6463.
[8] W.A. Banks, A.J. Kastin, Am. J. Physiol. 259 (1990) E1–E10.
[9] B.V. Zlokovic, J.M. Mackic, B. Djuricic, H. Davson, J. Neurochem. 3 (1989) 1333–1340.
[10] T. Pawson, Nature 373 (1995) 573–580.
[11] C.A. Hinchman, H. Matsumoto, T.W. Simmons, N. Ballatori, J. Biol. Chem. 266 (1991) 22179–22185.
[12] P. Henklein, M. Beyermann, M. Bienert, R. Knorr, in: E. Giralt, D. Andreu (eds.), Peptides, ESCOM, Leiden, 1990, p. 67.

[13] J. Oehlke, E. Mittag, H.-J. Klebsch, H. Niedrich, J. Label. Compd. Radiopharm. 27 (1989) 999–1005.
[14] J. Oehlke, T. Brankoff, M. Schmidt, M. Brudel, U. Kertscher, H. Berger, J. Label. Compd. Radiopharm. 33 (1993) 161–169.
[15] M. Bienert, J. Oehlke, E. Mittag, H. Niedrich, J. Label. Compd. Radiopharm. 28 (1990) 1401–1409.
[16] W. Halle, W.-E. Siems, K.-D. Jentzsch, Acta Biol. Med. Germ. 39 (1980) 1163–1175.
[17] K. Mertsch, T. Grune, W.G. Siems, A. Ladhoff, N. Saupe, I.E. Blasig, Cell. Mol. Biol. 41 (1995) 243–253.
[18] M.M. Bradford, Anal. Biochem. 72 (1976) 248–254.
[19] Q.R. Smith, Exp. Med. Biol. 331 (1993) 83–93.
[20] T. Mosmann, J. Immunol. Methods 65 (1983) 55–63.
[21] F.E. Palmieri, H.H. Bausback, P.E. Ward, Biochem. Pharmacol. 38 (1989) 173–180.
[22] G. Heder, M. Melzig, W.-E. Siems, Pharmazie 47 (1992) 226–228.
[23] M.M. Gottesman, I. Pastan, Annu. Rev. Biochem. 62 (1993) 385–427.
[24] S.P. Cole, G. Bhardwaj, J.H. Gerlach, J.E. Mackie, C.E. Grant, K.C. Almquist, A.J. Stewart, E.U. Kurz, A.M. Duncan, R.G. Deeley, Science 258 (1992) 1650–1654.
[25] H. Shen, S. Paul, L.M. Breuninger, P.J. Ciaccio, N.M. Laing, M. Helt, K.D. Tew, G.D. Kruh, Biochemistry 35 (1996) 5719–5725.
[26] G. Bartosz, H. Sies, P.M. Akerboom, Biochem. J. 292 (1993) 171–174.
[27] N. Ballatori, A.T. Truong, J. Biol. Chem. 270 (1995) 3594–3601.
[28] J. Lippincott-Schwartz, L.C. Yuan, J.S. Bonifacino, R.D. Klausner, Cell 56 (1989) 801–813.
[29] M.D. Marger, M.H. Saier, Trends Biochem. Sci. 18 (1993) 13–21.
[30] F.R. Maxfield, J. Cell Biol. 95 (1982) 676–681.
[31] A.M. Garland, E.F. Grady, D.G. Payan, S.R. Vignas, N.W. Bunnett, Biochem. J. 303 (1994) 177–186.
[32] V. Ganapathy, F.H. Leibach, Life Sci. 30 (1982) 2137–2146.
[33] D. Meredith, C.A.R. Boyd, J. Membr. Biol. 145 (1995) 1–12.
[34] R.C. Sharma, S. Inoue, J. Roitelman, R.T. Schimke, R.D. Simoni, J. Biol. Chem. 267 (1992) 5731–5734.
[35] P.S. Burton, R.A. Conradi, A.R. Hilgers, N.F.H. Ho, Biochem. Biophys. Res. Commun. 190 (1993) 760–766.
[36] F.J. Sharom, G. DiDiodato, X. Yu, K.J.D. Ashbourne, J. Biol. Chem. 270 (1995) 10334–10341.
[37] F.L. Guillot, K.L. Audus, T.J. Raub, Microvasc. Res. 39 (1990) 1–14.
[38] W.-C. Shen, J. Wan, H. Ekrami, Adv. Drug Deliv. Rev. 8 (1992) 93–113.
[39] D. Derossi, A.H. Joliot, G. Chassaing, A. Prochiantz, J. Biol. Chem. 269 (1994) 10444–10450.
[40] Y.-Z. Lin, S. Yao, R.A. Veach, T.R. Torgerson, J. Hawiger, J. Biol. Chem. 270 (1995) 14255–14258.
[41] J. Oehlke, E. Krause, B. Wiesner, M. Beyermann, M. Bienert, Protein Peptide Lett. 3 (1996) 393–398.

ELSEVIER

Biochimica et Biophysica Acta 1330 (1997) 61–70

BIOCHIMICA ET BIOPHYSICA ACTA
BBA

Charge-dependent insertion of β-lactoglobulin into monoglyceride monolayers

J.M. Leenhouts [1], R.A. Demel, B. de Kruijff, J.-W.P. Boots *

Department of Biochemistry of Membranes, Centre for Biomembranes and Lipid Enzymology, Institute of Biomembranes, Utrecht University, Padualaan 8, 3584 CH Utrecht, Netherlands

Received 16 April 1997; revised 10 June 1997; accepted 12 June 1997

Abstract

The interactions between β-lactoglobulin and 1-monostearoyl-glycerol were studied in order to gain insight into protein–gel-phase monoglyceride interactions. Using a monomolecular layer at the air–water interface, we determined the insertion of β-lactoglobulin into the monoglycerides under different conditions of protein and surface charge by varying the pH and/or incorporating charged amphiphiles into the monolayer, respectively, and using subphases with either a low or high ionic strength. The interactions were quantified by determining the binding of ^{14}C-labeled β-lactoglobulin to the monolayer. Our results show the importance of electrostatics for binding of β-lactoglobulin to condensed monoglycerides. Moreover, electrostatic interactions were found to be important for specific insertion of β-lactoglobulin into the monolayer. A negatively charged surface in particular allowed positively charged β-lactoglobulin to insert in a surface charge density-dependent manner, even at surface pressures as high as 36 mN/m, whereas under other conditions, the limiting insertion pressure was 32 mN/m. The rheological properties of the monolayer were not affected by the interactions with β-lactoglobulin. © 1997 Elsevier Science B.V.

Keywords: Protein-lipid interaction; Condensed monolayer; Monoglyceride; β-Lactoglobulin

1. Introduction

Aqueous dispersions of commonly used long chain saturated monoglycerides are able to form densely packed gel-phase bilayer structures that are separated by aqueous compartments [1–3]. The size of these aqueous compartments can be increased by adding small amounts of charged amphiphiles to the monoglyceride, providing such systems with interesting properties for application in the food industry, in particular in low-fat products [4]. Proteins may be entrapped in the aqueous compartments and could interact with the lipid phase and thus influence the properties of the monoglyceride system. In contrast to the interactions between proteins and other lipid bilayers, i.e. biological membranes, virtually nothing is known about a possible interaction between proteins and gel-phase monoglycerides. Such interactions

Abbreviations: β-LG, β-lactoglobulin; MSG, 1-monostearoyl-*rac*-glycerol; MPG, 1-mono-palmitoyl-*rac*-glycerol; MOG, 1-monooleoyl-*rac*-glycerol; DCP, dicetylphosphate; SA, stearylamine; IEP, isoelectric point; π_i, initial surface pressure; $\Delta\pi$, surface pressure increase; π_l, limiting surface pressure; ϵ, surface elasticity dilatation modulus

* Corresponding author. Fax: +31 30 2522478.

[1] Present address: Department of Biochemistry and Molecular Biology, University of British Colombia, 2146 Health Sciences Mall, Vancouver, British Colombia, Canada, V6T 1Z3.

0005-2736/97/$17.00 © 1997 Elsevier Science B.V. All rights reserved.
PII S0005-2736(97)00142-9

could involve binding and adsorption of a protein to the interface or even penetration of a protein into the bilayer. However, it is generally difficult for proteins to penetrate into gel-phase phospholipid bilayers. On the other hand, the nature and extent of any given lipid–protein interaction may not be entirely determined by the packing density of the lipids; the type of interface presented by the lipids is also an important parameter. Therefore, studying monoglyceride–protein interactions also offers many interesting opportunities from the point of view of understanding biomembrane structure and function, because a monoglyceride ''membrane'' presents a stable interface containing only free hydroxyls as polar groups to a protein. In this respect, it is intriguing that monoglyceride cubic phases allowed the crystallization of membrane proteins [5].

In the present study, we investigated, using the monolayer technique, the interaction between a globular protein and one layer of a gel-phase monoglyceride bilayer. For this purpose, the most abundant whey protein, β-lactoglobulin (β-LG), and a gel-phase-forming monoglyceride, 1-monostearoyl-glycerol (MSG), were used. The interactions between β-LG and MSG were characterized by determining the binding and insertion of β-LG into the monoglyceride monolayer and the effect of β-LG on the rheology of the monolayer. Bovine β-LG was used because it is a well-characterized globular protein of which two major, β-LG A and B, and several minor genetic variants are found in bovine milk. The protein consists of 162 amino acids and has a molecular weight of 18 kDa and an isoelectric point (IEP) of 5.2 [6]. The structure consists of an eight-stranded antiparallel β-barrel and one N-terminal α-helix, which is followed by a ninth β-strand. All of these structural elements are connected by large loops of random coil, which account for about 50% of the structure. The protein also contains one disulfide bridge and one free thiol group [7,8].

Since monoglycerides are uncharged, it can be envisioned that the addition of a surface charge will also affect the interaction between the monoglycerides and a protein. It has been shown that a surface charge can be an important factor for the interaction of peptides and proteins with membranes [9–11], including the interaction of β-LG with phospholipid monolayers [12]. Therefore, we included in our studies the effect of incorporating small amounts of dicetylphosphate (DCP) or stearylamine (SA) in the monolayer, to give a negatively or positively charged surface, respectively. The results show the importance of electrostatics for the interaction between β-LG and the monoglycerides, and, moreover, that the protein is, under specific conditions, able to penetrate into a densely packed MSG monolayer.

2. Materials and methods

2.1. Materials

Bovine β-lactoglobulin (a mixture of genetic variants A and B), 1-monostearoyl-*rac*-glycerol, 1-monopalmitoyl-*rac*-glycerol and 1-monooleoyl-*rac*-glycerol, DCP and SA were obtained from Sigma (St. Louis, MO, USA) and were used without further purification. Ultra-pure bovine β-lactoglobulin (genetic variant A) was a generous gift from Dr. C.G. de Kruif (NIZO, the Netherlands). Tris was obtained from Baker (Deventer, the Netherlands), sodium acetate, KH_2PO_4 and NaCl were from Merck (Darmstadt, Germany), fast-flow Q-Sepharose was from Pharmacia (Uppsala, Sweden), [^{14}C]formaldehyde (58 μCi/μmol) was from Dupont NEN (Mechelen, Belgium) and $NaBH_3CN$ was obtained from Across (Geel, Belgium).

2.2. Modification of β-LG

A ^{14}C label was introduced into β-LG by reductive methylation with [^{14}C]formaldehyde and $NaBH_3CN$ [13]. β-LG was dissolved to a final concentration of 54 μM in a 0.2-M KH_2PO_4 buffer at pH 7.0. [^{14}C]Formaldehyde and $NaBH_3CN$ were added to give final concentrations of 0.16 and 1.6 mM, respectively. The mixture was then incubated overnight at room temperature. After the reaction, the incubation mixture was loaded on a 0.5-ml fast-flow Q-Sepharose column that had been equilibrated with 20 mM Tris, pH 7.0. After washing the column with 5.0 ml of 20 mM Tris, pH 7.0, β-LG was eluted from the column with 1.0 ml of 500 mM NaCl, 20 mM Tris, pH 7.0. The resulting β-LG had a specific radioactivity of 105 000 dpm/nmol, corresponding to a stoichiometry of the reaction of 0.8 mole label/mole protein.

β-LG was heat-denatured under conditions reported to induce the formation of large covalent aggregates [14,15]. To this end, 15 mg of β-LG dissolved in 1 ml of 20 mM Tris, 10 mM NaCl, pH 7.0, were incubated overnight at 65°C.

2.3. Monolayer experiments

Surface pressures were measured by the Wilhelmy plate method in Teflon troughs at 22°C, using a paper (π–A curves) or platinum plate [16]. Buffers used were: 20 mM sodium acetate (pH 4.0 and pH 5.2) and 20 mM Tris (pH 7.0), with or without 100 mM NaCl. Appropriate amounts of lipid stock solutions, dissolved in $CHCl_3$–MeOH (3:1, v/v), were spread on the subphase. Unless stated otherwise, a 9:1 monoglyceride-charged amphiphile molar ratio was used for experiments requiring a charged monolayer.

Surface pressure–area (π–A) curves were measured using a 0.8-l trough (32.2 × 17.3 × 1.5 cm) equipped with a moveable barrier. The films were compressed at a rate of 80 cm^2/min.

The insertion of β-LG into monoglyceride monolayers was studied using a 6-ml Teflon dish with a surface area of 8.8 cm^2. The whole experimental set-up was placed in a thermostated box. The subphase was continuously stirred with a magnetic bar. Initial surface pressures ranged from 25 to 36 mN/m. A 10-μl volume of a β-LG stock solution (0.82 mM) was injected under the monolayer through a separate hole in the Teflon dish, giving a final β-LG concentration of 1.4 μM. The addition of more β-LG did not result in larger increases in the surface pressure. The error in these experiments was 0.2 mN/m.

Binding experiments were performed using a 20-ml trough (5.5 × 6 × 0.6 cm) that was connected to two reservoirs via a circulation pump. Initial surface pressures were 26 or 32 mN/m. A 50-μl volume of a [^{14}C]β-LG stock solution (26.6 μM) was injected under the monolayer, giving a final β-LG concentration of 0.07 μM. This lower β-LG concentration gave similar surface pressure increases as those observed using 1.4 μM β-LG, as used for the insertion experiments. The surface radioactivity was determined with a Berthold LB 203E gas flow counter. After the surface tension and radioactivity of the monolayer became stable, the subphase was washed with 100 ml of the appropriate buffer by flushing at a flow-rate of 6 ml/min. The monolayer was subsequently collected in a scintillation vial by aspiration through a glass capillary while manually decreasing the surface area with a barrier. The radioactivity of the samples was determined with a Packard TRI-CARB 1500 scintillation counter (Downers Grove, IL, USA), and the result was corrected for the value measured in an equal volume of subphase.

The surface dilatation elasticity was measured as described by Paternotte et al. [17] using a 1.2-l trough (45.0 × 15.2 × 1.5 cm) equipped with a moveable barrier. A 1.0-ml volume of a β-LG stock solution (1.4 mM) was injected under the monolayer, giving a final β-LG concentration of 1.2 μM in the subphase. The initial surface pressure was 20 mN/m and final surface pressures ranged from 38 to 47 mN/m. Measurements were performed at several surface pressures by compressing the monolayer in a stepwise manner. After each compression step, the dilatation elasticity was determined by oscillating the barrier sinusoidally at a frequency of 0.15 Hz and at an amplitude of 4% of the mean surface area.

3. Results

In order to characterize the state of the monolayer, the surface pressure–area (π–A) curve of 1-monostearoyl-glycerol (MSG) was determined and compared to those of: 1-monopalmitoyl-glycerol (MPG) and 1-monooleoyl-glycerol (MOG) (Fig. 1). The π–A curve of MOG is typical for lipids in the expanded-

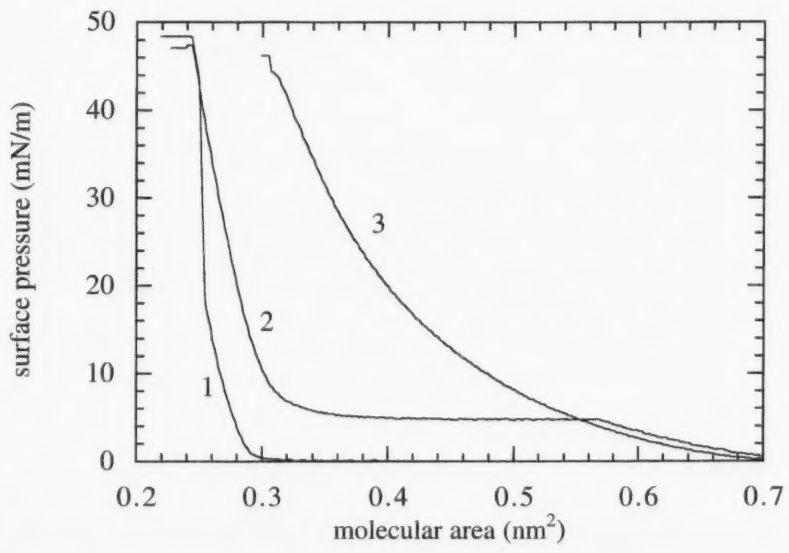

Fig. 1. Surface pressure–area curves for: 1-monostearoyl-glycerol (1), 1-monopalmitoyl-glycerol (2) and 1-monooleoyl-glycerol (3) at 22°C on water.

phase. The relatively large molecular area of 0.312 nm^2 at the collapse pressure can be attributed to the *cis*Δ9 double bond. MPG shows a phase transition from the expanded- to the condensed-phase at a surface pressure of 5 mN/m and a molecular area of 0.56 nm^2. In the expanded-phase, i.e. below 5 mN/m, the molecular area of MPG is comparable to that of MOG. The π–A curve of MSG is characteristic for a lipid in the condensed-phase with little compressibility, a phase similar to the gel-phase of lamellar systems, and its limiting molecular area of 0.254 nm^2 is significantly higher than those found for the single chain surfactants, stearic acid and stearyl alcohol [18]. This higher value of MSG could result from a tilted orientation of the acyl chain, as found in liquid crystals [1,19,20], or it could be attributed to the presence of the larger polar headgroup. The collapse pressure of 45 mN/m is remarkably high and comparable to that of phosphatidylcholines [16]. Because the aim of this study was to investigate the interaction between a protein and gel-phase, i.e. condensed monoglycerides, MSG was used for all further experiments. Furthermore, MSG forms very stable monolayers, whereas MPG shows a decline at higher surface pressures, as was also found by de la Fuente Feria and Rodriguez Patino [21].

In the absence of monoglycerides, the surface activity of β-LG results in a protein monolayer with

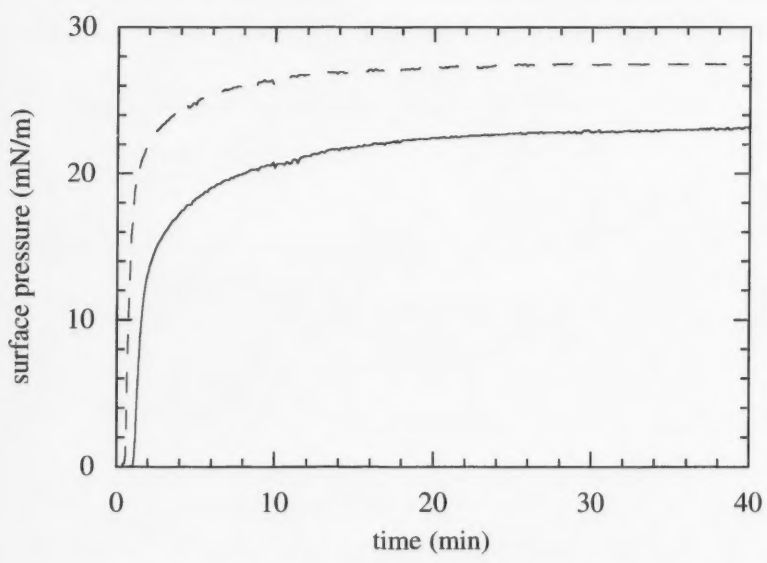

Fig. 2. Time dependence of the β-LG-induced surface pressure increase in the absence (solid line) or presence (dotted line) of 100 mM NaCl. The buffer used was 20 mM Tris, pH 7. At t = 0, β-LG was injected into the subphase to give a final concentration of 1.4 μM.

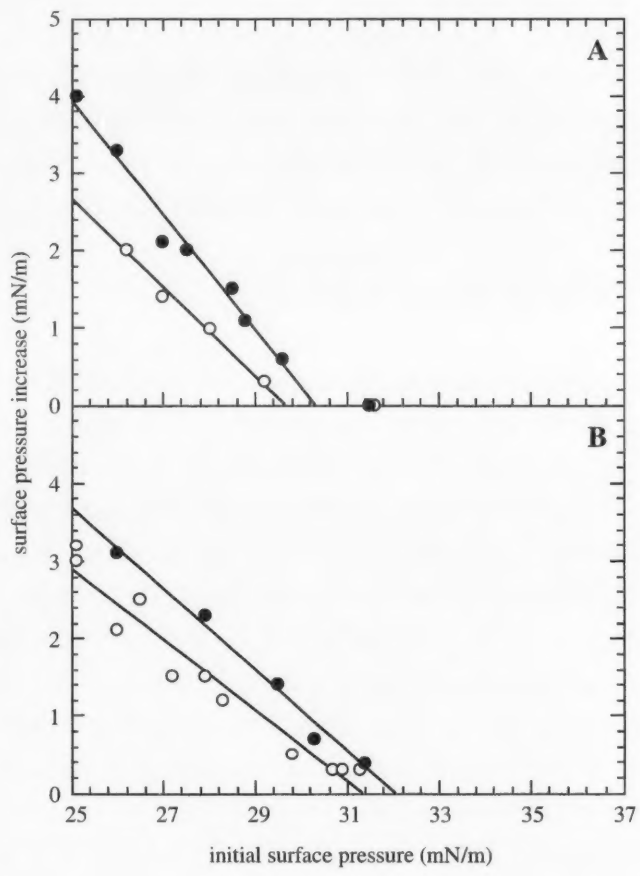

Fig. 3. β-LG-induced surface pressure increase as a function of the initial surface pressure of neutral MSG monolayers. The buffers used were 20 mM Tris, pH 7 (panel A) or 20 mM sodium acetate, pH 4 (panel B), either with (closed symbols) or without (open symbols) 100 mM NaCl. The β-LG concentration in the subphase was 1.4 μM.

a surface pressure of 22.8 mN/m, at pH 7 (Fig. 2) and pH 4 (not shown). The presence of 100 mM NaCl in the subphase increases the surface activity of β-LG at pH 7 to 27.4 mN/m (Fig. 2), indicating an increased hydrophobicity of the protein, while no significant effect was observed at pH 4 (not shown). Because of the surface activity of the protein, all insertion and binding experiments were performed using monolayers with initial surface pressures (π_i) of 25 mN/m or higher.

Injection of β-LG under a MSG monolayer leads to a protein-induced surface pressure increase ($\Delta\pi$) of the monolayer, the extent of which depends on the lipid composition of the monolayer, and on the pH and ionic strength of the subphase. The β-LG-induced $\Delta\pi$ as a function of the initial surface pressure of a neutral MSG monolayer (π_i–$\Delta\pi$) under various conditions is shown in Fig. 3. Extrapolation to high initial surface pressures provides the limiting inser-

tion pressure (π_l) at which the protein is no longer able to insert into the monolayer. At pH 7, the π_l for β-LG insertion into a neutral MSG monolayer is 30 mN/m (Fig. 3A), while at pH 4, this was found to be 32 mN/m (Fig. 3B). Similar results were obtained at pH 5.2, the IEP of β-LG (not shown). Addition of 100 mM NaCl to the subphase has a stimulating effect on β-LG insertion, at pH values of 7 and 4.

The addition of charged amphiphiles to the MSG monolayer affects the interaction between the monolayer and β-LG. Fig. 4 shows the effect of incorporating small amounts of the anionic amphiphile, DCP, into a MSG monolayer with a π_i of 25 mN/m at pH 4, i.e. with β-LG and the monolayer having opposite charges. A non-linear relationship was observed. Initially, at DCP concentrations up to 5 mole%, no additional effect is observed. Above 5 mole% DCP, however, larger surface pressure increases were induced by β-LG, an effect which leveled off at 10 mole% DCP. No reliable data could be obtained above 10 mole% as a result of the monolayer becoming less stable. The increased insertion observed in the 5–10 mole% DCP range is specific for this set of conditions. Larger β-LG-induced $\Delta\pi$s were not observed at pH 7, where β-LG and the monolayer are both negatively charged. Moreover, larger $\Delta\pi$s were also not observed when the charges of β-LG and the monolayer were reversed by incorporating SA into the monolayer and performing the experiment at pH

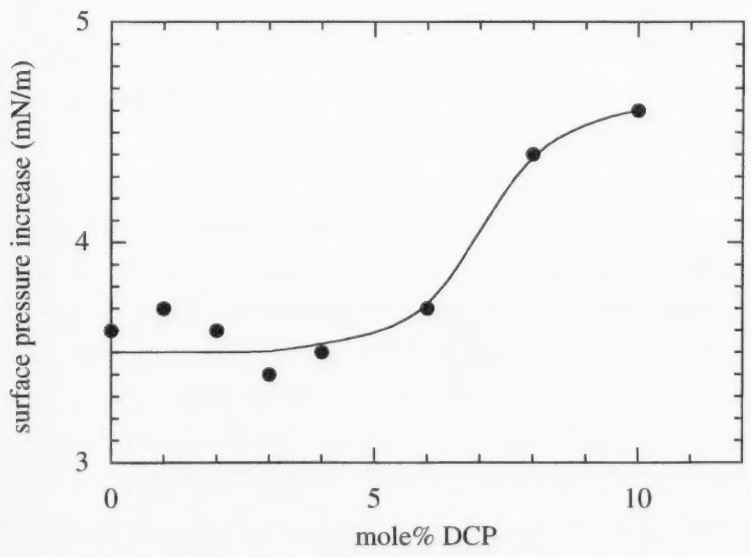

Fig. 4. β-LG-induced surface pressure increase as a function of the mole percentage of DCP in a MSG monolayer. The initial surface pressure was 25 mN/m. The buffer used was 20 mM sodium acetate, pH 4. The β-LG concentration in the subphase was 1.4 μM.

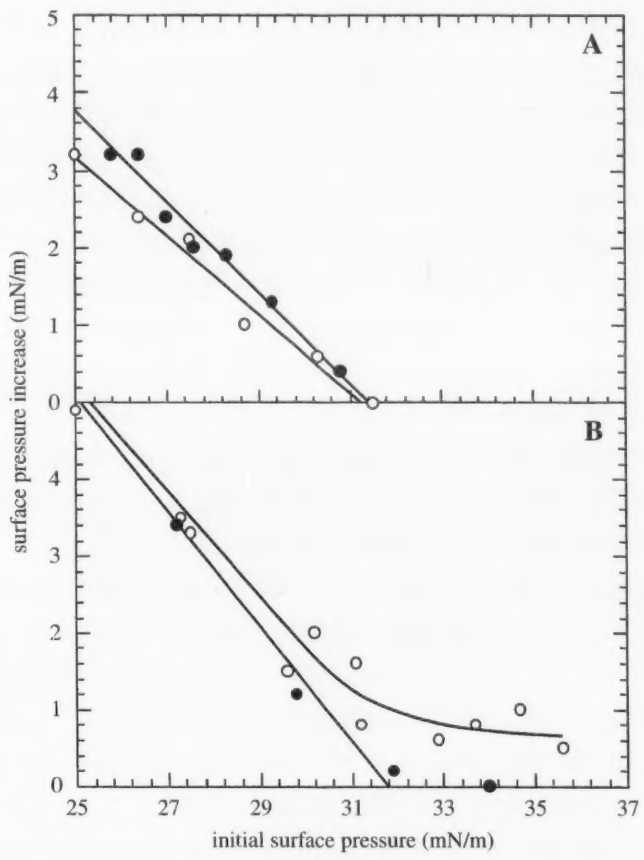

Fig. 5. β-LG-induced surface pressure increase as function of the initial surface pressure of negatively charged MSG/DCP monolayers. The concentration of DCP in the monolayer was 10 mole%. The buffers used were 20 mM Tris, pH 7 (panel A) or 20 mM sodium acetate, pH 4 (panel B), either with (closed symbols) or without (open symbols) 100 mM NaCl. The β-LG concentration in the subphase was 1.4 μM.

7. Based on these observations, all further experiments with charged monolayers were performed using a charged amphiphile concentration of 10 mole%.

Incorporation of 10 mole% DCP into a MSG monolayer had little effect on the π_i–$\Delta\pi$ curve at pH 7 (Fig. 5A). Both in the presence and absence of 100 mM NaCl, the π–$\Delta\pi$ curves are similar to those observed using neutral MSG monolayers, and a comparable π_l of 32 mN/m was found in both cases. However, at pH 4, with β-LG and the surface having opposite charges, another interaction is observed and, as a result, β-LG insertion is increased (Fig. 5B). Consequently, the β-LG-induced $\Delta\pi$s are larger (cf. Fig. 4) and no clear π_l seems to be reached, distinct β-LG-induced $\Delta\pi$s are also observed above 32 mN/m, at surface pressures as high as 36 mN/m. In the presence of 100 mM NaCl, no β-LG-induced $\Delta\pi$s were observed above a π_i of 32 mN/m, but the $\Delta\pi$s observed at surface pressures below 32 mN/m are still larger than those observed using neutral

monolayers. Interestingly, heat denaturation did not abolish the ability of β-LG to insert at high initial surface pressures and a curve similar to that observed with the native protein was obtained (not shown). Furthermore, using an ultra-pure sample of β-LG A also resulted in a curve similar to that observed with the mixture of β-LG A and B obtained from Sigma, ruling out the possibility of contamination effects.

No large effects on the β-LG-induced $\Delta\pi$s were observed when 10 mole% of the positively charged amphiphile, SA, were incorporated into MSG monolayer (Fig. 6). Also, no stimulating effect of a higher ionic strength was observed at pH 7, while at pH 4, where both β-LG and the monolayer are positively charged, there is even a small negative effect on the insertion of β-LG into the MSG/SA monolayer, possibly as a result of charge shielding.

In order to quantify the binding of β-LG to the MSG monolayers, ^{14}C-labeled β-LG was used. In Fig. 7, two typical experimental curves are depicted.

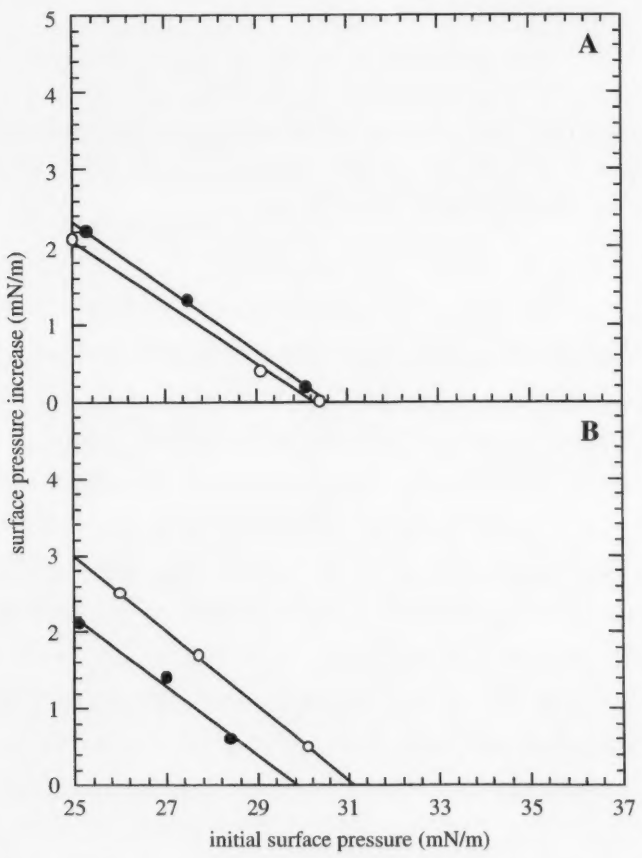

Fig. 6. β-LG-induced surface pressure increase as a function of the initial surface pressure of positively charged MSG/SA monolayers. The concentration of SA in the monolayer was 10 mole%. The buffers used were 20 mM Tris, pH 7 (panel A) or 20 mM sodium acetate, pH 4 (panel B), either with (closed symbols) or without (open symbols) 100 mM NaCl. The β-LG concentration in the subphase was 1.4 μM.

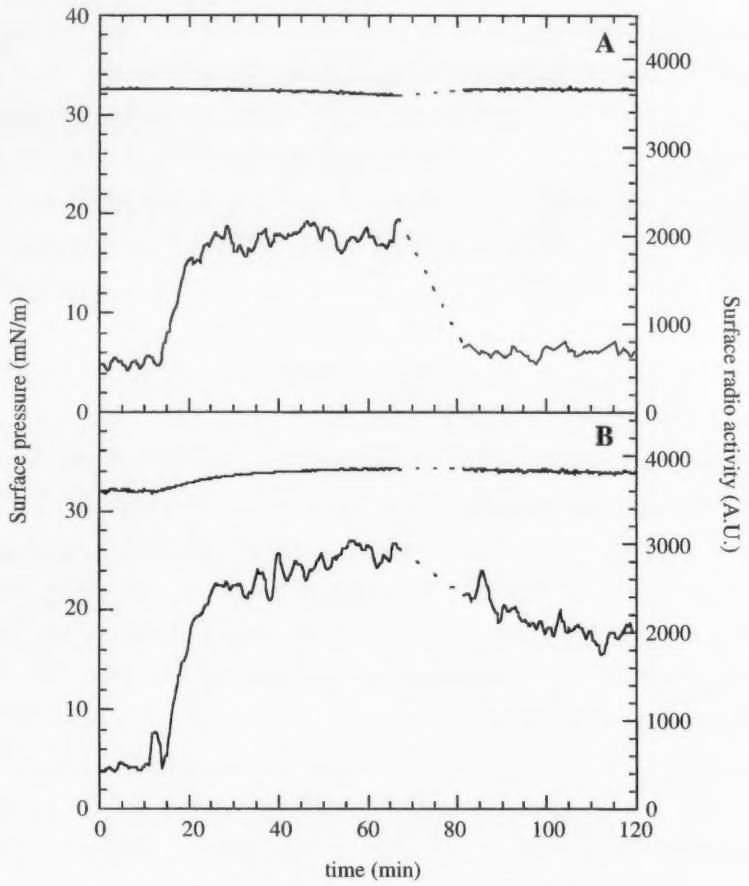

Fig. 7. Time dependence of β-LG binding (surface radioactivity) and insertion (surface pressure increase) into a MSG/SA monolayer at pH 7 (panel A) or a MSG/DCP monolayer at pH 4 (panel B). SA and DCP concentrations were 10 mole%. At t = 15 min, [^{14}C]β-LG was injected to give a final concentration of 0.07 μM in the subphase. Between t = 65 and t = 80 min, the subphase was washed with 100 ml of buffer (dotted line). The buffers used were 20 mM Tris, pH 7 or 20 mM sodium acetate, pH 4.

Although no insertion of β-LG into a MSG/SA monolayer with a π_i of 32 mN/m is observed at pH 7 (cf. Fig. 6), it is clear that β-LG binds to such a monolayer, as revealed by the increased surface radioactivity (Fig. 7A). However, most of the bound protein is removed from the monolayer upon washing, indicating a loose association. The interaction between β-LG and a MSG/DCP monolayer at 32 mN/m and pH 4 leads to insertion of the protein and a concomitant increase in the surface radioactivity (Fig. 7B). However, washing now results in only a partial loss of the β-LG bound to the surface. The role of electrostatics in the binding of β-LG to MSG monolayers is apparent from Fig. 8. When using monolayers containing a surface charge that is opposite to that of β-LG, optimal binding was observed with a low ionic strength in the subphase. A high

ionic strength in the subphase prevented the binding of β-LG to both positively and negatively charged MSG monolayers. Furthermore, a high ionic strength in the washing buffer resulted under all conditions in the removal of the β-LG bound to the monolayer. In contrast, a washing buffer with a low ionic strength did not completely remove the β-LG bound to MSG/DCP (cf. Fig. 7). Only small amounts of β-LG were found to interact with neutral MSG monolayers, even under conditions, i.e. at a π_i of 26 mN/m, where the protein does insert (cf. Fig. 3).

To gain further insight into the β-LG–MSG monolayer interaction, the effect of β-LG on the rheological properties of the monolayer were studied. In Fig. 9, the surface dilatation elasticity modulus (ϵ) of different MSG monolayers in the absence or presence of β-LG are shown as function of the surface pressure. The ϵ of the neutral MSG monolayer is comparable to that of a distearoylphosphatidylcholine monolayer [16]. Clear differences are indeed observed between the various MSG monolayers in the absence of β-LG, reflecting the sensitivity of this technique for small variations in the lipid composition of the monolayer. The presence of SA in the MSG monolayer causes a small decrease in ϵ at higher surface pressures, while ϵ is reduced at all surface pressures when DCP is added to the monolayer. However, the presence of β-LG had no detectable effect on ϵ under all of the conditions tested, indicating that the rheological properties are primarily determined by the lipid layer itself and less so by the adsorbed protein.

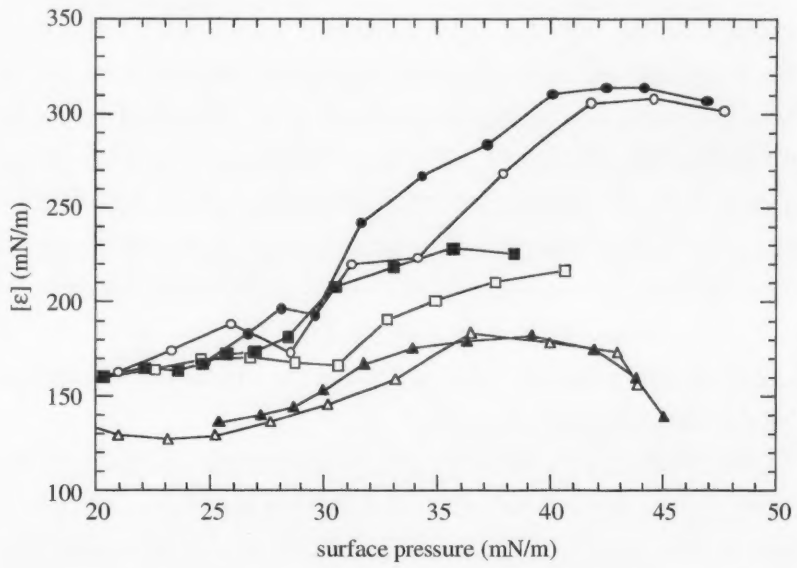

Fig. 9. Surface dilatation elasticity modulus (ϵ) of neutral MSG (circles), positively charged MSG/SA (squares) and negatively charged MSG/DCP (triangles) monolayers as a function of the surface pressure, either in the absence (open symbols) or presence (closed symbols) of β-LG. DCP and SA concentrations were 10 mole%. The buffers used were 20 mM Tris, pH 7 (positively charged monolayer) or 20 mM sodium acetate, pH 4 (neutral and negatively charged monolayers). The β-LG concentration in the subphase was 1.2 μM.

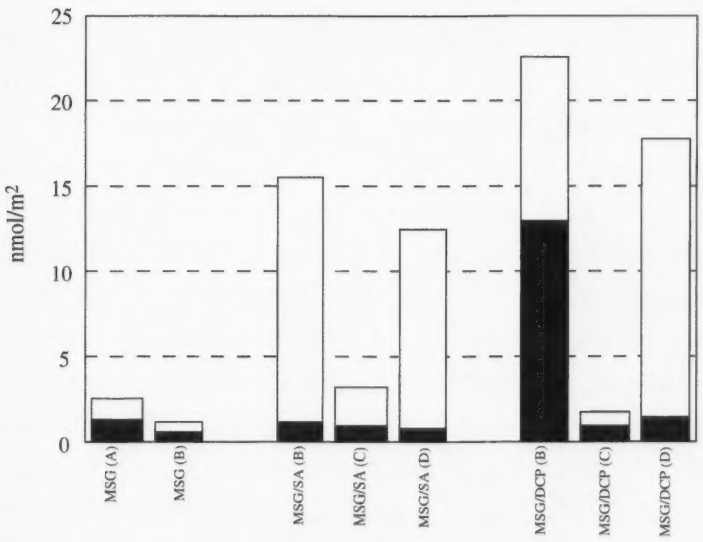

Fig. 8. Surface binding of [^{14}C]β-LG, before (open + closed bar) and after (closed bar) washing of the subphase, to MSG, MSG/SA and MSG/DCP monolayers at pH values of 5.2, 7 and 4, respectively. Conditions: (A) $\pi_i = 26$ mN/m, (B) $\pi_i = 32$ mN/m, (C) $\pi_i = 32$ mN/m with 100 mM NaCl added to the subphase and (D) $\pi_i = 32$ mN/m with 100 mM NaCl added to the washing buffer. The buffers used were 20 mM sodium acetate (pH 4), 20 mM sodium acetate (pH 5.2) and 20 mM Tris (pH 7). SA and DCP concentrations were 10 mole%. The [^{14}C]β-LG concentration in the subphase was 0.07 μM. β-LG binding was determined by measuring the surface radioactivity before and after washing and by measuring the radioactivity of the monolayers collected after washing of the subphase.

4. Discussion

It is clear from our results that β-LG is able to interact with condensed monoglyceride monolayers under various conditions. When using neutral MSG monolayers, the protein is able to insert into the monolayer at initial surface pressures of up to 32 mN/m. The hydrophobic nature of this interaction follows from the stimulating effect of the increased ionic strength of the subphase, in particular, at pH 4, where the hydrophobicity of the protein itself is unaffected. The interaction therefore probably in-

volves some of the hydrophobic patches on the surface of β-LG, one of which could be the putative binding site for retinol and other hydrophobic compounds [8]. The pH of the subphase, on the other hand, had no effect on the insertion of β-LG into a neutral MSG monolayer, indicating that, in contrast to a protein monolayer, the conformational change of β-LG, which occurs between pH values of 4 and 6 [22,23], does not affect its interaction with a neutral MSG monolayer.

No reduction of the β-LG-induced surface pressure increase was observed when a surface charge of the same sign as that of β-LG was introduced into the monolayer, meaning that an electrostatic repulsion by the monolayer does not affect the insertion of β-LG, further pointing to the importance of hydrophobic contacts for its insertion. The importance and effects of electrostatics were revealed by the interaction of β-LG with a monolayer that was oppositely charged. When injected under a positively charged MSG/SA monolayer, the binding of β-LG to the monolayer was found to be increased at pH 7. However, the insertion of β-LG into the monolayer was comparable to that observed with neutral monolayers, π_i not exceeding 31 mN/m, and the β-LG bound to a MSG/SA monolayer could be largely removed by washing with a low ionic strength buffer. Both of these observations indicate that the electrostatic interaction between β-LG and a positively charged monolayer is relatively weak. Interestingly, the reduced insertion of β-LG observed below 31 mN/m at pH 4 in the presence of a high ionic strength, i.e. as a result of charge shielding, indicates that this electrostatic interaction can still stimulate the insertion of β-LG into a MSG/SA monolayer, albeit weakly. In the reversed situation, with β-LG being positively- and the monolayer negatively charged, a stronger interaction was observed. Firstly, because, at pH 4, β-LG is able to insert into negatively charged MSG/DCP monolayers at initial surface pressures far above 32 mN/m. Secondly, only a fraction of β-LG was removed from the monolayer after washing. The importance of electrostatics for this stronger interaction between β-LG and a MSG/DCP monolayer follows from the results obtained in the presence of 100 mM NaCl. A high ionic strength first of all effectively prevented, or abolished, the binding of β-LG to the monolayer and, furthermore, abolished the ability of β-LG to insert at initial surface pressures higher than 32 mN/m.

From the amounts of protein associated with a monolayer, it is possible to estimate the average area occupied by a protein in the monolayer, assuming that the molecular areas of the components of a monolayer are additive and knowing the area occupied by the lipids as a function of surface pressure [24,25]. The observed amounts of β-LG bound to a MSG/DCP monolayer at pH 4 mean that, when taking into account the dimensions of β-LG (molecular area ≈ 21 nm^2 [7,8]), the protein covers 30 or 18% of the total available area before and after washing of the subphase, respectively. These amounts of β-LG induce a surface pressure increase of about 1 mN/m in a monolayer with an initial surface pressure of 32 mN/m. Inspection of the π–A curve of the monolayer shows that, under similar conditions, the area occupied by the lipids decreases by 0.06% and that only 0.07 nm^2, i.e. less then the area of a methyl group, is available per bound β-LG molecule for insertion. From this, we conclude that only a fraction of the β-LG bound to the MSG/DCP monolayer inserts and that, consequently, two populations of β-LG are present at the MSG/DCP surface, one inserted and one adsorbed. It is as yet unclear what the exact nature of the two different β-LG populations at the MSG/DCP monolayer is. It is, however, highly unlikely that this behavior of β-LG is due to the presence of minor contaminations in the protein sample, because similar results were obtained using an ultra pure sample prepared at the NIZO. The conclusion that only a fraction of the bound β-LG inserts into the monolayer is supported by the finding that only very small amounts of β-LG were bound to a neutral MSG monolayer under conditions, i.e. at a π_i of 26 mN/m, where a $\Delta\pi$ was observed that is higher than that observed with a MSG/DCP monolayer, of 32 mN/m at pH 4. Furthermore, no effects were observed on the surface dilatation elasticity, which can be expected when large amounts of protein insert into a lipid monolayer [17].

The difference in insertion of β-LG bound to either a MSG/SA monolayer at pH 7 or a MSG/DCP monolayer at pH 4 probably does not find its origin in simple electrostatics because the relationship between surface charge and β-LG-induced $\Delta\pi$s was either not observed (pH 7) or not linear (pH 4). Also,

the increased insertion of β-LG into a MSG/DCP monolayer below 32 mN/m at pH 4 was unaffected by a high ionic strength; a high ionic strength only affected the insertion above 32 mN/m. The observed difference could result from structural differences of β-LG bound to the surface. These structural differences are, however, not likely to be those found in solution, because no differences between pH 4 and pH 7 were observed with neutral monolayers and heat-denaturation of the protein also had no effect. We therefore propose that the difference results from an anionic amphiphile-induced structural change in β-LG. This structural change may not be very dramatic but is probably large enough to allow additional hydrophobic parts of the protein to insert into the densely packed monolayer. That anionic amphiphiles are able to affect the structure of a protein is not unlikely — SDS being a well known example, also for β-LG [26,27] — while cationic amphiphiles are normally less destructive, thus explaining the absence of an increased insertion of β-LG into a positively charged monolayer.

The different types of interactions observed at high surface pressures are schematically summarized in Fig. 10. Only weak interactions are found in the absence of charge differences between β-LG and the monolayer and the protein will thus be mainly present in solution (Fig. 10A). Above its IEP, i.e. when negatively charged, β-LG will bind to a positively charged surface. Binding in this case does not, however, result in an increased insertion of β-LG into the monolayer (Fig. 10B). Below its IEP, i.e. when positively charged, β-LG will bind strongly to a negatively charged monolayer and will probably undergo a structural change. As a result, parts of the protein will also insert into the monolayer (Fig. 10C).

In conclusion, the results presented in this study show the importance of a negatively charged surface for the insertion of β-LG into condensed-phase monoglyceride monolayers, which compares well with the reported importance of a negative charge for the interaction of β-LG with phospholipid monolayers [12]. This increase in understanding protein–monoglyceride interactions will not only prove valuable for industrial use, but, moreover, also for the application of monoglycerides in studies on biological systems, as so elegantly demonstrated by Landau and Rosenbusch [5] who recently used monoglyceride cubic phases for the crystallization of membrane proteins.

Acknowledgements

This work was supported by the IOP-industrial proteins project IIE95001a. The authors would like to thank I. Heertje, F.A.M. Kleinherenbrink, A. Sein, G. Wijngaards, L.G.J. Verhoeven and B. Klarenbeek for fruitful discussions. The authors also would like to thank M. Kooijman for help with the surface dilatation elasticity measurements.

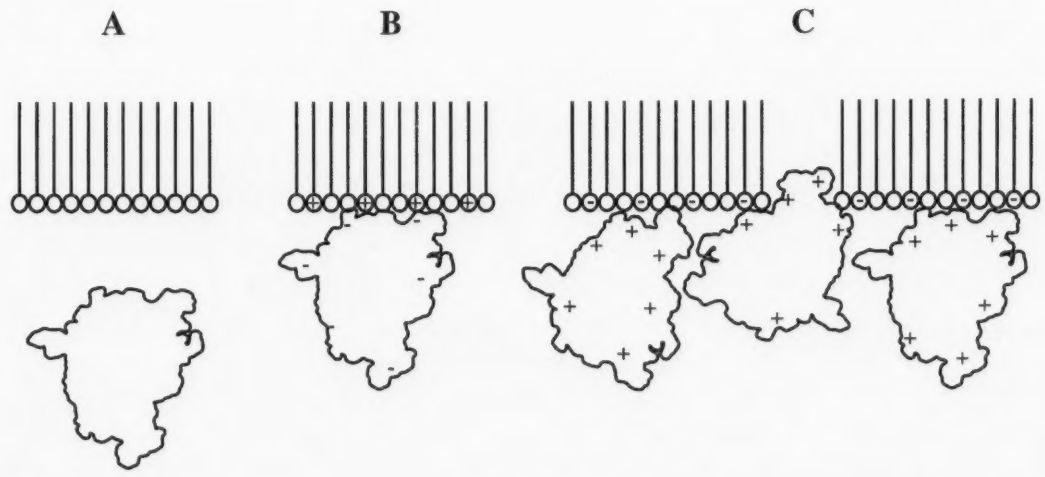

Fig. 10. Schematic representation of the observed interactions between β-LG and different MSG monolayers. β-LG does not bind to neutral monolayers (A). When negatively charged, β-LG is able to bind to positively charged monolayers. Binding does not, however, result in insertion (B). When positively charged, β-LG not only binds strongly to negatively charged monolayers but a fraction also inserts into the monolayer (C).

References

[1] N. Krog, K. Larson, Chem. Phys. Lipids 2 (1968) 129–143.
[2] I. Pezron, E. Pezron, B.A. Bergenstahl, P.M. Claesson, J. Phys. Chem. 94 (1990) 8255–8261.
[3] E.S. Lutton, J. Am. Oil Chem. Soc. 42 (1965) 1068–1070.
[4] N.J. Krog, in: K. Larsson, S.E. Friberg (eds.), Food emulsions, Marcel Dekker, New York and Basel, 1990, pp. 127–202.
[5] E.M. Landau, J.P. Rosenbusch, Proc. Natl. Acad. Sci. U.S.A. 93 (1996) 14532–14535.
[6] S.O. Hambling, A.S. McAlpine, L. Sawyer, in: P.F. Fox (ed.), Advanced Dairy Chemistry — 1: Proteins, Elsevier, London and New York, 1992.
[7] M.Z. Papiz, L. Sawyer, E.E. Eliopoulos, A.C.T. North, J.B.C. Findlay, R. Sivaprasadarao, T.A. Jones, M.E. Newcomer, P.J. Kraulis, Nature 324 (1986) 383–385.
[8] H.L. Monaco, G. Zanotti, P. Spadon, J. Mol. Biol. 197 (1987) 695–706.
[9] E. Breukink, R.A. Demel, O. de Korte-Kool, B. de Kruijff, Biochemistry 31 (1992) 1119–1124.
[10] N. Ben-Tal, B. Honig, R.M. Peitsch, G. Denisov, S. McLaughlin, Biophys. J. 71 (1996) 561–575.
[11] M. Dathe, M. Schumann, T. Wieprecht, A. WinMer, M. Beyermann, E. Krause, K. Matsuzaki, O. Murase, M. Bienert, Biochemistry 35 (1996) 12612–12622.
[12] D.O. Cornell, J. Colloid Interface Sci. 88 (1982) 536–545.
[13] D. Dottavio-Martin, J.M. Ravel, Anal. Biochem. 87 (1978) 562–565.
[14] P.F.M. Roefs, K.U. de Kruif, Eur. J. Biochem. 226 (1994) 883–889.
[15] M.A.M. Hoffman, S.P.F.M. Roefs, M. Verheul, P.J.J.M. van Mil, K.U. de Kruif, J. Dairy Res. 63 (1996) 423–440.
[16] R.A. Demel, Subcell. Biochem. 23 (1994) 83–120.
[17] T.A. Patemotte, R. Orsel, R.J. Hamer, J. Cereal Sci. 19 (1994) 123–129.
[18] U.L. Gaines, in: Insoluble Monolayers at Liquid–Gas Interfaces, Interscience, New York, 1966.
[19] U. Oehlert, G. Weidemann, D. Vollhardt, J. Colloid Interface Sci. 175 (1995) 393–399.
[20] D.R. Merker, B.F. Daubert, J. Am. Chem. Soc. 80 (1958) 516–519.
[21] J. de la Fuente Feria, J.M. Rodriguez Patino, Langmuir 10 (1994) 2317–2324.
[22] S.N. Timasheff, L. Mescanti, J.J. Bash, R. Townend, J. Biol. Chem. 241 (1966) 2496–2501.
[23] R. Townend, T.F. Kumosinski, S.N. Timasheff, J. Biol. Chem. 242 (1967) 4538–4545.
[24] L.K. Tamm, Biochemistry 25 (1986) 7470–7476.
[25] A.M. Batenburg, R.A. Demel, A.J. Verkleij, B. de Kruijff, Biochemistry 27 (1988) 5678–5685.
[26] M.N. Jones, A. Wilkinson, Biochem. J. 153 (1976) 713–718.
[27] A.J. Hillquist Damon, G.C. Kresheck, Biopolymers 21 (1982) 895–908.

ELSEVIER

Biochimica et Biophysica Acta 1330 (1997) 71–82

BIOCHIMICA ET BIOPHYSICA ACTA
BBA

Lysosome membrane permeability to amines

Carole L. Andrew, Ann R. Klemm, John B. Lloyd *

Division of Developmental Biology, Jefferson Medical College and Nemours Research Programs, Alfred I. duPont Institute, P.O. Box 269, Wilmington, DE 19899, USA

Received 16 May 1997; accepted 3 June 1997

Abstract

The permeability of rat liver lysosomes to xenobiotic organic compounds possessing nitrogen functions was investigated, using an osmotic-protection methodology. It was first shown that rat liver lysosomes are stable for at least one hour when incubated in 250 mM sucrose within the pH range 5 to 9. Primary and tertiary amines with pK_a values within this pH range, and with differing numbers of aliphatic hydroxy or ether groups, were chosen for study and their permeability investigated at a range of pH values. The results indicate that uncharged amines can cross the lysosome membrane, and that the permeability of such molecules can be predicted from their total hydrogen-bonding capacity. The notional hydrogen-bonding capacity of an uncharged tri-substituted nitrogen with no attached hydrogen atom, as in pyridine or in a tertiary aliphatic amine, is deduced to be approximately 1, and that of an uncharged primary amine approximately 2. A hydrogen-bonding capacity of at least 11 is deduced for cationic nitrogen, implying that most if not all molecules containing a charged nitrogen atom cannot cross the lysosome membrane by passive diffusion. The implications for lysosome physiology and pharmacology are discussed. © 1997 Elsevier Science B.V.

Keywords: Lysosome membrane; Amine (organic)

1. Introduction

The lysosome membrane constitutes a physiologically important barrier between the lysosome matrix and the surrounding cytoplasm. The membrane's impermeability to macromolecules ensures the retention within the organelle of both the lysosomal enzymes and their substrates. By contrast, the products of lysosomal metabolism must leave the lysosome. Most of these metabolites are thought to cross the membrane by transport on substrate-specific porters, although a contribution from passive diffusion is likely in a few cases (see [1] for a review).

Passive diffusion is certain to be the only mechanism available for most non-physiological molecules to cross the lysosome membrane. Several current approaches to targeted drug delivery require the drug to cross the lysosome membrane in order to reach the subcellular site where its action is desired [2]. It will be valueless to target a drug efficiently to some cell type if the drug remains trapped in the lysosomes. An ability to predict how well a given xenobiotic structure will cross the lysosome membrane is therefore of potential practical utility.

In our first study addressing this topic [3], we tested some 40 organic non-electrolytes containing aliphatic hydroxy, ether, hemiacetal and ester moi-

* Corresponding author. Fax: +1 (302) 651-6876; E-mail: jlloyd@aidi.nemours.org

0005-2736/97/$17.00 © 1997 Elsevier Science B.V. All rights reserved.
PII S0005-2736(97)00145-4

eties. The results showed that the rate of passive diffusion of solutes across the rat liver lysosome membrane is not significantly influenced by their molecular weight. However there was a strong inverse correlation between rate of penetration and a substance's notional hydrogen-bonding capacity, a parameter calculated from the number and nature of the functional groups the molecule possesses. The ability of these non-electrolytes to cross the lysosome membrane appeared to be wholly predictable from chemical structure.

Solute permeabilities across biological membranes are commonly correlated with oil–water partition coefficients. This approach is of limited value for many molecules of biochemical interest, since they are too hydrophilic for their partition coefficients to be determined with accuracy. Stein [4] was the first to point out the high degree of correlation between oil–water partition coefficient and notional hydrogen-bonding capacity, and to demonstrate the ability of the latter parameter to predict solute permeabilities across a variety of biological membranes.

Stein [4] proposed theoretically derived numerical values for the hydrogen-bonding capacity of several common functional groups found in organic molecules. Subsequently Diamond and Wright [5] slightly modified these values in respect of some functional groups; we used Stein's values and these modifications in our study [3] on the permeability of the lysosome membrane to organic non-electrolytes. A subsequent study of the permeability of rat kidney lysosomes to seven low (< 100) molecular weight non-electrolytes [6] revealed a good correlation between measured permeability for 6 of the 7 solutes and their partition coefficients in various oil–water systems. Using the permeability data from that publication and Stein's [4] values for functional group hydrogen-bonding capacities, a good correlation can be demonstrated between these two parameters (Fig. 1). The correlation coefficient (including all 7 compounds) is 0.88, greater than that reported [6] for three out of the four sets of partition coefficients.

Since drug moieties possess many functional groups other than the three oxygen-containing functions previously [3] studied, it is of value to obtain direct evidence on the ability of substances with such groups to cross the lysosome membrane. Our ultimate aim is to make the permeability of any organic

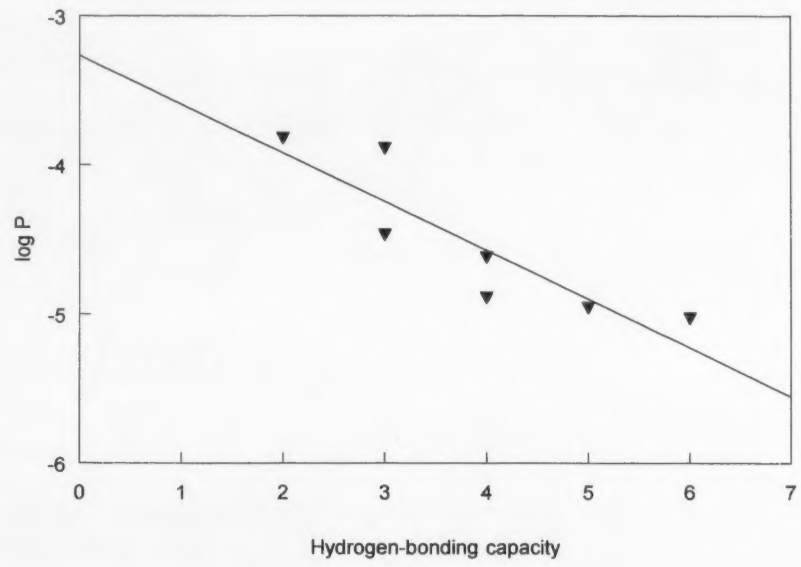

Fig. 1. Relationship between the logarithm of the measured permeability of rat kidney lysosomes and the notional hydrogen-bonding capacity of solutes. Points on the graph are, from left to right, for butanol, butyramide (upper point), acetamide (lower point), propylene glycol (upper point), ethanolamine (lower point), urea and glycerol. Permeability data are from Piqueras et al. [6]; hydrogen-bonding capacities are calculated from Table 3.2 of Stein [4].

molecule across the lysosome membrane reliably predictable from its structural formula. In the work reported in the present paper we have extended our previous studies to embrace organic molecules containing nitrogen atoms that have or can acquire a positive charge.

The permeability of the lysosome membrane to organic amines has attracted much attention in the past. This is because of an early observation that cells exposed to certain weak bases, such as chloroquine, accumulate them to high concentration in the lysosomes. The phenomenon was explained as resulting from the pH difference between the lysosome matrix and the cytoplasm and from the differential permeability of the lysosome membrane to the unprotonated and protonated form of amines. The early data and the underlying theory were discussed in detail by de Duve et al. [7]. Briefly, amines enter the lysosome by crossing the membrane from the cytoplasmic side in the uncharged form. In the more acidic environment of the lysosome the amine acquires a proton, thus generating the much less permeable cationic form. The law of mass action predicts a lysosome:cytosol concentration ratio with maximum value equal to the antilogarithm of the pH difference. Ohkuma and Poole [8] studied a large number of organic weak

bases for their ability to accumulate in and vacuolize macrophage lysosomes. With a few exceptions, their results were broadly consistent with theory. Their data additionally provided an early indication that the presence of multiple hydroxy groups on an aliphatic amine decreases its permeability. They found that triethanolamine and Tris fail to vacuolize lysosomes, despite having pK_a values above neutrality, and concluded that this is because ''the compounds are relatively hydrophilic even in their neutral forms and probably would not permeate easily through membranes''.

Stein [4] assigned notional hydrogen-bonding capacities of 2 to the uncharged nitrogen of primary amines and 1 to that of secondary amines. It is implicit in these assignments that the uncharged nitrogen of tertiary amines has zero hydrogen-bonding capacity. These values may each be one unit too low. In theory any uncharged aliphatic amine can accept a hydrogen bond, by virtue of the nitrogen's unshared electron pair, while the hydrogen atoms of primary and secondary amines can additionally donate two or one hydrogen bonds respectively [5].

We have previously studied the ability of some charged but electrically neutral molecules to cross the rat liver lysosome membrane. Our data [9] on ω-amino-aliphatic acids and dipeptides indicated that the combination of a protonated primary amine group and an anionic carboxylate group renders a molecule rather impermeant. It was proposed by Ginsburg and Stein [10] that the combination of these two charged groups contributes a hydrogen-bonding capacity of 11, and it has been tentatively inferred [11] from their data that the protonated amino group may account for 8 or 9 of this total.

The present investigation is a systematic study of the permeability of the lysosome membrane to charged and uncharged nitrogenous compounds. The principal aims were to discover whether permeability can be explained in terms of hydrogen-bonding capacity and, if so, to determine which of the theory-derived numerical assignments [4,5] are correct. As in our previous reports [3,9] we investigated the permeability of lysosomes by making use of the osmotic properties of these organelles. This indirect approach avoids the impracticable custom synthesis of a multitude of labeled molecules. We believe it also has an advantage over methods that demand the preparation of highly purified lysosomes, since the latter represent a very small and likely unrepresentative fraction of the entire lysosome population. Furthermore, if due caution is used, the results can be interpreted with more confidence than might be expected of an essentially indirect method of approach.

In order to reach reliable conclusions about the effect of different functional groups on permeability, one should study as many compounds as possible. In our work on non-electrolytes [3] we tested over 40. In the present work we used fewer, as each had to be tested at several pH values in order to evaluate the effect of protonation on permeability. We chose only non-physiological compounds, so as to minimize any influence from the metabolite porters that are present in the lysosome membrane.

2. Materials and methods

All chemicals were from Aldrich or Sigma.

Solutions of the test compounds were prepared at 250 mM in water. The pH was adjusted by adding 250 mM HCl to achieve the desired value. This method ensures that the total osmolarity of every solution was 250 mOsm/l. The amount of HCl added varied from compound to compound, according to the pK_a and with the target pH. It is possible to calculate, for each solution, the fraction of the total osmolarity due to the amine and that due to chloride.

A lysosome-rich subcellular fraction was prepared from the liver of an overnight-starved rat. The liver was pushed through a sieve and the pulp homogenized in 10 ml of ice-cold 250 mM sucrose per gram, followed by centrifugation at 4°C and $1100 \times g$ for 10 min. The pellet was discarded and 20 ml of the supernate centrifuged at 4°C and $22\,500 \times g$ for 10 min. The resulting pellet was gently resuspended in 1 ml of ice-cold 250 mM sucrose.

To test the ability of various salts to afford osmotic protection to lysosomes, 200 μl of the resuspended lysosome-rich pellet was added to 3.8 ml of test solution at 25°C. This diluted suspension was maintained at 25°C and 50- or 100-μl samples taken at 0, 30 and 60 min.

The integrity of the lysosomes in these samples was measured by determining the free activity of *N*-acetyl-β-glucosaminidase at 25°C. The assay mix-

ture contained the substrate 4-methylumbelliferyl *N*-acetyl-β-D-glucosaminide (2.5 mM) and sucrose (250 mM) in 200 mM sodium citrate–HCl buffer pH 5.0. Incubation was for 2 or 5 min and was terminated by the addition of 5 volumes of sodium carbonate (1 M). Liberated 4-methylumbelliferone was measured by determining the fluorescence of a 400-μl sample in the well-plate attachment of a Perkin Elmer LS 50B luminescence spectrometer (λ_{ex} 360 nm; λ_{em} 448 nm). In controls, substrate was added after the sodium carbonate. The free activity was expressed as a percentage of the total activity of *N*-acetyl-β-glucosaminidase, as measured in simultaneous parallel assays in the presence of Triton X-100 (0.2%).

3. Results

Table 1 shows the *N*-acetylglucosaminidase free activity of rat liver lysosomes incubated at 25°C in 5 mM potassium phosphate buffers containing 250 mM sucrose. Lysosomes were stable for at least 60 min when the pH was within the range 5.0 to 9.0. At pH 4 or 10 the lysosomes began to break, despite the protective effect of the 250 mM sucrose, and similar results were seen at pH 4.5 and 9.5. This experiment identifies the range of pH within which osmotic protection experiments can be used to indicate lysosome membrane permeability. It was shown that lysosomes break immediately when suspended in 5 mM potassium phosphate buffer without sucrose (results not shown).

Typical aliphatic amines have pK_a above 10, and consequently exist almost entirely in the protonated form within the pH range 5–9. In order to study the permeability of lysosomes to amines in their unprotonated form, we required substances with much lower pK_a. We identified three groups of molecules suitable for the purpose of this project: some substituted pyridines, some *N*-alkyl-morpholines and some hydroxylated alkylamines. The pyridines have pK_a values between 4 and 6, the *N*-alkyl-morpholines values around 7, and the alkylamines values between 6 and 10, so that these molecules change from the unprotonated to the protonated form within the pH range feasible for this investigation. Moreover, within each of these three groups, compounds are commercially available containing different numbers of aliphatic hydroxy groups, which we and others have shown substantially decrease a molecule's ability to cross biomembranes. Thus, as in our study of non-electrolytes [3], we aimed to distinguish between the effects of two parameters, in this case pK_a and hydrogen-bonding capacity, on a molecule's permeability. Table 2 shows the structures, pK_a values and notional hydrogen-bonding capacities of the compounds studied.

Table 3 shows the results of incubating rat liver lysosomes in 250 mOsm/l solutions of each of the eight bases at pH values within the range 5–9. Sev-

Table 1
Free activity of *N*-acetyl-β-D-hexosaminidase in rat liver lysosomes pre-incubated in 250 mM sucrose buffered with 5 mM potassium phosphate

pH of the buffered sucrose solution [a]	Number of experiments	Free activity (% of total activity)		
		0 min	30 min	60 min
3.0	5	13±5	23±4	32±10
4.0	4	6±1	13±2	22±6
4.5	3	8±5	13±7	21±7
5.0	4	7±1	9±2	12±2
6.0	4	6±2	10±2	8±1
7.0	3	7±1	8±1	11±3
8.0	3	6±1	8±1	9±1
9.0	3	6±1	8±0	10+1
9.5	3	9±5	13±3	21±2
10.0	3	6±2	12±4	29±6

[a] The solutions also contained valinomycin (2.5 μg per ml) to enhance K^+ permeability.

A lysosome-rich fraction from rat liver was diluted into the buffered sucrose at 4°C, and then incubated at 25°C. Samples were removed for assay of *N*-acetyl-β-D-glucosaminidase at the indicated times. Free enzyme activity is expressed as a percentage of the total activity measured in the presence of Triton X-100 (0.2%). Values shown are the mean±SD for the number of experiments shown.

[a] pK_a values were determined by titration. They confirm published values where shown as available [12,13].
[b] Excluding any contribution from the nitrogen function.
[c] Hydrogen-bonding capacities are calculated by reckoning 2.0 for each C-O-H group and 0.8 for each C–O–C. These values are those assigned in Ref. [3].

Table 2
Structures, pK_a values and hydrogen-bonding capacities of the compounds studied

Name	Structure	pK_a(25°C)[a]	Hydrogen-bonding capacity[b,c]
PYRIDINES			
4-Methyl	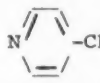	6.0 [12]	0
4-Hydroxymethyl	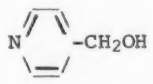	5.3 [13]	2.0
2,6-Di(hydroxymethyl)	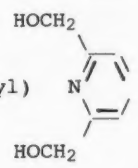	4.3	4.0
MORPHOLINES			
N-Methyl		7.4 [12]	0.8
N-(2-Hydroxyethyl)	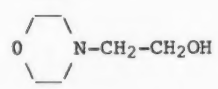	6.8	2.8
N-(2,3-Dihydroxypropyl)	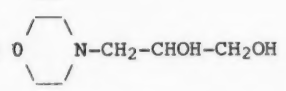	6.6	4.8
ALKYLAMINES			
Triethanolamine	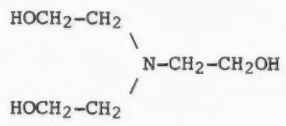	7.8 [12]	6.0
Bis-Tris	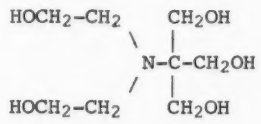	6.5 [13]	10.0
2-Amino-2-methyl-1-propanol	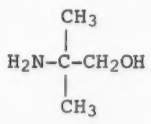	9.7 [12]	2.0
2-Amino-2-methyl-1,3-propanediol	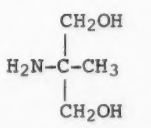	8.8 [12]	4.0
Tris	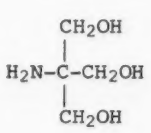	8.1 [12]	6.0
QUATERNARY AND STRONG BASES			
Choline	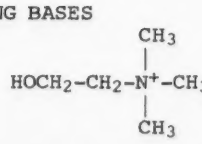	not applicable	2.0
Dimethylamine	$CH_3-NH_2^+-CH_3$	10.8 [12]	0
N-Methylglucamine	$CH_3-NH_2^+-CH_2-(CHOH)_4-CH_2OH$	9.3	10.0

Table 3
Free activity of *N*-acetyl-β-D-glucosaminidase in rat liver lysosomes pre-incubated in 250 mOsm solutions of organic bases

Solute	pH	Number of experiments	Free activity (% of total activity)		
			0 min	30 min	60 min
Pyridines					
4-Methyl	5.0	3	10 ± 4	85 ± 12	94 ± 13
	6.0	3	43 ± 10	94 ± 14	102 ± 21
	7.0	3	110 ± 14	118 ± 3	96 ± 9
4-Hydroxymethyl	5.0	3	17 ± 1	80 ± 3	93 ± 14
	6.0	3	60 ± 5	84 ± 6	91 ± 4
	7.0	3	85 ± 8	94 ± 4	106 ± 7
2,6-Di(hydroxymethyl)	5.0	3	74 ± 9	95 ± 10	94 ± 10
	6.0	3	91 ± 13	86 ± 11	90 ± 2
	7.0	3	93 ± 13	94 ± 9	94 ± 4
Morpholines					
N-Methyl	5.0	3	7 ± 2	50 ± 4	76 ± 12
	6.0	3	11 ± 2	18 ± 5	25 ± 4
	7.0	3	45 ± 9	66 ± 6	62 ± 6
	8.0	3	102 ± 13	89 ± 10	110 ± 4
N-2-Hydroxyethyl	5.0	3	11 ± 6	40 ± 5	79 ± 8
	6.0	3	15 ± 3	25 ± 9	26 ± 6
	7.0	3	72 ± 8	85 ± 4	85 ± 13
	8.0	3	101 ± 5	101 ± 17	103 ± 21
N-2,3-Dihydroxypropyl	5.0	5	10 ± 4	32 ± 8	56 ± 4
	6.0	5	12 ± 1	22 ± 2	23 ± 2
	7.0	4	55 ± 15	85 ± 12	79 ± 10
	8.0	5	86 ± 7	109 ± 10	110 ± 12
Alkylamines					
Triethanolamine	7.0	3	8 ± 2	31 ± 4	41 ± 5
	8.0	3	9 ± 5	103 ± 13	90 ± 10
	9.0	3	22 ± 11	88 ± 8	98 ± 4
Bis-Tris	5.0	6	10 ± 2	13 ± 3	21 ± 6
	6.0	6	10 ± 2	12 ± 2	18 ± 3
	7.0	8	8 ± 5	13 ± 6	19 ± 4
	8.0	6	13 ± 3	16 ± 4	46 ± 15
2-Amino-2-methyl-1-propanol	7.0	3	5 ± 1	27 ± 2	35 ± 1
	8.0	3	11 ± 4	52 ± 2	58 ± 8
	9.0	3	72 ± 8	98 ± 10	100 ± 5
2-Amino-2-methyl-1,3-propanediol	7.0	3	5 ± 1	11 ± 1	20 ± 3
	8.0	3	4 ± 1	71 ± 7	67 ± 7
	9.0	3	7 ± 3	109 ± 12	96 ± 5
Tris	7.0	3	5 ± 4	13 ± 3	13 ± 2
	8.0	3	6 ± 2	55 ± 19	61 ± 17
	9.0	3	1 ± 1	78 ± 3	95 ± 5

A lysosome-rich fraction from rat liver was diluted into the indicated solution, at 4°C, and then incubated at 25°C. Samples were removed for assay of *N*-acetyl-β-D-glucosaminidase at the indicated times. Free enzyme activity is expressed as a percentage of the total activity measured in the presence of Triton X-100 (0.2%). Values shown are the mean ± SD for the number of experiments shown.

eral of the compounds tested caused a degree of inhibition of *N*-acetylglucosaminidase, but this does not affect the validity of the osmotic protection data, as both the free and the total activity were measured in the presence of the same concentration of amine. Inhibition by the hydroxylated alkylamines and morpholines was 40–60% at 30 mM, the maximum concentration encountered in the osmotic protection assays; the three pyridines were not significantly inhibitory.

The results shown in Table 3 indicate that lysosomes break immediately when suspended in some of the test solutions. This finding can arise either because the solution actively disrupts the lysosome membrane, or because the solute enters the lysosomes so quickly that it fails to provide even initial osmotic protection. These alternative explanations can be distinguished by incubating lysosomes in the test solution to which sucrose has been added to a concentration of 250 mM. If the solution now provides initial osmotic protection, the solute is not actively membrane-lytic. This experiment was performed for each of the solutions that gave an initial free activity greater than 20%, as shown in Table 3. In no case was the initial free activity greater than 20% when 250 mM sucrose was also present (data not shown). Moreover, when incubations were continued for 60 min, free activity remained low in most cases. Exceptions were incubations at pH 6 or 7 in sucrose-containing 4-methylpyridine, when free activity reached 100% by 30 min, and in *N*-(2-hydroxyethyl)morpholine and *N*-(2,3-dihydroxypropyl)morpholine at pH 8, where a substantial increase in free activity was seen at 30 min of incubation, and a further rise by 60 min.

Table 4 shows the results of incubating lysosomes in 250 mOsm/l solutions of some quaternary or strong organic base hydrochlorides. These bases have no significant buffering capacity at neutral pH. Choline chloride and dimethylammonium hydrochloride were dissolved in water at 125 mM and the pH measured but not adjusted. *N*-Methylglucamine was dissolved in water, the pH adjusted to approximately 7.0 with HCl and the volume adjusted to give a final concentration of 125 mM. The results obtained with dimethylammonium chloride indicated the necessity to repeat the experiments at pH 7.0. This was done by adding KOH to the 125 mM solution; the amount needed was very small, adding less than 1 mOsm to the osmolarity of the solution.

The complete osmotic protection offered by 125 mM choline or *N*-methylglucamine chloride (Table 4) provides a striking demonstration of the inability of a permeant anion to enter lysosomes when its counter-cation is impermeant.

4. Discussion

4.1. Methodology

As indicated in the introduction, the osmotic protection methodology has two major advantages for

Table 4
Free activity of *N*-acetyl-β-D-glucosaminidase in rat liver lysosomes pre-incubated in solutions of quaternary and strong organic base hydrochlorides

Solution	pH	Number of experiments	Free activity (% of total activity)		
			0 min	30 min	60 min
Choline chloride (125 mM)	4.76	4	5.7 ± 1.7	7.0 ± 1.4	8.0 ± 2.7
Dimethylammonium chloride (125 mM)	5.43	3	8.1 ± 1.9	14.0 ± 3.3	22.2 ± 1.8
	7.00	3	7.8 ± 1.7	19.6 ± 0.6	27.1 ± 3.2
N-Methylglucamine chloride (125 mM)	6.56	4	6.9 ± 1.7	7.5 ± 1.9	8.5 ± 1.0

A lysosome-rich fraction from rat liver was diluted into the indicated solution, at 4°C, and then incubated at 25°C. Samples were removed for assay of *N*-acetyl-β-D-glucosaminidase at the indicated times. Free enzyme activity is expressed as a percentage of the total activity measured in the presence of Triton X-100 (0.2%). Values shown are the mean ± SD for the number of experiments shown.

structure-permeability correlation studies such as this. It demands neither the preparation of a highly purified lysosome fraction nor the availability of the desired compounds in radiolabeled form. It is currently the only practicable method available for testing a large number of xenobiotic amines, such as those studied here. However there are limitations: although the results give a reliable indication of the rank order of permeation rates for the compounds tested, they do not yield absolute rates. Our analysis (Fig. 1) of the recently published permeability data for rat kidney lysosomes [6] indicates however that their permeability to small non-electrolytes decreases approximately two-fold with each additional hydrogen bond.

Another pertinent issue is the relevance of osmotic-protection data to lysosome permeability in situ. Here an analysis [11] of the rather sparse data is encouraging — endocytosed substances that accumulate in lysosomes all have hydrogen-bonding capacity 11.5 or higher. By contrast substances below this threshold seem able to escape into the cytoplasm. Passive diffusion is of course not a threshold phenomenon and every compound will diffuse at some rate. There are as yet no comparative quantitative data available on rates of passive diffusion across the lysosome membrane in situ.

4.2. Effect of pH on lysosome stability

We first showed that rat liver lysosomes suspended in 250 mOsm sucrose show no significant loss of latency at pH values in the range 5 to 9. However, below 5 and above 9, the lysosomal enzyme monitored becomes progressively more available to added impermeant substrate. We have not sought to discover whether the membrane becomes more permeable or begins to break at these extremes of pH, as our purpose was to identify a pH range within which pH alone does not affect the stability of the lysosomes.

4.3. The uncharged nitrogen of an aromatic heterocycle

The three substituted pyridines studied in this investigation have pK_a values between 4 and 6. Thus they exist principally in their uncharged form at pH 7. Table 3 shows that none of the amines give even initial osmotic protection to lysosomes at pH 7.0, indicative of very rapid passage across the lysosome membrane. At pH 6.0, however, results with the three compounds differed — 4-methylpyridine provided a transient osmotic protection, although this was lost after 30 min of incubation; similar but slightly poorer protection was offered by 4-hydroxymethylpyridine; 2,6-di(hydroxymethyl)pyridine provided no initial protection. At pH 5.0 these three amines respectively provided complete, good and poor (albeit some) initial osmotic protection, although in all cases the protection was lost after 30 min incubation. Reference to Table 2 shows that these results correlate with the different pK_a values of the three amines, and are explicable in terms of the pyridines having a lower permeability when the ring nitrogen is protonated.

An alternative explanation of the very high initial free activity seen in many of these experiments is that the pyridine derivative actively disrupts the lysosome membrane, in a similar fashion to detergents such as Triton X-100. This possibility was excluded by repeating experiments with 250 mM sucrose present with the substituted pyridine — in each case and at all pH values, the lysosomes were fully latent at time-zero. In most cases the lysosomes remained intact for the full 60 min of the incubation, although rapid loss of latency was seen with 4-methylpyridine at pH 6.0 and 7.0. This finding does not affect the interpretation of the data.

In our earlier study [3] on non-electrolytes, we found that substances failing to offer even initial osmotic protection to lysosomes, all had a hydrogen-bonding capacity below 7.5. The failure of 2,6-di(hydroxymethyl)pyridine to provide initial protection suggests that the unprotonated ring-nitrogen cannot contribute more than 3.5 units of hydrogen-bonding capacity. The two other pyridines tested have less hydrogen-bonding capacity than 2,6-di(hydroxymethyl)pyridine (Table 2) and their inability to provide osmotic protection is unsurprising.

Even at the most acidic pH tested (5.0), the three pyridines exist significantly in the uncharged form. Therefore the data on these compounds in Table 3 cannot be used to draw any conclusions about the permeability of their protonated forms.

4.4. The uncharged nitrogen of aliphatic tertiary amines

We consider next the three morpholine derivatives tested. Table 2 shows that they have rather similar pK_a values (range 6.6–7.4), but a wider spectrum of hydrogen-bonding capacities (0.8–4.8), reflecting the differing complement of aliphatic hydroxy groups. Table 3 shows that at pH 8.0, when these molecules all exist substantially in the unprotonated form, there is no indication of even initial osmotic protection. That this indicates rapid permeation, and not a detergent-like action, was clear from the initial lysosome stability seen when lysosomes were incubated with the morpholine derivatives in the presence of 250 mM sucrose. Using the argument deployed above in respect of 2,6-di(hydroxymethyl)pyridine, the result with *N*-(2,3-dihydroxypropyl)morpholine indicates that its uncharged tertiary nitrogen contributes no more than 2.7 units of hydrogen-bonding capacity.

As pH is decreased from 8 to 7 and 6, the *N*-alkyl morpholines provide lysosomes with increasing osmotic protection. This result is consistent with a decreasing proportion of amine in the unprotonated form and an increasing proportion in the less permeant charged form. The pH 6 data in Table 3 are similar for all the three morpholines; likewise the pH 7 data. This finding is explicable in terms of pK_a values and hydrogen-bonding capacities (Table 2). With increasing side-chain length, pK_a decreases, thus increasing the proportion of molecules in the uncharged form at any given pH and thus increasing permeability. Concomitantly, the number of hydroxy groups increases, decreasing permeability. Thus, the two effects of the side-chain substituents counteract each other.

The results on osmotic protection by the three morpholines at pH 5.0 were a surprise. At this pH, the amines are principally in the protonated form and therefore were expected to show their lowest permeability. However in all three cases, osmotic protection at pH 5 was poorer than at pH 6. Several possible explanations of this observation can be excluded. First, the results in Table 1, and indeed the data on Bis-Tris (Table 3) show that the pH itself cannot be responsible. Secondly, this is not a membrane-lytic effect: lysosomes incubated in any of the three morpholines in the presence of 250 mM sucrose at pH 5, 6 or 7 remained intact for at least 60 min at all four pH values. A third possible explanation focuses on the composition of the amine solution. As explained above, the solutions were formulated to be 250 mOsm at all pH values: at pH values below the pK_a, a substantial contribution to the osmolarity comes from the counter-anion chloride. Although it had been assumed that little counter-ion would be able to cross the lysosome membrane without its compensating cation, it could be argued that the poorer osmotic protection at pH 5 than 6 reflected the lower concentration of amine. There are strong arguments against this possibility. First, the amine concentration in an iso-osmotic solution changes most significantly around the pK_a value. In a 250 mOsm solution of an amine hydrochloride, the total amine concentration (RNH_2 plus RNH_3^+) is 167 mM at the pK_a, 131 mM at one pH unit below the pK_a and 126 mM at two pH units below. The difference between the osmotic protection data for 4-methylmorpholine (pK_a 7.3) at pH 5.0 and 6.0, as shown in Table 3, is too great to be explicable in terms of decreased total amine concentration. A second argument is to be found in the results with choline chloride (Table 4), where a 125 mM solution gave total osmotic protection even at the low pH of 4.76. At present we have no convincing explanation for the apparently high permeability of the morpholines at pH 5.0.

We turn now to the two tertiary aliphatic amines Bis-Tris and triethanolamine. Lysosomes incubated in Bis-Tris in the presence of 250 mM sucrose remained intact for at least 60 min at all four pH values. Lysosomes suspended in Bis-Tris alone showed only slow loss of latency, even at pH 8.0, when only 3% of Bis-Tris molecules are protonated. Because it can be confidently assumed that the protonated species will be less permeable than the uncharged amine, the permeability of Bis-Tris at pH 8.0 must be attributable to the uncharged amine. The slow loss of latency seen at pH 8.0 is similar to that of non-electrolytes with a hydrogen-bonding capacity between 10 and 11 [3]. The five hydroxy groups in Bis-Tris contribute 10 units of hydrogen-bonding capacity (Table 2), indicating that the tertiary amine nitrogen of Bis-Tris contributes 0–1 units of hydrogen-bonding capacity.

Triethanolamine has a pK_a of 7.8, higher than that of any of the molecules discussed thus far. Pre-

dictably, its permeability is greater at pH values above its pK_a (Table 3), but the most noteworthy result is the initial free activity at pH 9.0, when 94% of the amine is in the free form. The pattern seen at this pH, an initial low free activity, followed by a rapid lysis, is reminiscent of molecules with a total hydrogen-bonding capacity between 7.2 and 8.0 [3]. Since triethanolamine has three aliphatic hydroxy groups, we conclude that its tertiary nitrogen has a hydrogen-bonding capacity between 1 and 2.

Taken together, the data from the pyridines, the morpholines and the tertiary aliphatic amines indicate a value of approximately unity for the hydrogen-bonding capacity of an uncharged tri-substituted nitrogen atom.

4.5. The uncharged nitrogen of aliphatic primary amines

In the amines discussed thus far the nitrogen atom has had no directly attached hydrogen atoms. Secondary amines, which have one such hydrogen, are stronger bases than their cognate primary or tertiary amines. As shown in Table 2, the pK_a of dimethylamine is 10.8. We were unable to identify any secondary amine with a low enough pK_a to be useful for the present study.

Although most primary amines are also strong bases, tri-hydroxylated *t*-butylamine (Tris) has a pK_a of 8.1. This compound was therefore investigated at pH 7, 8 and 9. For comparison the mono- and di-hydroxylated *t*-butylamines, 2-amino-2-methyl-1-propanol and 2-amino-2-methyl-1,3-propanediol, were also included in the study, notwithstanding their high pK_a values (see Table 2).

2-Amino-2-methyl-1-propanol has a hydrogen-bonding capacity of only 2.0 in addition to the contribution of the primary amine moiety. At pH 9.0, when 83% is in the protonated form, this amine fails to afford lysosomes even initial osmotic protection, indicative of a rapid penetration of the unprotonated form. This is a clear indication that an uncharged primary amine moiety cannot possess a hydrogen-bonding capacity in excess of about 5. With decreasing pH 2-amino-2-methyl-1-propanol provides good osmotic protection, indicative of a hydrogen-bonding capacity of at least 9 for the $-NH_3^+$ group.

2-Amino-2-methyl-1,3-propanediol at pH 9.0 affords lysosomes initial protection, but this is entirely lost by 30 min of incubation, a pattern typical of substances of hydrogen-bonding capacity about 8 [3]. A rather similar pattern is seen at pH 8.0. Since this molecule is substantially (39% and 86% respectively) in protonated form at pH 9.0 and 8.0, and since its two hydroxy groups contribute 4.0 units of hydrogen-bonding capacity, the uncharged $-NH_2$ group cannot contribute more than 4 units. Decreasing the pH to 7.0 leads to a marked increase in osmotic protection by 2-amino-2-methyl-1,3-propanediol, again indicative of the greater hydrogen-bonding capacity of the $-NH_3^+$ group.

Turning finally to Tris, we see patterns similar to those described above for 2-amino-2-methyl-1,3-propanediol. Tris at pH 9.0 is 89% uncharged, and even at pH 8.0 is 44% uncharged, so that the permeability seen at these pH values represents that of the uncharged amine. Comparison with earlier data [3] indicates that the uncharged $-NH_2$ group contributes approximately 2 units of hydrogen-bonding capacity.

4.6. Charged nitrogen atoms

Although the data of Table 3 show that the weak bases are all much less permeable at pH values below their pK_a, several of the cationic forms are apparently significantly permeant. However, because even at low pH values a fraction of the amine exists as the free base, it is possible that the cationic form is wholly impermeant and that permeation at low pH is due to the small fraction of unprotonated amine. In order to throw light on this question, we studied the permeation of some organic amines that cannot exist in unionized form or whose pK_a values are so high that an explanation in terms of free base penetration is implausible. Choline is a quaternary amine that bears a permanent positive charge, and dimethylamine is a strong base of pK_a 10.8. *N*-Methylglucamine is a polyhydroxylated derivative of dimethylamine.

Table 4 shows that 125 mM choline chloride is as good an osmotic protector as sucrose or mannitol [3], even at the low pH of 4.8. This finding indicates that the combination of a charged nitrogen and one aliphatic hydroxy equates to a hydrogen-bonding ca-

pacity of at least 12. Thus the charged nitrogen must contribute at least 10 units of hydrogen-bonding capacity. *N*-Methylglucamine chloride (125 mM) likewise gave full osmotic protection, a result consistent with its possessing a hydrogen-bonding capacity of approximately 10 in addition to that conferred by the protonated nitrogen. The strong secondary amine dimethylammonium chloride, also at 125 mM, gave a degree of osmotic protection typical of a substance with hydrogen-bonding capacity of about 11 [3]. Since this was observed at pH 5.43, over 5 pH units lower than its pK_a, it is difficult to attribute the permeation to free base. This result can be explained in two ways. Either the charged nitrogen contributes a hydrogen-bonding capacity of about 11, or its permeation is carrier-mediated.

4.7. General conclusions and implications for lysosome physiology and pharmacology

Two overall conclusions can be drawn from this work. The first is that non-physiological organic compounds containing an uncharged nitrogen atom can diffuse across the lysosome membrane, and that the effect of such groups is predictable in terms of hydrogen-bonding capacity, as was previously shown to be the case for some oxygen-containing functions. The second conclusion concerns the hydrogen-bonding capacities of nitrogen atoms in organic structures. We propose the following assignments: 1 for an uncharged nitrogen with no attached hydrogen, as in a tertiary aliphatic amine or an aromatic structure such as pyridine; 2 for an uncharged nitrogen with two attached hydrogen atoms, as in a primary amine. These values are broadly consistent with theory [4,5]. We do not propose a value for an uncharged nitrogen with one attached hydrogen, as in a secondary amine, since our data do not include any such compounds. However the matter is largely academic in the context of permeability through biological membranes in situ, owing to the high pK_a of secondary amines.

Many investigators take it as axiomatic that the possession of a positively charged nitrogen function makes a molecule incapable of diffusion through biological membranes, and that any observed permeation must be due to the uncharged moiety or to the presence of a carrier or channel, such as the organic cation/proton exchanger recently described [14] in rat liver lysosomes. Our data are consistent with this interpretation. However, they do not exclude the possibility that passive diffusion of a molecule such as dimethylamine could still occur. This diffusion may be too slow to be observable in most experimental systems, but may yet have physiological and pharmacological relevance to the penetration across small organelles such as the lysosome, in which the surface:volume ratio is very high compared with, for example, that of the whole cell. We note that Ohkuma and Poole [8] also envisioned some charged nitrogenous bases passively traversing lysosome membranes because they are ''lipophilic even in their protonated forms''. We conclude that the hydrogen-bonding capacity of a cationic nitrogen is at least 11.

The results we report are relevant to two issues, one physiological and one pharmacological. As discussed elsewhere [1], there are some products of the lysosomal catabolism of macromolecules that bear positive charges and for which no carrier has been identified in the lysosome membrane. Sphingosine is one such metabolite. It is a primary amine with two aliphatic hydroxy groups, and so can be assigned a total hydrogen-bonding capacity of 6 in the uncharged form and at least 15 in the charged form. At the pH of the lysosome interior, the latter form must predominate and it is unclear whether or how sphingosine can escape into the cytoplasm.

In the context of drug delivery, the results we report make it possible to compute the total hydrogen-bonding capacity of a wider range of structures than hitherto. As explained elsewhere [11], lysosomes in situ are effectively impermeable to molecules of hydrogen-bonding capacity greater than about 11.5. Many xenobiotics contain nitrogen atoms that are present in aromatic or heterocyclic structures and have low pK_a values, such that a significant fraction is uncharged at lysosomal pH. Their ability to cross the lysosome membrane will depend chiefly on the other functional groups they contain. By contrast all or most chemical moieties containing a charged nitrogen will not diffuse across the lysosome membrane at a significant rate. Here the lysosomal organic cation–proton exchanger [14] is potentially of great significance in achieving what diffusion cannot. It will be valuable to know more about the substrate specificity of this system.

Acknowledgements

We thank Nemours Research Programs for their support of this work.

References

[1] J.B. Lloyd, in: J.B. Lloyd, R.W. Mason (Eds.), Biology of the Lysosome, Subcellular Biochemistry, Vol. 27, Chapter 11, Plenum Press, New York, 1996, pp. 361–386.
[2] R. Duncan, Anti-Cancer Drugs 3 (1992) 175–210.
[3] G.P. Iveson, S.J. Bird, J.B. Lloyd, Biochem. J. 261 (1989) 451–456.
[4] W.D. Stein, The Movement of Molecules across Cell Membranes, Academic Press, New York, 1967.
[5] J.M. Diamond, E.M. Wright, Annu. Rev. Physiol. 31 (1969) 581–646.
[6] A.-I. Piqueras, M. Somers, T.G. Hammond, K. Strange, H.W. Harris, M. Gawryl, M.L. Zeidel, Am. J. Physiol. 266 (1994) C121–133.
[7] C. De Duve, T. de Barsy, B. Poole, A. Trouet, P. Tulkens, F. van Hoof, Biochem. Pharmacol. 23 (1974) 2495–2531.
[8] S. Ohkuma, B. Poole, J. Cell Biol. 90 (1981) 656–664.
[9] S.J. Bird, J.B. Lloyd, Biochim. Biophys. Acta 1024 (1990) 267–270.
[10] H. Ginsburg, W.D. Stein, J. Membr. Biol. 96 (1987) 1–10.
[11] J.B. Lloyd, in: J.G. Thoene (Ed.), Pathophysiology of Lysosomal Transport, Chapter 7, CRC Press, Boca Raton, 1992, pp. 295–308.
[12] D.D. Perrin, Dissociation Constants of Organic Bases in Aqueous Solution, Butterworths, London, 1965.
[13] D.D. Perrin, Dissociation Constants of Organic Bases in Aqueous Solution: Supplement 1972, Butterworths, London, 1972.
[14] R.H. Moseley, R.W. Van Dyke, Am. J. Physiol. 268 (1995) G480–G486.

ELSEVIER

Biochimica et Biophysica Acta 1330 (1997) 83–93

BIOCHIMICA ET BIOPHYSICA ACTA
BBA

Activation of the Na^+/K^+ pump current by intra- and extracellular Li ions in single guinea-pig cardiac cells

An Nathalie Hermans [a], Helfried Günther Glitsch [b,*], Fons Verdonck [a]

[a] *Interdisciplinary Research Centre, Catholic University of Leuven, Campus Kortrijk, B-8500 Kortrijk, Belgium*
[b] *Arbeitsgruppe Muskelphysiologie, Ruhr-Universität, D-44780 Bochum, Germany*

Received 21 April 1997; revised 9 June 1997; accepted 12 June 1997

Abstract

Li^+ is the only ion that can replace the physiological intra- and extracellular activator cations of the Na^+/K^+ pump. In order to study this singular property of Li^+ in some detail, the activation of the Na^+/K^+ pump current (I_p) by intra- and extracellular Li^+ (Li_i^+; Li_o^+) was measured in isolated guinea-pig ventricular myocytes by means of whole cell recording at 34°C and a holding potential of −20 mV. I_p was identified as current blocked by dihydro-ouabain. Half-maximal I_p activation occurred at 23 mM Li_o^+ ($K_{0.5}$ value) in cells containing Na^+ (50 or 100 mM) and at 73 mM Li_o^+ in myocytes containing Li^+ (100 mM). The $K_{0.5}$ value of I_p activation by Li_o^+ increased with depolarisation, suggesting the transfer of 0.2 of an elementary charge across the electric field of the sacrolemma during Li_o^+-binding. An intracellular Li^+ concentration of 36 mM caused half-maximal I_p activation in cells superfused with Na^+- and Li^+-free media containing 1 mM K^+. In Na^+-free solutions, the I_p–V curve displayed a positive slope at negative membrane potentials. A negative slope at positive potentials was observed in Li^+-containing media. It is concluded that Li^+ is less efficacious and potent than the physiological pump activator cations. The shape of the I_p–V curves in Na^+-free solutions supports the view that the cardiac Na^+/K^+ pump contains a channel-like structure and suggests that there are voltage-sensitive steps in the pump cycle, apart from the binding of external cations. © 1997 Elsevier Science B.V.

Keywords: Na^+/K^+ pump; Pump current; Whole-cell recording; Cardiac myocyte; Li ion

1. Introduction

The Na^+/K^+ pump in the cell membrane of animal cells generates a pump current, I_p. Since the pump is activated by various species of extracellular monovalent cations, an effect of these ions on I_p would not be surprising. In fact, it is known for various cells (e.g. [1,2]), including cardiac cells [3,4], that Tl^+, Rb^+, Cs^+ or NH_4^+ mimic, to a certain degree, the activation of I_p by extracellular K^+. These ions are unable to replace intracellular Na^+ in the activation of the cardiac Na^+/K^+ pump [5]. However, a recent abstract [6] reports that Li ions can substitute for internal Na^+ in the mechanism of cardiac I_p activation. This is in contrast to earlier observations on cardiac preparations, which suggested rather that Li^+ cannot replace Na^+ at the intracellular cation binding sites of the Na^+/K^+ pump [5,7], but, is in line with findings in erythrocytes [8,9] and neurons [10], where Li^+ acts as a

* Corresponding author. Fax: +49 (234) 7094 129.

0005-2736/97/$17.00 © 1997 Elsevier Science B.V. All rights reserved.
PII S0005-2736(97)00143-0

(poor) substitute for intracellular Na^+ in the mechanism of Na^+/K^+ pump activation. Interestingly, Li^+ is also known to be a weak extracellular activator cation of the Na^+/K^+ pump in red blood cells [8], nerve [11] and cardiac preparations [5]. In addition, Eisner and Lederer [12] found that extracellular Li^+ activates I_p in cardiac Purkinje fibres. Thus, Li^+ has the singular property among the monovalent activator cations of being able to activate the Na^+/K^+ pump at intra- and extracellular sites. The aim of the patch clamp experiments described below is to analyse quantitatively the effect of intra- and extracellular Li ions and membrane potential on the current generated by the Na^+/K^+ pump in cardiac cells. The voltage dependency of I_p has offered valuable information on ion translocation in the Na^+/K^+ pump cycle [2,13]. As Li^+ is widely used in the treatment of manic depressive disorders (for a recent review, see [14]), a detailed knowledge of the cellular actions of this ion species seems desirable.

2. Materials and methods

2.1. Preparation of single myocytes

Guinea-pigs (≈ 400 g) were killed under deep ether anaesthesia by cervical dislocation. Ventricular myocytes were isolated at 35°C from the excised heart by means of a Langendorff perfusion with Ca^{2+}-free solutions containing collagenase and protease. The procedure has been described in detail previously [3,15]. The digested ventricles were cut into pieces and carefully stirred at room temperature in a small plastic beaker containing a low Ca^{2+}, enzyme-free medium. The Ca^{2+} concentration of the solution was stepwise increased to 1.8 mM within about 60 min. Isolated ventricular cells were then transferred using a Pasteur pipette to a culture dish (diameter, 3.6 cm) installed on the stage of an inverted microscope.

2.2. Solutions

Two basic solutions containing either 50 mM (A) or 100 mM Na^+ (B) were used in the patch pipettes for intracellular perfusion. Solution A contained (mM): 110 caesium aspartate, 40 NaOH, 10 EGTA, 40 HEPES, 5 $MgCl_2$ (free $Mg^{2+} \approx 2$ mM), 0.15 $CaCl_2$ (free $Ca^{2+} \approx 10^{-9}$ M), 5 glucose, 5 MgATP, 5 sodium creatine phosphate (adjusted to pH 7.3 at 34°C with HCl). Solution B contained (mM): 100 sodium aspartate, 10 EGTA, 40 HEPES, 6 $MgCl_2$ (free $Mg^{2+} \approx 3$ mM), 0.15 $CaCl_2$ (free $Ca^{2+} \approx 10^{-9}$ M), 5 glucose, 5 MgATP, 20 tetraethylammonium chloride (TEACl; adjusted to pH 7.3 at 34°C with NaOH). A medium containing 100 mM Li^+ instead of 100 mM Na^+ was obtained by replacing the sodium aspartate in solution B with lithium aspartate, the other constituents of solution B remained unchanged (pH adjusted with LiOH). Finally, a Na^+-free solution was made from solution B by substituting 100 mM TEACl for sodium aspartate. Thus, this Na^+-free medium contained 120 mM TEACl plus the residual constituents of solution B (pH adjusted to 7.3 with CsOH). High Na^+ concentrations of solutions A and B were selected in order to reduce the effect on the I_p amplitude of a possible Na^+ depletion beneath the cell membrane during strong activation of the Na^+/K^+ pump [16]. Solution A was used in the experiments if not stated otherwise. The standard extracellular superfusion medium contained (mM): 144 NaCl, 0–5.4 KCl, 0.5 $MgCl_2$, 1.8 $CaCl_2$, 10 HEPES and 10 glucose (adjusted to pH 7.3 at 34°C with NaOH). In order to decrease K^+ and Ca^{2+} conductances and the Na^+/Ca^{2+} exchange of the sarcolemma, 2 mM $BaCl_2$ and 5 mM $NiCl_2$ were added to the solution. In Na^+-free superfusion media, NaCl was replaced either by 150 mM choline chloride (plus $5 \cdot 10^{-6}$ M atropine sulphate), by 150 mM LiCl (pH of both solutions adjusted to 7.3 with LiOH) or by 150 mM *N*-methyl-D-glucamine (NMDG, pH adjusted to 7.3 with HCl). In Na^+-free superfusion media containing various Li^+ concentrations, [choline] plus $[Li^+]$ was always 150 mM.

2.3. Drugs

The cardiac glycoside, dihydro-ouabain (DHO; Sigma, Deisenhofen, Germany), was used to identify I_p in cells superfused with Na^+-free solutions. In these media, the affinity of the Na^+/K^+ pump for K_o^+ increased by a factor of ten and, thus, $[K^+]_o$ in the submillimolar range substantially activated I_p. Therefore, DHO was used (instead of a K^+-free solution) to check for exact zero I_p.

2.4. Experimental procedure and whole-cell recording

The experiments were carried out in culture dishes containing several hundred isolated, rod-shaped myocytes. A dish was fixed to the stage of an inverted microscope (IM; Zeiss, Oberkochen, Germany). The volume of the dishes was reduced to ≈ 0.3 ml by means of an annular plastic device, which was pressed down to the bottom of the dish. The device included an inlet and an outlet for the external media, which superfused the myocytes in the dish at ≈ 2 ml/min and 34°C. The cell under study was additionally superfused with test solutions that were successively applied close to the myocyte via a multibarrelled pipette (inner tip diameter, ≈ 150 μm). A command valve unit regulated solution release under gravitational force from reservoirs that were kept about 30 cm above the culture dish. The solution change at the surface of the cell was complete within 250 ms (cf. [3]). The temperature in the immediate vicinity of the cell dropped by 1–1.5°C during superfusion with one of the test media. The membrane current of the myocyte was measured at pre-set membrane potentials in the whole-cell recording mode of the patch clamp technique [17] by means of an Axoclamp 2A voltage clamp amplifier (Axon Instruments, Burlingame, CA, USA). The initial resistance of the patch pipettes filled with one of the intracellular solutions varied between 2 and 3.5 MΩ. Membrane current and voltage were recorded on a pen recorder (Multicorder; Watanabe, Tokyo, Japan). The holding potential was -20 mV throughout. I_p was identified as the outward current blocked by K^+-free and/or DHO-containing solutions. The cell surface area was estimated from the capacitive current flowing during small hyperpolarizing voltage pulses. The specific membrane capacitance was assumed to be 1 μF cm^{-2} (for more details, see [18]).

2.5. Statistics

Whenever possible, data are presented as means ± S.E.M., and S.E.M. is presented in the figures only if the size of the symbols is exceeded. The symbol, n, indicates the number of cells studied. Differences between means were tested by Student's one-tailed t-test. They were deemed significant if $P < 0.05$.

3. Results

3.1. I_p activation by K^+ or Li^+ in Na^+-free solution. Inhibition of I_p by DHO

Under normal physiological conditions, the Na^+/K^+ pump extrudes 3 Na^+ and takes up 2 K^+ into the cell during each cycle and, thus, I_p is an outward current. The bottom trace in Fig. 1 shows the membrane current (I) of a guinea-pig ventricular myocyte superfused with Na^+-free solution at the holding potential of -20 mV. The intracellular perfusion medium contained 50 mM Na^+ (solution A). The upper traces specify the solutions applied. First, the myocyte was superfused with a K^+-free medium in which NaCl was completely replaced by choline chloride. Active Na^+/K^+ transport was strongly inhibited by this solution and, thus, I_p was almost absent. The addition of 0.2 mM K^+_o evoked an outward current of 130 pA which was partially (82%) and reversibly inhibited by $5 \cdot 10^{-5}$ M DHO. The current was nearly blocked again following reapplication of the K^+-free, choline-containing solution. This current was considered to represent I_p. Switching to a K^+-free medium containing 150 mM LiCl instead of choline chloride shifted the current once more in the outward direction. The application of DHO ($5 \cdot 10^{-5}$ or 10^{-3} M) caused a concentration-dependent, reversible inward shift of the current and thus revealed the presence of I_p under these conditions. The I_p

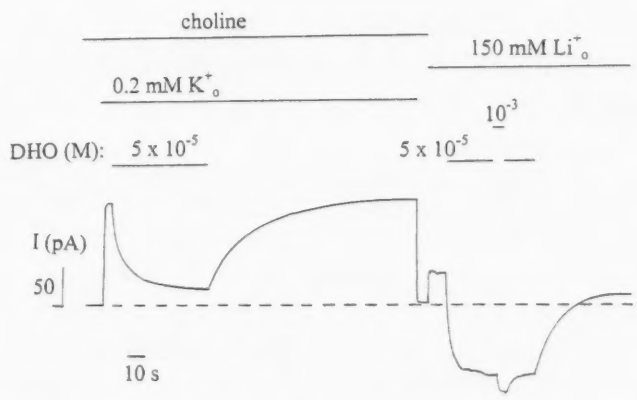

Fig. 1. Membrane current of a guinea-pig ventricular myocyte in various Na^+-free solutions. The current was measured at the holding potential (-20 mV) in media in which NaCl was replaced by choline chloride (left) or LiCl (right), as indicated by the lines above the current trace. The application of DHO is marked by horizontal bars. The lower end of the current calibration bar and the broken line indicate zero current level. Membrane capacitance, 158 pF.

inhibition evoked by $5 \cdot 10^{-5}$ M DHO amounted to 86% of the I_p blockade under 10^{-3} M DHO. In line with earlier observations [3,6,12], the experiment suggests that Li^+, like K^+, acts as an extracellular activator cation of the cardiac I_p.

The current shift upon switching from the choline-containing to the Li^+-containing solution is caused by two mechanisms. First, there is an activation of the outwardly directed I_p by Li_o^+. Secondly, there is, at the same time, an inward leak current because of a higher membrane permeability for Li^+ than for choline. The net result, compared to the current in K^+-free, choline-containing medium, can be an outward or an inward current shift, depending on the relative magnitude of I_p and the Li^+-leak current at -20 mV. In Fig. 1, a small net outward shift results when choline is replaced by Li^+. Upon applying DHO, the holding current shifted inwardly, since I_p is inhibited. The current level attained with $1 \cdot 10^{-3}$ M DHO indicates zero I_p.

3.2. Concentration–response curves of I_p inhibition by DHO in Na^+-free media

The application of various DHO concentrations to myocytes in experiments like that illustrated in Fig. 1 resulted in the concentration–response curves of I_p inhibition by DHO shown in Fig. 2. The figure displays the normalized inhibition of I_p versus the logarithm of the DHO concentration tested. The I_p inhibition caused by $1 \cdot 10^{-3}$ M DHO was arbitrarily set to 100%. I_p amounted to 0.64 ± 0.03 μA cm^{-2} ($n = 21$) in a choline solution containing 0.2 mM K^+ (●) and to 0.80 ± 0.02 μA cm^{-2} ($n = 16$) in myocytes superfused with the Na^+-, K^+-free medium containing 150 mM Li^+ (○). The sigmoid curves fitted to the data by least-squares non-linear regression obey the Hill equation:

$$\text{Percentage } I_p \text{ inhibition} = \frac{100 \times [\text{DHO}]^{n_H}}{(K'_D)^{n_H} + [\text{DHO}]^{n_H}}. \quad (1a)$$

The resulting Hill coefficient (n_H) of 1.08 for both curves reflects a one-to-one binding of DHO to the Na^+/K^+ pump (cf. [19]). The apparent K_D value K'_D ([DHO] for half-maximal I_p inhibition) amounted to $0.8 \cdot 10^{-5}$ M DHO in Li^+-containing medium and to $1.2 \cdot 10^{-5}$ M DHO in the choline-containing solution. Thus, the concentration–response curve of I_p inhibition by DHO in Li^+-containing medium was (significantly) shifted to the left, although I_p was slightly larger in the Li^+-containing solution. This is surprising because a stronger pump activation by a higher external activator cation concentration normally increases the K'_D value for DHO binding [19]. The present finding recalls an earlier observation of the authors that the inhibition of I_p by DHO in rat and guinea-pig ventricular cells occurs at somewhat lower [DHO] in Na^+-containing than in Na^+-free, choline-containing media, if the activation of I_p under both conditions is comparable [19]. Therefore, Li_o^+ seems to promote DHO binding to the Na^+/K^+ pump in a similar way as Na_o^+. This is also evident from the higher rate of I_p inhibition by $5 \cdot 10^{-5}$ M DHO when the current is activated by 150 mM Li_o^+ instead of 0.2 mM K_o^+ (Fig. 1). Table 1 summarizes the mean values of the apparent association and dissociation rate constants and the derived K'_D values of DHO binding from experiments like that shown in Fig. 1 (see [15] for details of the methodology used).

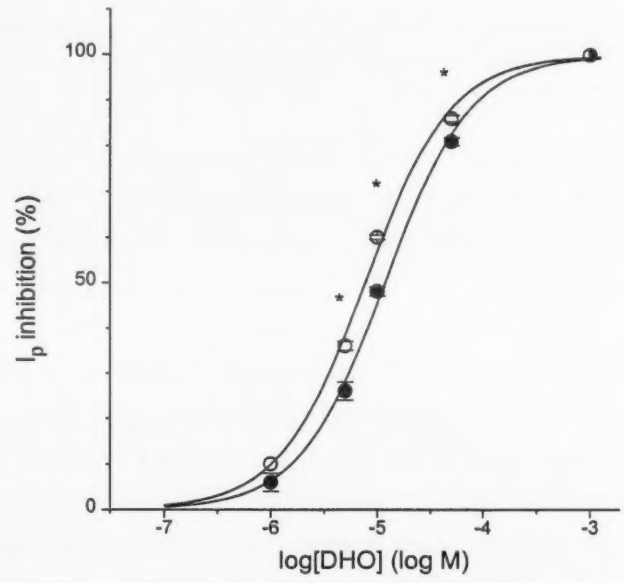

Fig. 2. Concentration–response curves of steady-state I_p inhibition by DHO in ventricular myocytes at the holding potential of -20 mV. I_p inhibition caused by $1 \cdot 10^{-3}$ M DHO was arbitrarily set to 100% (◑). Sigmoid curves fitted to the data points obey Eq. 1a. ●, 0.2 mM K_o^+, Na^+-free medium containing choline chloride; K'_D value ([DHO] for half-maximal I_p inhibition), $1.2 \cdot 10^{-5}$ M DHO ($n = 3$–8). ○, 150 mM Li_o^+; K'_D value, $0.8 \cdot 10^{-5}$ M DHO ($n = 2$–6). *, $P < 0.05$ for the difference between the data points. $r^2 = 0.99$.

Table 1
Kinetics of I_p inhibition by DHO in ventricular myocytes

I_p activated by:	k_1 10^3 M^{-1} s^{-1}	k_2 s^{-1}	K'_D 10^{-5} M	n
0.2 mM K_o^+, choline	1.9 ± 0.3 [a]	0.055 ± 0.003 [a]	3.4 ± 0.5 *	11
150 mM Li_o^+	7.2 ± 0.7 [a]	0.079 ± 0.005 [a]	1.2 ± 0.1 *	11

I_p was activated either by 0.2 mM K_o^+ (in choline medium) or by 150 mM Li_o^+.
k_1, apparent association rate constant.
k_2, apparent dissociation rate constant.
K'_D, mean of apparent K_D values determined for each cell (k_2/k_1).
[DHO] from $1 \cdot 10^{-5}$ to $1 \cdot 10^{-4}$ M.
[a] Significant difference ($P < 0.05$).

To rule out a possible effect of choline on the dose–response curve, NMDG was also used as a Na^+ substitute, but no difference in the sensitivity of the pump towards DHO was found between myocytes in choline or NMDG-containing solution (data not shown).

3.3. I_p activation by various $[Li^+]_o$ in Na^+-containing cells

The concentration dependence of I_p activation by Li_o^+ was studied in some detail in Na^+-containing myocytes superfused with Na^+-free media at constant $[Li^+]_o + [choline]_o$ (150 mM). The measurements were carried out at the holding potential similar to the procedure depicted in the left part of Fig. 1. However, instead of 0.2 mM K_o^+, various $[Li^+]_o$ were applied to the myocytes. DHO-containing solutions ($1 \cdot 10^{-4}$ or $1 \cdot 10^{-3}$ M) were used to estimate the I_p amplitude at the various $[Li^+]_o$. In the presence of 150 mM Li^+, the amount of I_p blocked by $1 \cdot 10^{-4}$ M DHO amounted to 95% (see Fig. 2). No significant difference between I_p determined either with $1 \cdot 10^{-4}$ or $1 \cdot 10^{-3}$ M DHO was found when $[Li^+]_o$ was lower than 100 mM. Therefore, $1 \cdot 10^{-3}$ M DHO was applied in experiments where $[Li^+]_o$ exceeded 100 mM. The results are presented in Fig. 3 (●). Normalized I_p amplitudes were plotted versus $[Li^+]_o$. The pump current density amounted to 0.55 ± 0.04 $\mu A\ cm^{-2}$ ($n = 21$) at 150 mM Li_o^+. This I_p density was arbitrarily set to 100%. The curve fitted to the data represents the Hill equation:

$$I_p = \frac{I_{p,max} \times [Li^+]_o^{n_H}}{(K_{0.5})^{n_H} + [Li^+]_o^{n_H}}. \quad (1b)$$

The fitting procedure yielded a Hill coefficient, n_H, of 1.4 and an $I_{p,max}$ of 106%. The $K_{0.5}$ value, the $[Li^+]_o$ for half-maximal I_p activation, was 23 mM. A small I_p was still observed in the absence of Li_o^+ [0.021 ± 0.006 $\mu A\ cm^{-2}$ ($n = 8$); checked with $1 \cdot 10^{-3}$ M DHO]. It might be caused by a small amount of K^+ (≈ 10 μM; determined by atomic absorption spectrometry) present as an impurity in nominally K^+-free solutions and was subtracted from the I_p densities observed at the various $[Li^+]_o$. Experiments on four cells internally perfused with solution B (100

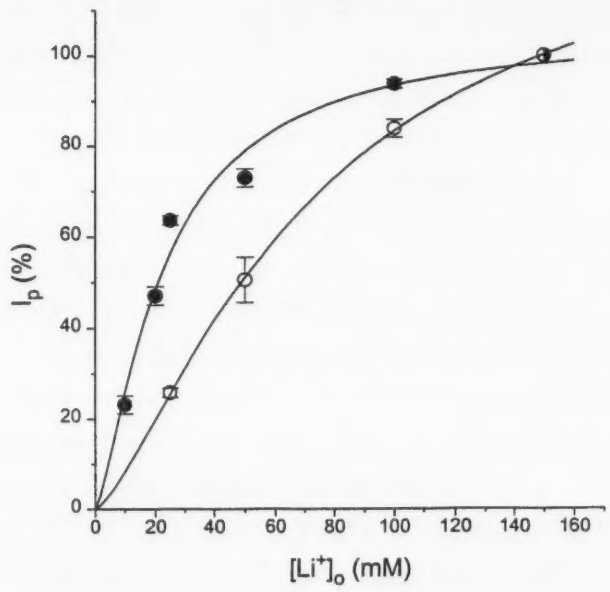

Fig. 3. I_p activation by Li_o^+ in ventricular myocytes containing Na^+ or Li^+. I_p amplitudes were estimated at −20 mV by the application of $1 \cdot 10^{-4}$–$1 \cdot 10^{-3}$ M DHO. I_p activated by 150 mM Li_o^+ was arbitrarily set to 100% (◑). At this $[Li^+]_o$, I_p amounted to 0.55 ± 0.04 $\mu A\ cm^{-2}$ in cells containing 50 mM Na^+ ($n = 21$) and to 0.33 ± 0.05 $\mu A\ cm^{-2}$ in myocytes that were internally perfused with 100 mM Li^+ (plus 20 mM TEACl; $n = 10$). $K_{0.5}$ value for Na^+-containing cells (●), 23 mM Li_o^+; $I_{p,max}$, 106%; n_H, 1.4 ($n = 8$–21); $r^2 = 0.98$. $K_{0.5}$ value for Li^+-containing myocytes (○), 73 mM Li_o^+; $I_{p,max}$, 137.5%; n_H, 1.4 ($n = 5$–10); $r^2 > 0.99$.

mM Na^+) resulted in the same I_p activation by Li_o^+. Compared to the activation of I_p by K_o^+ in Na^+-free, choline-containing media under otherwise similar conditions [19], Li_o^+ exhibits at least a 100-fold weaker potency in activating the cardiac Na^+/K^+ pump, and the maximal I_p activated by Li_o^+ tends to be smaller than the (maximal) I_p evoked by K_o^+ [1.02 ± 0.05 μA cm^{-2} ($n = 30$) in a Na^+-free (choline) medium containing 5.4 mM K^+].

3.4. I_p activation by various $[Li^+]_o$ in Li^+-containing myocytes

We tested to see if I_p activation by Li_o^+ differed in myocytes internally perfused with 100 mM Li^+ instead of 50 (or 100) mM Na^+. First, we checked whether Li ions actually activate the cardiac Na^+/K^+ pump at internal sites. The original records of different cells depicted in Fig. 4 illustrate the test. The pump current was activated in a Na^+-free, choline-containing solution by 1 mM K_o^+ (indicated by a fast upward deflection of the current trace). The upper record displays the change of I_p when a myocyte was internally perfused with a Na^+-free (TEA) pipette solution in order to reduce $[Na^+]_i$ to zero. I_p declined rapidly and, 90 s after establishing the whole-cell configuration, amounted to $< 10\%$ of the initial I_p amplitude, most probably because of the decline in $[Na^+]_i$. Intracellular perfusion with a Na^+-free medium containing 100 mM Li^+ caused a quite different time course of I_p decline (middle record). The I_p amplitude measured 90 s after the first I_p activation still reached $\approx 50\%$ of the initial I_p amplitude. About 2 min later, I_p amounted to 41% of the current measured at first and remained nearly constant thereafter for several minutes. For comparison, an original record of a cell internally perfused with 50 mM Na^+ (solution A) is also shown (bottom record). We conclude from the test that Li^+ activates the cardiac Na^+/K^+ pump at intracellular sites.

I_p activated by Li_o^+ in cells internally perfused with Li ions was estimated by applying superfusion media containing $1 \cdot 10^{-3}$ M DHO. The other experimental conditions remained the same as those in the experiments performed with Na^+ in the pipette and illustrated in Fig. 3 (●). The results are also shown in Fig. 3 (○). Normalized I_p densities were plotted versus $[Li^+]_o$. The I_p density measured at 150 mM

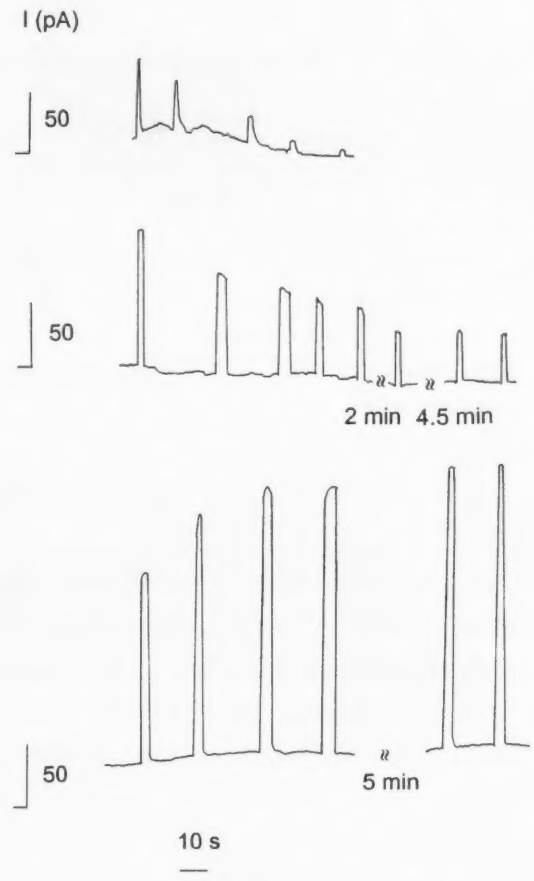

Fig. 4. Time course of I_p activation by 1 mM K_o^+ in three myocytes. Na^+-free (choline chloride) bathing medium was used. I_p activation causes a step-like current shift in the outward direction. Upper current trace: I_p in a cell internally perfused with Na^+-free solution containing 120 mM TEACl. Membrane capacitance, 174 pF. Middle trace: I_p in a myocyte that was internally perfused with 100 mM Li^+. Membrane capacitance, 120 pF. Interruption of the current trace indicates omission of records for the time period stated. Lower trace: I_p in a cell that was internally perfused with 50 mM Na^+. Membrane capacitance, 248 pF. Interruption of the current trace indicates omission of records for the time period stated. The lower end of the current calibration bars marks zero current level.

Li_o^+ amounted to 0.33 ± 0.05 μA cm^{-2} ($n = 10$). It was arbitrarily set to 100%. The curve fitted to the data obeys Eq. (1b), with $n_H = 1.4$, $I_{p,max} = 137.5\%$, and a $[Li^+]_o$ for half-maximal I_p activation of 73 mM ($K_{0.5}$ value; $n = 5$–10). Again, a small I_p was present in the nominal absence of K_o^+ and Li_o^+ (0.023 ± 0.004 μA cm^{-2} ($n = 10$); checked with $1 \cdot 10^{-3}$ M DHO). This value of I_p was subtracted from the I_p densities derived for the various $[Li^+]_o$. Compared to the data from Na^+-containing cells (●), the I_p density of myocytes internally perfused with Li^+ (○) is smaller at 150 mM Li_o^+ (0.33 versus 0.55 μA cm^{-2}) and at the other $[Li^+]_o$ tested. Furthermore, the $K_{0.5}$ value, the $[Li^+]_o$ required for half-

maximal I_p activation, was larger in myocytes containing 100 mM Li^+ than in cells intracellularly perfused with 50 (or 100) mM Na^+ (73 versus 23 mM Li_o^+).

3.5. Binding of Li_o^+ to the Na^+/K^+ pump is voltage-dependent

In single cardiac Purkinje cells, I_p activation by K_o^+ and its congeners Tl_o^+, NH_{4o}^+ and Cs_o^+ is voltage-dependent [4]. Depolarization increases and hyperpolarization decreases the extracellular concentration of activator cations required for half-maximal I_p activation ($K_{0.5}$ value). This means that hyperpolarization of the sarcolemma, at a constant concentration of an extracellular activator cation, or an increase in the ionic concentration at a constant membrane potential exerts an equivalent activation of I_p. We tested to see if the I_p activation by Li_o^+ in ventricular myocytes is also voltage-dependent. For this purpose, we carried out experiments as illustrated in Fig. 5A. The membrane potential of a myocyte was clamped to preset values (indicated by the upper trace) and the resulting current was measured in Na^+-free superfusion fluid containing 50 mM Li^+ with (right part of the figure) or without (left part) DHO ($1 \cdot 10^{-4}$ M). The cardiac glycoside was used to estimate I_p as the difference in current. As indicated by the dashed lines, the DHO-sensitive current (ΔI) is clearly smaller at +20 mV than at −40 mV. In this way, I_p was measured in media containing various [Li^+]. In all solutions, [choline chloride] plus

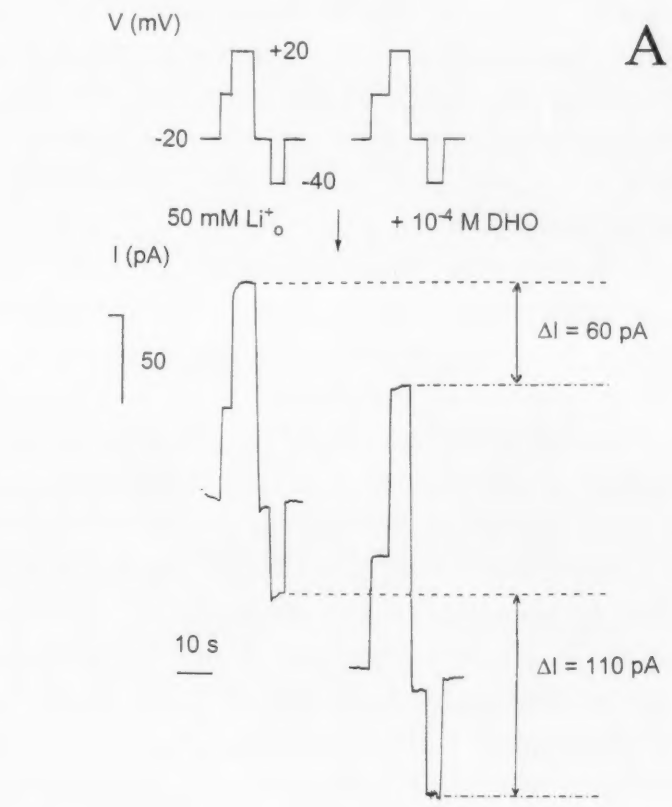

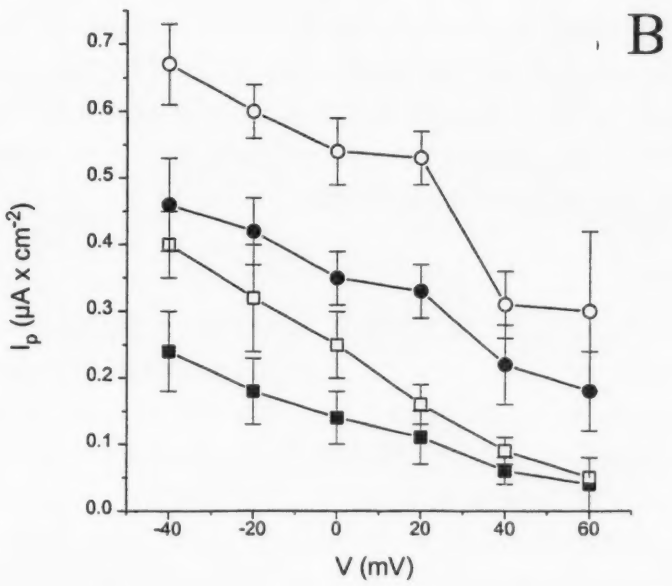

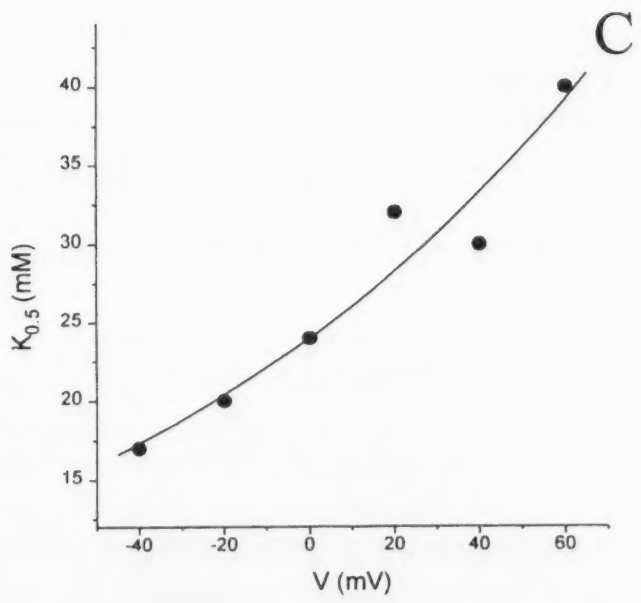

Fig. 5. I_p activation by Li_o^+ is voltage-dependent. I_p was estimated by application of $1 \cdot 10^{-4}$ M DHO. Pipette solution B (100 mM Na^+). (A) Original records of membrane current (bottom traces) at various membrane potentials (top traces) in Na^+-free (choline chloride) solution containing 50 mM Li^+ with (right part) or without DHO. The dashed lines indicate that the inward shift of membrane current (ΔI) caused by DHO is larger at −40 mV than at +20 mV. Membrane capacitance, 148 pF. The upper end of the current calibration bar marks zero current level. (B) I_p densities as a function of membrane potential at four $[Li^+]_o$. $[Li^+]_o$ plus [choline] was 150 mM throughout. ■, 10 mM Li_o^+ ($n = 2$–9); □, 20 mM Li_o^+ ($n = 2$–6); ●, 50 mM Li_o^+ ($n = 2$–9); ○, 150 mM Li_o^+ ($n = 2$–8). (C) $K_{0.5}$ value for I_p activation by Li_o^+ in myocytes as a function of membrane potential. The curve fitted to the data points obeys Eq. 2. $K_{0.5}$ value at zero potential [$K_{0.5(V=0\ mV)}$], 24 mM Li_o^+; δ, 0.22; $r^2 = 0.93$.

[LiCl] was 150 mM. Mechanisms different from the binding of external activator cations to the Na^+/K^+ pump govern the shape of the cardiac I_p–V curve at membrane potentials that are more negative than −40 mV [3,20]. Therefore, only I_p densities observed at more positive potentials were plotted versus voltage in Fig. 5B. The data were obtained at four $[Li^+]_o$. Surprisingly, the I_p density of the myocytes decreased with depolarization, even at 150 mM Li_o^+. This is in contrast to the cardiac I_p–V relationship at concentrations of K_o^+ or of the aforenamed congeners above their respective $K_{0.5}$ values. Under these conditions, I_p remained constant at potentials that were more positive than −40 mV [4]. As can be seen from Fig. 5B, I_p also declined at lower $[Li^+]_o$ upon depolarization. A closer inspection of the figure suggests that the percentage of I_p activated by the three lower $[Li^+]_o$ decreased with depolarization. This is more clearly seen in Fig. 5C where the Li_o^+ concentrations required for half-maximal I_p activation ($K_{0.5}$ values) were plotted as a function of the membrane potential (for details of the procedure, see [4]). The $K_{0.5}$ value increased by a factor of 2.5 over the potential range studied. The data points were fitted by a curve which obeys the exponential function:

$$K_{0.5(V)} = K_{0.5(V=0\ mV)} \exp(\delta FV/RT) \qquad (2)$$

where $K_{0.5(V)}$ denotes the $K_{0.5}$ value at the membrane potential, V; $K_{0.5(V=0\ mV)}$ stands for the $K_{0.5}$ value at zero potential (24 mM Li_o^+), and R, T and F have their usual meanings. Delta (δ) influences the steepness of the function. It represents the fraction of the electrical field across the sarcolemma sensed by extracellular monovalent ions in the process of binding to the Na^+/K^+ pump [21] and was calculated to be 0.22. Thus, binding of Li_o^+ to the cardiac Na^+/K^+ pump is voltage-dependent and is facilitated by hyperpolarization.

3.6. Activation of I_p in myocytes at various intracellular $[Li^+]$

In order to study quantitatively the activation of I_p by intracellular Li^+, I_p was measured at four internal Li^+ concentrations. Each $[Li^+]_i$ was tested in a different group of myocytes ($n = 4$–16). The measurements were carried out at the holding potential of −20 mV. The media used for intracellular perfusion contained various $[Li^+]$, but [LiCl] plus [TEACl] was always 120 mM (Na^+-free solution B). The external Na^+-free (choline chloride) solution contained 1 mM K^+. At this $[K^+]_o$, the extracellular binding sites of the cardiac Na^+/K^+ pump for activator cations are nearly saturated [3,22]. In addition, I_p was estimated in cells intracellularly perfused with a medium containing no activator cation of the Na^+/K^+ pump. Under these conditions (1 mM K_o^+; 120 mM TEACl inside the myocytes), I_p amounted to 0.03 ± 0.01 μA cm^{-2} ($n = 8$; checked with $1 \cdot 10^{-3}$ M DHO). This I_p value was subtracted from the I_p densities observed at the various $[Li^+]_i$. Fig. 6 shows the results. The I_p density was plotted versus the Li concentration of the pipette solution ($[Li^+]_{pip}$). The current density increased with increasing $[Li^+]_{pip}$ towards a maximum value $I_{p,max}$ that amounted to 0.54 μA cm^{-2}, according to the Hill equation fitted to the data. Half-maximal I_p activation occurred at 36 mM Li_i^+. Thus, the maximal I_p density was lower (by a factor of two) and the $K_{0.5}$ value for the activation of I_p by intracellular Li^+ was larger (by a factor of four) than the corresponding values for I_p activation by Na_i^+ (see ref. [22]).

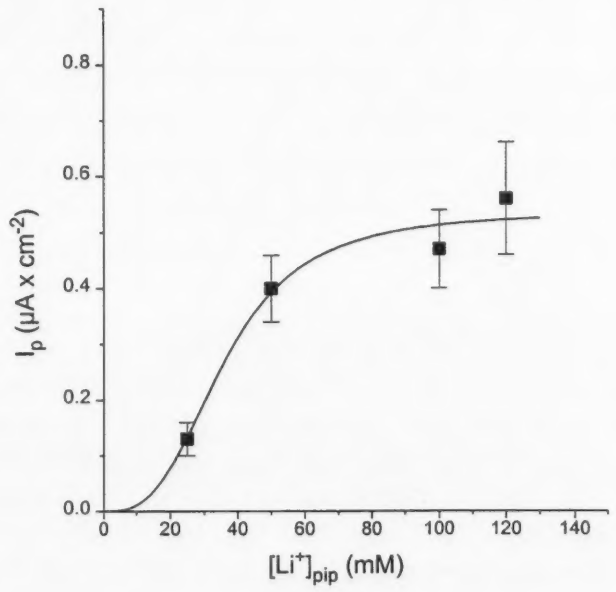

Fig. 6. I_p activation by internal Li^+ in myocytes superfused with Na^+-free (choline) medium containing 1 mM K_o^+. I_p densities are plotted versus $[Li^+]$ of the pipette solution for internal perfusion ($[Li^+]_{pip}$). Four different groups of four–sixteen cells were internally perfused at the holding potential with one of the four $[Li^+]_{pip}$. I_p was estimated by the application of $1 \cdot 10^{-3}$ M DHO. The curve fitted to the data points obeys Eq. 1b. $I_{p,max}$, 0.54 μA cm^{-2}; $K_{0.5}$ value, 36 mM Li_{pip}^+; $n_H = 3.1$; $r^2 = 0.97$.

3.7. I_p–V curves of cells containing Na_i^+ or Li_i^+ in Na^+-free solutions

We studied the I_p–V relationship of Na_i^+-containing ventricular myocytes superfused with Na^+-free media in the membrane potential range between −100 mV and +40 mV. Solution B (100 mM Na^+) was used for the internal perfusion of the cells in order to saturate the internal Na^+-binding sites of the Na^+/K^+ pump and to evoke maximal pump activation intracellularly. The external Na^+-free media contained either 150 mM Li^+ or 1 mM K^+ (NaCl replaced by choline chloride) to also strongly activate the pump at the external cation-binding sites of the pump. Mean I_p densities ± S.E.M. as a function of membrane potential are shown in Fig. 7. Open squares represent the I_p–V curve of cells in Na^+-, K^+-free solution containing 150 mM Li^+ ($n = 8$–9). Filled squares indicate the I_p–V relationship of myocytes superfused with Na^+-free (choline chloride) medium containing 1 mM K^+ ($n = 6$–8). Fig. 7 reveals a positive slope of the I_p–V curve at negative membrane potentials in myocytes superfused with the choline chloride solution containing 1 mM K^+ (■). The curve flattens at positive potentials. The I_p–V curve of cells in the medium containing 150 mM Li^+ (□) not only shows a positive slope at negative potentials up to −40 mV but also a markedly negative slope (significantly different from the slope observed in the choline chloride medium containing 1 mM K^+) at more positive voltages (as already noted in context with Fig. 5B).

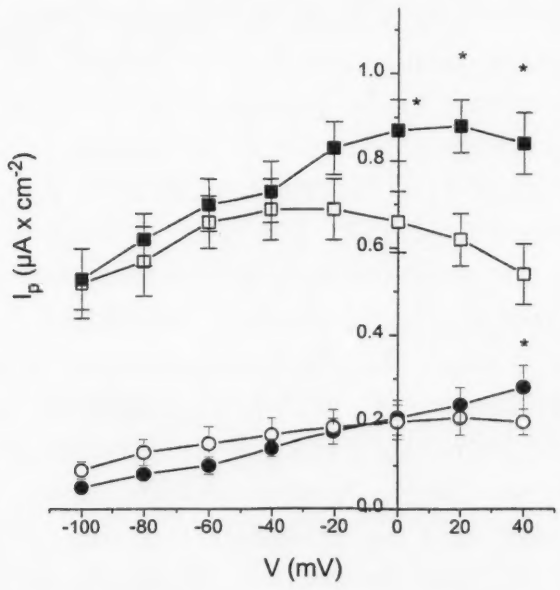

Fig. 7. I_p–V relationships of myocytes internally perfused with 100 mM Na^+ (squares) or 100 mM Li^+ (circles). I_p was estimated by the application of $5 \cdot 10^{-4}$–$1 \cdot 10^{-3}$ M DHO. ■, ●: 1 mM K_o^+ ($n = 6$–8); NaCl of the superfusion medium was replaced by choline chloride. □, ○: 150 mM Li_o^+ ($n = 6$–9). Both superfusion media were successively applied to the same cells containing 100 mM Li^+ (○, ●). *, $P < 0.05$ for the difference between corresponding data points. The positive slope of the curves at negative membrane potentials differs significantly from zero.

I_p–V relationships of myocytes internally perfused with a solution containing 100 mM Li^+ (circles) and superfused either with the K^+- and Na^+-free medium containing 150 mM Li^+ (○) or the choline chloride solution containing 1 mM K^+ (●) are also depicted in Fig. 7. Both media were successively applied to the same cells ($n = 6$–7). As in Na^+-containing myocytes, the I_p–V curve of the cells at 1 mM K_o^+ displays a positive slope at negative membrane potentials. The I_p–V relationship of the myocytes in the medium containing 150 mM Li^+ exhibits a more shallow slope at negative potentials. In these cells, I_p is nearly voltage-independent at positive membrane potentials. In this voltage range, the slopes of the I_p–V curves in Li^+-containing and K^+-containing solution differ significantly. The results suggest that internal perfusion of the cells with a solution containing 100 mM Li^+ instead of 100 mM Na^+ evokes a smaller I_p. The voltage dependence of I_p at negative potentials persists in Na^+-free solution, especially in the choline chloride medium containing 1 mM K^+.

4. Discussion

4.1. Activation of cardiac I_p by Li_o^+

The concentration-dependent inhibition by DHO of the Li_o^+-activated current (Fig. 1) clearly demonstrated that the activated current was indeed I_p. This is in line with earlier reports on Li_o^+ as an activator cation of the cardiac Na^+/K^+ pump current [3,6,12]. The data displayed in Fig. 5C indicate that 24 mM Li_o^+ is required at zero potential for half-maximal I_p activation in Na^+-containing ventricular myocytes superfused with Na^+-free solution. Under these conditions, K_o^+ exerts an ≈ 100-fold stronger I_p activation [19,22]. I_p tends to be smaller in Li^+-containing than in K^+-containing media (Figs. 4 and 7). This finding agrees well with earlier Na^+ efflux measurements on frog sartorius muscles in Na^+-free solution containing K^+ or Li^+ [23]. It also recalls biochemical

studies that demonstrated a smaller potency and efficacy of Li^+ compared to K^+ for the activation of the Na^+/K^+ ATPase [11,24]. The $[Li^+]_o$ required for half-maximal I_p activation is larger for cells internally perfused with Li^+ than in Na^+-perfused myocytes (73 versus 23 mM; Fig. 3). Interestingly, the $K_{0.5}$ value for the Na^+/K^+ pump activation by K_o^+ in Na^+- and Li^+-free media was very much the same in myocytes internally perfused either with Na^+ or Li^+ (data not shown). Thus, the increased $K_{0.5}$ value seems to be specific for Li_o^+. Li_o^+-induced alterations in the transition between the conformational E_2P-states in the Na^+ limb of the Na^+/K^+ pump cycle may be involved.

4.2. I_p activation by intracellular Li^+

According to a recent abstract [6], Li^+ can replace Na^+ at intracellular binding sites of the cardiac Na^+/K^+ pump in the mechanism of I_p activation. The results described above (Figs. 3, 4, 6 and 7) extend these observations. The I_p density is lower in myocytes internally perfused with media containing 100 mM Li^+ instead of 100 mM Na^+ (Fig. 7). The different current densities may be partly due to a lower affinity of the pump's intracellular binding sites for Li^+ (Fig. 6; $K_{0.5}$ value, 36 mM) than for Na^+ ($\approx$ 10 mM; see [22,25]). Since the difference between the I_p densities is large, even at high intracellular $[Na^+]$ and $[Li^+]$ (comp. Fig. 7), an additional factor seems to be involved. This factor may be a decreased $I_{p,max}$. Compared to Na^+, Li^+ is a less potent and less efficacious activator of ATP hydrolysis by the Na^+/K^+ ATPase in cells [8] and in K^+-free or K^+-containing media [11,26]. Since ATP splitting is a prerequisite for ion translocation by the Na^+/K^+ pump, it seems reasonable that $I_{p,max}$ is smaller in Li^+-containing than in Na^+-containing myocytes. Based on notoriously difficult net ion flux measurements, a change of the usual 3:2 coupling ratio for active Na_i^+–K_o^+ exchange to a ratio near or equal to 1:1 for the Li_i^+–K_o^+ exchange in erythrocytes has been suggested [9]. While the I_p data presented in Fig. 6 clearly show that the coupling ratio of active Li_i^+–K_o^+ exchange must be > 1, they do not exclude a ratio different from 3:2. Additional experimental evidence is required to prove a change in the coupling ratio.

4.3. I_p activation by Li_o^+ is voltage-dependent

The $K_{0.5}$ value for the activation of I_p by Li_o^+ is voltage-dependent (Fig. 5C). This and other observations [2] are interpreted to mean that binding of extracellular activator cations to the Na^+/K^+ pump might occur at the bottom of a 'high field narrow access channel' [27]. About 0.25 of an elementary charge traverses the electric field across the sarcolemma during the binding of extracellular cations. The data illustrated in Fig. 5C are in quantitative agreement with these considerations and lend further support to the hypothesis that the Na^+/K^+ pump molecule contains a channel-like structure.

4.4. I_p–V curves of ventricular myocytes in Na^+-free media containing K^+ or Li^+

The persistence of a positive slope in the I_p–V relationship at negative voltages in Na^+-free solutions is in line with earlier reports on isolated cardiac Purkinje cells [3,4] and *Xenopus* oocytes [28], but is at variance with other observations on *Xenopus* oocytes [29,30] and squid axons [21]. These inconsistent observations are most probably not due to the different Na^+/K^+ ATPase isoenzymes expressed in various cells. Guinea-pig ventricular myocytes express predominantly the α_1 isoenzyme [31]. However, in contrast to the present results, earlier studies on these cells revealed only a shallow (if any) voltage dependence of I_p at negative membrane potentials in Na^+-free media [20,32]. The latter findings constitute the experimental basis of the generally accepted hypothesis that voltage-dependent binding of Na^+ from the extracellular solution is an important mechanism for the decrease in I_p with hyperpolarization in cells superfused with Na^+-containing, 'physiological' media [2,13,30]. The I_p-V relationships shown in Fig. 7 suggest that this is probably not the only factor involved. As can be seen from the figure, the decrease in I_p with increasingly more negative potentials is most pronounced in Na^+-free solutions containing choline chloride, although choline has no effect on the cardiac Na^+/K^+ ATPase [5].

Another interesting feature of the I_p–V curve of Na^+-containing myocytes superfused with Li^+-containing medium is the negative slope that was observed at positive membrane potentials (Fig. 5B and Fig. 7). Such a negative slope is usually thought to be

caused by voltage-dependent binding of K^+ or its congeners to the Na^+/K^+ pump. It can be easily demonstrated in cells superfused with solutions containing low ($< K_{0.5}$ value) concentrations of external activator cations [1,4,29], but it is absent in cardiac cells at nearly saturating concentrations of these ions [4]. However, the figures display a negative slope of the I_p–V relationship at a high Li_o^+ concentration ($\approx$ six times the $K_{0.5}$ value at 0 mV) in myocytes internally perfused with a saturating $[Na^+]$. Thus, the negative slope of the I_p–V curves at positive potentials is probably not due solely to voltage-dependent Li_o^+-binding. An additional voltage-sensitive partial reaction of the pump cycle probably affects the slope of the I_p–V relationship under these conditions.

4.5. Li^+ transport by the Na^+/K^+ pump in Li^+-treated patients

The intracellular Li^+ concentration in Li^+-treated patients is normally less than 1.0 mM and is lower than expected from a passive distribution across the cell membrane [33]. Thus, Li^+-transport out of the cells occurs against an electrochemical gradient for Li^+. However, the present study suggests that a large active Li^+ efflux via the Na^+/K^+ pump is not performed if Li^+ acts as a partial agonist at the Na_i^+- and K_o^+-binding sites of the Na^+/K^+ pump. In vivo, the physiological activator cations Na_i^+ and K_o^+ are present at relatively high concentrations. Both cation species exhibit a higher apparent affinity than Li^+ for the respective binding sites. Thus, the main Li^+ efflux seems to be mediated by a mechanism that is different from that of active Na^+/K^+ transport.

Acknowledgements

The authors are indebted to Professor W. Schwarz (Frankfurt) for helpful comments on an earlier draft of the manuscript. This work has been supported by a grant from the Belgian F.G.W.O. and a grant from the Research Council of the University of Leuven.

References

[1] H.S. Omay, W. Schwarz, Biochim. Biophys. Acta 1104 (1992) 167–173.
[2] L.A. Vasilets, W. Schwarz, Biochim. Biophys. Acta 1154 (1993) 201–222.
[3] F.V. Bielen, H.G. Glitsch, F. Verdonck, J. Physiol. 442 (1991) 169–189.
[4] F.V. Bielen, H.G. Glitsch, F. Verdonck, J. Physiol. 465 (1993) 699–714.
[5] H.J. Portius, K.R.H. Repke, Acta Biol. Med. Germ. 19 (1967) 907–938.
[6] P.D. Hemsworth, H.H. Rasmussen, Biophys. J. 68 (1995) W-Pos 297.
[7] E.E. Carmeliet, J. Gen. Physiol. 47 (1964) 501–530.
[8] R. Whittam, M.E. Ager, Biochem. J. 93 (1964) 337–348.
[9] P.B. Dunham, O. Senyk, Proc. Natl. Acad. Sci. U.S.A. 74 (1977) 3099–3103.
[10] R.C. Thomas, W. Simon, M. Oehme, Nature 258 (1975) 754–756.
[11] J.C. Skou, Biochim. Biophys. Acta 42 (1960) 6–23.
[12] D.A. Eisner, W.J. Lederer, J. Physiol. 303 (1980) 441–474.
[13] D.C. Gadsby, R.F. Rakowski, P. De Weer, Science 260 (1993) 100–103.
[14] J.R. Atack, H.B. Broughton, S.J. Pollack, Trends Neurosci. 18 (1995) 343–349.
[15] F.V. Bielen, H.G. Glitsch, F. Verdonck, Naunyn-Schmiedeberg's Arch. Pharmacol. 345 (1992) 100–107.
[16] F.V. Bielen, H.G. Glitsch, F. Verdonck, Biochim. Biophys. Acta 1065 (1991) 269–271.
[17] O.P. Hamill, A. Marty, E. Neher, B. Sakmann, F.J. Sigworth, Pflüg. Arch. Eur. J. Physiol. 391 (1981) 85–100.
[18] A.N. Hermans, H.G. Glitsch, F. Verdonck, J. Physiol. 481 (1994) 279–291.
[19] A.N. Hermans, H.G. Glitsch, F. Verdonck, J. Physiol. 484 (1995) 617–628.
[20] D.C. Gadsby, M. Nakao, J. Gen. Physiol. 94 (1989) 511–537.
[21] R.F. Rakowski, D.C. Gadsby, P. De Weer, J. Gen. Physiol. 93 (1989) 903–941.
[22] M. Nakao, D.C. Gadsby, J. Gen. Physiol. 94 (1989) 539–565.
[23] L. Beaugé, J. Physiol. 246 (1975) 397–420.
[24] J.D. Robinson, Biochim. Biophys. Acta 384 (1975) 250–264.
[25] H.G. Glitsch, T. Krahn, H. Pusch, Pflüg. Arch. Eur. J. Physiol. 414 (1989) 52–58.
[26] L. Beaugé, Biochim. Biophys. Acta 527 (1978) 472–484.
[27] P. Läuger, H.-J. Apell, Eur. Biophys. J. 13 (1986) 309–321.
[28] L.A. Vasilets, T. Ohta, S. Noguchi, M. Kawamura, W. Schwarz, Eur. Biophys. J. 21 (1993) 433–443.
[29] R.F. Rakowski, L.A. Vasilets, J. La Tona, W. Schwarz, J. Membr. Biol. 121 (1991) 177–187.
[30] A. Sagar, R.F. Rakowski, J. Gen. Physiol. 103 (1994) 869–894.
[31] K. Sweadner, Biochim. Biophys. Acta 988 (1989) 185–220.
[32] D.C. Gadsby, M. Nakao, J. Physiol. 382 (1987) 106P.
[33] L. Gyulai, S.W. Wicklund, R. Greenstein, M.S. Bauer, P. Ciccione, P.C. Whybrow, J. Zimmerman, G. Kovachich, W. Alves, Biol. Psychiatry 29 (1991) 1161–1170.

ELSEVIER

Biochimica et Biophysica Acta 1330 (1997) 94–102

BIOCHIMICA ET BIOPHYSICA ACTA
BBA

Na^+-dependent γ-aminobutyric acid (GABA) transport in the choroid plexus of rabbit

Vikram K. Ramanathan [a,c], Claire M. Brett [b], Kathleen M. Giacomini [a,c,*]

[a] *Graduate Program in Pharmaceutical Chemistry, S-926, Box 0446, School of Pharmacy, University of California, San Francisco, CA 94143, USA*

[b] *Department of Anesthesia, Box 0624, School of Medicine, University of California, San Francisco, CA 94143, USA*

[c] *Departments of Biopharmaceutical Sciences and Pharmaceutical Chemistry, S-926, Box 0446, School of Pharmacy, University of California, San Francisco, CA 94143, USA*

Received 29 May 1997; accepted 3 June 1997

Abstract

The goal of this study was to examine the mechanisms of transport of γ-aminobutyric acid (GABA) in the choroid plexus. Choroid plexus slices from the rabbit were depleted of ATP with 2,4-dinitrophenol. GABA accumulated in the choroid plexus slices in a concentrative manner in the presence of an inwardly-directed Na^+ gradient. Uptake occurred in the presence of Cl^-; replacement of Cl^- with gluconate abolished uptake. SCN^-, NO_3^- or Br^- were able to support uptake in the absence of Cl^- to a significant extent (80, 68 and 61% of control, respectively). GABA uptake was saturable (K_m of 37 ± 8.5 μM, V_{max} of 409 ± 43 nmol/g/min). Na^+-driven GABA uptake was inhibited by β-alanine ($IC_{50} = 22.9$ μM) and hypotaurine ($IC_{50} = 21.9$ μM) but less potently by nipecotic acid ($IC_{50} = 244$ μM) and hydroxy-nipecotic acid ($IC_{50} = 284$ μM). Betaine, L-(2,4)-diaminobutyric acid, guvacine and 4,5,6,7-tetrahydroisoxazolo[4,5-c]pyridin-3-ol were weak inhibitors ($IC_{50} > 500$ μM). GABA inhibited Na^+-driven uptake of taurine ($IC_{50} = 230$ μM); taurine, however, did not inhibit GABA uptake ($IC_{50} > 1$ mM). RT–PCR, using degenerate primers for cloned GABA transporters, did not result in the amplification of a band from rat choroid plexus RNA. The location of the choroid plexus in the ventricles of the brain, and its role in the secretion of the cerebrospinal fluid, suggest a role for the choroid plexus Na^+-GABA transporter in the disposition of GABA in the brain. © 1997 Elsevier Science B.V.

Keywords: γ-Aminobutyric acid; Taurine; Transport; Epithelium; Choroid plexus

Abbreviations: GABA, γ-aminobutyric acid; L-DABA, L-(2,4)-diaminobutyric acid; THPO, 4,5,6,7-tetrahydroisoxazolo[4,5-c]pyridin-3-ol; CSF, cerebrospinal fluid; DNP, 2,4-dinitrophenol; GAT, GABA transporter

* Corresponding author. Fax: +1 415-476-0688; E-mail: kmg@itsa.ucsf.edu

0005-2736/97/$17.00 © 1997 Elsevier Science B.V. All rights reserved.
PII S0005-2736(97)00146-6

1. Introduction

γ-Aminobutyric acid (GABA) is a neurotransmitter amino acid which is found throughout the central nervous system of vertebrates, formed in neuronal cells by the decarboxylation of glutamic acid and further metabolized by GABA-α-keto-glutarate transaminase. Upon release into the synaptic cleft, GABA binds to post-synaptic $GABA_A$ receptors and elicits a neuroinhibitory response by activating Cl^- channels. Na^+ and Cl^--coupled GABA transporters terminate the actions of GABA by mediating its rapid removal from the synapse. Previously, it was proposed that there were two types of GABA transporters based on their different sensitivity to β-alanine [1,2]. The recent cloning and heterologous expression of GABA transporters has made it clear that multiple subtypes of this transporter exist, and that these can be differentiated on the basis of pharmacological sensitivities to GABA transport inhibitors [3–7].

Studies of GABA transport have focused on neuronal and glial cells [1,2,8,9]. In addition, GABA transport has been described in the epithelia of the retina [10], stomach [11], duodenum [12], kidney [13] and oviduct [14], although the significance of these processes is generally less clear. The choroid plexus epithelium, which secretes the cerebrospinal fluid (CSF), is a major site for transport mechanisms into and out of the brain via the ventricles of the brain [15–17]. The location of the choroid plexus within the ventricles of the brain and its production of the CSF suggest a physiological role for the choroid plexus in maintaining the protected milieu of the brain. A previous study, in vivo, suggested bi-directional transport of GABA between the CSF and blood; the transport of GABA from the CSF to blood was inhibited by probenecid (an inhibitor of the organic anion transporter) [18]. In addition, an early, preliminary in vitro study reported saturable uptake of GABA in the choroid plexus of the cat [19]; however, the mechanisms of the uptake were not characterized.

The goal of this study was to determine the mechanisms of GABA transport in the choroid plexus. Our data provide the first evidence for a Na^+-dependent GABA transporter in the choroid plexus. The choroid plexus is increasingly being recognized as a target tissue for hormones [20] and neurotransmitters [21]. The GABA transporter in the choroid plexus may play a role in CSF production or in maintaining homeostasis of GABA in the CSF and ultimately in the extracellular fluids of the brain.

2. Methods

2.1. Preparation of ATP-depleted choroid plexus

Choroid plexus was obtained from brains of New Zealand White rabbits and depleted of ATP using a modification of the method of Carter-Su and Kimmich [22] that has been described previously [23–25]. The animals were anesthetized with ketamine (5 mg/kg) and decapitated. The choroid plexus was quickly removed from the lateral ventricles and placed in one of the following buffers at room temperature (mM): KCl (120), mannitol (40), and HEPES (25) or NaCl (120), mannitol (40), and HEPES (25); the pH of each buffer was adjusted to 7.4 with 1 M Tris. Each choroid plexus was cut into 2–3-mm pieces and depleted of ATP by placing them in appropriate pre-loading buffers containing 250 μM 2,4-dinitrophenol (DNP), for 20 min at 37°C. Following ATP-depletion, all tissue pieces in the DNP-containing buffer were stored on ice until the start of the uptake studies. The tissue pieces were removed from the pre-loading buffer and blotted gently on laboratory tissue. Uptake commenced with placing the pieces in the appropriate uptake medium.

2.2. Uptake studies

Uptake of GABA into the choroid plexus was studied by incubating the tissue in 140 μl of uptake medium (37°C), which contained [^{3}H]GABA (0.01 μM), [^{14}C]mannitol (17.9 μM) and unlabeled GABA (1 μM), in appropriate buffer (indicated in the figure legends). The uptake medium contained DNP (250 μM) to ensure continued depletion of ATP. Uptake in the presence of Na^+ increased linearly and reproducibly with time, until 2.5 min (Fig. 1). Therefore, uptake was determined at 1 min in all subsequent studies.

For Michaelis–Menten studies, the uptake medium contained [^{3}H]GABA and [^{14}C]mannitol and different amounts of unlabeled GABA (to obtain the indicated

GABA concentrations). For IC_{50} studies, the uptake medium consisted of [^{3}H]GABA, [^{14}C]mannitol, unlabeled GABA (1 μM) and different amounts of unlabeled compounds. Data for both Michaelis–Menten and inhibition studies were generated by measuring GABA uptake into the tissue at 1 min.

Uptake was terminated in each choroid plexus tissue piece by removing it from the uptake medium and blotting it gently on laboratory tissue. Preliminary experiments showed that rinsing tissue in ice cold buffer versus blotting on laboratory tissue had equal effect in stopping the uptake reaction. The blotted tissue piece was placed on a pre-weighed piece of aluminum foil, dried under an IR-lamp heater (approximately 15 cm away from tissue) for 1 h, and then weighed to calculate the net dry tissue weight. The tissue was carefully detached from the foil using forceps and digested in 50 μl of 3 M KOH solution in a liquid scintillation counting vial. After dissolution was complete, 50 μl of 3 M HCl solution was added to neutralize the KOH. The corresponding aluminum foil was then added to the vials and the tissue-associated radioactivity was determined by liquid scintillation. In addition, the uptake medium (50 μl) was sampled and added to separate vials for liquid scintillation counting. Quantitation of ^{14}C and $_3$H was done by dual isotope liquid scintillation counting on a Beckman Model 1801 liquid scintillation counter (Beckman Instruments, Fullerton, CA). Counting efficiency of ^{3}H ranged from 45% to 47% and that of ^{14}C ranged from 92% to 94%.

Uptake of taurine into the choroid plexus pieces was examined in a manner identical to GABA except that, in this case, the uptake medium contained [^{3}H]taurine (0.0391 μM), [^{14}C]mannitol (17.9 μM) and different amounts of GABA. Taurine uptake into the tissue was measured at 15 min [24].

2.3. Reverse transcriptase–polymerase chain reaction (RT–PCR)

Specific oligonucleotide primers corresponding to nucleotides 242–276 and 1108–1139 of GAT-3/GAT-B were synthesized (UCSF Biomolecular Resource Center); the sequences were: sense, ACAAGAACGGCGGAGGGGCATTCCTGATTCCTTA and antisense, ATGAAAGCCAGTCCAGGACCTGATTCTGCCA. Degenerate oligonucleotide primers, previously described [5], corresponding to transmembrane domains II and VI of GAT-1 protein, were synthesized (UCSF Biomolecular Resource Center); the sequences were: sense, CCGCTCGAGAAGAACGG(C/T)GG(C/T)GG(C/T)GC(C/T)TTC-(C/T)T(G/A)AT(C/T)CC(A/G)TA and antisense, GCTCTAGAAA(G/A)AAGATCTG(G/A)GT(G/T)GC(G/A)GC(G/A)TC-(G/A/C)A(G/T)CCA. RNA was isolated from rat choroid plexus and rat brain using Trizol® reagent, according to the manufacturer's protocol. cDNA was generated from the RNA using a SuperScript™ preamplification kit (GIBCO-BRL). Polymerase chain reaction was performed with the cDNAs and oligonucleotide primers, using Taq DNA-polymerase (Boehringer Mannheim). Briefly, denaturation was performed for 3 min at 94°C; followed by 40 cycles each of 30 s at 94°C, 30 s at 55°C and 30 s at 72°C. Finally, 2 cycles were performed at 72°C for 7 min.

2.4. Data analysis

The uptake of GABA into the choroid plexus is expressed as a volume of distribution (V_d, ml/g dry tissue), calculated from the following equation [23,24]:

$$V_d = \frac{\text{dpm}[^3\text{H}]\text{GABA in choroid plexus/g of choroid plexus}}{\text{dpm}[^3\text{H}]\text{GABA in uptake medium/ml of uptake medium}} - \frac{\text{dpm}[^{14}\text{C}]\text{mannitol in choroid plexus/g of choroid plexus}}{\text{dpm}[^{14}\text{C}]\text{mannitol choroid plexus/ml of uptake medium}} \quad (1)$$

For Michaelis–Menten studies, the initial rate of GABA uptake is expressed as nmol/g dry choroid plexus tissue per minute and plotted against the concentration of GABA. The data were fit to the following equation:

$$\text{Rate} = \frac{V_{max} \cdot C}{K_m + C} \quad (2)$$

where V_{max} is the maximal rate of uptake, K_m is concentration of GABA at which the rate of uptake is 50% of the maximal rate and C is the concentration of GABA in the uptake medium. The parameters were estimated using a non-linear regression program on Minim 3.0.8® (obtained from Dr. R.D. Purves, University of Otago, New Zealand).

Inhibition of Na^+-GABA uptake by various test compounds was evaluated by estimation of IC_{50} values: the data were fit to the following four-parameter logistic function using a non-linear fitting routine on Minim 3.0.8:

$$V_d = \frac{(V_{d,0} - V_{d,ns})}{1 + (C/IC_{50})^n} + V_{d,ns} \quad (3)$$

where V_d is the volume of distribution of GABA in the choroid plexus; $V_{d,0}$ is the volume of distribution of GABA in the absence of inhibitor and in the presence of an inwardly directed Na^+-gradient; $V_{d,ns}$, the non-specific diffusional component, is the volume of distribution of GABA in the absence of a Na^+ gradient; C is the concentration of inhibitor in the uptake mixture; and n is the Hill coefficient. The IC_{50} of GABA in inhibiting Na^+-stimulated taurine uptake was computed in a manner similar to that described for GABA.

For each data point, 3–5 measurements were made per experiment; between one and five experiments were performed (see figure legends). Data are presented as mean ± SE of all determinations. All parameter estimates (Michaelis–Menten and IC_{50} studies), which were generated using non-linear regression (Minim 3.0.8), are expressed as mean ± SD of the estimates. Means were compared using unpaired Student's t-test or one-way ANOVA and a probability, P, of less than 0.05 was considered significant.

2.5. Materials

[^{3}H]Taurine (specific activity: 21.9 Ci/mmol) and [^{3}H]GABA (specific activity: 88.4 Ci/mmol) were obtained from Du Pont–New England Nuclear (Boston, MA). [^{14}C]Mannitol was obtained from Moravek Biochemicals (Brea, CA). Guvacine, nipecotic acid, OH-nipecotic acid (hydroxy-nipecotic acid) and 4,5,6,7-tetrahydroisoxazolo[4,5-c]pyridin-3-ol (THPO) were from RBI (Natick, MA). All other chemicals were purchased from Sigma (St. Louis, MO). Cytoscint ES scintillation fluid was obtained from ICN (Irvine, CA). New Zealand white rabbits (2–3 kg) were purchased from Nitabell Rabbitry (Hayward, CA).

3. Results

3.1. Time dependence

Uptake of GABA into ATP-depleted tissue pieces was examined in the presence and absence of an inwardly-directed Na^+ gradient (Fig. 1). A distinct ''overshoot'' phenomenon, typical of Na^+-driven uptake in ATP-depleted tissue preparations, was observed in the presence of an initial Na^+ gradient. Uptake in the presence of the Na^+ gradient increased linearly as a function of time, until 2.5 min. It reached a maximum at 15 min ($V_d = 27.7 \pm 2.9$ ml/g) and then declined at 30 min ($V_d = 8.58 \pm 2.01$ ml/g). Uptake at 30 min was not significantly different from that at 60 min, suggesting that an equilibrium value of uptake was reached by 30 min.

GABA uptake in the presence of an inwardly-directed Na^+ gradient was significantly higher than that when Na^+ was present in equal concentration inside and outside the tissue (120 mM), at all time points studied (Fig. 1). In addition, absence of Na^+

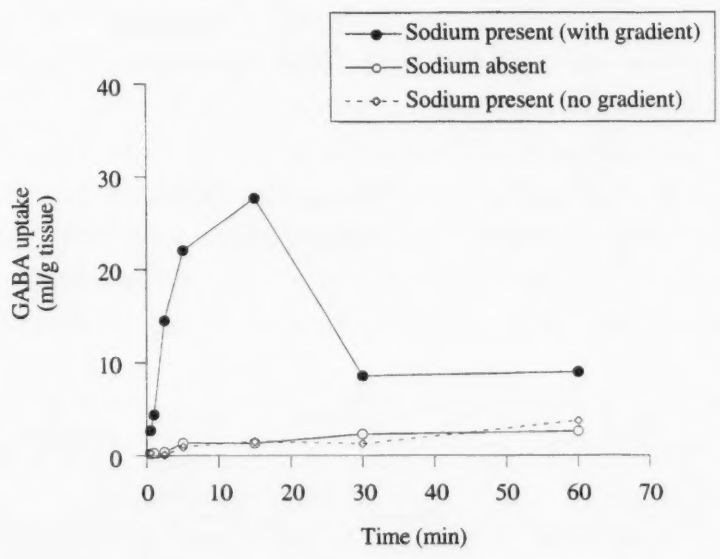

Fig. 1. Temporal profile of GABA accumulation in ATP-depleted rabbit choroid plexus. Uptake (expressed as V_d) of GABA was determined at 37°C. Points represent means ± SE of data obtained from two separate experiments, each performed in quadruplicate. Uptake at all time points in the presence of a Na^+-gradient was significantly greater than that in the absence of Na^+ and the absence of a Na^+ gradient ($P < 0.001$). Key: 120 mM inwardly-directed Na^+ gradient (filled circles); 120 mM equal K^+ inside and outside of the tissue (open circles); 120 mM equal Na^+ inside and outside of the tissue (open diamonds).

from the reaction mixture (equal K^+ inside and outside, 120 mM) resulted in an uptake that was not significantly different from that when equal Na^+ was present inside and outside the tissue, at all time points studied. These data suggest that a Na^+-gradient can drive the uptake of GABA in the choroid plexus.

3.2. Ion dependence

Replacement of Na^+ with choline in the uptake mixture abolished GABA uptake (5.08 ± 0.58 vs. 0.17 ± 0.05 ml/g, mean $\pm$ SE, $P < 0.001$) indicating a strong Na^+-dependence. Replacement of Cl^- with SCN^-, NO_3^- or Br^- resulted in a partial attenuation of transport which was, however, insignificant (80, 68 and 61% of control uptake, respectively) (Table 1). When gluconate was used as the anion in place of Cl^-, there was a complete loss of Na^+-dependent GABA uptake (5.08 ± 0.58 vs -0.04 ± 0.04 ml/g, mean $\pm$ SE, $P < 0.001$). These results suggest a moderately selective anion requirement for Na^+–GABA transport in the rabbit choroid plexus.

3.3. Concentration dependence

The initial rate of uptake of GABA (at 1 min) was measured as a function of concentration in the presence of an inwardly-directed Na^+ gradient. The rate of uptake increased initially with increasing substrate concentration and then achieved a plateau in a manner consistent with saturable kinetics (Fig. 2). The data were fitted to the Michaelis–Menten equation describing a single saturable component. The estimated V_{max} and K_m (mean $\pm$ SD) were 409 ± 43 nmol/g per min and 37 ± 9 μM, respectively. The uptake values at the 4 highest GABA concentrations were not significantly different from each other (ANOVA, $P = 0.741$), indicating that a non-saturable component was not a major component of GABA transport into the tissue. Hence, a linear term was not included in the equation used to fit the data.

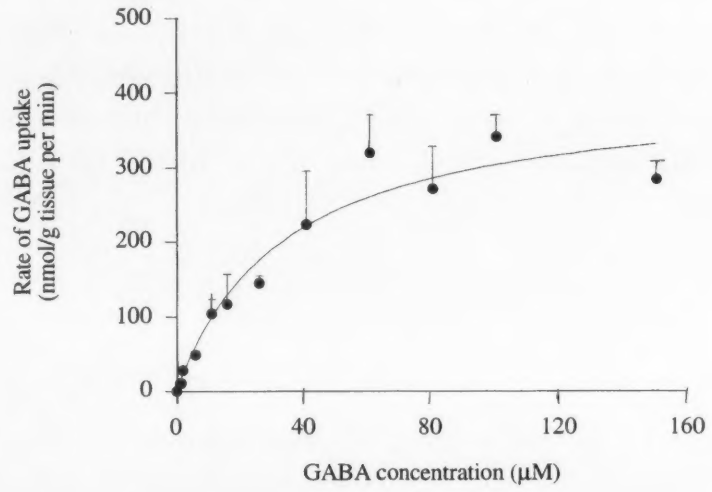

Fig. 2. Concentration dependency of Na^+-driven GABA uptake in ATP-depleted choroid plexus. Uptake at 1 min in nmol/g tissue was measured at 37°C in the presence of a Na^+ gradient (120 mM). Points represent the mean $\pm$ SE of between 1 to 3 experiments, each performed in triplicate or quadruplicate. GABA uptakes at the four highest substrate concentrations were not significantly different from each other ($P = 0.741$, ANOVA). The estimated V_{max} and K_m were 409 ± 43 nmol/g per min and 37 ± 9 μM, respectively (mean $\pm$ SD).

3.4. Inhibition

Various compounds previously shown to inhibit GABA transport in other tissue were tested for their ability to inhibit GABA transport in choroid plexus

Table 1
Ion-dependence of GABA uptake

Condition	V_d of GABA (ml/g)	% of control	P value compared to control
Na^+, Cl^- (control)	5.08 ± 0.58 (2)	100	–
Na^+, SCN^-	4.06 ± 0.28 (2)	80	n.s.
Na^+, NO_3^-	3.49 ± 0.35 (2)	68	n.s.
Na^+, Br^-	3.13 ± 0.67 (1)	61	n.s.
Na^+, Gluconate$^-$	-0.04 ± 0.04 (2)	0	< 0.001
Choline$^+$, Cl^-	0.17 ± 0.05 (2)	3	< 0.001

ATP-depleted choroid plexus pieces were pre-incubated in choline Cl (120 mM), KCl (40 mM) and HEPES (15 mM) pH 7.4. For uptake studies, tissue was incubated with [^{3}H]GABA in either buffer containing NaCl (120 mM), KCl (40 mM) and HEPES (15 mM) pH 7.4, or in buffers which were identical except for equimolar replacement of Cl^- with SCN^-, NO_3^-, Br^- or gluconate$^-$, or in which Na^+ was replaced with choline$^+$. Data represent mean $\pm$ SE of uptake (determined at 1 min); the number of experiments are indicated in parentheses. Each experiment was performed in replicates of five; n.s. denotes not significant.

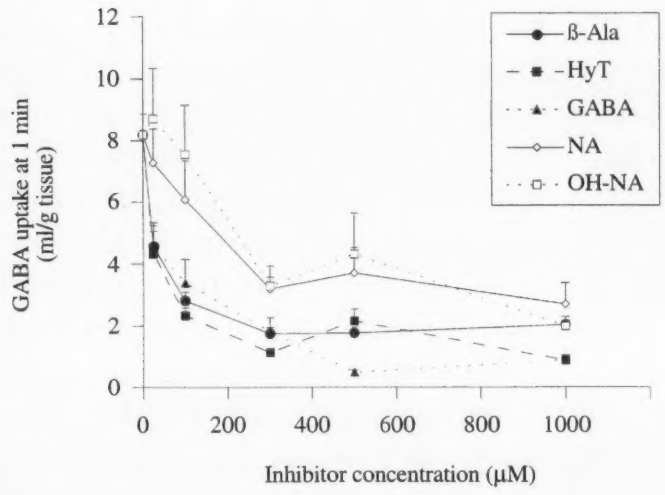

Fig. 3. Effect of various inhibitors on Na^+-driven GABA uptake in ATP-depleted choroid plexus tissue. Uptake (ml/g) of GABA (1 μM) was measured at 37°C in the presence of various concentrations (0, 25, 100, 300, 500 and 1000 μM) of unlabeled compounds. Key: β-Ala, β-Alanine; HyT, hypotaurine; NA, nipecotic acid; OH-NA, hydroxy-nipecotic acid. Points represent mean ± SE of between 1 and 4 experiments, each performed in quadruplicate. Where error bars are not visible, they are encompassed within the point. Points are connected by a simple linear spline. See Table 1 for a summary of these and other results.

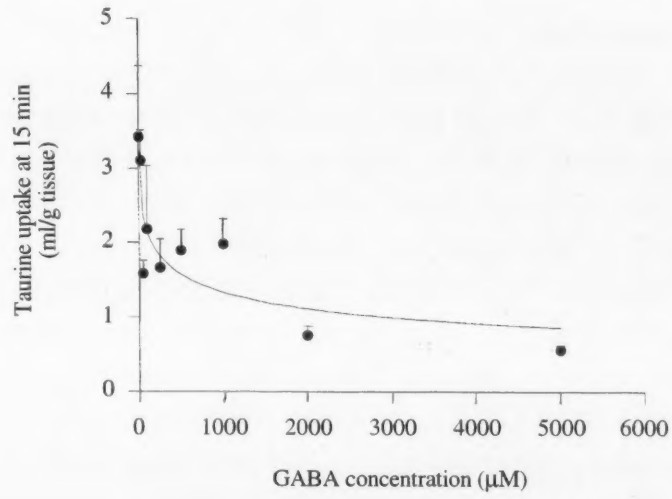

Fig. 4. Effect of GABA on Na^+-driven taurine uptake in ATP-depleted choroid plexus tissue. Uptake (ml/g) of taurine 25 μM) was measured at 37°C in the presence of various concentrations (25, 50, 100, 250, 500, 1000, 2000 and 5000 μM) of unlabeled GABA. Points represent mean ± SE of 1 experiment, performed in quadruplicate. The curve represents the best fit to the data and was generated using the equation for IC_{50} (see Section 2). The IC_{50} was estimated to be 230 μM.

tissue pieces. All potential compounds were tested at various concentrations (0, 25, 100, 300, 500 and 1000 μM), and IC_{50} values (mean ± SD) were obtained (Fig. 3, Table 2). Hypotaurine (IC_{50} = 21.9 ± 17.3 μM) and β-alanine (IC_{50} = 22.9 ± 18.1 μM) were potent inhibitors of Na^+-driven GABA uptake in choroid plexus tissue pieces. Nipecotic Acid (IC_{50} = 244 ± 113 μM) and OH-nipecotic acid (IC_{50} = 284 ± 128 μM) were moderately potent in their ability to inhibit Na^+-driven GABA uptake. Betaine, L-(2,4)-diaminobutyric acid (L-DABA), guvacine and THPO showed weak inhibitory activity, with IC_{50}values of > 1 mM. Neither taurine nor L-alanine, an isomer of β-alanine, significantly inhibited GABA uptake (IC_{50} > 1 mM).

Table 2
Inhibitor sensitivity of GABA uptake in rabbit choroid plexus

Inhibitor	IC_{50} (μM)	K_i (μM)
β-Alanine	22.9 ± 18.1	22.2 ± 17.5
Hypotaurine	21.9 ± 17.3	21.2 ± 16.7
Nipecotic acid	244 ± 113	236 ± 109
OH-Nipecotic acid	284 ± 128	275 ± 124
Guvacine	565 ± 208	547 ± 201
THPO	> 1 mM	> 1 mM
L-DABA	> 1 mM	> 1 mM
Taurine	> 1 mM	> 1 mM
Betaine	> 1 mM	> 1 mM
L-Alanine	> 1 mM	> 1 mM

For IC_{50} estimates, the Na^+-driven uptake (1 min) of [^{3}H]GABA was measured in the presence of various inhibitors. Each inhibitor was tested at 0, 25, 100, 300, 500 μM and 1 mM. Uptake values, which were corrected for non-specific Na^+-independent uptake, were pooled from between 1–5 experiments and fitted to the equation as described in Section 2. Each experiment was performed in quadruplicate. IC_{50} and K_i values are the mean ± SD of the estimate; Fig. 3 depicts some of the data. To allow comparison with other studies, K_i values were generated from IC_{50} determinations using the Cheng and Prusoff relationship [41], which assumes competitive inhibition: $K_i = IC_{50}/(1 + S)$, where S = concentration of GABA/K_m of GABA.

The effect of GABA on the Na^+-dependent uptake of taurine (25 μM) into the tissue pieces was determined at 15 min. GABA inhibited taurine uptake with an IC_{50} value of 230 μM (Fig. 4). Since an inhibitor may not necessarily be a substrate of the transporter, further studies are required to determine if GABA is a substrate of the Na^+-taurine transporter in choroid plexus.

3.5. RT–PCR

RT–PCR with primers specific to GAT-3, resulted in the amplification of a band of predicted size from the rat brain but not from the choroid plexus (data not shown). Identical results were obtained using primers degenerate for GAT-1, which were designed to amplify both GAT-1 and GAT-3 (data not shown).

4. Discussion

GABA is the dominant inhibitory neurotransmitter in the brain and is present throughout the central nervous system. The neurotransmitter actions of GABA in the synaptic cleft are terminated by its reuptake via Na^+ and Cl^- coupled transporters; both neuronal and glial cells express one or more members of this closely related family of transporters [3–7]. Imbalances in GABA function in the brain have been associated with psychiatric [26] and neurological diseases [27,28]. Studies with post-mortem human brains suggest that an increased level of expression of GABA transporters may be involved in schizophrenia [29]. In various species, including humans [30], GABA transporters have been implicated in epilepsy and are an active target of drug design efforts for the disease [31–35]. Inhibitors of GABA transporters have demonstrated usefulness in animal models of seizures [36–38] presumably by sustaining the concentration of GABA in the synaptic cleft. Our finding of a GABA transporter in the choroid plexus of the brain suggests an additional mechanism that may govern the disposition of GABA in the brain.

In vivo studies suggest that the transfer of GABA from blood to the CSF and the disposition of GABA in the CSF is governed by a carrier-mediated process [18]. An early, preliminary study reported saturable uptake of GABA in the choroid plexus of the cat [19]. However, neither the driving force for GABA transport in the choroid plexus nor the specificity of the observed transport process was determined. Here, we provide evidence for a Na^+-dependent GABA transporter (CP–GABA transporter) in the choroid plexus of the rabbit brain. Following ATP-depletion of the tissue, we determined that GABA uptake was driven by an initial inwardly-directed Na^+-gradient (Fig. 1). This Na^+-gradient-dependent uptake is characteristic of concentrative accumulation of a substrate by the tissue, and it is similar to that seen for GABA uptake in other tissue. As with other GABA transporters, Cl^- supported GABA transport optimally; replacement of Cl^- with gluconate completely abolished transport. However, SCN^-, NO_3^- and Br^- were also able to sustain GABA transport, suggesting that Cl^- is not absolutely necessary for GABA transport in the choroid plexus. Similar results have been obtained for Na^+-GABA transport in the retina [10]. In contrast, while Cl^- replacement has been less well studied for the Na^+-GABA transporters in the brain, they generally show a strong requirement for Cl^- and in some cases Br^- [3,4,6]. These results suggest that the CP–GABA transporter may be similar to the GABA transporter in the retina. In this study, the estimated K_m (37 ± 8 μM) indicates that the affinity of the GABA transporter in the choroid plexus for GABA is similar to that of other GABA transporters in the brain [3,4,6,7] and other tissues [10,13,14]. We note that the K_m for GABA reported by Lorenzo (K_m = 230 μM) in the cat choroid plexus is considerably higher than the one we obtained in this study [19]. The reason for this discrepancy is not clear; it is possible that it results from methodological or species differences.

To determine the selectivity of the CP–GABA transporter, we examined the potency of various compounds known to inhibit GABA transport in other tissues. Of the compounds tested, β-alanine (IC_{50} = 22.9 μM) and hypotaurine (IC_{50} = 21.9 μM) were the most potent, whereas L-DABA and betaine were not able to effectively inhibit Na^+-driven GABA transport in choroid plexus. These data suggest that the CP–GABA transporter is most similar to GAT-3/GAT-B, which is sensitive to β-alanine but insensitive to L-DABA (GAT-1 is insensitive to β-alanine and GAT-2 is sensitive to L-DABA). However, the anion requirements (Table 1) suggest that there may be functional differences in the two transporters. Finally, the choroid plexus transporter is also different from the GABA-transporting renal epithelial transporter, BGT, by virtue of its refractoriness to betaine.

Because hypotaurine and β-alanine, both potent inhibitors of Na^+-GABA uptake in the rabbit choroid plexus, also inhibit taurine uptake via the Na^+-taurine transporter in the choroid plexus, we asked if both uptake processes were mediated via the same transporter. The finding that GABA inhibits the uptake of taurine (Fig. 4, IC_{50} = 230 μM), but taurine does not inhibit GABA uptake significantly (Table 2), suggests that the Na^+-GABA transporter, which we have characterized in the choroid plexus, is distinct from the Na^+-taurine transporter.

RT–PCR of rat brain RNA using oligonucleotide probes degenerate for the rat GAT-1 [5] resulted in amplification of a band of predicted size (data not

shown). Similarly probes specific for GAT-3/GAT-B resulted in the amplification of the predicted band (data not shown). We did not observe amplification of corresponding bands, with either set of probes, when RNA from rat choroid plexus was used. These data suggest that the rat choroid plexus may not express a GABA transporter similar to GAT-1 or GAT-3/GAT-B. However, alternative RT–PCR conditions may be necessary to identify GAT-1 or GAT-3 mRNA transcripts in the choroid plexus.

The presence of a $GABA_A$ receptor in the choroid plexus epithelium of the rat has been documented [39]; in vivo studies indicate that benzodiazepine ligands reduce the secretion rate of the CSF by up to 50% [40]. The concomitant presence of a GABA transporter is consistent with the suggested involvement of GABA-ergic mechanisms in modulation of CSF production. Furthermore, the transporter for GABA in the choroid plexus may play a role in maintaining homeostasis of GABA in the CSF, and ultimately the brain. Such a transporter may also be important in the targeting of GABA analogs to the central nervous system.

Acknowledgements

This work was supported by National Institutes of Health Grant GM 26691.

References

[1] R. Radian, O.P. Ottersen, J. StormMathisen, M. Castel, B.I. Kanner, J. Neurosci. 10 (1990) 1319–1330.
[2] N.J. Mabjeesh, M. Frese, T. Rauen, G. Jeserich, B.I. Kanner, FEBS Lett. 299 (1992) 99–102.
[3] J. Guastella, N. Nelson, H. Nelson, L. Czyzyk, S. Keynan, M.C. Miedel, N. Davidson, H.A. Lester, B.I. Kanner, Science 249 (1990) 1303–1306.
[4] K.E. Borden, P.R. Smith, T.A. Hartig, Branchek, R.L.J. Weinshank, Biol. Chem. 267 (1992) 21098–21104.
[5] J.A. Clark, A.Y. Deutch, P.Z. Gallipoli, S.G. Amara, Neuron 9 (1992) 337–348.
[6] B. Lopez-Corcuera, Q.R. Liu, S. Mandiyan, H. Nelson, N. Nelson, J. Biol. Chem. 267 (1992) 17491–17493.
[7] Q.R. Liu, B. Lopez-Corcuera, S. Mandiyan, H. Nelson, N. Nelson, J. Biol. Chem. 268 (1993) 2106–2112.
[8] S.G. Amara, Nature 360 (1992) 420–442.
[9] J.A. Clark, S.G. Amara, Bioessays 15 (1993) 323–332.
[10] S. Sivakami, V. Ganapathy, F.H. Leibach, Y. Miyamoto, Biochem. J. 283 (1992) 391–397.
[11] K.R. Jessen, J.M. Hills, A.R. Limbrick, Gut 29 (1988) 1549–1556.
[12] P. Gilon, B. Reusens-Billen, C. Remacle, P. Janssens de Varebeke, G. Pauwels, J.J. Hoet, Cell Tissue Res. 249 (1987) 93–600.
[13] P.R. Goodyer, R. Rozen, C.R. Scriver, Biochim. Biophys. Acta 818 (1985) 45–54.
[14] S.L. Erdo, F. Amenta, Eur. J. Pharmacol. 130 (1986) 287–294.
[15] H.F. Cserr, Physiol. Rev. 51 (1986) 273–311.
[16] E.M. Wright, Physiol. Biochem. Pharmacol. 83 (1978) 33–34.
[17] C.E. Johanson in: E.A. Neuwelt (Ed.), Implications of the Blood-brain Barrier and its Manipulation Vol. 1: Basic Clinical Aspects, Plenum Publishing Corporation, New York, 1989, pp. 223–260.
[18] W. Loscher, H.H. Frey, J. Neurochem. 38 (1982) 1072–1079.
[19] A.V. Lorenzo, Fed. Proc. 33 (1974) 2079–2085.
[20] L.A. Tartaglia, M. Dembski, X. Weng, N. Deng, J. Culpepper, R. Devos, G.J. Richards, L.A. Campfield, F.T. Clark, J. Deeds, C. Muir, S. Sankar, A. Moriarty, K.J. Moore, J.S. Smutko, G. Mays, E.A. Woolf, C.A. Monroe, R. Tepper, Cell 83 (1995) 1263–1271.
[21] E.L. Barker, E. Sanders-Bush, Mol. Pharmacol. 44 (1993) 725–730.
[22] C. Carter-Su, G.A. Kimmich, Am. J. Physiol. 237 (1979) C64–C74.
[23] X. Wu, G. Yuan, C.M. Brett, A.C. Hui, K.M. Giacomini, J. Biol. Chem. 267 (1992) 8813–8818.
[24] S.J. Chung, V. Ramanathan, K.M. Giacomini, C.M. Brett, Biochim. Biophys. Acta 1193 (1994) 10–16.
[25] H. Suzuki, Y. Sawada, Y. Sugiyama, T. Iga, M. Hanano, J. Pharmacol. Exp. Ther. 243 (1987) 1147–1152.
[26] F.M. Benes, S.L. Vincent, G. Alsterberg, E.D. Bird, J.P. SanGiovanni, J. Neurosci. 12 (1992) 924–929.
[27] C.R. Scriver, S. Pueschel, E. Davies, N. Engl. J. Med. 274 (1966) 635–643.
[28] T.L. Perry, S. Hansen, M. Kloster, N. Engl. J. Med. 288 (1973) 337–342.
[29] G.P. Reynolds, C. Czudek, H.B. Andrews, Biol. Psychiatry 27 (1990) 1038–1044.
[30] M.J. During, M.K. Ryder, D.D. Spencer, Nature 376 (1995) 174–177.
[31] P. Krogsgaard-Larsen, E. Falch, O.M. Larsson, A. Schousboe, Epilepsy Res. 1 (1987) 77–93.
[32] R.J. Porter, M.A. Rogawski, Epilepsia 33 (Suppl. 1) (1992) S1–S6.
[33] B.S. Meldrum, Adv. Neurol. 57 (1992) 635–641.
[34] P.D. Suzdak, J.A. Jansen, Epilepsia 36 (1995) 612–626.
[35] B. Meldrum, Nature 376 (1995) 122–123.
[36] A.M. Coenen, E.H. Blezer, E.L. van Luijtelaar, Epilepsy Res. 21 (1995) 89–194.

[37] S.E. Smith, N.S. Parvez, A.G. Chapma, B.S. Meldrum, Eur. J. Pharmacol. 273 (1995) 259–265.
[38] A. Schousboe, O.M. Larsson, J.D. Wood, P. Krogsgaard-Larsen, Epilepsia 24 (1983) 531–538.
[39] F. Amenta, C. Cavallotti, W.L. Collier, F. Ferrante, P. Napoleone, Pharmacol. Res. 21 (1989) 369–373.
[40] G.L. Williams, M. Pollay, T. Seale, B. Hisey, P.A. Roberts, J. Neurosurg. 72 (1978) 759–762.
[41] Y. Cheng, W.H. Prusoff, Biochem. Pharmacol. 22 (1973) 3099–3108.

Send for a Free Sample Copy!

BBA - Lipids and Lipid Metabolism

One of the ten topical sections of Biochimica et Biophysica Acta, the International Journal of Biochemistry, Biophysics and Molecular Biology

- **Thematic special issues on current "hot" topics**

Executive Editors:

D.E. Vance, *Edmonton, AB, Canada* and **H. van den Bosch**, *Utrecht, The Netherlands*

AIMS AND SCOPE:

Covers the novel aspects of lipid biosynthesis and metabolism, including protein modification by lipids, in all organisms. Emphasis is given to the enzymology and molecular biology of the enzymes involved in lipid metabolism. In addition, molecular genetics of the genes involved will be emphasized in the future.
Sub-section: 'Lipids in Signalling and Recognition' concentrates on all biochemical and biophysical aspects of lipids and lipid-derived messenger molecules, including their structure, physicochemical properties and transport, regulation and enzymology of their biosynthesis and metabolic inactivation, and the recognition processes underlying their biological activities.

Types of papers published: regular papers, rapid reports, short sequence papers, reviews and mini-reviews.

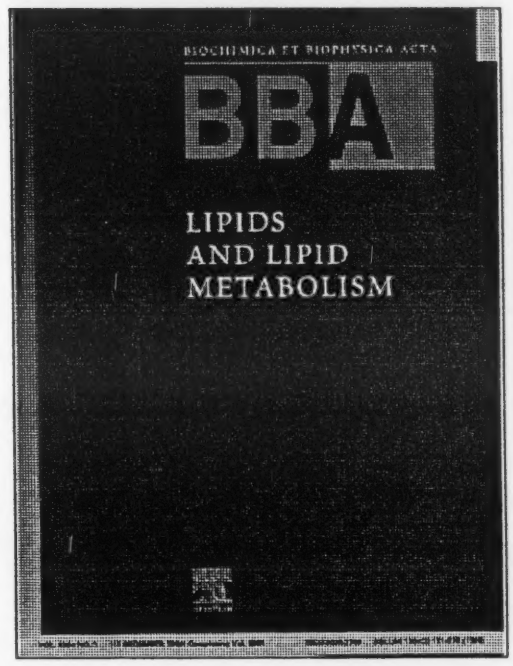

For:
Biochemists, Biophysicists, Chemists, Cell biologists, Molecular biologists, Physiologists, Pharmacologists, Nutritionists

BBA - Lipids and Lipid Metabolism
For more information, access http://www.elsevier.nl/locate/bbalip

❑ Please send me a **FREE Sample Copy** including instructions to authors

Name: ..... Initials: .....
Position: ..... Title: .....
Institute/Company: .....
Department: .....
Address: .....
Post/Zip Code: ..... City: .....
Country: ..... Tel: .....
Fax: ..... E-mail address: .....

ELSEVIER SCIENCE

New York
Tel: (+1) 212-633-3730
[Toll Free number for North American customers: 1-888-4ES-INFO (437-4636)]
Fax: (+1) 212-633-3680
E-mail: usinfo-f@elsevier.com

Amsterdam
Tel: (+31) 20-485-3757
Fax: (+31) 20-485-3432
E-mail: nlinfo-f@elsevier.nl

Tokyo
Tel: (+81) 3-5561-5033
Fax: (+81) 3-5561-5047
E-mail: info@elsevier.co.jp

Singapore
Tel: (+65) 434-3727
Fax: (+65) 337-2230
E-mail: asiainfo@elsevier.com.sg

Please quote the following code with all requests: GB7

057-12/97

Interested in Associative Learning?

OPAL is the answer! Open Programs for Associative Learning is an interactive system using computer technology and hypermedia principles to present a revolutionary approach to learning and teaching. OPAL modules provide the tools for intuitive and associative learning. By browsing freely the User can create his/her own knowledge trail.

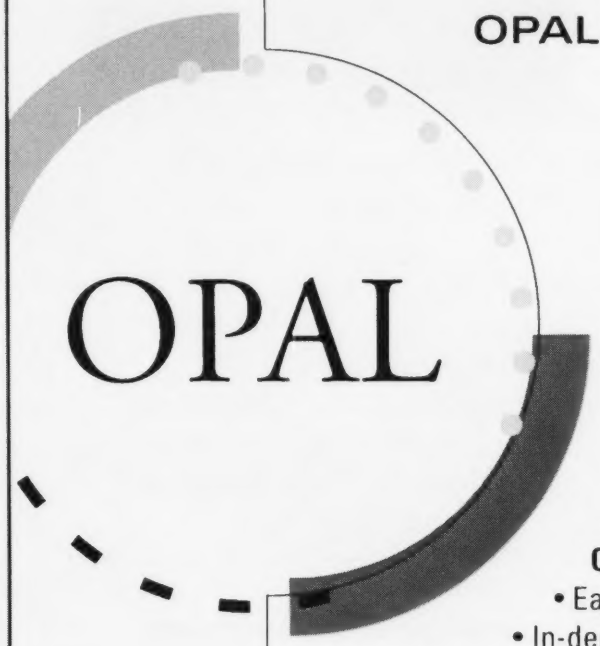

OPAL Modules available:

OPAL Module 1	Neural Communication
OPAL Module 2	Calcium as a Messenger
OPAL Module 3	Immune Cells
OPAL Module 4	Endocrine Cells
OPAL Module 5	Autonomic Nervous System
OPAL Module 6	Brain Aging
OPAL Module 7	Cell Structure
OPAL Module 8	Pain: Basic Science

Options

- Easy to use
- In-depth information
- Interactive animations and simulations
- Knowledge evaluation through electronic questionnaire

Seeing is believing....

so log into the OPAL Website today!

http://www.elsevier.com/locate/opal
http://www.elsevier.nl/locate/opal

ELSEVIER SCIENCE

Check out the OPAL Website for information on and demos of the OPAL Modules.

Publication information
Biochimica et Biophysica Acta (Biomembranes) (ISSN 0005-2736). For 1997 volumes 1323–1331 (including Reviews) are scheduled for publication. *Biochimica et Biophysica Acta* full subscription for 1997 consists of Volumes 1318–1362. Subscription prices are available upon request from the Publisher. Subscriptions are accepted on a prepaid basis only and are entered on a calendar year basis. Issues are sent by surface mail except to the following countries where Air delivery via SAL mail is ensured: Argentina, Australia, Brazil, Canada, Hong Kong, India, Israel, Japan, Malaysia, Mexico, New Zealand, Pakistan, PR China, Singapore, South Africa, South Korea, Taiwan, Thailand, USA. For all other countries airmail rates are available upon request. Claims for missing issues should be made within six months of our publication (mailing) date.

Orders, claims, and product enquiries: please contact the Customer Support Department at the Regional Sales Office nearest you:

New York, Elsevier Science, P.O. Box 945, New York, NY 10159-0945, USA. Tel. (+1)212-633-3730, [Toll free number for North American Customers:1-888-4ES-INFO (437-4636)], Fax (+1)212-633-3680, E-mail: usinfo-f@elsevier.com
Amsterdam, Elsevier Science, P.O. Box 211, 1000 AE Amsterdam, The Netherlands. Tel. (+31)20-4853757, Fax (+31)20-4853432, E-mail: nlinfo-f@elsevier.nl
Tokyo, Elsevier Science, 9-15, Higashi-Azabu 1-chome, Minato-ku, Tokyo 106, Japan. Tel. (+81)3-5561-5033, Fax (+81)3-5561-5047, E-mail: info@elsevier.co.jp
Singapore, Elsevier Science, No. 1 Temasek Avenue, #17-01 Millenia Tower, Singapore 039192. Tel. (+65)434-3727, Fax (+65)337-2230, E-mail: asiainfo@elsevier.com.sg

Enquiries concerning manuscripts and proofs
Questions arising after acceptance of the manuscript, especially those relating to proofs, should be directed to Issue Manager, *BBA,* Elsevier Science B.V., P.O. Box 2759, 1000 CT Amsterdam, The Netherlands. Courier address: Sara Burgerhartstraat 25, 1055 KV Amsterdam, The Netherlands. Tel. (+31) 20 485 3273; Fax: (+31) 20 485 2775.

Authors in Japan please note: Upon request, Elsevier Science Japan will provide authors with a list of people who can check and improve the English of their paper (*before submission*). Please contact our Tokyo office: Elsevier Science Japan, 1-9-15 Higashi-Azabu, Minato-ku, Tokyo 106; Tel. (03)-5561-5032; Fax (03)-5561-5045.

BBA has no page charges and 50 offprints are provided free to the corresponding author of each published paper.

Colour figures
Colour figures are published at the author's expense: 750 Dutch guilders for the first page and 500 Dutch guilders for each subsequent page, excluding sales tax.

This journal is in the *ADONIS* Service, whereby copies of individual articles can be printed out from CD-ROM on request. An explanatory leaflet can be obtained by writing to ADONIS B.V., P.O. Box 17005, 1001 JA Amsterdam, The Netherlands.

US mailing notice – Biochimica et Biophysica Acta (*Biomembranes*) (ISSN 0005-2736) is published monthly, except semimonthly in Jan., April, July and Oct. (total 16 issues) by Elsevier Science B.V. (Molenwerf 1, Postbus 211, 1000 AE Amsterdam, The Netherlands).
Annual subscription price in the USA US$ 2889 (valid in North, Central and South America), including air speed delivery. Periodicals postage paid at Jamaica, NY 11431.
USA POSTMASTER: Send address changes to *Biochimica et Biophysica Acta* (*Biomembranes*), Publications Expediting, Inc., 200 Meacham Avenue, Elmont, NY 11003.
AIRFREIGHT AND MAILING in the USA by Publications Expediting Inc., 200 Meacham Avenue, Elmont, NY 11003.

0005-2736(19971113)1330:1;1-U